

**NASA TECHNICAL NOTE**



**NASA TN D-2387**

*C.1*

NASA TN D-2387

LOAN COPY: RETURN  
AFWL (WLIL-2)  
KIRTLAND AFB, N ME



**HEAT-TRANSFER AND PRESSURE  
MEASUREMENTS ON DELTA WINGS  
AT MACH NUMBERS OF 3.51 AND 4.65  
AND ANGLES OF ATTACK FROM  $-45^{\circ}$  TO  $45^{\circ}$**

*by Robert L. Stallings, Jr., Paige B. Burbank,  
and Dorothy T. Howell*

*Langley Research Center  
Langley Station, Hampton, Va.*



HEAT-TRANSFER AND PRESSURE MEASUREMENTS ON DELTA WINGS  
AT MACH NUMBERS OF 3.51 AND 4.65 AND ANGLES OF ATTACK  
FROM  $-45^{\circ}$  TO  $45^{\circ}$

By Robert L. Stallings, Jr., Paige B. Burbank,  
and Dorothy T. Howell

Langley Research Center  
Langley Station, Hampton, Va.

NATIONAL AERONAUTICS AND SPACE ADMINISTRATION

---

For sale by the Office of Technical Services, Department of Commerce,  
Washington, D.C. 20230 -- Price \$3.00

# HEAT-TRANSFER AND PRESSURE MEASUREMENTS ON DELTA WINGS

AT MACH NUMBERS OF 3.51 AND 4.65 AND ANGLES OF ATTACK

FROM  $-45^{\circ}$  TO  $45^{\circ}$

By Robert L. Stallings, Jr., Paige B. Burbank,  
and Dorothy T. Howell  
Langley Research Center

## SUMMARY

Heat-transfer and pressure measurements were determined on  $70^{\circ}$  swept hyper-sonic wings having a sharp or blunt nose and having dihedral angles of  $0^{\circ}$  and  $24.3^{\circ}$  in the Langley Unitary Plan wind tunnel. All models were tested at Mach numbers 3.51 and 4.65 at nominal Reynolds numbers per foot of  $2.9 \times 10^6$  and  $4.1 \times 10^6$ . The models having a dihedral angle of  $0^{\circ}$  were tested through an angle-of-attack range from  $0^{\circ}$  to  $45^{\circ}$  and the models with  $24.3^{\circ}$  dihedral were tested at angles of attack from  $-45^{\circ}$  to  $45^{\circ}$ .

Throughout the angle-of-attack range for which the stagnation line remained on the wing cylindrical leading edge, the pressure distributions on the leading edges of the models through  $60^{\circ}$  expansion leeward of the stagnation line were predicted by both Newtonian flow and a modified version of the compressible Bernoulli equation based on normal Mach number components. For expansion angles from  $60^{\circ}$  to  $90^{\circ}$ , the experimental data were in agreement with the compressible Bernoulli equation. For angles of attack for which the stagnation line shifts from the geometrical wing leading edges to the ridge line, the pressure distributions on the wing leading edges (now trailing edges) were approximated only by the Newtonian flow. The windward-panel center-line pressures for both sharp-nose models were correlated throughout the Mach number and angle-of-attack ranges of this investigation by the parameter  $M \sin \alpha$ , where  $M$  is the free-stream Mach number and  $\alpha$  is the angle of attack. The pressures obtained off the center line on the windward panel of the body with  $24.3^{\circ}$  dihedral were correlated by the same parameter based on the effective angle of attack of the wing panel.

The heat-transfer-coefficient distributions on the leading edge of the wings with  $0^{\circ}$  dihedral and for which the boundary layer remained laminar were in good agreement with laminar swept-cylinder theory for angles of attack from  $0^{\circ}$  to  $37.5^{\circ}$ . Good agreement was also obtained with swept-cylinder theory for the portion of the leading edge of the  $24.3^{\circ}$  dihedral wing not affected by turbulence at angles of attack from  $-37.5^{\circ}$  to  $22.5^{\circ}$ . At an angle of attack of  $45^{\circ}$ , the heating rates on both wings were overpredicted by the swept-cylinder theory. There was no apparent trend of nose effect on the heat transfer or pressure distribution downstream of 4.5 nose diameters throughout the range of this investigation.

## INTRODUCTION

High heating rates on the wing leading edges of vehicles operating at hypersonic speeds produce very large temperatures and associated structural problems. One of the conventional methods of reducing these high heating rates is to add sweep and bluntness, thereby reducing the normal Mach number and increasing the volume and surface area. The panel heating rates for a constant lift coefficient can be decreased by adding dihedral to the lower wing surfaces. The hypersonic wing with a blunt leading edge and with dihedral has been the subject of many investigations. (See refs. 1 to 6.) In the majority of these investigations the size of the model prevents detailed instrumentation on the leading edges and permits only limited spanwise and chordwise instrumentation. It is the purpose of this investigation to determine detailed heat-transfer and pressure distribution and correlations with existing theories on wings with a planform sweep of  $70^\circ$  and with  $0^\circ$  and  $24.3^\circ$  dihedral. Both configurations were tested with pointed and blunted apexes to determine the magnitude and extent of nose blunting on local heat-transfer coefficients. The range of the angle of attack of the wing planform is from  $-45^\circ$  to  $45^\circ$  at Mach numbers 3.51 and 4.65. The Reynolds number per foot is varied from  $2.9 \times 10^6$  to  $4.1 \times 10^6$ , and the maximum Reynolds number based on center-line chord is  $7 \times 10^6$ .

## SYMBOLS

$a_{x=0}$	speed of sound along stagnation line of infinite swept cylinder, ft/sec
$C_p$	pressure coefficient, $\frac{p - p_\infty}{q_\infty}$
$c$	specific heat of model skin, Btu/lb- $^\circ$ R
$D$	diameter of cylindrical leading edge, in.
$h$	heat-transfer coefficient, Btu/(sec)(sq ft)( $^\circ$ R)
$M$	free-stream Mach number
$M_n$	normal Mach number component
$N_{St}$	Stanton number
$p$	pressure, lb/sq ft
$P_{t,nom}$	nominal free-stream stagnation pressure, lb/sq ft
$P_{t,2}$	stagnation pressure behind normal shock, lb/sq ft

$P_{x=0}$	pressure along stagnation line of cylindrical leading edge, lb/sq ft
$q$	dynamic pressure, lb/sq ft
$R$	free-stream Reynolds number per foot
$r$	wing leading-edge radius, in.
$s'$	length of wing leading edge of sharp-nose models, 21.28 in.
$T_e$	measured wall equilibrium temperature, °R
$T_t$	stagnation temperature, °R
$T_w$	wall temperature, °R
$t$	time, sec
$v_l$	local velocity, ft/sec
$w$	weight of model skin per unit area, lb/sq ft
$x, s, z$	coordinates of model relative to plane perpendicular to leading edge (fig. 1), in.
$y', z'$	coordinates of model measured in plane perpendicular to ridge line, in.
$\alpha$	angle of attack of ridge line (fig. 19), deg
$\alpha'$	angle of attack of wing planform, deg
$\alpha_{eff}$	effective angle of attack of windward wing panel, deg
$\alpha_{e_e}$	angle of attack at which effective sweep of wing leading edge and ridge line are equal, deg
$\Gamma$	dihedral angle measured in plane perpendicular to ridge line, deg
$\gamma$	ratio of specific heats, 1.4
$\delta$	angle between normal Mach number component and dihedral surface measured in plane perpendicular to wing leading edge, deg
$\epsilon_e$	angle between wing leading edge and free-stream velocity vector, complement of $\Lambda_e$ , deg
$\epsilon_n$	angle between ridge line and plane containing axes of wing cylindrical leading edges, deg

$\epsilon_0$	angle between leading edge and ridge line of wing, deg
$\epsilon_p$	planform semiapex angle, deg
$\Lambda_e$	effective sweep of leading edge, complement of $\epsilon_e$ , deg
$\xi$	angle between ridge line and intersection line of lower wing panel with plane of effective angle of attack (fig. 19(a)), deg
$\Phi$	local surface slope in plane perpendicular to wing leading edge, deg
$\Phi_{stag}$	location of stagnation line on wing leading edge in terms of $\Phi$ , deg
$\psi'$	local surface slope in plane perpendicular to ridge line, deg
Subscripts:	
$l$	local conditions
$t$	stagnation
$\infty$	free stream
$0,1,2,3,\dots,n$	time sequence

#### DESCRIPTION OF MODEL AND INSTRUMENTATION

The models used in this investigation and shown in figure 1 have a planform semiapex angle of  $20^\circ$ , hemicylindrical leading edges, and dihedral angles of  $0^\circ$  and  $24.3^\circ$  (dihedral was added to the lower surface only). Each model was tested with two apex configurations to determine the effect of nose bluntness. In the planform view one configuration was pointed, and the other configuration had a nose radius of 0.5 inch (equal to the radius of the hemicylindrical leading edge). All models were constructed of 0.030-inch inconel with a minimum of internal structure and were supported by a sting at the model base. Relative to the vertical plane of symmetry, the models were instrumented with iron-constantan thermocouples on one-half of the model (see fig. 1 for detail of thermocouple installation) and with static-pressure orifices of 0.030-inch inside diameter on the other half. This instrumentation was located in planes normal to the leading edge, except the pressure orifices along the top and bottom center lines which are displaced to prevent conduction effects to the heat-transfer measurements. The panel sections were reinforced with balsa wood to prevent deflection of the flat surfaces from aerodynamic loads. In order that internal conduction and convection be minimized, the balsa was relieved a

distance of 0.5 inch from each thermocouple and the model interior was vented to base pressure. Photographs illustrating the model installation in the tunnel test section are shown in figure 2. A complete listing of the instrumentation locations is presented in table I.

The thermocouple output was recorded on a multichannel sequential analog digital converter discussed in reference 7. The pressures were measured by electrical transducers, and each electrical output was recorded on digital self-balancing potentiometers. The tunnel free-stream static and stagnation pressures were measured on precision mercury manometers. The test-section stagnation temperature was measured with probes mounted at the model base, as shown in figure 2.

### APPARATUS AND TEST CONDITIONS

This investigation was conducted in the high Mach number test section of the Langley Unitary Plan wind tunnel described in reference 8. This variable-pressure continuous-flow tunnel has an asymmetrical sliding-block nozzle that permits a continuous variation in the test-section Mach number from 2.3 to 4.65. The deviation in Mach number in the entire 4- by 4-foot test section for Mach numbers of 3.51 and 4.65 is  $\pm 0.05$ . Heat-transfer and pressure measurements were obtained for the following test conditions:

Configuration	Test	Angle of attack, $\alpha'$ , deg (a)	Mach number	Reynolds number (nominal)
1 and 2	Static pressure and heat transfer	0, 7.5, 15, 22.5, 30, 37.5, and 45	3.51	$4.0 \times 10^6$ and $2.9 \times 10^6$
1 and 2	Static pressure and heat transfer	0, 7.5, 15, 22.5, 30, 37.5, and 45	4.65	$4.1 \times 10^6$ and $2.9 \times 10^6$
3 and 4	Static pressure	0, $\pm 7.5$ , $\pm 15$ , $\pm 22.5$ , $\pm 30$ , $\pm 37.5$ , and $\pm 45$	3.51	$4.0 \times 10^6$ and $2.9 \times 10^6$
3 and 4	Static pressure	0, $\pm 7.5$ , $\pm 15$ , $\pm 22.5$ , $\pm 30$ , $\pm 37.5$ , and $\pm 45$	4.65	$4.1 \times 10^6$ and $2.9 \times 10^6$
3	Heat transfer	0, $\pm 7.5$ , $\pm 15$ , $\pm 22.5$ , $\pm 30$ , $\pm 37.5$ , and $\pm 45$	3.51	$4.0 \times 10^6$
3	Heat transfer	0, $\pm 7.5$ , $\pm 15$ , $\pm 22.5$ , $\pm 30$ , 37.5, and 45	3.51	$2.9 \times 10^6$
3	Heat transfer	0, 7.5, 15, 22.5, 30, 37.5, and 45	4.65	$4.1 \times 10^6$
3	Heat transfer	0, 7.5, $\pm 15$ , 22.5, 30, 37.5, and $\pm 45$	4.65	$2.9 \times 10^6$
4	Heat transfer	0, $\pm 7.5$ , $\pm 15$ , $\pm 22.5$ , $\pm 30$ , $\pm 37.5$ , and $\pm 45$	3.51	$4.0 \times 10^6$ and $2.9 \times 10^6$
4	Heat transfer	0, $\pm 7.5$ , $\pm 15$ , $\pm 22.5$ , $\pm 30$ , $\pm 37.5$ , and $\pm 45$	4.65	$4.1 \times 10^6$ and $2.9 \times 10^6$

<sup>a</sup>The negative range of  $\alpha'$  was obtained by rolling the models 180°.

## METHOD OF HEAT-TRANSFER-DATA REDUCTION

The heat-transfer coefficients were obtained from transient skin-temperature measurements resulting from a stepwise increase in stagnation temperature. (See ref. 7.) The following relation, which assumes constant temperature through the skin, negligible lateral heat flow, negligible heat flow to the model interior, and no heat losses due to radiation, was used:

$$h = \frac{wc \frac{dT_w}{dt}}{T_e - T_w}$$

This equation can be integrated and written in the following form for complete machine calculation:

$$h = \frac{wc(T_{w,n} - T_{w,0})}{\frac{T_e}{T_t} \int T_t dt - \int T_w dt}$$

The integrals are evaluated over increments of 0.5 second, according to the trapezoidal rule

$$\int T dt = \Delta t \left( \frac{1}{2} T_0 + \frac{1}{2} T_n + T_1 + T_2 \dots + T_{n-1} \right)$$

and the ratio  $T_e/T_t$  is experimentally determined.

The magnitude of the lateral heat flow for a thin-skin model as discussed in reference 9 is negligible. The heat flow by radiation is dependent on the term  $(T_w^4 - T_a^4)$ , where  $T_a$  is the tunnel-wall temperature, and this term is negligible.

### ACCURACY

The accuracy of the temperature measurements, including recorder resolution, thermocouple-wire calibration, and cold junctions, is  $\pm 2^\circ$  F; however, this error occurs in temperature level rather than in random temperature fluctuations. A temperature error of  $\pm 2^\circ$  F could result in ratios of wall equilibrium temperature to stagnation temperature  $T_e/T_t$  greater than 1 in stagnation regions of the model. Also, as discussed in reference 9, in regions of low heat transfer ( $h < 0.001$ ) the ratio  $T_e/T_t$  may be questionable because the wall temperature may not have reached equilibrium from the preceding test point.



An estimation of the accuracy of heat-transfer measurements in the Langley Unitary Plan wind tunnel has been determined by the repeatability of data in the tests discussed in reference 9. The accuracy is dependent on the magnitude of the heat-transfer coefficient. For  $h > 0.0150$ , the accuracy is within 10 percent; for  $0.0010 < h < 0.0150$ , within 15 percent; for  $h < 0.0010$ , within 20 percent. Although  $h < 0.0010$  is within the accuracy of data reduction, no significance is attached to the magnitude of  $h$ , other than to indicate the regions of low heat transfer.

The accuracy of the precision manometers is within 0.5 pound per square foot. Therefore, the accuracy of the system is limited to that of the electrical transducer, which is 0.5 percent of the full-scale deflection. The error in the pressure coefficient resulting from the inaccuracy of the electrical transducer depends on  $M$  and  $R$  as the error varies from 0.0135 at  $M = 3.51$  and  $R = 4 \times 10^6$  to 0.0288 at  $M = 4.65$  and  $R = 2.9 \times 10^6$ .

### THEORY

The theoretical pressure distributions around the cylindrical wing leading edges were calculated by two methods. Both methods assume that the stagnation-line pressure corresponds to Newtonian flow, as defined in the following relation:

$$\frac{p_{x=0}}{p_{t,2}} = \cos^2 \Lambda_e + \frac{p_\infty}{p_{t,2}} \sin^2 \Lambda_e \quad (1)$$

which is analogous to the product  $\left(\frac{p_{t,2}}{p_\infty}\right)_{M_n} \left(\frac{p_\infty}{p_{t,2}}\right)_{M_\infty}$ , where  $(p_\infty)_{M_n} = (p_\infty)_{M_\infty}$ ,

as presented in reference 4.

One method of defining the local pressure distribution on the leading edge uses a modified Newtonian theory based on the normal Mach number component, and the second method uses Bernoulli's compressible equation based on the assumption that the surface velocity component is a linear function of the surface length. The expression for the modified Newtonian theory is simply

$$C_p = C_{p,max} \cos^2 \phi$$

where  $C_{p,max}$  is the pressure coefficient along the leading edge and can be expressed as

$$C_{p,max} = \frac{\frac{p_{x=0}}{p_{t,2}} - \frac{p_{\infty}}{p_{t,2}}}{\frac{q_{\infty}}{p_{t,2}}} \quad (2)$$

The second theoretical approximation using the assumption that  $v_z = 2.13 \left( \frac{a_{x=0}}{D} \right) x$ , as discussed in reference 10, can be written

$$C_p = \frac{\left( \frac{p}{p_{x=0}} \frac{p_{x=0}}{p_{t,2}} \right) - \frac{p_{\infty}}{p_{t,2}}}{\frac{q_{\infty}}{p_{t,2}}} \quad (3)$$

where

$$\frac{p}{p_{x=0}} = \left[ 1 - \frac{\gamma - 1}{2} \left( 2.13 \frac{x}{D} \right)^2 \right]^{\gamma/\gamma-1}$$

Equations (1) to (3) are valid approximations only within the angle-of-attack range for which the wing geometrical leading edge acts aerodynamically as a leading edge. It has been shown in reference 11 that the stagnation line on wings incorporating dihedral shifts from the wing geometrical leading edge to the ridge line at angles of attack for which the effective angle of sweep of the ridge line is less than the effective angle of sweep for the geometric wing leading edge. The wing leading edge in the aerodynamic sense then becomes a trailing edge. This shift of stagnation line from wing leading edge to ridge line occurs at approximately the angle of attack  $\alpha_{\epsilon_e}$  at which the angle of sweep of the ridge line is equal to the effective angle of sweep of the wing leading edges. This angle is defined as follows:

$$\alpha_{\epsilon_e} = \tan^{-1} \frac{1 - \cos \epsilon_0}{\sin \epsilon_0 \sin \Gamma} \quad (4)$$

At angles of attack less than  $\alpha_{\epsilon_e}$  for the dihedral wings and at all angles of attack for the  $0^\circ$  dihedral wings, the position of the stagnation line with angle of attack was determined from the following expression, as developed in appendix A:

$$\cos \Phi_{\text{stag}} = \frac{\tan \epsilon_p}{\tan \epsilon_e} \quad (5)$$

If Newtonian theory is to be applied to the wing leading edges at angles of attack greater than  $\alpha_{\epsilon_e}$ , the local surface inclination must be known in a plane perpendicular to the ridge line. A transformation for calculating this inclination from the corresponding inclination on the cylindrical leading edge in a plane perpendicular to the wing leading edge is developed in appendix B. The resulting equation is:

$$C_p = C_{p,\text{max}}' \cos^2 \psi' \quad (6)$$

where  $C_{p,\text{max}}'$  is the pressure coefficient on the ridge line and

$$\psi' = \tan^{-1} \left( \frac{1}{\tan \Phi} \sqrt{\tan^2 \epsilon_n + \cos^2 \epsilon_p} \right) \quad (7)$$

Throughout the angle-of-attack range, the Newtonian theory can be used to predict pressures on the windward panels of bodies with dihedral by assuming that the plane surfaces are at an effective angle of attack so that

$$\sin \alpha_{\text{eff}} = \sin \alpha \cos \Gamma \quad (8)$$

as derived in appendix C.

It is to be noted that the definition and notation of the basic geometrical parameters used in the present analysis are in accordance with those presented in the symbols and in figure 1 of reference 11. The variations of the basic angles with angle of attack are presented in figure 3 of this report.

## RESULTS AND DISCUSSION

Schlieren photographs of the sharp-nose flat wing and of both the sharp- and blunt-nose dihedral wings are presented in figures 4, 5, and 6. The visible shocks occurring on the surface of the models through the range of angle of attack apparently emanate from the regions of the model where the model skin is attached to the supporting bulkheads. It is believed that these localized shocks had no effect on either the pressure or heat-transfer data greater than the data accuracy, except for the possibility of promoting boundary-layer transition.

The schlieren photographs of configuration 1 (fig. 4) show the shape of the nose shock in the vertical plane of symmetry at zero  $\alpha'$  to have some curvature in the nose region of the model, but it approaches a straight line with increasing  $s/s'$ . The straight portion of the shock moves toward the nose region of the model with increasing  $\alpha'$ . It is interesting to note that the angle between the flat surface of the model and the shock wave decreases with increasing angle of attack for  $\alpha' \leq 15^\circ$ . For greater angles of attack, this angle remains approximately constant and equal to  $10^\circ$  and  $7^\circ$  for  $M = 3.51$  and  $4.65$ , respectively. The corresponding angle between a two-dimensional oblique shock and a wedge for wedge angles less than or approximately equal to  $15^\circ$  also decreases with increasing angle of attack; however, for greater wedge angles this angle increases with wedge angle to the point of shock detachment.

The shock formations shown in the schlieren photographs obtained for configuration 3 (fig. 5) are very similar throughout the negative  $\alpha'$  range to the results obtained for configuration 1. The trend of the variation of the angle between the shock wave and the model ridge line with positive angles of attack is also the same as was obtained for configuration 1. The magnitude of the limiting value of this angle for configuration 3 at Mach numbers of  $3.51$  and  $4.65$  is approximately  $6^\circ$  and  $4^\circ$ , respectively. Schlieren photographs showing the shock formation for the planform of configuration 3 are presented in figure 5(c) for a range of angle of attack from  $0^\circ$  to  $20^\circ$ . Throughout this range of  $\alpha'$  the planform shock formation remains approximately constant.

The effect of nose bluntness on the shock formation in the vertical plane of symmetry of configuration 4 as shown in figure 6 is confined to the immediate nose region of the model throughout the positive range of angle of attack.

Complete lists of the pressure and heat-transfer data obtained for all models throughout the range of test variables are presented in tables II to IX.

### Pressures

The effect of angle of attack on the pressure-coefficient distribution normal to the wing leading edge at three spanwise locations of configuration 1 is shown in figure 7. The selection of the parameter  $x/D$  as the ordinate renders geometric similarity at the three spanwise stations for a constant  $x/D$  to the instrumentation located on the cylindrical leading edge, that is, for  $-0.785 \leq x/D \leq 0.785$ . In order to clarify the discussion of data beyond these limits, the experimental data at the wing center line are identified by the solid symbols and at  $\epsilon_p/2$  by the half-solid symbols. Theoretical pressure distributions presented in figure 7(a) consist of both the Newtonian equation (eq. (2)) and the compressible Bernoulli equation (eq. (3)). The location of the stagnation line on the cylindrical leading edge was determined from equation (5). The data presented in figure 7(a) are for a Mach number of  $3.51$ , a Reynolds number of  $4.00 \times 10^6$ , and angles of attack  $\alpha'$  from  $0^\circ$  to  $45^\circ$ .

Prior to any comparison of experimental results with theoretical predictions, the following general observations should be noted:

(1) Theory predicts that for a wing with  $0^\circ$  dihedral the stagnation line (for the angle-of-attack range of this investigation) will remain on the leading edge.

(2) For a constant  $x/D$  there is a variation of the experimental values of  $C_p$  with  $s/s'$ .

Comparison of the two theoretical curves with the experimental data shows that the maximum theoretical value of  $C_p$  is within the deviation of the experimental data with  $s/s'$  throughout the  $\alpha'$  range. The pressure distribution about the leading edge from the aerodynamic stagnation line through an expansion angle of  $60^\circ$  is predicted by both theories. At larger expansion angles,  $C_p$  becomes negative and generally is only in agreement with the compressible Bernoulli equation. It is interesting to note that the compressible Bernoulli equation is in good agreement with the experimental data from the stagnation line through an expansion of  $90^\circ$  leeward throughout the angle-of-attack range at an  $s/s'$  of 0.442. For  $\alpha'$  from  $0^\circ$  to  $22.5^\circ$  there is a good correlation between the experimentally measured and the theoretically predicted location of the stagnation line. The anticipated expansion on the windward side of the theoretical stagnation line does not occur for  $\alpha' > 30^\circ$ ; however, the agreement of theory with experimental data on the leeward side of the stagnation line indicates that the location of the stagnation line is in the vicinity of the theoretical location. Similar agreement of experimental data with Bernoulli's equation for  $M = 4.65$  is shown in figure 7(b).

The effect of angle of attack on the pressure-coefficient distribution normal to the wing leading edge of configuration 3 is shown in figure 8 at three spanwise locations. The data presented in figure 8(a) are for  $M = 3.51$ ,  $R = 4.00 \times 10^6$ , and  $-45^\circ \leq \alpha' \leq 45^\circ$ . For angles of attack  $\alpha'$  from  $-45^\circ$  to  $15^\circ$ , theory predicts that the stagnation line is located on the cylindrical leading edges. The stagnation-line location is also indicated by the experimental data as a result of the good agreement of the data with the predicted pressure distribution leeward of the theoretical stagnation line throughout the range of  $\alpha'$  from  $-45^\circ$  to  $15^\circ$ . For angles of attack greater than  $\alpha_{\epsilon_e}$  ( $\alpha_{\epsilon_e} = 25.2^\circ$ , which corresponds to  $\alpha' = 15.7^\circ$  for this configuration, as determined from eq. (4)), the angle of sweep of the ridge line is less than the angle of sweep of the wing leading edge; thus, the stagnation-line location should shift from the wing leading edge to the ridge line. This anticipated stagnation-line shift is indicated by the experimental data for  $\alpha'$  greater than  $15^\circ$ . For  $\alpha'$  greater than  $15^\circ$ , the wing leading edge becomes a trailing edge, and the assumption of a linear velocity in the compressible Bernoulli equation is no longer valid. Application of the theory at  $\alpha' = 22.5^\circ$  does not predict the maximum measured  $C_p$  but does predict the  $C_p$  distribution from the theoretical stagnation-line location through an expansion angle of  $90^\circ$ . Application of the Newtonian theory for  $\alpha > \alpha_{\epsilon_e}$  to these trailing edges necessitates measuring the local flow deflection in a plane normal to the ridge line as outlined in appendix B. The maximum  $C_p$  in equation (6) is assumed to be the measured  $C_p$  at  $s/s' = 0.113$  on the ridge line. The agreement of this

method of prediction with experimental data for  $22.5^\circ \leq \alpha' \leq 45^\circ$  is illustrated in figure 8(a), the best agreement being obtained at the highest angles of attack. A more detailed comparison of the two theories with experiment is shown in the insert of figure 8(a). Similar distributions with approximately the same agreement between experiment and theory are shown in figure 8(b) for  $M = 4.65$ .

Pressure measurements obtained along the bottom center line (windward side at  $\alpha > 0^\circ$ ) of configurations 1 and 3 at  $s/s' = 0.276$  and  $0.652$  are presented in figure 9 at Mach numbers of 3.51 and 4.65 and angles of attack from  $0^\circ$  to  $45^\circ$ . The experimental data are expressed in terms of the ratio  $p_1/p_\infty$  as a function of the correlation parameter  $M \sin \alpha$  suggested by both hypersonic oblique-shock theory and Newtonian theory, as discussed in reference 12. This parameter correlates data obtained at various free-stream Mach numbers. Both two-dimensional oblique-shock theory and Newtonian theories are presented in the figure for reference. For the wing with  $0^\circ$  dihedral (fig. 9(a)), good agreement was obtained between experimental data and the two-dimensional oblique-shock theory, except at the maximum  $\alpha$  for which a large longitudinal pressure gradient occurred in the experimental data. For the wing incorporating dihedral (fig. 9(b)), good agreement was obtained with the Newtonian theory for angles of attack less than  $\alpha_{\epsilon_e}$ .

The experimental data obtained on the windward wing panel at  $\epsilon_p/2$  of configuration 3 is shown in figure 10. Good correlation of the experimental data was obtained by using the parameter  $M \sin \alpha_{\text{eff}}$ , where  $\alpha_{\text{eff}}$  is the effective angle of attack of the wing panel defined by equation (8). The experimental data are between the two-dimensional and Newtonian predicted values.

The effect of nose bluntness on the measured pressure-coefficient distributions obtained along the center line and wing leading edges of configurations 1 and 2 is presented in figure 11 at angles of attack from  $0^\circ$  to  $45^\circ$  and for Mach numbers 3.51 and 4.65. At both Mach numbers, the nose effect on the wing leading edge extends downstream to approximately  $s/s' = 0.3$  (approximately 4.5 nose diameters) throughout the angle-of-attack range. Although the extent of this nose effect (a pressure relief for the blunt body) does not decrease with increasing  $\alpha'$ , it is believed that these low pressure coefficients within this range of  $s/s'$  resulted from the overexpansion occurring at the juncture of the nose and leading edge. There is no apparent effect of nose bluntness on the measured pressure distribution on the bottom center line for a Mach number of 3.51 at angles of attack from  $0^\circ$  and  $7.5^\circ$ . However, at angles of attack equal to and greater than  $15^\circ$  an adverse pressure gradient occurs on both configurations at  $0.2 \lesssim s/s' \lesssim 0.4$ .

The effect of nose bluntness on the configurations having dihedral is shown in figure 12 for a range of angle of attack from  $-45^\circ$  to  $45^\circ$ . As would be expected, the measured distributions on the windward wing-panel center line are very similar throughout the negative  $\alpha'$  range (flat surface windward) to the results obtained for configurations 1 and 2. On the wing leading edge, however, there is apparently a much larger effect of nose bluntness for  $\alpha'$  approaching  $-45^\circ$  at  $s/s' < 0.4$  on the dihedral bodies as compared with the

flat bodies. This larger effect is attributed to the fact that as the angle of attack is increased, the geometric wing stagnation line ( $\Phi = 0^\circ$ ) approaches the separation line which occurs on the leeward surfaces; therefore, the pressures in this region become more sensitive to the afterbody shape, in particular, at the nose region of the model. There is no apparent effect of bluntness on the pressure distributions for  $s/s' > 0.4$  throughout the complete negative range of angle of attack; this trend is the same as that obtained for the flat wings. This trend can be explained by results obtained from oil-flow photographs of configuration 3 (which were not suitable for reproduction) in which the indicated separation line at an angle of attack of  $45^\circ$  was initially visible on the leeward wing panel at the nose region of the model and extended to the wing leading edge at larger values of  $s/s'$ . The exact location where this separation line initially intersected the leading edge could not be determined from these photographs. For angles of attack from  $0^\circ$  to  $45^\circ$ , the extent of the bluntness effect for the models with dihedral is also approximately the same as for the flat models; however, the trend of this effect is reversed for the wing leading edge for  $\alpha' \geq 15^\circ$ . This reversed effect of nose bluntness, consisting of a decrease in the  $C_p$  distribution, is apparently associated with the shift of the stagnation line from the wing leading edge to the ridge line of the models with dihedral.

#### Heat Transfer

The occurrence of natural boundary-layer transition on all configurations renders a complex distribution of the experimental heat-transfer coefficients and limits the application of theoretical predictions to these measured distributions. The extent of the wing surface affected by transitional and turbulent flow was determined from contour plots of the experimental heat-transfer coefficients, as illustrated in figure 13. In order that the complete heat-transfer distributions over the model be presented, the drawings in figure 13 were constructed by unfolding the model surface area from the vertical plane of symmetry about  $\Phi = 0^\circ$ . For configuration 1 at  $M = 3.51$ ,  $R \approx 4.1 \times 10^6$ , and  $\alpha' = 0^\circ$  (fig. 13(a)), the area affected by boundary-layer transition is confined to the upper and lower wing panels with no apparent effects on the wing leading edge. Although not presented in the figure, similar results were noted at angles of attack of  $7.5^\circ$  and  $15^\circ$ . At angles of attack of  $22.5^\circ$  and  $37.5^\circ$  the transition region extends to the leading edge, initially indicated by rapid increase in heating rates at  $s/s' = 0.442$  for  $\alpha' = 22.5^\circ$ . The area of the leading edge affected by transition increases with increasing angle of attack through  $\alpha' = 37.5^\circ$ . At  $\alpha' = 45^\circ$  no apparent regions of transition exist. For the same free-stream variables, similar results were noted for configuration 3, with one major exception: the experimental data (fig. 13(b)) indicate that the wing leading edges are influenced by turbulence at an angle of attack of  $15^\circ$ . Configuration 3 was also apparently free of turbulent flow at an angle of attack of  $45^\circ$ .

Because of the arbitrary location of transition, the major portion of the discussion pertaining to the heat-transfer data is concerned with the measured heating rates on the wing leading edges having a laminar boundary layer (as

determined from the contour plots). A complete listing of the measurements obtained from all four configurations are presented in tables VI to IX.

The effect of angle of attack on the distribution of heat-transfer coefficient normal to the leading edge of configuration 1 is shown in figure 14 at three spanwise stations for angles of attack from  $0^\circ$  to  $45^\circ$ . The laminar swept-cylinder theory of reference 10 is included in the figure for comparison with the leading-edge stations having a laminar boundary layer. For angles of attack from  $0^\circ$  to  $15^\circ$  at  $M = 3.51$  and  $R = 2.90 \times 10^6$  (fig. 14(a)), the experimental heat-transfer coefficients on the wing leading edge at all three spanwise stations are in fair agreement with the theoretical distribution. For angles of attack from  $22.5^\circ$  to  $37.5^\circ$ , only the experimental data at the most forward station ( $s/s' = 0.113$ ) have a laminar boundary layer and are in agreement with the swept-cylinder theory. At an angle of attack of  $45^\circ$ , the experimental data at all three stations are overpredicted by the theoretical distributions.

The heat-transfer-coefficient distribution about the wing leading edge of configuration 1 for a Mach number of 3.51 and a Reynolds number of  $4.00 \times 10^6$  is presented in figure 14(b). The data obtained at a Mach number of 4.65 and at Reynolds numbers of  $2.90 \times 10^6$  and  $4.10 \times 10^6$  are presented in figures 14(c) and 14(d). The heat-transfer distributions presented in these figures for this range of variable are similar to that presented for  $M = 3.51$  in figure 14.

The experimental heat-transfer data obtained for configuration 3 at a Mach number of 3.51 and at Reynolds numbers  $2.90 \times 10^6$  and  $4.00 \times 10^6$  are presented in figures 15(a) and 15(b). Measurements were obtained at the high Reynolds number through an angle-of-attack range from  $-45^\circ$  to  $45^\circ$ . The laminar swept-cylinder theory (ref. 7) is included in figure 15 for comparison with leading-edge data throughout the angle-of-attack range where the theoretical stagnation line as determined from equation (5) lies on the wing leading edge. At the high Reynolds number (fig. 15(b)) for angles of attack from  $-45^\circ$  (flat surface windward) to  $7.5^\circ$ , the magnitude and distribution of the experimental heat-transfer data on the cylindrical leading edge are in fair agreement with theory and is very similar to the experimental data obtained for configuration 1 (fig. 14(b)). At angles of attack from  $15^\circ$  to  $37.5^\circ$ , the major portion of the data for the wing leading edge is affected by turbulence; however, at  $\alpha' = 15^\circ$  and  $22.5^\circ$ , the data at  $s/s' = 0.113$  are in fair agreement with the swept cylinder theory, even though the theoretical stagnation-line location at the latter angle of attack is on the ridge line. Because of the similarity of data obtained at the negative angles of attack for configurations 1 and 3 and because of the incompleteness of the data for negative angles of attack for configuration 3, only the experimental data obtained at angles of attack from  $0^\circ$  to  $45^\circ$  are presented in figure form for  $R = 2.90 \times 10^6$  at  $M = 3.51$  and for  $R = 2.90 \times 10^6$  and  $4.10 \times 10^6$  at  $M = 4.65$ . (See figs. 15(a), 15(c), and 15(d), respectively.) As shown in figure 15, the effect of the range of free-stream variables on the heating rates for the area unaffected by the turbulent boundary layer was predominantly to the magnitude of the heat-transfer rates with negligible effects to the  $h$  distribution.

The effect of nose bluntness on the distribution of heat-transfer coefficient on the flat wing is shown in figure 16 for Mach numbers of 3.51 and 4.65,



Reynolds numbers of  $4.00 \times 10^6$  and  $4.10 \times 10^6$ , and angles of attack from  $0^\circ$  to  $45^\circ$ . The circular data symbols correspond to the experimental data obtained at the wing leading-edge geometrical stagnation line and the square data symbols correspond to the data obtained at the windward wing-panel center line. At both Mach numbers, throughout the range of angle of attack, the data along the wing geometrical stagnation line indicate no apparent trend in nose effect greater than the accuracy of the experimental data. The increase in  $h$  with  $s/s'$  along the bottom center line for both configurations is attributed to boundary-layer transition and is apparently associated with the adverse pressure gradient located in the same region, as mentioned in the section entitled "Pressures." Similar results are shown in figure 17 for the models with dihedral.

The measured heat-transfer-coefficient distributions at three spanwise stations along the windward wing panel at  $\epsilon_p/2$  of configuration 3 are presented in figure 18 for a Mach number of 3.51, Reynolds numbers  $4.10 \times 10^6$  and  $2.90 \times 10^6$ , and angles of attack from  $0^\circ$  to  $45^\circ$ . An approximation of the measured  $h$  distribution is obtained with Van Driest turbulent flat-plate theory (ref. 13), using measured static pressures, a total pressure corresponding to that behind a two-dimensional oblique shock at the same angle as the shock inclination on the model (measured from schlieren photographs), and a Reynolds number based on the length from the mating line of the nose-body juncture. (See fig. 1.) The variation of  $h$  with angle of attack is generally approximated, but the magnitude of the measured and theoretical distributions indicates large discrepancies. These discrepancies are to be expected, however, since the selection of a location for the origin of the turbulent boundary layer was arbitrary and was assumed to remain constant throughout the angle-of-attack range.

#### CONCLUDING REMARKS

The results of pressure and heat-transfer measurements on  $70^\circ$  swept hyper-sonic wings with dihedral angles of  $0^\circ$  and  $24.3^\circ$  tested through an angle-of-attack range from  $-45^\circ$  to  $45^\circ$  at Mach numbers of 3.51 and 4.65 lead to the following concluding remarks:

1. For angles of attack where the stagnation line is on the leading edge, the pressures on the hemicylindrical leading edge of the wings with  $0^\circ$  and  $24.3^\circ$  dihedral were predicted through  $60^\circ$  of expansion by both the Newtonian and modified Bernoulli equations and by using normal Mach numbers.

2. For expansion angles from  $60^\circ$  to  $90^\circ$  on the model with  $0^\circ$  dihedral, the experimental leading-edge pressure coefficients were in good agreement with the compressible Bernoulli equation.

3. For angles of attack for which the stagnation line shifted from the wing leading edge to the ridge line on the wing with  $24.3^\circ$  dihedral, the pressure distributions on the wing leading edges (now trailing edges) were predicted by Newtonian flow using a local surface slope in a plane perpendicular to the ridge line.

4. The windward-panel center-line pressures for all the models were correlated for the Mach numbers and angle-of-attack range of this investigation by the parameter  $M \sin \alpha$ , where  $M$  is the free-stream Mach number and  $\alpha$  is the angle of attack of the ridge line. Pressures obtained off the center line of the windward panel of the body with  $24.3^\circ$  dihedral were correlated by the parameter  $M \sin \alpha_{\text{eff}}$ , where  $\alpha_{\text{eff}}$  is the effective angle of attack of the windward wing panel.

5. The windward center-line pressure distribution on the wing with  $0^\circ$  dihedral was in good agreement with two-dimensional oblique-shock theory.

6. The windward center-line pressure distributions for the wing with  $24.3^\circ$  dihedral are in good agreement with Newtonian flow for all angles of attack where the stagnation line is located on the wing leading edge.

7. The distribution of the heat-transfer coefficient on the leading edge of the wing with  $0^\circ$  dihedral, where the boundary-layer remained laminar, was in good agreement with laminar swept-cylinder theory for angles of attack from  $0^\circ$  to  $37.5^\circ$ . Good agreement was also obtained with swept-cylinder theory on the wing with  $24.3^\circ$  dihedral at angles of attack from  $-45^\circ$  to  $22.5^\circ$  on the portion of the wing where the boundary layer remained laminar. At an angle of attack of  $45^\circ$ , the heating rates on both wings were overpredicted by the swept-cylinder theory.

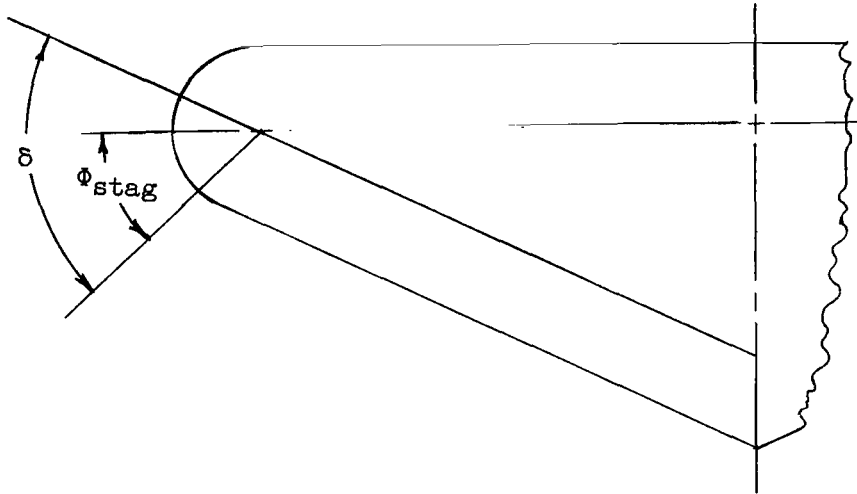
8. Throughout the range of variables of this investigation, there was no apparent trend in nose effect on the heat-transfer or pressure distribution at stations downstream of approximately 4.5 nose diameters.

Langley Research Center,  
National Aeronautics and Space Administration,  
Langley Station, Hampton, Va., March 25, 1964.

APPENDIX A

FLOW DEFLECTION ANGLE RELATIVE TO THE PLANE CONTAINING  
THE AXES OF THE WING LEADING EDGES

The angular stagnation-line shift  $\Phi_{\text{stag}}$  is illustrated in sketch (a), which is a sectional view perpendicular to the wing leading edge of a typical blunt wing incorporating dihedral.



Sketch (a)

These angles are further illustrated by the geometrical model presented in figure 19.

From the construction of the model in figure 19(b), it is readily seen that the angle  $adD'$  is a right angle. Hence,

$$\cos \Phi_{\text{stag}} = \frac{(ad)}{(aD')} = \frac{(Oa)\tan \epsilon_p}{(Oa)\tan \epsilon_e} = \frac{\tan \epsilon_p}{\tan \epsilon_e}$$

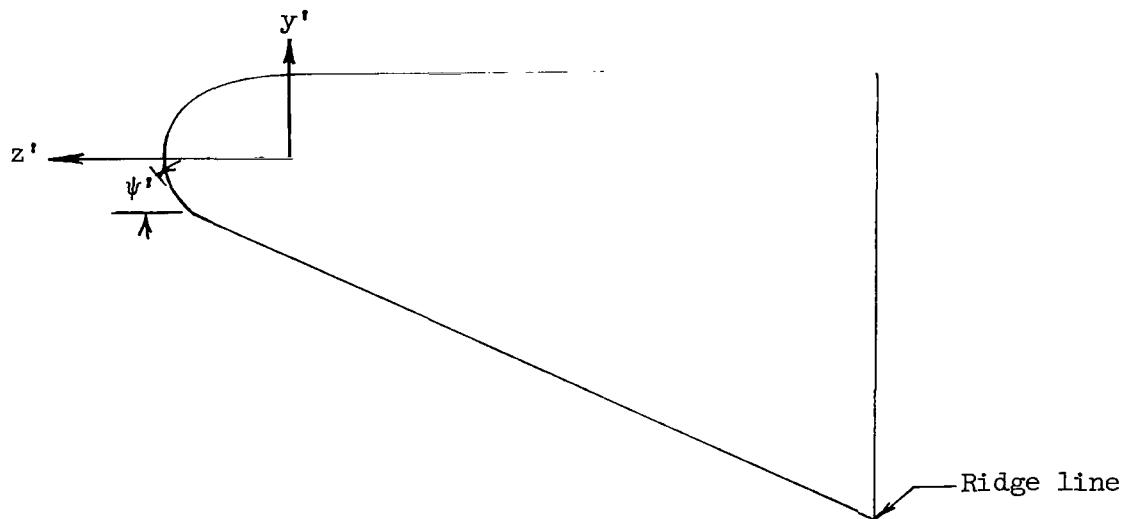
The stagnation-line shift in reference 11 is defined in terms of the angle  $\delta$ , which is measured relative to the plane of the surface with dihedral.

## APPENDIX B

### TRANSFORMATION OF SLOPE OF CYLINDRICAL LEADING-EDGE SURFACE OF BODIES WITH DIHEDRAL IN A PLANE NORMAL TO THE LEADING EDGE TO THE CORRESPONDING SLOPE IN A PLANE NORMAL TO THE RIDGE LINE

Calculation of pressure distribution from Newtonian flow based on the free-stream Mach number component normal to the ridge line necessitates definition of the leading-edge geometry in a plane normal to the ridge line.

A sectional view in a plane normal to the ridge line of a sweptback wing with dihedral and with cylindrical leading edges is shown in sketch (b).



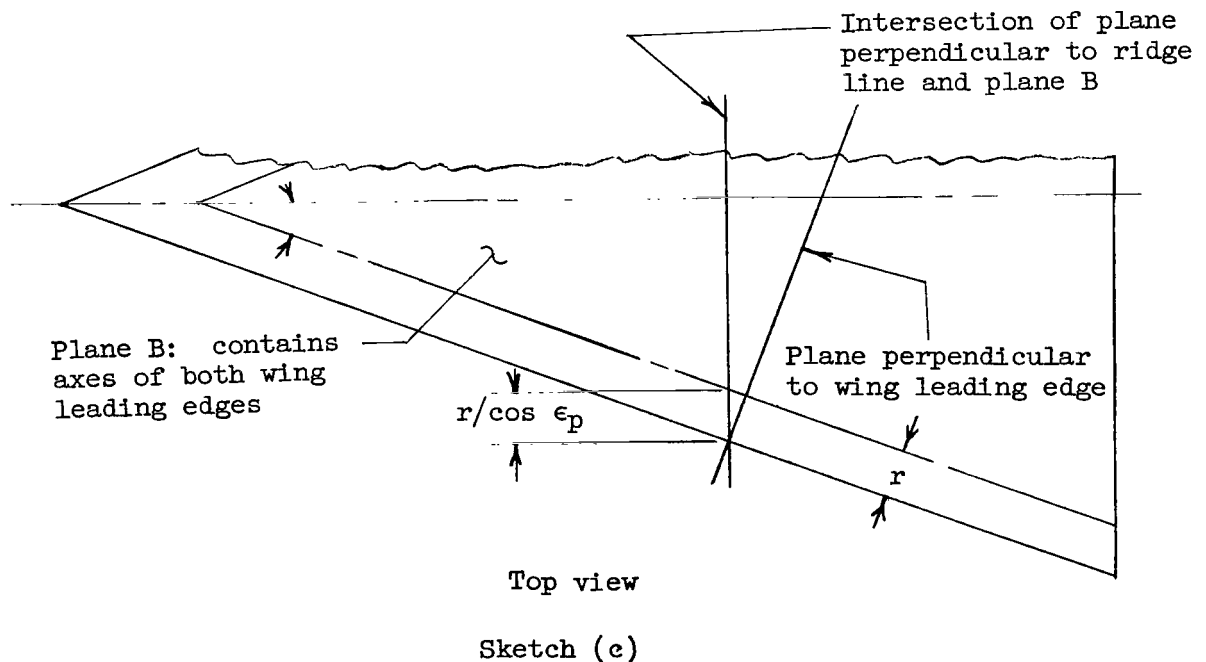
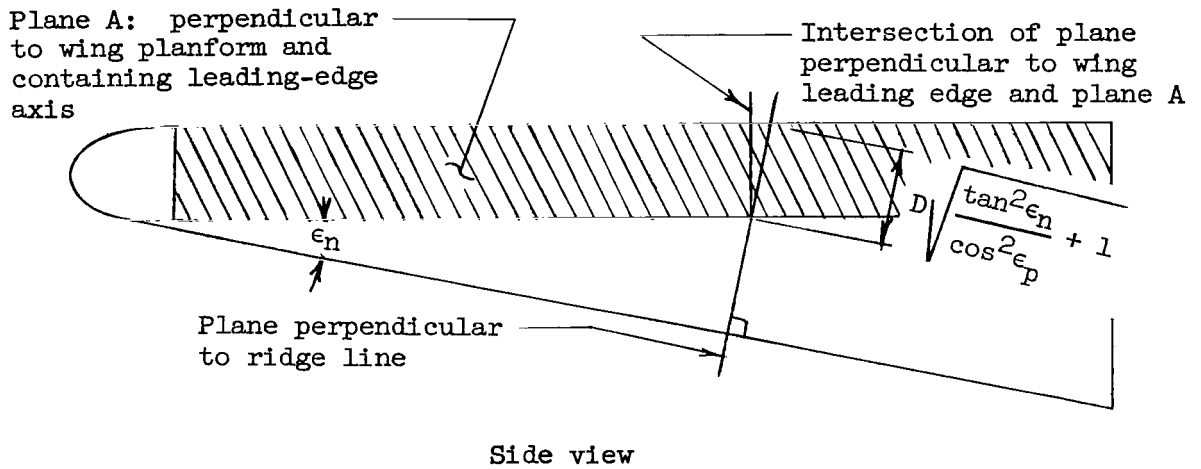
Sketch (b)

With the assumption that the stagnation line occurs at the ridge line and that the local flow governing the pressure distribution on the geometrical wing leading edge is in a plane perpendicular to the ridge line, the Newtonian theory can be expressed as:

$$C_p = C_{p,\max}' \cos^2 \psi' \quad (B1)$$

where  $C_{p,max}'$  is the pressure coefficient at the ridge line and  $\psi'$  is the surface inclination in a plane perpendicular to the ridge line.

In a plane perpendicular to the wing leading edge, the leading-edge surface is cylindrical with radius  $r$ . In a plane perpendicular to the ridge line, the projection of the cylindrical leading edge is an ellipse, as is illustrated in sketch (b). The intercepts  $y'$  and  $z'$  of the elliptical leading edge can be readily determined from the geometry presented in sketch (c).



Thus, for the  $y', z'$  coordinate system, the equation of the ellipse is:

$$\frac{(z')^2}{a^2} + \frac{(y')^2}{b^2} = 1 \quad (\text{B2})$$

where  $a$  and  $b$ , by utilization of sketch (c), can be written:

$$\left. \begin{aligned} a &= r \sec \epsilon_p \\ b &= r \sqrt{\frac{\tan^2 \epsilon_n}{\cos^2 \epsilon_p} + 1} \end{aligned} \right\} \quad (\text{B3})$$

Solving equation (B2) for  $y'$ , substituting the values of the constants  $a$  and  $b$  from equations (B3), and differentiating yield:

$$\frac{dy'}{dz'} = \left( \frac{z'}{\sqrt{r^2 \sec^2 \epsilon_p - (z')^2}} \right) \sqrt{\tan^2 \epsilon_n + \cos^2 \epsilon_p} \quad (\text{B4})$$

The right-hand side of equation (B4) can be transformed to the unprimed system using the transformation  $z' = z \sec \epsilon_p$ . Thus, equation (B4) becomes:

$$\frac{dy'}{dz'} = \left( \frac{z}{\sqrt{r^2 - z^2}} \right) \sqrt{\tan^2 \epsilon_n + \cos^2 \epsilon_p} \quad (\text{B5})$$

Substituting the expression  $z = r \cos \Phi$  into equation (B5) simplifies the equation so that:

$$\tan \psi' = \frac{dy'}{dz'} = \frac{1}{\tan \Phi} \sqrt{\tan^2 \epsilon_n + \cos^2 \epsilon_p} \quad (\text{B6})$$

## APPENDIX C

### EFFECTIVE ANGLE OF ATTACK

A geometrical model of a wing incorporating dihedral and illustrating the basic angles is shown in figure 19. It should be noted that this geometrical model differs from the experimental models in that the base of the experimental models is perpendicular to the axis of symmetry and to the plane of the leading edges, whereas the base of the geometrical model is in a plane perpendicular to the ridge line. The latter model simplifies the development for an expression of  $\alpha_{\text{eff}}$ .

From the law of cosines and the aid of figure 19(a), the effective angle of attack can be expressed as follows:

$$\begin{aligned} \cos \alpha_{\text{eff}} &= \frac{(OO')^2 + (OC)^2 - (O'C)^2}{2(OO')(OC)} \\ &= \frac{(OB)^2 \sec^2 \alpha + (OB)^2 \sec^2 \xi - (O'B)^2 \cos^2 \Gamma}{2(OB)^2 (\sec \alpha \sec \xi)} \end{aligned} \quad (C1)$$

$$\cos \alpha_{\text{eff}} = \frac{\sec^2 \alpha + \sec^2 \xi - \tan^2 \alpha \cos^2 \Gamma}{2 \sec \alpha \sec \xi} \quad (C2)$$

where  $\tan \alpha = \frac{O'B}{OB}$ .

The angle  $\xi$  in equation (C2) can be expressed in terms of  $\alpha$  and  $\Gamma$  from the following relation:

$$\sec \xi = \sqrt{1 + \tan^2 \xi} = \sqrt{1 + \tan^2 \alpha \sin^2 \Gamma}$$

thus, equation (C2) becomes:

$$\cos \alpha_{\text{eff}} = \frac{\sec^2 \alpha + (1 + \tan^2 \alpha \sin^2 \Gamma) - \tan^2 \alpha \cos^2 \Gamma}{2 \sec \alpha \sqrt{1 + \tan^2 \alpha \sin^2 \Gamma}} \quad (C3)$$

Substituting the following trigonometric identities,

$$\sec^2\alpha = 1 + \tan^2\alpha$$

and

$$\cos^2\Gamma = 1 - \sin^2\Gamma$$

into equation (C3) and simplifying yield:

$$\cos \alpha_{\text{eff}} = \cos \alpha \sqrt{1 + \tan^2\alpha \sin^2\Gamma} \quad (\text{C4})$$

Equation (C4) can be further simplified by expressing  $\cos \alpha_{\text{eff}}$  in terms of  $\sin \alpha_{\text{eff}}$  as follows:

$$\sin \alpha_{\text{eff}} = \sqrt{1 - \cos^2\alpha_{\text{eff}}} = \sqrt{1 - \cos^2\alpha(1 + \tan^2\alpha \sin^2\Gamma)}$$

or

$$\sin \alpha_{\text{eff}} = \sin \alpha \cos \Gamma \quad (\text{C5})$$



## REFERENCES

1. Stainback, P. Calvin: Preliminary Heat-Transfer Measurements on a Hypersonic Glide Configuration Having  $79.5^\circ$  Sweepback and  $45^\circ$  Dihedral at a Mach Number of 4.95. NASA TM X-247, 1960.
2. Stainback, P. Calvin: Heat-Transfer Measurements at a Mach Number of 4.95 on Two  $60^\circ$  Swept Delta Wings With Blunt Leading Edges and Dihedral Angles of  $0^\circ$  and  $45^\circ$ . NASA TN D-549, 1961.
3. Gunn, Charles R.: Heat-Transfer Measurements on the Apexes of Two  $60^\circ$  Sweptback Delta Wings (Panel Semiapex Angle of  $30^\circ$ ) Having  $0^\circ$  and  $45^\circ$  Dihedral at a Mach Number of 4.95. NASA TN D-550, 1961.
4. Gunn, Charles R.: Pressure Measurements on the Apexes of Two  $60^\circ$  Sweptback Delta Wings (Panel Semiapex Angle of  $30^\circ$ ) Having  $0^\circ$  and  $45^\circ$  Dihedral at a Mach Number of 4.95. NASA TM X-421, 1961.
5. Dunavant, James C.: Investigation of Heat Transfer and Pressures on Highly Swept Flat and Dihedraled Delta Wings at Mach Numbers of 6.8 and 9.6 and Angles of Attack to  $90^\circ$ . NASA TM X-688, 1962.
6. Seidman, Mitchell: Pressure Distribution for Blunted Delta Wings at Mach 21. Tech. Rep. 205 (Contract No. AF 33(616)-6692), Gen. Appl. Sci. Labs., Inc., Jan. 6, 1961.
7. Burbank, Paige B., and Hodge, B. Leon: Distribution of Heat Transfer on a  $10^\circ$  Cone at Angles of Attack From  $0^\circ$  to  $15^\circ$  for Mach Numbers of 2.49 to 4.65 and a Solution to the Heat-Transfer Equation That Permits Complete Machine Calculations. NASA MEMO 6-4-59L, 1959.
8. Anon: Manual for Users of the Unitary Plan Wind Tunnel Facilities of the National Advisory Committee for Aeronautics. NACA, 1956.
9. Taylor, Nancy L., Hodge, Ward F., and Burbank, Paige B.: Heat-Transfer and Pressure Measurements of a  $1/7$ -Scale Model of a Mercury Capsule at Angles of Attack From  $0^\circ$  to  $\pm 20^\circ$  at Mach Numbers of 3.50 and 4.44. NASA TM X-522, 1961.
10. Goodwin, Glen, Creager, Marcus O., and Winkler, Ernest L.: Investigation of Local Heat-Transfer and Pressure Drag Characteristics of a Yawed Circular Cylinder at Supersonic Speeds. NACA RM A55H31, 1956.
11. Cooper, Morton, and Stainback, P. Calvin: Influence of Large Positive Dihedral on Heat Transfer to Leading Edges of Highly Swept Wings at Very High Mach Numbers. NASA MEMO 3-7-59L, 1959.
12. Bertram, Mitchel H., and Henderson, Arthur, Jr.: Recent Hypersonic Studies of Wings and Bodies. ARS Jour., vol. 31, no. 8, Aug. 1961, pp. 1129-1139.

13. Van Driest, E. R.: The Problem of Aerodynamic Heating. *Aero. Eng. Rev.*, vol. 15, no. 10, Oct. 1956, pp. 26-41.





TABLE II.- TABULATION OF PRESSURE MEASUREMENTS FOR CONFIGURATION 1

(a) M = 3.51; P<sub>t, nom</sub> = 5,040 lb/sq ft

Orifice	C <sub>p</sub> at α of -						
	0°	7.5°	15.0°	22.5°	30.0°	37.5°	45.0°
	T <sub>t</sub> = 575° R; P <sub>t</sub> = 5,041.0 <sup>a</sup>	T <sub>t</sub> = 581° R; P <sub>t</sub> = 5,050.0 <sup>a</sup>	T <sub>t</sub> = 585° R; P <sub>t</sub> = 5,037.0 <sup>a</sup>	T <sub>t</sub> = 583° R; P <sub>t</sub> = 5,052.0 <sup>a</sup>	T <sub>t</sub> = 584° R; P <sub>t</sub> = 5,044.0 <sup>a</sup>	T <sub>t</sub> = 584° R; P <sub>t</sub> = 5,055.0 <sup>a</sup>	T <sub>t</sub> = 585° R; P <sub>t</sub> = 5,042.0 <sup>a</sup>
1	0.2351	0.1644	0.1184	0.0943	0.0772	0.0652	0.0537
2	.2643	.2520	.2415	.2404	.2234	.2170	.1557
3	.1825	.2696	.3762	.5091	.6153	.7428	.6388
4	.1049	.0400	.0082	-.0083	-.0137	-.0083	-.0082
5	.1825	.1002	.0481	.0185	.0011	-.0108	-.0340
6	.2410	.2404	.2356	.2346	.2234	.2170	.1531
7	.1707	.2520	.3528	.4624	.5510	.6492	.5218
8	.0953	.1854	.3194	.5048	.7112	.9330	.9465
9	-.0080	-.0353	-.0566	-.0783	-.0836	-.0783	-.0729
10	-.0190	-.0568	-.0891	-.0836	-.0944	-.0783	-.0729
11	.0457	-.0298	-.0728	-.0891	-.0944	-.0730	-.0729
12	.1707	.0943	.0422	.0185	-.0048	-.0108	-.0340
13	.2175	.2170	.2121	.2111	.1999	.1994	.1531
14	.1531	.2346	.3293	.4331	.5218	.6201	.5977
15	.0350	.1433	.2830	.4748	.6870	.9088	.9646
16	-.0133	.0709	.2045	.4084	.6568	.9449	1.1519
17	-.0012	.0709	.1924	.3844	.6326	.9209	1.1398
19	-.0244	-.0675	-.0944	-.0783	-.0891	-.0783	-.0674
20	.2116	.2053	.2004	.2053	.1940	.1936	.1590
21	-.0375	.0527	.1924	.3903	.6326	.9028	1.1035
23	.0080	-.0353	-.0673	-.0783	-.0944	-.0730	-.0674
24	-.0137	-.0730	-.0944	-.0783	-.0836	-.0730	-.0674
25	-.0405	-.0730	-.0997	-.0783	-.0836	-.0730	-.0674
26	.0240	-.0407	-.0835	-.0783	-.0891	-.0675	-.0674
27	.1531	.0826	.0248	.0009	-.0224	-.0341	-.0516
28	.2058	.2053	.2004	.2053	.1940	.1936	.1649
29	.1357	.2170	.3001	.3981	.4807	.5617	.5686
30	.0169	.1131	.2529	.4386	.6586	.8545	.9707
31	-.0436	.0588	.2045	.4145	.6447	.9209	1.1640
32	-.0254	.0588	.1803	.3724	.5965	.8786	1.1640
33	-.0133	.0588	.1742	.3603	.6025	.8967	1.2303
34	-.0028	-.0407	-.0673	-.0783	-.0944	-.0730	-.0674
35	-.0082	-.0730	-.0997	-.0783	-.0944	-.0675	-.0674
36	-.0514	-.0783	-.0997	-.0783	-.0836	-.0675	-.0674
37	.1999	.1994	.1945	.1936	.1883	.1762	.1473
38	-.0557	.0527	.2045	.4024	.6326	.8907	1.1459
39	-.0194	.0588	.1863	.3724	.6086	.9028	1.2122
40	-.0073	.0709	.1984	.3963	.6265	.9209	1.2424
41	-.0567	-.0836	-.0997	-.0783	-.0891	-.0675	-.0674
42	.0295	-.0353	-.0782	-.0836	-.0944	-.0675	-.0621
43	.1357	.0710	.0189	-.0050	-.0224	-.0400	-.0574
44	.1883	.1820	.1770	.1820	.1707	.1527	.1298
45	.1240	.2053	.2942	.3923	.4692	.5382	.5744
46	.0048	.1010	.2590	.4507	.6447	.8245	.9828
47	-.0557	.0588	.2166	.4205	.6628	.9269	1.1940
60	-.0082	-.0407	-.0673	-.0836	-.0836	-.0675	-.0674
61	-.0082	-.0783	-.0891	-.0783	-.0891	-.0622	-.0621
62	-.0621	-.0891	-.0891	-.0783	-.0836	-.0622	-.0621
63	.0240	-.0407	-.0728	-.0891	-.0891	-.0622	-.0621
64	.1531	.0943	.0540	.0243	.0011	-.0226	-.0398
65	.1825	.1879	.1888	.1879	.1766	.1586	.1240
66	.1240	.1994	.2825	.3747	.4398	.4739	.4866
67	-.0073	.0950	.2529	.4446	.6265	.7701	.8983
68	-.0615	.0648	.2287	.4446	.6689	.9088	1.1217
70	-.0133	.0648	.1924	.4084	.6447	.9149	1.2364
71	-.0082	-.0407	-.0728	-.0675	-.0729	-.0622	-.0621
72	-.0137	-.0730	-.0835	-.0730	-.0783	-.0622	-.0621
73	-.0674	-.0891	-.0944	-.0730	-.0729	-.0622	-.0621
74	-.0133	-.0407	-.0782	-.0730	-.0783	-.0622	-.0621
75	.1240	.0710	.0248	-.0050	-.0283	-.0458	-.0574
76	.1825	.1820	.1770	.1644	.1357	.1002	.0596
77	.1240	.1994	.2766	.3597	.3754	.3747	.3580
78	.0169	.1192	.2770	.4326	.5723	.6677	.7413
79	-.0496	.1192	.2408	.4326	.6628	.7943	1.0612
81	-.0133	.0648	.1984	.3903	.6326	.9209	1.2122
83	-.0137	-.0675	-.0782	-.0675	-.0674	-.0568	-.0621
84	-.0674	-.0891	-.0673	-.0675	-.0674	-.0622	-.0567
85	.0135	-.0407	-.0728	-.0675	-.0729	-.0568	-.0567
86	.1181	.0933	.0130	-.0226	-.0226	-.0457	-.0516
87	.1707	.1762	.1633	.1410	.1005	.0652	.0302
88	.1181	.1936	.2766	.3338	.3521	.3514	.3228
89	.0108	.1131	.2770	.4265	.5842	.6314	.6870
90	-.0676	.0648	.2469	.4386	.6326	.8124	.9828
93	-.0674	-.0622	-.0458	-.0568	-.0674	-.0515	-.0567
94	.0133	-.0407	-.0513	-.0568	-.0621	-.0515	-.0567
95	.1181	.0652	.0189	-.0167	-.0457	-.0517	-.0516
96	.1649	.1644	.1477	.1119	.0713	.0417	.0069
97	.1240	.1936	.2707	.3104	.3169	.3047	.2701
98	.0108	.1192	.2770	.4145	.5179	.5833	.6326
99	-.0615	.0709	.2529	.4326	.6086	.7762	.9285

<sup>a</sup> P<sub>t</sub> is in lb/sq ft.

TABLE II.- TABULATION OF PRESSURE MEASUREMENTS FOR CONFIGURATION 1 - Continued

(b) M = 3.51;  $P_{t,nom} = 7,200$  lb/sq ft

Orifice	$C_p$ at $\alpha$ of -							
	$0^\circ$	$7.5^\circ$	$15.0^\circ$	$22.5^\circ$	$30.0^\circ$	$37.5^\circ$	$45.0^\circ$	
	$T_t = 596^\circ R;$ $P_t = 7,186.0^a$	$T_t = 593^\circ R;$ $P_t = 7,034.0^a$	$T_t = 590^\circ R;$ $P_t = 7,201.0^a$	$T_t = 588^\circ R;$ $P_t = 7,215.0^a$	$T_t = 585^\circ R;$ $P_t = 7,200.0^a$	$T_t = 585^\circ R;$ $P_t = 7,207.0^a$	$T_t = 585^\circ R;$ $P_t = 7,182.0^a$	
1	0.2043	0.1359	0.0807	0.0435	0.0274	0.0151	0.0115	
2	.2413	.2491	.2446	.2315	.2160	.2156	.1512	
3	.1550	.2618	.3758	.5013	.6174	.7476	.6650	
4	.0920	.0154	-.0179	-.0406	-.0291	-.0331	-.0251	
5	.1633	.0939	.0480	.0026	-.0095	-.0177	-.0337	
6	.2167	.2365	.2364	.2274	.2200	.2196	.1512	
7	.1427	.2491	.3552	.4605	.5519	.6575	.6075	
8	.0831	.1654	.3111	.5000	.7043	.9483	.9869	
9	.0087	-.0348	-.0594	-.0746	-.0745	-.0745	-.0592	
10	-.0177	-.0696	-.0858	-.0859	-.0745	-.0745	-.0630	
11	.0428	-.0387	-.0745	-.0933	-.0745	-.0745	-.0630	
12	.1509	.0897	.0438	.0026	-.0136	-.0177	-.0337	
13	.1961	.2156	.2160	.2071	.1995	.2033	.1594	
14	.1304	.2323	.3307	.4278	.5232	.6207	.6280	
15	.0366	.1309	.2815	.4746	.6874	.9273	1.0547	
16	-.0142	.0573	.2054	.4071	.6577	.9694	1.2074	
17	-.0015	.0616	.1927	.3861	.6323	.9400	1.1396	
19	-.0252	-.0773	-.0896	-.0783	-.0782	-.0708	-.0592	
20	.1920	.2030	.2036	.1947	.1913	.1869	.1594	
21	-.0354	.0399	.1927	.3904	.6323	.9188	1.1226	
23	.0087	-.0426	-.0631	-.0783	-.0820	-.0669	-.0592	
24	-.0025	-.0811	-.0933	-.0783	-.0782	-.0669	-.0592	
25	-.0366	-.0851	-.0971	-.0783	-.0820	-.0669	-.0592	
26	.0240	-.0503	-.0782	-.0820	-.0820	-.0708	-.0554	
27	.1387	.0770	.0274	-.0097	-.0258	-.0382	-.0502	
28	.1878	.2030	.2036	.1988	.1913	.1869	.1677	
29	.1181	.2114	.3019	.3910	.4781	.5553	.5787	
30	.0154	.1005	.2561	.4409	.6450	.8638	1.0462	
31	-.0397	.0443	.2054	.4114	.6335	.9357	1.1904	
32	-.0185	.0529	.1842	.3735	.6070	.8934	1.1819	
33	-.0100	.0486	.1757	.3735	.6028	.9146	1.2625	
34	.0012	-.0464	-.0669	-.0783	-.0820	-.0669	-.0554	
35	-.0025	-.0811	-.0933	-.0820	-.0820	-.0708	-.0554	
36	-.0479	-.0927	-.0971	-.0783	-.0820	-.0708	-.0592	
37	.1797	.1945	.1954	.1824	.1791	.1706	.1389	
38	-.0482	.0399	.2011	.4029	.6366	.9061	1.1693	
39	-.0142	.0443	.1842	.3777	.6281	.9146	1.2456	
40	-.0015	.0573	.1969	.3945	.6577	.9400	1.2838	
41	-.0479	-.0967	-.0971	-.0783	-.0820	-.0669	-.0554	
42	.0315	-.0426	-.0745	-.0820	-.0820	-.0669	-.0554	
43	.1222	.0645	.0193	-.0178	-.0340	-.0464	-.0544	
44	.1674	.1862	.1791	.1791	.1627	.1500	.1266	
45	.1016	.2030	.2938	.3910	.4658	.5347	.5828	
46	.0069	.0918	.2603	.4494	.6408	.8343	.9996	
47	-.0397	.0443	.2138	.4198	.6577	.9400	1.2159	
60	-.0064	-.0464	-.0669	-.0746	-.0782	-.0669	-.0592	
61	-.0064	-.0735	-.0933	-.0746	-.0782	-.0669	-.0592	
62	-.0593	-.0927	-.0933	-.0746	-.0782	-.0632	-.0592	
63	.0315	-.0387	-.0707	-.0783	-.0782	-.0632	-.0554	
64	.1346	.0981	.0521	.0190	-.0095	-.0259	-.0420	
65	.1633	.1903	.1872	.1865	.1709	.1500	.1225	
66	.1016	.1987	.2856	.3747	.4413	.4734	.4883	
67	-.0015	.0833	.2518	.4494	.6450	.7920	.9148	
68	-.0524	.0399	.2350	.4494	.6874	.9188	1.1353	
70	-.0354	.0573	.2350	.3987	.6874	.9568	1.2753	
71	-.0064	-.0464	-.0669	-.0708	-.0707	-.0595	-.0554	
72	-.0101	-.0696	-.0858	-.0708	-.0745	-.0632	-.0592	
73	-.0630	-.0967	-.0896	-.0708	-.0745	-.0595	-.0554	
74	.0164	-.0503	-.0745	-.0708	-.0707	-.0595	-.0592	
75	.1098	.0686	.0233	-.0138	-.0581	-.0546	-.0544	
76	.1633	.1820	.1791	.1621	.1340	.0928	.0567	
77	.1057	.1945	.2774	.3378	.3752	.3578	.3567	
78	.0238	.1135	.2772	.4452	.5689	.6781	.7451	
79	.0069	.0529	.2772	.4494	.6620	.8892	1.0845	
81	-.0057	.0616	.2011	.4029	.6408	.9400	1.2456	
83	-.0101	-.0696	-.0707	-.0670	-.0631	-.0595	-.0592	
84	-.0630	-.1005	-.0669	-.0595	-.0594	-.0556	-.0592	
85	.0201	-.0464	-.0707	-.0633	-.0594	-.0556	-.0554	
86	.0976	.0561	.0111	-.0301	-.0463	-.0546	-.0544	
87	.1509	.1694	.1668	.1335	.1011	.0641	.0320	
88	.0976	.1862	.2774	.3338	.3593	.3465	.3239	
89	.0154	.1092	.2815	.4367	.5562	.6400	.6985	
90	-.0227	.0616	.2815	.4409	.6281	.8259	.9996	
93	-.0630	-.0735	-.0567	-.0595	-.0594	-.0556	-.0516	
94	.0164	-.0464	-.0405	-.0595	-.0594	-.0556	-.0516	
95	.1016	.0603	.0152	-.0301	-.0463	-.0546	-.0502	
96	.1509	.1610	.1462	.1089	.0766	.0355	.0074	
97	.1016	.1903	.2733	.3092	.3225	.3015	.2745	
98	.0196	.1092	.2815	.4240	.5225	.5936	.6348	
99	-.0524	.0529	.2518	.4367	.6198	.7878	.9403	

<sup>a</sup>  $P_t$  is in lb/sq ft.

TABLE II.- TABULATION OF PRESSURE MEASUREMENTS FOR CONFIGURATION 1 - Continued

(c)  $M = 4.65$ ;  $P_{t, nom} = 8,640$  lb/sq ft

Orifice	$C_p$ at $\alpha$ of -						
	$0^\circ$	$7.5^\circ$	$15.0^\circ$	$22.5^\circ$	$30.0^\circ$	$37.5^\circ$	$45.0^\circ$
	$T_t = 604^\circ R$ $P_t = 8,645.0^a$	$T_t = 600^\circ R$ $P_t = 8,649.0^a$	$T_t = 600^\circ R$ $P_t = 8,640.0^a$	$T_t = 602^\circ R$ $P_t = 8,633.0^a$	$T_t = 600^\circ R$ $P_t = 8,646.0^a$	$T_t = 602^\circ R$ $P_t = 8,640.0^a$	$T_t = 600^\circ R$ $P_t = 8,641.0^a$
1	0.2933	0.2581	0.2232	0.2145	0.2057	0.1969	0.1969
2	.2669	.2581	.2494	.2318	.2057	.2057	.1268
3	.1793	.2645	.3897	.5123	.5912	.7052	.4774
4	.1598	.1196	.0954	.0954	.0871	.1034	.0954
5	.1881	.1180	.0741	.0567	.0392	.0392	.0128
6	.2494	.2494	.2406	.2145	.2145	.2145	.1268
7	.1793	.2757	.3722	.4774	.5387	.6263	.4422
8	.1511	.2414	.3588	.5488	.7025	.9196	.7659
9	.0147	-.0096	-.0338	-.0338	-.0338	-.0176	-.0176
10	-.0016	-.0338	-.0418	-.0338	-.0338	-.0176	-.0256
11	.0549	-.0016	-.0338	-.0338	-.0338	-.0176	-.0258
12	.1793	.1180	.0741	.0567	.0392	.0304	.0128
13	.2406	.2406	.2232	.2232	.2145	.2145	.1444
14	.1705	.2669	.3546	.4598	.5299	.6175	.4947
15	.0514	.1601	.2957	.5128	.6934	.9015	.8112
16	-.0027	.0786	.2051	.4132	.6484	.9287	.9196
17	-.0064	.0786	.1961	.4132	.6594	.9015	.9740
19	-.0096	-.0338	-.2318	-.2318	-.0418	-.0176	-.0258
20	.2232	.2318	.2232	.2318	.2232	.2232	.1617
21	-.0117	.0695	.1961	.4223	.6484	.8834	.9559
23	-.0067	-.0176	-.0338	-.0338	-.0338	-.0176	-.0258
24	-.0016	-.0338	-.0338	-.0338	-.0338	-.0176	-.0258
25	-.0096	-.0418	-.0418	-.0338	-.0338	-.0176	-.0176
26	.0469	-.0096	-.0338	-.0338	-.0338	-.0176	-.0176
27	.1705	.1092	.0653	.0392	.0216	.0128	.0040
28	.2318	.2318	.2232	.2232	.2232	.2057	.1705
29	.1705	.2494	.3282	.4334	.5123	.5650	.5211
30	.0424	.1420	.2776	.4857	.6665	.8474	.9106
31	-.0117	.0786	.2142	.4404	.6665	.9106	1.0462
32	-.0117	.0695	.1782	.3951	.6122	.8562	1.0733
33	-.0117	.0605	.1782	.3860	.6122	.8653	1.1549
34	.0067	-.0258	-.0338	-.0338	-.0338	-.0176	-.0176
35	-.0016	-.0338	-.0338	-.0338	-.0338	-.0176	-.0176
36	-.0176	-.0418	-.0338	-.0338	-.0338	-.0176	-.0176
37	.2232	.2318	.2232	.2232	.2145	.2057	.1705
38	-.0117	.0695	.2142	.4404	.6575	.8834	1.0824
39	-.0117	.0605	.1870	.4041	.6213	.8743	1.1458
40	.0064	.0786	.1961	.4223	.6594	.8925	1.1908
41	-.0096	-.0418	-.0338	-.0338	-.0338	-.0176	-.0176
42	.0549	-.0016	-.0338	-.0258	-.0338	-.0176	-.0176
43	.1617	.1004	.0567	.0392	.0216	.0128	.0040
44	.2145	.2145	.2057	.2057	.1969	.1793	.1529
45	.1529	.2406	.3282	.4334	.5035	.5475	.5736
46	.0424	.1420	.2867	.4947	.6665	.8293	.9740
47	-.0117	.0786	.2232	.4585	.6756	.9106	1.1730
60	.0067	-.0258	-.0338	-.0258	-.0338	-.0176	-.0176
61	.0067	-.0338	-.0338	-.0258	-.0258	-.0176	-.0176
62	-.0096	-.0418	-.0338	-.0258	-.0258	-.0176	-.0258
63	.0631	.0067	-.0258	-.0258	-.0338	-.0176	-.0258
64	.1793	.1268	.0916	.0653	.0480	.0304	.0216
65	.2057	.2232	.2232	.2057	.2057	.1881	.1705
66	.1529	.2406	.3194	.4071	.4686	.5123	.5211
67	.0333	.1239	.2685	.4766	.6484	.7931	.9196
68	-.0117	.0786	.2323	.4766	.6847	.9106	1.1186
70	-.0117	.0786	.1961	.4675	.6594	.9649	1.1908
71	.0067	-.0258	-.0258	-.0176	-.0258	-.0096	-.0258
72	.0067	-.0338	-.0338	-.0176	-.0258	-.0096	-.0258
73	-.0096	-.0418	-.0338	-.0176	-.0258	-.0096	-.0258
74	.0549	-.0016	-.0258	-.0176	-.0258	-.0096	-.0258
75	.1617	.1092	.0653	.0480	.0304	.0128	.0040
76	.2145	.2232	.2145	.2057	.1793	.1529	.1180
77	.1617	.2406	.3109	.3810	.4159	.4246	.3983
79	.0514	.1511	.2957	.4766	.6031	.7116	.7569
81	.0155	.1511	.2504	.4766	.6847	.8203	1.0522
83	-.0027	.0786	.1961	.4132	.6484	.9377	1.2361
84	.0067	-.0176	-.0258	-.0096	-.0176	-.0176	-.0258
85	-.0096	-.0176	-.0176	-.0016	-.0176	-.0176	-.0258
86	.1529	.1004	-.0258	-.0096	-.0176	-.0176	-.0258
87	.2057	.1004	.0567	.0392	.0216	.0040	-.0136
88	.1529	.2057	.1881	.1617	.1617	.1268	.0829
89	.0514	.2318	.3109	.3810	.4159	.4071	.3810
90	.0424	.1511	.2957	.4766	.5941	.6934	.7478
93	-.0096	.0876	.2595	.4766	.6665	.8562	1.0281
94	-.0096	.0067	-.0176	-.0016	-.0176	-.0176	-.0258
95	.0631	.0067	-.0176	-.0016	-.0176	-.0176	-.0258
96	.1529	.1092	.0653	.0392	.0216	.0040	-.0136
97	.2057	.2057	.1881	.1617	.1356	.1004	.0653
98	.1617	.2406	.3109	.3634	.3810	.3722	.3282
99	.0514	.1511	.3048	.4766	.5669	.6484	.6847
	.0064	.0876	.2776	.4766	.6484	.8384	.9830

<sup>a</sup>  $P_t$  is in lb/sq ft.

TABLE II.- TABULATION OF PRESSURE MEASUREMENTS FOR CONFIGURATION 1 - Concluded

(d) M = 4.65;  $p_{t,nom} = 12,240$  lb/sq ft

Orifice	$C_p$ at $\alpha$ of -						
	0°	7.5°	15.0°	22.5°	30.0°	37.5°	45.0°
	$T_t = 604^\circ R$ ; $P_t = 12,255.0^a$	$T_t = 607^\circ R$ ; $P_t = 12,211.0^a$	$T_t = 603^\circ R$ ; $P_t = 12,265.0^a$	$T_t = 604^\circ R$ ; $P_t = 12,235.0^a$	$T_t = 604^\circ R$ ; $P_t = 12,217.0^a$	$T_t = 604^\circ R$ ; $P_t = 12,235.0^a$	$T_t = 604^\circ R$ ; $P_t = 12,247.0^a$
1	0.2427	0.1879	0.1562	0.1384	0.1259	0.1259	0.1130
2	.2611	.2560	.2489	.2249	.2063	.2003	.1130
3	.1809	.2807	.3970	.5035	.5903	.7017	.4773
4	.1102	.0651	.0533	.0480	.0480	.0651	.0589
5	.1809	.1135	.0698	.0392	.0267	.0267	.0081
6	.2427	.2436	.2489	.2311	.2125	.2125	.1254
7	.1747	.2682	.3786	.4726	.5408	.6274	.4463
8	.1186	.2087	.3480	.5282	.6944	.9244	.7431
9	.0021	-.0205	-.0319	-.0376	-.0318	-.0205	-.0148
10	-.0148	-.0376	-.0377	-.0376	-.0376	-.0205	-.0148
11	.0419	-.0147	-.0319	-.0433	-.0318	-.0205	-.0148
12	.1747	.1011	.0698	.0392	.0329	.0267	.0081
13	.2303	.2311	.2303	.2187	.2063	.2125	.1378
14	.1685	.2560	.3600	.4540	.5222	.6212	.4897
15	.0550	.1639	.3099	.5026	.6880	.9180	.8195
16	-.0024	.0809	.2143	.4260	.6432	.9372	.9280
17	.0039	.0809	.2016	.4068	.6304	.9116	.9661
19	-.0206	-.0433	-.0377	-.0376	-.0318	-.0205	-.0148
20	.2241	.2249	.2241	.2187	.2125	.2125	.1562
21	-.0150	.0745	.2080	.4132	.6432	.8988	.9724
23	.0021	-.0262	-.0319	-.0376	-.0318	-.0205	-.0148
24	-.0092	-.0433	-.0319	-.0376	-.0318	-.0205	-.0148
25	-.0206	-.0489	-.0319	-.0376	-.0318	-.0205	-.0148
26	-.0362	-.0147	-.0319	-.0433	-.0318	-.0205	-.0148
27	.1685	.1011	.0636	.0329	.0145	.0083	-.0043
28	.2241	.2249	.2241	.2187	.2125	.2125	.1624
29	.1624	.2374	.3352	.4231	.5097	.5654	.5267
30	.0422	.1448	.2844	.4770	.6816	.8604	.9280
31	-.0150	.0809	.2271	.4324	.6816	.9244	1.0680
32	-.0086	.0681	.1952	.3940	.6304	.8732	1.0744
33	-.0024	.0681	.1952	.3876	.6304	.8796	1.1573
34	.0021	-.0318	-.0263	-.0433	-.0318	-.0205	-.0148
35	-.0092	-.0433	-.0319	-.0376	-.0318	-.0205	-.0148
36	-.0263	-.0546	-.0319	-.0376	-.0318	-.0205	-.0148
37	.2179	.2187	.2179	.2187	.2125	.2003	.1624
38	-.0150	.0745	.2271	.4324	.6688	.8988	1.0999
39	-.0086	.0745	.2016	.3940	.6368	.8860	1.1637
40	-.0024	.0809	.2143	.4196	.6688	.9116	1.2082
41	-.0263	-.0489	-.0319	-.0376	-.0262	-.0147	-.0148
42	.0477	-.0090	-.0263	-.0433	-.0318	-.0147	-.0148
43	.1562	.0887	.0574	.0267	.0145	.0083	-.0043
44	.2055	.2063	.2055	.2003	.1941	.1816	.1562
45	.1500	.2311	.3290	.4231	.5035	.5470	.5760
46	.0358	.1384	.2971	.4898	.6752	.8348	.9788
47	-.0150	.0809	.2397	.4516	.6880	.9308	1.1763
60	-.0036	-.0318	-.0263	-.0376	-.0262	-.0205	-.0148
61	-.0036	-.0489	-.0319	-.0376	-.0262	-.0205	-.0148
62	-.0263	-.0489	-.0319	-.0376	-.0262	-.0147	-.0148
63	.0477	-.0090	-.0263	-.0376	-.0262	-.0147	-.0148
64	.1747	.1135	.0882	.0578	.0392	.0267	.0205
65	.1995	.2063	.2179	.2125	.2003	.1879	.1624
66	.1438	.2249	.3228	.3983	.4664	.4975	.5081
67	.0295	.1320	.2844	.4706	.6624	.7966	.9216
68	-.0214	.0809	.2461	.4706	.6944	.9180	1.1318
70	-.0150	.0745	.2461	.4196	.6560	.9626	1.2082
71	-.0036	-.0318	-.0263	-.0262	-.0262	-.0090	-.0148
72	-.0036	-.0433	-.0263	-.0318	-.0262	-.0147	-.0092
73	-.0263	-.0489	-.0263	-.0318	-.0262	-.0147	-.0092
74	.0419	-.0090	-.0263	-.0376	-.0262	-.0147	-.0092
75	.1500	.0887	.0636	.0329	.0145	.0083	-.0043
76	.2055	.2003	.2055	.1941	.1692	.1444	.1068
77	.1500	.2187	.3044	.3736	.4107	.4294	.3970
78	.0486	.1512	.3035	.4644	.6112	.7262	.7622
79	.0486	.0937	.2907	.4706	.6496	.9308	.9980
81	-.0024	.0809	.2080	.4132	.6688	.9690	1.2018
83	-.0036	-.0376	-.0206	-.0262	-.0205	-.0205	-.0206
84	-.0263	-.0489	-.0148	-.0262	-.0205	-.0147	-.0148
85	.0477	-.0206	-.0318	-.0318	-.0205	-.0147	-.0148
86	.1438	.0826	.0512	.0267	.0083	-.0041	-.0229
87	.1995	.1941	.1995	.1754	.1444	.1197	.0822
88	.1500	.2187	.3106	.3736	.4045	.4045	.3786
89	.0422	.1448	.3035	.4706	.5984	.7070	.7431
90	.0422	.0809	.2652	.4706	.6688	.8668	1.0299
93	-.0206	-.0090	-.0206	-.0205	-.0205	-.0147	-.0206
94	.0477	-.0034	-.0148	-.0205	-.0205	-.0147	-.0148
95	.1500	.0887	.0574	.0267	.0083	-.0041	-.0167
96	.1933	.1879	.1871	.1506	.1259	.0949	.0574
97	.1500	.2125	.3106	.3550	.3674	.3674	.3228
98	.0486	.1512	.3099	.4706	.5666	.6560	.6731
99	-.0024	.0873	.2780	.4644	.6560	.8476	.9724

<sup>a</sup>  $p_t$  is in lb/sq ft.



TABLE III.-- TABULATION OF PRESSURE MEASUREMENTS FOR CONFIGURATION 2

(a)  $M = 3.51$ ;  $P_{t, nom} = 5,040 \text{ lb/sq ft}$

Orifice	$C_p$ at $\alpha$ of -						
	$0^\circ$	$7.5^\circ$	$15.0^\circ$	$22.5^\circ$	$30.0^\circ$	$37.5^\circ$	$45.0^\circ$
	$T_t = 581^\circ R$ ; $P_t = 5,045.0^a$	$T_t = 580^\circ R$ ; $P_t = 5,037.0^a$	$T_t = 580^\circ R$ ; $P_t = 5,028.0^a$	$T_t = 582^\circ R$ ; $P_t = 5,043.0^a$	$T_t = 585^\circ R$ ; $P_t = 5,045.0^a$	$T_t = 585^\circ R$ ; $P_t = 5,043.0^a$	$T_t = 585^\circ R$ ; $P_t = 5,045.0^a$
4	0.1049	0.0566	0.0300	0.0133	0.0025	0.0025	-0.0082
5	.1766	.1126	.0778	.0302	.0187	-.0107	-.0340
6	.2234	.2004	.2068	.1883	.1940	.1766	.1122
7	.1999	.2474	.3241	.3930	.4925	.5744	.5334
8	.1133	.1865	.3140	.4757	.6991	.9525	.9767
9	.0025	-.0242	-.0350	-.0567	-.0729	-.0729	-.0783
10	.0225	-.0404	-.0673	-.0836	-.0944	-.0783	-.0836
11	.0295	-.0242	-.0566	-.0891	-.0944	-.0783	-.0891
12	.1414	.0775	.0425	.0011	-.0011	-.0165	-.0340
13	.1940	.1712	.1716	.1590	.1707	.1473	.1064
14	.1473	.1888	.2713	.3580	.4633	.5218	.4633
15	.0350	.1138	.2474	.4334	.6568	.8741	.9225
16	.0048	.0714	.1928	.3852	.6507	.9465	1.0533
17	.0108	.0654	.1807	.3671	.6265	.9104	1.1277
19	-.0137	-.0620	-.0835	-.0998	-.0944	-.0783	-.0836
20	.1825	.1594	.1657	.1590	.1649	.1473	.1122
21	-.0133	.0593	.1928	.3911	.6447	.9164	1.1579
23	.0025	-.0351	-.0512	-.0783	-.0836	-.0729	-.0836
24	.0025	-.0673	-.0890	-.0944	-.0836	-.0783	-.0836
25	-.0190	-.0673	-.0835	-.0944	-.0891	-.0729	-.0836
26	.0133	-.0458	-.0781	-.0944	-.0891	-.0729	-.0783
27	.1298	.0540	.0191	-.0165	-.0224	-.0457	-.0574
28	.1825	.1712	.1775	.1649	.1707	.1473	.1181
29	.1240	.1888	.2831	.3696	.4633	.5101	.5218
30	.0048	.0956	.2535	.4395	.6507	.8620	1.0130
31	-.0254	.0533	.1989	.3971	.6447	.9104	1.1640
32	-.0012	.0654	.1928	.3911	.6507	.9285	1.1940
33	-.0012	.0533	.1686	.3489	.5965	.8620	1.0975
34	-.0028	-.0404	-.0566	-.0836	-.0836	-.0729	-.0783
35	-.0028	-.0782	-.0890	-.0944	-.0891	-.0729	-.0783
36	-.0244	-.0728	-.0890	-.0944	-.0891	-.0729	-.0783
37	.1825	.1712	.1775	.1649	.1649	.1473	.1240
38	-.0315	.0593	.2333	.4395	.6991	.9525	1.1880
39	-.0073	.0533	.1868	.3610	.6145	.8922	1.1940
40	-.0073	.0474	.1686	.3368	.5844	.8681	1.1940
41	-.0352	-.0782	-.0944	-.0891	-.0891	-.0836	-.0783
42	.0240	-.0404	-.0728	-.0891	-.0891	-.0783	-.0783
43	.1357	.0598	.0191	-.0165	-.0283	-.0516	-.0574
44	.1825	.1712	.1775	.1649	.1590	-.0516	.1122
45	.1240	.1888	.2831	.3637	.4339	.4807	.5101
46	.0048	.0896	.2535	.4274	.6145	.7836	.9285
47	-.0496	.0413	.1989	.3792	.6025	.8499	1.0914
60	-.0028	-.0404	-.0673	-.0783	-.0783	-.0783	-.0729
61	.0025	-.0782	-.0944	-.0891	-.0836	-.0729	-.0729
62	-.0567	-.0891	-.0890	-.0891	-.0836	-.0729	-.0729
63	.0349	-.0236	-.0619	-.0891	-.0891	-.0674	-.0729
64	.1649	.0949	.0601	.0187	.0069	-.0283	-.0398
65	.1940	.1888	.1950	.1825	.1766	.1531	.1240
66	.1357	.2063	.2949	.3696	.4457	.4807	.4866
67	.0048	.0956	.2656	.4395	.6447	.8017	.9164
68	-.0557	.0533	.2333	.4395	.6870	.9225	1.1398
70	-.0557	.0654	.2110	.3792	.6447	.9104	1.2364
71	.0025	-.0404	-.0673	-.0836	-.0729	-.0674	-.0674
72	-.0028	-.0728	-.0890	-.0891	-.0783	-.0674	-.0674
73	-.0567	-.0891	-.0835	-.0891	-.0729	-.0674	-.0674
74	.0240	-.0404	-.0728	-.0891	-.0783	-.0621	-.0674
75	.1414	.0716	.0307	-.0107	-.0283	-.0457	-.0574
76	.1940	.1829	.1834	.1590	.1357	.1005	.0654
77	.1357	.2004	.2831	.3345	.3754	.3754	.3521
78	.0290	.1199	.2836	.4334	.5723	.6689	.7352
79	.0290	.0593	.2776	.4515	.6568	.8741	.9949
81	-.0012	.0654	.2050	.3911	.6386	.9285	1.2122
83	.0025	-.0673	-.0835	-.0729	-.0729	-.0621	-.0674
84	-.0567	-.0891	-.0835	-.0674	-.0729	-.0567	-.0621
85	.0295	-.0351	-.0673	-.0674	-.0729	-.0567	-.0621
86	.1298	.0598	.0191	-.0224	-.0398	-.0574	-.0633
87	.1825	.1712	.1716	.1357	.1064	.0713	.0361
88	.1298	.1945	.2831	.3345	.3580	.3404	.3228
89	.0108	.1138	.2897	.4274	.5421	.6447	.6931
90	.0048	.0593	.2596	.4334	.6265	.8199	.9888
93	-.0567	-.0513	-.0566	-.0567	-.0729	-.0567	-.0621
94	.0295	-.0351	-.0619	-.0514	-.0729	-.0567	-.0674
95	.1357	.0657	.0250	-.0224	-.0398	-.0633	-.0574
96	.1766	.1653	.1481	.1064	.0772	.0361	.0069
97	.1357	.1945	.2772	.3110	.3169	.2995	.2701
98	.0169	.1199	.2897	.4092	.5179	.5904	.6205
99	-.0375	.0775	.2656	.4153	.6145	.7775	.9346

<sup>a</sup>  $P_t$  is in lb/sq ft.

TABLE III.- TABULATION OF PRESSURE MEASUREMENTS FOR CONFIGURATION 2 - Continued

(b)  $M = 3.51$ ;  $P_{t, nom} = 7,200 \text{ lb/sq ft}$

Orifice	$C_p$ at $\alpha$ of -						
	$0^\circ$	$7.5^\circ$	$15.0^\circ$	$22.5^\circ$	$30.0^\circ$	$37.5^\circ$	$45.0^\circ$
	$T_t = 587^\circ R$ ; $P_t = 7,205.0^a$	$T_t = 584^\circ R$ ; $P_t = 7,199.0^a$	$T_t = 582^\circ R$ ; $P_t = 7,212.0^a$	$T_t = 585^\circ R$ ; $P_t = 7,193.0^a$	$T_t = 585^\circ R$ ; $P_t = 7,208.0^a$	$T_t = 583^\circ R$ ; $P_t = 7,211.0^a$	$T_t = 585^\circ R$ ; $P_t = 7,209.0^a$
4	0.0915	0.0349	0.0009	-0.0178	-0.0331	-0.0368	-0.0331
5	.1668	.1135	.0641	.0234	-.0014	-.0218	-.0423
6	.2077	.2036	.1951	.1875	.1788	.1747	.1091
7	.1831	.2446	.3138	.3967	.4816	.5839	.5388
8	.0912	.1715	.2980	.4765	.6950	.9610	1.0285
9	.0161	-.0217	-.0406	-.0593	-.0820	-.0820	-.0820
10	.0047	-.0443	-.0708	-.0933	-.1046	-.0896	-.0858
11	.0349	-.0254	-.0632	-.0895	-.1046	-.0896	-.0820
12	.1340	.0766	.0272	-.0011	-.0177	-.0259	-.0423
13	.1831	.1750	.1624	.1588	.1542	.1500	.1132
14	.1340	.1913	.2646	.3598	.4489	.5308	.5184
15	.0278	.1123	.2472	.4343	.6527	.8765	.9779
16	.0024	.0744	.1923	.3878	.6485	.9483	1.1384
17	.0066	.0659	.1797	.3708	.6232	.9103	1.1342
19	-.0103	-.0631	-.0820	-.0971	-.1046	-.0858	-.0820
20	.1709	.1586	.1542	.1547	.1500	.1418	.1091
21	-.0187	.0574	.1923	.3961	.6400	.9188	1.1596
23	.0047	-.0330	-.0536	-.0819	-.0972	-.0858	-.0820
24	.0047	-.0535	-.0972	-.1009	-.1009	-.0896	-.0820
25	-.0179	-.0707	-.0896	-.0971	-.1009	-.0896	-.0820
26	.0161	-.0481	-.0820	-.0971	-.1009	-.0896	-.0783
27	.1217	.0562	.0068	-.0216	-.0382	-.0464	-.0627
28	.1709	.1709	.1665	.1671	.1583	.1459	.1173
29	.1094	.1872	.2769	.3722	.4489	.5184	.5184
30	.0024	.0954	.2472	.4427	.6485	.8555	1.0160
31	-.0314	.0532	.1966	.4004	.6400	.9146	1.1722
32	-.0017	.0659	.1966	.3920	.6442	.9357	1.2060
33	-.0102	.0489	.1670	.3496	.5936	.8680	1.1680
34	.0010	-.0405	-.0632	-.0858	-.0933	-.0858	-.0783
35	.0047	-.0820	-.0933	-.0933	-.1009	-.0896	-.0820
36	-.0291	-.0745	-.0933	-.0933	-.1009	-.0896	-.0783
37	.1709	.1750	.1706	.1630	.1542	.1459	.1173
38	-.0399	.0617	.2262	.4427	.6950	.9610	1.2060
39	-.0102	.0574	.1797	.3666	.6147	.9019	1.1975
40	-.0102	.0489	.1627	.3454	.6020	.8850	1.2186
41	-.0405	-.0820	-.0972	-.0972	-.0972	-.0896	-.0783
42	.0237	-.0443	-.0783	-.0933	-.1009	-.0896	-.0783
43	.1258	.0603	.0109	-.0175	-.0382	-.0505	-.0627
44	.1709	.1709	.1665	.1671	.1542	.1418	.1132
45	.1094	.1872	.2728	.3639	.4325	.4898	.5184
46	-.0017	.0912	.2472	.4258	.6105	.7878	.9273
47	-.0610	.0362	.1881	.3793	.6063	.8555	1.1088
60	-.0027	-.0443	-.0708	-.0858	-.0858	-.0858	-.0745
61	.0010	-.0820	-.0972	-.0972	-.0972	-.0858	-.0745
62	-.0555	-.0896	-.1009	-.0933	-.0933	-.0820	-.0745
63	.0349	-.0330	-.0708	-.0895	-.0972	-.0820	-.0745
64	.1544	.0971	.0519	.0195	-.0055	-.0259	-.0423
65	.1831	.1872	.1869	.1834	.1706	.1500	.1255
66	.1217	.2036	.2893	.3763	.4489	.4816	.4939
67	-.0017	.0954	.2599	.4555	.6569	.8005	.9146
68	-.0568	.0532	.2304	.4470	.7034	.9230	1.1384
70	-.0102	.0532	.1923	.4004	.6611	.9610	1.2608
71	.0010	-.0443	-.0669	-.0782	-.0820	-.0745	-.0708
72	-.0027	-.0745	-.0972	-.0933	-.0858	-.0783	-.0745
73	-.0555	-.0933	-.0933	-.0933	-.0820	-.0783	-.0708
74	.0237	-.0405	-.0745	-.0933	-.0820	-.0783	-.0708
75	.1258	.0684	.0192	-.0135	-.0341	-.0546	-.0627
76	.1831	.1872	.1747	.1588	.1296	.0928	.0601
77	.1258	.1995	.2769	.3593	.3711	.3752	.3547
78	.0235	.1208	.2768	.4385	.5767	.6738	.7329
79	-.0483	.1208	.2430	.4385	.6611	.8259	1.0751
81	-.0060	.0659	.2008	.4004	.6485	.9400	1.2271
83	-.0027	-.0631	-.0933	-.0744	-.0783	-.0708	-.0669
84	-.0555	-.0933	-.0933	-.0707	-.0783	-.0669	-.0669
85	.0274	-.0405	-.0745	-.0707	-.0783	-.0669	-.0669
86	.1176	.0603	.0068	-.0257	-.0505	-.0627	-.0627
87	.1709	.1750	.1624	.1343	.0969	.0601	.0314
88	.1176	.1913	.2769	.3353	.3547	.3465	.3220
89	.0151	.1166	.2811	.4343	.5513	.6315	.6865
90	-.0610	.0617	.2514	.4385	.6358	.8216	.9906
93	-.0555	-.0707	-.0595	-.0555	-.0783	-.0669	-.0669
94	.0274	-.0367	-.0669	-.0555	-.0783	-.0669	-.0669
95	.1217	.0109	.0109	-.0257	-.0505	-.0627	-.0627
96	.1668	.1627	.1418	.1055	.0723	.0355	.0027
97	.1217	.1954	.2687	.3065	.3179	.3015	.2687
98	.0108	.1166	.2811	.4173	.5176	.5809	.6147
99	-.0526	.0659	.2557	.4343	.6190	.7836	.9315

<sup>a</sup> $P_t$  is in lb/sq ft.

TABLE III.- TABULATION OF PRESSURE MEASUREMENTS FOR CONFIGURATION 2 - Continued

(c)  $M = 4.65$ ;  $P_{t, nom} = 8,640$  lb/sq ft

Orifice	$C_p$ at $\alpha$ of -						
	$0^\circ$ $T_t = 605^\circ R$ ; $P_t = 8,644.0^a$	$7.5^\circ$ $T_t = 605^\circ R$ ; $P_t = 8,634.0^a$	$15.0^\circ$ $T_t = 605^\circ R$ ; $P_t = 8,633.0^a$	$22.5^\circ$ $T_t = 605^\circ R$ ; $P_t = 8,617.0^a$	$30.0^\circ$ $T_t = 605^\circ R$ ; $P_t = 8,611.0^a$	$37.5^\circ$ $T_t = 603^\circ R$ ; $P_t = 8,671.0^a$	$45.0^\circ$ $T_t = 607^\circ R$ ; $P_t = 8,651.0^a$
4	0.1609	0.1356	0.1111	0.1041	0.0877	0.0870	0.0879
5	.1732	.1375	.0914	.0655	.0391	.0295	.0037
6	.2177	.2171	.1963	.1971	.1883	.1688	.0908
7	.1998	.2526	.3189	.3988	.4601	.5511	.3961
8	.1694	.2328	.3415	.5066	.6791	.9327	.7851
9	.0232	.0067	-.0096	-.0174	-.0337	-.0337	-.0418
10	.0232	-.0096	-.0338	-.0417	-.0498	-.0337	-.0418
11	.0474	.0067	-.0258	-.0417	-.0498	-.0337	-.0418
12	.1468	.0932	.0565	.0391	.0305	.0210	.0037
13	.1822	.1817	.1614	.1707	.1707	.1512	.0996
14	.1468	.1995	.2664	.3638	.4424	.5163	.4137
15	.0426	.1332	.2510	.4521	.6610	.8608	.7398
16	.0155	.0879	.1966	.3975	.6519	.9146	.8666
17	.0155	.0789	.1875	.3796	.6339	.8785	.9300
19	.0069	-.0258	-.0418	-.0498	-.0498	-.0337	-.0418
20	.1822	.1729	.1702	.1795	.1795	.1772	.1257
21	-.0027	.0698	.1966	.4066	.6519	.8876	.9291
23	.0069	-.0096	-.0258	-.0417	-.0498	-.0419	-.0336
24	.0069	-.0258	-.0501	-.0498	-.0498	-.0419	-.0336
25	-.0013	-.0258	-.0501	-.0498	-.0498	-.0419	-.0336
26	.0312	-.0096	-.0418	-.0498	-.0498	-.0337	-.0336
27	.1377	.0754	.0389	.0217	.0128	.0034	-.0051
28	.1910	.1905	.1790	.1883	.1795	.1688	.1257
29	.1377	.2083	.3016	.3988	.4775	.5163	.4920
30	.0155	.1151	.2781	.4793	.6701	.8427	.8847
31	-.0208	.0698	.2057	.4248	.6610	.8876	1.0478
32	-.0027	.0698	.1966	.4066	.6610	.8966	1.0749
33	-.0027	.0607	.1785	.3705	.5976	.8427	1.0749
34	.0069	-.0096	-.0338	-.0498	-.0417	-.0337	-.0256
35	-.0013	-.0338	-.0501	-.0417	-.0501	-.0337	-.0256
36	-.0093	-.0338	-.0501	-.0498	-.0498	-.0337	-.0256
37	.1910	.1995	.1963	.1971	.1883	.1772	.1433
38	-.0208	.0698	.2419	.4702	.7064	.9417	1.1474
39	-.0117	.0607	.1875	.3796	.6067	.8608	1.1293
40	-.0117	.0517	.1694	.3614	.5885	.8337	1.1293
41	-.0173	-.0418	-.0581	-.0498	-.0498	-.0337	-.0256
42	.0474	-.0016	-.0338	-.0417	-.0498	-.0337	-.0256
43	.1468	.0932	.0477	.0217	.0040	.0034	-.0139
44	.1910	.1995	.1963	.1883	.1795	.1688	.1345
45	.1377	.2259	.3016	.3900	.4601	.4991	.5096
46	.0155	.1241	.2691	.4611	.6430	.7886	.9210
47	-.0298	.0517	.2057	.4066	.6248	.8337	1.0568
60	-.0013	-.0258	-.0418	-.0417	-.0498	-.0337	-.0256
61	-.0093	-.0338	-.0418	-.0417	-.0417	-.0337	-.0336
62	-.0256	-.0418	-.0501	-.0417	-.0417	-.0337	-.0336
63	.0637	.0067	-.0258	-.0417	-.0498	-.0337	-.0418
64	.1732	.1287	.0826	.0655	.0391	.0295	.0125
65	.2086	.2171	.2139	.2145	.1969	.1860	.1694
66	.1468	.2347	.3189	.4077	.4775	.5076	.5269
67	.0245	.1241	.2781	.4793	.6430	.8156	.9210
68	-.0298	.0698	.2419	.4611	.6973	.9236	1.1293
70	-.0117	.0607	.1875	.3795	.6430	.9417	1.1836
71	-.0013	-.0258	-.0338	-.0417	-.0417	-.0337	-.0336
72	-.0013	-.0338	-.0418	-.0417	-.0337	-.0337	-.0256
73	-.0256	-.0418	-.0418	-.0417	-.0417	-.0337	-.0336
74	.0394	-.0016	-.0338	-.0417	-.0417	-.0337	-.0336
75	.1556	.1020	.0565	.0391	.0217	.0122	.0037
76	.2086	.2083	.2051	.1883	.1707	.1512	.1084
77	.1556	.2259	.3016	.3723	.4074	.4208	.3961
78	.0426	.1423	.2872	.4702	.5976	.7167	.7489
79	.0336	.0789	.2872	.4702	.6158	.9056	.9481
81	-.0117	.0698	.1966	.3975	.6519	.9327	1.2199
83	-.0093	-.0338	-.0418	-.0337	-.0417	-.0337	-.0256
84	-.0256	-.0418	-.0418	-.0337	-.0417	-.0337	-.0256
85	.0474	.0067	-.0258	-.0417	-.0417	-.0337	-.0256
86	.1468	.0932	.0565	.0217	.0040	.0034	-.0139
87	.1998	.1995	.1878	.1707	.1530	.1165	.0908
88	.1468	.2259	.3016	.3723	.4074	.4033	.3788
89	.0426	.1423	.2962	.4611	.5976	.6896	.7398
90	-.0208	.0789	.2600	.4611	.6610	.8608	1.0297
93	-.0256	-.0176	-.0258	-.0337	-.0337	-.0257	-.0256
94	.0474	.0067	-.0258	-.0417	-.0337	-.0337	-.0176
95	.1468	.1020	.0565	.0217	.0128	-.0053	-.0139
96	.1910	.1905	.1790	.1533	.1268	.0990	.0647
97	.1556	.2259	.3016	.3550	.3723	.3598	.3263
98	.0426	.1513	.3053	.4611	.5612	.6673	.6673
99	-.0027	.0970	.2781	.4611	.6430	.8337	.9753

<sup>a</sup>  $P_t$  is in lb/sq ft.

TABLE III.- TABULATION OF PRESSURE MEASUREMENTS FOR CONFIGURATION 2 - Concluded

(d) M = 4.65; P<sub>t, nom</sub> = 12,240 lb/sq ft

Orifice	C <sub>p</sub> at α of -							
	0° T <sub>t</sub> = 605° R; P <sub>t</sub> = 12,240.0 <sup>a</sup>	7.5° T <sub>t</sub> = 605° R; P <sub>t</sub> = 12,231.0 <sup>a</sup>	15.0° T <sub>t</sub> = 605° R; P <sub>t</sub> = 12,214.0 <sup>a</sup>	22.5° T <sub>t</sub> = 605° R; P <sub>t</sub> = 12,234.0 <sup>a</sup>	30.0° T <sub>t</sub> = 605° R; P <sub>t</sub> = 12,236.0 <sup>a</sup>	37.5° T <sub>t</sub> = 605° R; P <sub>t</sub> = 12,237.0 <sup>a</sup>	45.0° T <sub>t</sub> = 605° R; P <sub>t</sub> = 12,229.0 <sup>a</sup>	
4	0.1335	0.0936	0.0708	0.0593	0.0480	0.0536	0.0536	
5	.1816	.1259	.0887	.0516	.0529	.0207	-.0041	
6	.2187	.2125	.2003	.2003	.1816	.1692	.0949	
7	.2003	.2498	.3179	.3983	.4602	.5592	.4107	
8	.1512	.2087	.3238	.4962	.6816	.9308	.7902	
9	.0309	-.0034	-.0090	-.0147	-.0318	-.0262	-.0318	
10	.0252	-.0147	-.0318	-.0376	-.0489	-.0262	-.0318	
11	.0480	.0023	-.0262	-.0376	-.0489	-.0262	-.0318	
12	.1444	.0949	.0578	.0392	.0207	.0207	.0021	
13	.1879	.1754	.1692	.1568	.1568	.1568	.0949	
14	.1506	.2003	.2682	.3736	.4416	.5222	.4045	
15	.0553	.1256	.2598	.4644	.6560	.8668	.7518	
16	.0297	.0873	.2023	.4132	.6432	.9244	.8988	
17	.0233	.0745	.1895	.3940	.6240	.8924	.9562	
19	.0081	-.0262	-.0433	-.0433	-.0489	-.0262	-.0318	
20	.1816	.1692	.1692	.1816	.1692	.1692	.1135	
21	.0041	.0681	.2023	.4396	.6560	.9052	.9882	
23	.0137	-.0147	-.0318	-.0376	-.0376	-.0318	-.0376	
24	.0137	-.0376	-.0489	-.0489	-.0489	-.0318	-.0376	
25	.0023	-.0318	-.0489	-.0433	-.0489	-.0318	-.0376	
26	.0365	-.0147	-.0376	-.0433	-.0489	-.0318	-.0376	
27	.1384	.0764	.0392	.0207	.0083	.0021	-.0104	
28	.1941	.1879	.1879	.1941	.1816	.1692	.1259	
29	.1384	.2063	.3055	.4045	.4789	.5222	.4851	
30	.0361	.1128	.2790	.4834	.6944	.8604	.9180	
31	-.0023	.0617	.2151	.4324	.6816	.9052	1.0584	
32	.0105	.0681	.2023	.4196	.6752	.9180	1.0968	
33	.0105	.0553	.1831	.3812	.6240	.8540	1.0776	
34	.0137	-.0147	-.0318	-.0433	-.0376	-.0318	-.0318	
35	.0081	-.0376	-.0489	-.0376	-.0489	-.0262	-.0262	
36	-.0034	-.0376	-.0489	-.0376	-.0489	-.0262	-.0318	
37	.2003	.1941	.1941	.1941	.1816	.1754	.1444	
38	-.0085	.0681	.2470	.4834	.7262	.9562	1.1416	
39	.0041	.0617	.1895	.3940	.6504	.8732	1.1288	
40	.0041	.0553	.1705	.3748	.6112	.8476	1.1544	
41	-.0147	-.0433	-.0489	-.0376	-.0433	-.0262	-.0318	
42	.0480	-.0090	-.0318	-.0376	-.0489	-.0262	-.0318	
43	.1506	.0826	.0592	.0267	.0083	.0021	-.0104	
44	.2003	.1941	.1816	.1816	.1692	.1444	.1444	
45	.1444	.2187	.2995	.3983	.4602	.5055	.5159	
46	.0561	.1192	.2790	.4706	.6560	.7966	.9244	
47	-.0149	.0553	.2151	.4196	.6368	.8476	1.0776	
60	.0081	-.0262	-.0433	-.0376	-.0433	-.0262	-.0262	
61	-.0034	-.0376	-.0546	-.0433	-.0433	-.0262	-.0262	
62	-.0147	-.0433	-.0546	-.0376	-.0376	-.0262	-.0262	
63	.0651	.0023	-.0262	-.0318	-.0376	-.0262	-.0262	
64	.1879	.1259	.0764	.0578	.0392	.0267	.0207	
65	.2125	.2125	.2125	.2249	.2003	.1879	.1754	
66	.1630	.2311	.3179	.4107	.4602	.4975	.5284	
67	.0425	.1256	.2662	.4898	.6752	.8158	.9434	
68	-.0085	.0745	.2406	.4770	.7134	.9308	1.1416	
70	-.0085	.0617	.2023	.4132	.6816	.9562	1.2054	
71	.0081	-.0262	-.0376	-.0318	-.0376	-.0262	-.0262	
72	.0081	-.0376	-.0433	-.0376	-.0376	-.0262	-.0262	
73	-.0090	-.0433	-.0433	-.0376	-.0318	-.0262	-.0205	
74	.0536	-.0034	-.0318	-.0376	-.0376	-.0262	-.0205	
75	.1568	.0949	.0578	.0529	.0145	.0083	.0083	
76	.2125	.2063	.2003	.1941	.1692	.1444	.1197	
77	.1630	.2187	.2995	.3736	.4045	.4231	.4045	
78	.0617	.1448	.2918	.4706	.6176	.7262	.7646	
79	.0617	.0873	.2854	.4770	.7008	.9244	.9818	
81	.0041	.0681	.2023	.4132	.6752	.9626	1.2054	
83	.0081	-.0376	-.0433	-.0262	-.0318	-.0205	-.0205	
84	-.0090	-.0433	-.0433	-.0262	-.0318	-.0205	-.0205	
85	.0593	.0023	-.0262	-.0318	-.0318	-.0205	-.0205	
86	.1568	.0887	.0516	.0267	.0083	-.0041	-.0041	
87	.2063	.1941	.1754	.1754	.1444	.1197	.0949	
88	.1568	.2187	.3055	.3736	.3983	.3983	.3859	
89	.0425	.1384	.2982	.4706	.6048	.6944	.7582	
90	.0425	.0809	.2598	.4770	.6816	.8668	1.0458	
93	-.0090	-.0205	-.0262	-.0262	-.0318	-.0205	-.0205	
94	.0593	.0023	-.0262	-.0262	-.0318	-.0205	-.0205	
95	.1568	.0949	.0516	.0267	.0083	-.0041	-.0041	
96	.2003	.1879	.1754	.1568	.1197	.0949	.0702	
97	.1630	.2249	.3055	.3550	.3674	.3612	.3302	
98	.0553	.1448	.3110	.4770	.5956	.6560	.6816	
99	-.0085	.0809	.2662	.4770	.6624	.8476	.9882	

<sup>a</sup> P<sub>t</sub> is in lb/sq ft.























TABLE VI. - TABULATION OF HEAT-TRANSFER MEASUREMENTS  
FOR CONFIGURATION 1 - Continued

(a)  $M = 3.51$ ;  $P_{t, \text{nom}} = 5,040 \text{ lb/sq ft}$

Thermo- couple	$T_e/T_t$	$T_w$ , OR	$h$ ,	$N_{St}$
			$\frac{\text{Btu}}{\text{sec-ft}^2\text{-}^\circ\text{R}}$	
$\alpha' = 45.0^\circ$ ; $T_f = 705^\circ\text{R}$ ;				
$P_t = 5,042.0 \text{ lb/sq ft}$				
1	.93359	565.1	.00336	.000941
2	.94962	583.5	.00591	.001638
3	.96565	612.1	.01016	.002816
4	.93473	550.5	.00120	.000433
5	.92672	551.1	.00254	.000704
6	.93874	572.5	.00492	.001364
7	.95477	597.5	.00810	.002245
8	.96851	613.8	.00989	.002741
9	.95305	560.1	.00089	.000247
10	.94962	557.5	.00088	.000244
11	.94275	554.5	.00125	.000346
12	.93473	555.5	.00230	.000637
13	.93301	569.5	.00490	.001358
14	.94847	593.8	.00804	.002228
15	.96507	612.1	.00985	.002730
16	.97366	617.8	.01005	.002785
17	.97425	617.5	.00984	.002727
18	.96908	568.8	.00089	.000244
19	.96450	566.5	.00088	.000244
20	.93359	572.5	.00543	.001505
21	.96965	623.1	.01231	.003412
22	.97080	622.1	.01189	.003295
23	.98454	577.8	.00090	.000249
24	.98053	576.1	.00099	.000274
25	.96794	569.5	.00108	.000299
26	.95420	562.8	.00147	.000407
27	.93817	564.8	.00263	.000729
28	.93759	575.8	.00574	.001591
29	.94904	601.5	.00996	.002760
30	.96221	620.1	.01265	.003506
31	.96965	626.1	.01312	.003636
32	.97080	624.1	.01260	.003492
33	.97252	624.1	.01211	.003356
34	.98969	581.1	.00090	.000249
35	.99542	585.8	.00111	.000308
36	.96851	574.1	.00142	.000394
37	.94217	579.8	.00601	.001666
38	.96908	627.8	.01379	.003822
39	.97309	627.1	.01287	.003567
40	.97652	626.8	.01200	.003326
41	.97538	579.5	.00188	.000521
42	.96965	577.5	.00205	.000568
43	.94790	569.5	.00343	.000951
44	.94389	582.5	.00611	.001693
45	.95992	609.1	.00988	.002738
46	.97080	626.1	.01244	.003448
47	.97137	629.1	.01347	.003733
60	1.00343	586.5	.00058	.000161
61	.99656	582.8	.00062	.000172
62	.96507	566.5	.00088	.000244
63	.95820	566.5	.00118	.000327
64	.94332	560.5	.00216	.000599
65	.93359	568.1	.00473	.001311
66	.94733	596.8	.00893	.002475
67	.96336	621.1	.01255	.003478
68	.97366	631.5	.01390	.003852
69	.97767	628.8	.01247	.003456
70	.97939	627.1	.01136	.003148
71	.99255	584.1	.00112	.000310
72	.98339	578.1	.00101	.000280
73	.96851	570.5	.00111	.000308
74	.95763	567.1	.00119	.000330
75	.89122	516.8	.00060	.000166
76	.93931	575.1	.00426	.001181
77	.95362	597.8	.00779	.002159
78	.96107	615.8	.01152	.003193
79	.97366	631.5	.01388	.003847
80	.97881	629.5	.01243	.003445
81	.98912	625.8	.00978	.002710
83	.98511	581.1	.00139	.000385
84	.96679	571.1	.00145	.000402
85	.95763	569.1	.00162	.000449
86	.94504	561.5	.00216	.000599
87	.93702	566.5	.00420	.001164
88	.94103	587.8	.00758	.002101
89	.95763	613.1	.01130	.003132
90	.97080	629.5	.01387	.003844
91	.98225	628.5	.01126	.003121
93	.95820	565.8	.00105	.000291
94	.95248	563.8	.00120	.000333
95	.93645	554.5	.00199	.000552
96	.92786	558.1	.00359	.000995
97	.93759	584.5	.00734	.002034
98	.95505	608.8	.01067	.002957
99	.96851	626.5	.01329	.003683







TABLE VI. - TABULATION OF HEAT-TRANSFER MEASUREMENTS  
FOR CONFIGURATION 1 - Continued

(b)  $M = 3.51$ ;  $P_{t, \text{nom}} = 7,200 \text{ lb/sq ft}$

Thermo- couple	$T_e/T_t$	$T_w$ , OR	$h$ ,	$N_{St}$
			$\frac{\text{Btu}}{\text{sec-ft}^2\text{-}^\circ\text{R}}$	
			$\alpha' = 45.0^\circ$ ; $T_t = 708^\circ\text{R}$ ; $P_t = 7,182.0 \text{ lb/sq ft}$	
1	.92591	568.1	.00415	.000809
2	.94358	588.8	.00692	.001350
3	.96238	626.5	.01015	.001980
4	.93161	561.5	.00201	.000392
5	.92135	559.5	.00304	.000593
6	.92933	575.5	.00591	.001153
7	.95099	605.1	.00908	.001771
8	.96523	622.1	.01077	.002101
9	.95383	566.1	.00130	.000254
10	.94928	565.8	.00142	.000277
11	.94073	559.5	.00179	.000349
12	.93104	560.5	.00326	.000636
13	.92819	576.8	.00617	.001203
14	.94757	604.8	.00935	.001824
15	.96409	624.8	.01136	.002216
16	.97207	631.1	.01179	.002300
17	.97207	638.8	.01131	.002206
18	.96865	574.1	.00131	.000256
19	.96295	571.1	.00147	.000287
20	.92933	581.1	.00694	.001354
21	.96808	643.1	.01300	.002536
22	.96751	632.8	.01317	.002569
23	.98005	581.1	.00133	.000259
24	.97663	579.5	.00141	.000275
25	.96466	573.8	.00171	.000334
26	.95099	567.8	.00209	.000408
27	.93332	565.8	.00395	.000770
28	.93446	585.5	.00711	.001387
29	.94757	613.1	.01137	.002218
30	.96124	631.5	.01383	.002698
31	.96808	637.5	.01449	.002826
32	.96808	634.8	.01412	.002754
33	.97036	634.8	.01347	.002627
34	.98062	581.5	.00120	.000234
35	.98575	586.1	.00144	.000281
36	.96409	575.5	.00189	.000369
37	.94073	589.5	.00704	.001373
38	.96865	638.5	.01465	.002857
39	.97264	638.5	.01394	.002719
40	.97435	636.5	.01269	.002475
41	.96922	584.5	.00192	.000374
42	.96181	579.8	.00258	.000503
43	.94415	576.1	.00428	.000835
44	.94244	592.1	.00769	.001500
45	.96124	620.5	.01065	.002077
46	.96751	634.5	.01294	.002524
47	.97093	639.1	.01395	.002721
48	.98290	580.1	.00085	.000166
49	.97891	577.5	.00090	.000176
50	.95725	566.5	.00118	.000230
51	.94814	563.5	.00152	.000296
52	.93503	562.1	.00304	.000593
53	.92990	575.5	.00579	.001129
54	.94586	608.1	.01046	.002040
55	.96295	631.8	.01331	.002596
56	.97321	642.5	.01498	.002922
57	.97609	639.8	.01385	.002701
58	.97777	636.8	.01185	.002311
59	.97891	582.5	.00154	.000300
60	.96979	575.8	.00137	.000267
61	.95839	569.1	.00145	.000283
62	.95042	565.8	.00165	.000322
63	.93731	562.5	.00288	.000562
64	.93332	574.8	.00536	.001045
65	.94700	606.5	.01010	.001970
66	.95896	627.5	.01350	.002633
67	.97093	642.1	.01577	.003076
68	.97663	640.8	.01428	.002785
69	.98290	634.1	.01133	.002210
70	.97549	584.5	.00221	.000431
71	.95782	570.8	.00178	.000347
72	.95440	569.8	.00202	.000394
73	.94187	565.8	.00300	.000585
74	.93161	572.1	.00531	.001036
75	.93845	598.8	.00983	.001917
76	.95554	625.8	.01407	.002744
77	.96808	641.1	.01645	.003209
78	.97720	638.8	.01329	.002592
79	.94814	561.8	.00127	.000248
80	.94415	560.8	.00150	.000293
81	.92933	563.8	.00246	.000480
82	.92192	569.5	.00473	.000923
83	.93446	595.1	.00922	.001798
84	.95156	621.1	.01348	.002629
85	.96694	638.8	.01566	.003054





TABLE VI. - TABULATION OF HEAT-TRANSFER MEASUREMENTS  
FOR CONFIGURATION 1 - Continued

(c)  $M = 4.65$ ;  $P_{t, \text{nom}} = 8,640 \text{ lb/sq ft}$

Thermo- couple	$T_e/T_t$	$T_w$ OR	$h$	$N_{St}$
			$\frac{\text{Btu}}{\text{sec-ft}^2\text{-}^\circ\text{R}}$	
$\alpha' = 45.0^\circ$ ; $T_t = 670^\circ\text{R}$ ; $P_t = 8,641.0 \text{ lb/sq ft}$				
1	.95609	572.8	.00222	.000935
2	.96920	589.8	.00309	.001501
3	.98289	611.1	.00412	.001735
4	.96236	567.8	.00102	.000429
5	.95153	566.5	.00170	.000716
6	.95723	581.8	.00263	.001107
7	.96977	596.8	.00395	.001663
8	.98232	609.5	.00471	.001983
9	.98517	576.1	.00031	.000131
10	.97462	572.5	.00047	.000198
11	.96635	568.8	.00087	.000366
12	.95495	567.8	.00153	.000644
13	.94811	576.8	.00266	.001120
14	.95837	590.1	.00377	.001587
15	.97263	604.8	.00449	.001891
16	.98118	610.5	.00485	.002042
17	.98289	614.1	.00481	.002025
18	1.00057	584.1	.00037	.000156
20	.94468	574.8	.00303	.001276
21	.97662	612.8	.00559	.002354
22	.97890	617.1	.00575	.002421
23	1.01482	592.5	.00033	.000139
24	1.00741	589.1	.00039	.000164
25	.98802	580.1	.00070	.000295
26	.97263	573.8	.00112	.000472
27	.95267	570.8	.00186	.000763
28	.94526	575.5	.00313	.001318
29	.95723	594.8	.00484	.002048
30	.96977	608.8	.00596	.002510
31	.97776	615.5	.00618	.002602
32	.97091	613.5	.00616	.002594
33	.98118	618.8	.00597	.002514
34	1.01938	596.1	.00044	.000185
35	1.02164	599.5	.00056	.000236
36	.98688	581.5	.00097	.000408
37	.95096	580.8	.00342	.001440
38	.97719	616.8	.00628	.002644
39	.98232	618.5	.00647	.002724
40	.98517	621.5	.00565	.002379
41	.99201	587.8	.00121	.000509
42	.98346	586.8	.00155	.000653
43	.96008	576.5	.00222	.000935
44	.95210	585.5	.00338	.001423
45	.96749	602.8	.00495	.002084
46	.97947	616.1	.00613	.002581
47	.97890	617.8	.00640	.002695
60	1.03649	605.5	.00038	.000160
61	1.02965	601.8	.00037	.000156
62	.98688	579.8	.00067	.000292
63	.97320	574.5	.00103	.000434
64	.95837	573.5	.00190	.000800
65	.94640	575.1	.00308	.001297
66	.95780	595.1	.00481	.002025
67	.97205	612.5	.00629	.002649
68	.98175	621.1	.00717	.003019
69	.98574	624.5	.00670	.002821
70	.98745	623.1	.00584	.002459
71	1.01995	598.5	.00056	.000236
72	1.01482	594.5	.00051	.000215
73	.99201	583.8	.00082	.000345
74	.97719	576.8	.00108	.000455
75	.88367	522.2	.00586	.002467
76	.95609	581.8	.00293	.001234
77	.96749	600.1	.00472	.001987
78	.97377	612.1	.00634	.002670
79	.98745	625.5	.00718	.003023
80	.98859	626.5	.00690	.002905
81	1.00228	628.1	.00512	.002156
83	1.02337	597.8	.00035	.000147
84	.98631	577.8	.00047	.000198
85	.98232	579.1	.00089	.000375
86	.95666	568.5	.00163	.000686
87	.95210	575.1	.00285	.001200
88	.95324	590.1	.00477	.002009
89	.97091	610.8	.00575	.002421
90	.98403	624.5	.00687	.002893
91	.99714	634.5	.00485	.002042
93	.96806	567.8	.00060	.000253
94	.96179	566.1	.00080	.000337
95	.94524	561.1	.00163	.000686
96	.94126	570.5	.00282	.001187
97	.95153	589.1	.00491	.002067
98	.96749	608.5	.00665	.002800
99	.98346	623.8	.00853	.003592





TABLE VI. - TABULATION OF HEAT-TRANSFER MEASUREMENTS  
FOR CONFIGURATION 1 - Concluded

(d)  $M = 4.65$ ;  $P_{t, \text{nom}} = 12,240 \text{ lb/sq ft}$

Thermo- couple	$T_e/T_t$	$T_w$ , OR	$h$ ,	$N_{St}$
			$\frac{\text{Btu}}{\text{sec-ft}^2 \cdot ^\circ\text{R}}$	
$\alpha = 45.0^\circ$ ; $T_t = 675^\circ\text{R}$ ;				
$P_t = 12,247.0 \text{ lb/sq ft}$				
1	.95053	571.1	.00283	.000843
2	.96417	594.8	.00406	.001209
3	.97953	614.8	.00513	.001528
4	.96076	569.8	.00124	.000369
5	.94769	567.8	.00200	.000596
6	.95280	581.8	.00346	.001030
7	.96531	597.5	.00495	.001474
8	.97896	616.5	.00560	.001667
9	.98351	577.8	.00043	.000128
10	.97611	575.5	.00060	.000179
11	.96417	569.8	.00092	.000274
12	.95223	568.1	.00200	.000596
13	.94427	580.8	.00362	.001078
14	.95621	593.1	.00488	.001453
15	.97157	609.1	.00611	.001819
16	.98009	615.5	.00639	.001903
17	.98123	621.8	.00638	.001900
20	.94200	576.8	.00463	.001379
21	.97555	622.8	.00726	.002162
22	.97668	623.1	.00731	.002177
23	1.00909	592.8	.00048	.000143
24	1.00341	590.1	.00058	.000173
25	.98578	583.1	.00090	.000268
26	.97157	577.5	.00125	.000372
27	.95110	570.5	.00242	.000721
28	.94655	581.8	.00406	.001209
29	.95565	598.8	.00614	.001828
30	.96929	618.5	.00697	.002075
31	.97668	624.8	.00754	.002245
32	.96929	619.8	.00775	.002308
33	.97896	622.1	.00787	.002343
34	1.01194	595.8	.00058	.000173
35	1.01592	600.1	.00087	.000259
36	.98521	583.8	.00109	.000325
37	.94882	589.5	.00474	.001411
38	.97611	625.8	.00784	.002334
39	.98066	627.1	.00761	.002266
40	.98351	629.1	.00656	.001953
41	.98805	590.1	.00149	.000444
42	.98237	589.8	.00200	.000596
43	.95792	578.1	.00293	.000872
44	.95053	588.5	.00439	.001307
45	.96702	606.5	.00603	.001796
46	.97839	620.1	.00689	.002052
47	.97725	626.1	.00750	.002233
60	1.02615	601.8	.00046	.000137
61	1.02217	599.8	.00074	.000140
62	.98464	582.1	.00074	.000220
63	.97100	575.5	.00110	.000328
64	.95565	574.5	.00222	.000661
66	.95678	599.1	.00648	.001930
67	.97213	617.5	.00790	.002352
68	.98123	633.1	.00862	.002567
69	.98407	630.5	.00827	.002463
70	.98521	628.1	.00693	.002064
71	1.01137	595.1	.00055	.000164
72	1.00796	592.5	.00061	.000182
73	.98919	584.8	.00098	.000292
74	.97498	579.5	.00124	.000369
75	.95678	580.8	.00228	.000679
76	.95337	580.8	.00392	.001167
77	.96588	603.5	.00641	.001909
78	.97327	622.8	.00810	.002412
79	.98635	635.8	.00958	.002853
80	.98749	633.5	.00868	.002585
81	1.00000	632.1	.00584	.001739
83	1.00852	592.1	.00046	.000137
84	.98180	577.5	.00054	.000161
85	.97327	574.8	.00077	.000229
86	.95394	568.8	.00183	.000545
87	.94882	579.5	.00364	.001084
88	.95280	594.1	.00651	.001938
89	.97157	616.1	.00888	.002644
90	.98464	633.1	.01097	.003266
91	.99488	632.5	.00786	.002340
93	.96417	568.1	.00063	.000188
94	.95849	568.1	.00093	.000277
95	.94257	562.1	.00168	.000500
96	.93802	572.1	.00348	.001036
97	.95053	593.1	.00670	.001995
98	.96759	613.5	.00951	.002832
99	.98464	635.8	.01042	.003103







TABLE VII. - TABULATION OF HEAT-TRANSFER MEASUREMENTS  
FOR CONFIGURATION 2 - Continued

(a)  $M = 3.51$ ;  $p_{t, \text{nom}} = 5,040 \text{ lb/sq ft}$

Thermo- couple	$T_e/T_t$	$T_w$ OR	$h$	$N_{St}$
			$\frac{Btu}{\text{sec-ft}^2 \cdot \text{OR}}$	
$\alpha' = 45.0^\circ$ ; $T_t = 704^\circ \text{ R}$ ; $p_t = 5,045.0 \text{ lb/sq ft}$				
4	.93741	551.5	.00141	.000391
5	.92880	559.8	.00291	.000806
6	.94086	576.8	.00556	.001540
7	.96038	603.8	.00784	.002171
8	.97416	621.1	.00991	.002745
9	.96095	566.1	.00128	.000355
10	.95292	559.1	.00108	.000299
11	.94430	555.1	.00153	.000424
12	.93167	559.5	.00256	.000709
13	.93627	572.1	.00492	.001363
14	.95062	595.5	.00725	.002008
15	.96727	615.5	.00928	.002570
16	.97646	620.1	.00901	.002495
17	.97875	620.8	.00906	.002509
18	.97071	569.5	.00103	.000285
19	.96153	563.5	.00088	.000244
20	.93225	570.8	.00507	.001404
21	.97186	625.8	.01093	.003027
22	.97358	626.1	.01154	.003196
23	.96727	567.8	.00100	.000277
24	.97014	568.5	.00087	.000241
25	.96325	565.1	.00113	.000313
26	.95119	560.1	.00141	.000391
27	.93914	560.8	.00285	.000789
28	.93052	570.5	.00517	.001432
29	.95005	600.1	.00856	.002371
30	.96325	620.1	.00875	.002423
31	.97301	629.1	.01080	.002991
32	.96268	635.5	.01222	.003384
33	.97416	627.8	.01203	.003332
34	.96727	567.8	.00100	.000277
35	.98162	575.8	.00092	.000255
36	.96382	565.5	.00088	.000244
37	.94316	577.8	.00493	.001365
38	.97186	628.8	.01069	.002961
39	.97646	636.8	.01124	.003113
40	.97760	649.1	.00927	.002567
41	.96899	568.5	.00088	.000244
42	.96497	569.1	.00099	.000274
43	.95005	568.8	.00216	.000598
44	.94373	577.1	.00451	.001249
45	.95981	605.5	.00733	.002030
46	.97014	624.5	.00942	.002609
47	.97129	646.1	.00919	.002545
50	.93052	555.1	.00289	.000800
51	.94603	571.8	.00407	.001127
52	.96482	613.5	.00870	.002410
53	.99023	640.5	.00970	.002687
54	.99425	654.5	.00987	.002734
55	.93052	559.8	.00298	.000825
56	.93741	574.8	.00532	.001473
57	.96268	609.5	.00843	.002335
58	.98736	638.8	.00987	.002734
59	.99138	648.8	.01098	.003041
60	.97244	569.1	.00078	.000216
61	.97990	572.8	.00074	.000205
62	.95866	560.8	.00078	.000216
63	.95119	558.1	.00119	.000330
64	.94316	559.8	.00218	.000604
65	.93454	569.1	.00469	.001299
66	.94890	598.8	.00795	.002202
67	.96382	621.5	.01010	.002797
68	.97531	646.1	.01149	.003182
69	.98105	645.8	.01080	.002991
70	.97818	635.5	.01059	.002933
71	.98507	578.5	.00097	.000269
72	.97473	569.1	.00069	.000191
73	.96382	565.1	.00104	.000288
74	.95521	561.1	.00131	.000363
75	.94086	561.1	.00207	.000573
76	.93856	568.5	.00420	.001163
77	.95464	598.8	.00734	.002033
78	.96095	637.1	.00993	.002750
79	.97588	646.1	.01144	.003168
80	.97646	629.8	.01142	.003163
81	.98736	639.5	.00856	.002371
83	.98851	578.5	.00083	.000230
84	.96325	566.1	.00125	.000346
85	.98449	580.1	.00148	.000410
86	.94258	560.1	.00230	.000637
87	.94086	569.8	.00422	.001169
88	.94201	589.1	.00722	.002000
89	.95981	614.5	.00966	.002675
90	.97014	642.1	.01135	.003144
91	.98220	642.1	.00957	.002651
93	.95119	558.8	.00109	.000302
94	.94717	559.1	.00127	.000352
95	.93225	550.8	.00201	.000557
96	.93052	565.5	.00371	.001028
97	.93741	585.5	.00718	.001989
98	.95292	609.5	.00993	.002750
99	.96727	642.1	.01196	.003312





TABLE VII. - TABULATION OF HEAT-TRANSFER MEASUREMENTS  
FOR CONFIGURATION 2 - Continued

(b)  $M = 3.51$ ;  $P_{t, \text{nom}} = 7,200 \text{ lb/sq ft}$

Thermo- couple	$T_e/T_t$	$T_w$ , OR	$h$ ,	$N_{St}$
			Btu $\text{sec-ft}^2\text{-}^\circ\text{R}$	
$\alpha' = 45.0^\circ$ ; $T_s = 705^\circ\text{R}$ ; $P_t = 7,200.0 \text{ lb/sq ft}$				
4	.93749	553.8	.00170	.000330
5	.92544	562.8	.00390	.000756
6	.93691	581.8	.00740	.001435
7	.95756	611.8	.01174	.002276
8	.97247	637.8	.01256	.002435
9	.95985	568.1	.00171	.000332
10	.95240	561.5	.00147	.000285
11	.94322	557.8	.00180	.000349
12	.92716	557.1	.00373	.000723
13	.93175	585.1	.00690	.001358
14	.94838	605.8	.01134	.002203
15	.96673	635.1	.01269	.002461
16	.97534	641.1	.01312	.002544
17	.97648	641.8	.01330	.002579
18	.97075	571.8	.00132	.000256
19	.96157	567.8	.00132	.000256
20	.92831	585.8	.00737	.001429
21	.97017	645.8	.01533	.002972
22	.97132	645.5	.01532	.002971
23	.96903	570.1	.00118	.000229
24	.97189	571.1	.00106	.000206
25	.96387	567.1	.00116	.000225
26	.95068	562.5	.00195	.000378
27	.93634	569.5	.00388	.000752
28	.92774	585.1	.00740	.001435
29	.95010	619.1	.01157	.002243
30	.96272	638.5	.01415	.002744
31	.97132	647.1	.01543	.002992
32	.96272	640.5	.01565	.003035
33	.97247	646.8	.01562	.003029
34	.96903	570.8	.00120	.000233
35	.98279	578.5	.00119	.000231
36	.96444	567.8	.00108	.000209
37	.94035	584.1	.00732	.001419
38	.97017	646.5	.01523	.002953
39	.97476	647.1	.01510	.002928
40	.97591	646.5	.01442	.002796
41	.97017	571.5	.00107	.000207
42	.96559	570.5	.00109	.000211
43	.94838	573.1	.00290	.000562
44	.94150	589.8	.00630	.001222
45	.95813	621.8	.01031	.001999
46	.96845	640.5	.01308	.002536
47	.97017	644.1	.01418	.002749
50	.92716	556.1	.00363	.000704
51	.94093	581.5	.00525	.001018
52	.96100	619.8	.01151	.002232
53	.98853	652.1	.01224	.002373
54	.99311	656.1	.01229	.002383
55	.92716	556.5	.00354	.000686
56	.93347	578.1	.00679	.001317
57	.95928	622.8	.01081	.002096
58	.98451	657.8	.01333	.002585
59	.98853	655.1	.01331	.002581
60	.96731	567.8	.00096	.000186
61	.97534	571.8	.00094	.000182
62	.95297	557.8	.00096	.000186
63	.94666	557.8	.00158	.000268
64	.93749	560.5	.00303	.000588
65	.93003	573.5	.00620	.001202
66	.94724	606.8	.01227	.002379
67	.96272	639.5	.01448	.002808
68	.97362	651.1	.01637	.003174
69	.97763	642.5	.01710	.003316
70	.97591	638.5	.01566	.003017
71	.97419	574.5	.00128	.000248
72	.96559	566.1	.00087	.000169
73	.95698	563.5	.00132	.000256
74	.94781	559.1	.00148	.000287
75	.93405	560.8	.00274	.000531
76	.93232	571.1	.00564	.001094
77	.95182	607.5	.01049	.002034
78	.95028	635.1	.01436	.002784
79	.97476	651.5	.01632	.003164
80	.97476	649.1	.01587	.003077
81	.98336	641.1	.01165	.002259
83	.97648	574.5	.00131	.000254
84	.95756	566.5	.00172	.000334
85	.97992	584.1	.00205	.000397
86	.94035	561.8	.00282	.000568
87	.93921	575.8	.00538	.001043
88	.94035	597.5	.01044	.002024
89	.95813	638.1	.01377	.002670
90	.96845	639.1	.01755	.003403
91	.97820	643.8	.01273	.002468
93	.94609	557.8	.00147	.000285
94	.94265	556.8	.00160	.000310
95	.92831	551.1	.00251	.000487
96	.92659	562.8	.00493	.000956
97	.93577	593.8	.01024	.001986
98	.95240	628.5	.01383	.002682
99	.96845	638.5	.01729	.003352







TABLE VII. - TABULATION OF HEAT-TRANSFER MEASUREMENTS  
FOR CONFIGURATION 2 - Continued

(c)  $M = 4.65$ ;  $P_{t, \text{nom}} = 8,640 \text{ lb/sq ft}$

Thermo- couple	$T_e/T_t$	$T_w$ , OR	$h$ ,	$N_{St}$
			$\frac{\text{Btu}}{\text{sec-ft}^2\text{-}^\circ\text{F}}$	
$\alpha' = 45.0^\circ$ ; $T_t = 672^\circ \text{R}$ ;				
$P_t = 8,651.0 \text{ lb/sq ft}$				
4	.95269	567.5	.00094	.000396
5	.94537	567.1	.00186	.000784
6	.95494	584.5	.00354	.001493
7	.97127	599.8	.00500	.002109
8	.98479	613.1	.00579	.002442
9	.97747	578.5	.00039	.000164
10	.96508	571.5	.00055	.000232
11	.95551	567.1	.00076	.000321
12	.94312	564.8	.00179	.000755
13	.94424	576.8	.00316	.001333
14	.95551	589.1	.00471	.001986
15	.97240	609.5	.00568	.002395
16	.98141	610.8	.00595	.002509
17	.98366	612.5	.00609	.002568
18	.99098	586.1	.00041	.000173
19	.97465	577.5	.00047	.000198
20	.93805	571.5	.00346	.001459
21	.97578	611.5	.00489	.002096
22	.97803	613.1	.00702	.002960
23	.99155	586.8	.00043	.000181
24	.98986	585.8	.00041	.000173
25	.97691	581.8	.00065	.000274
26	.96226	572.5	.00099	.000418
27	.94706	568.5	.00188	.000793
28	.92904	571.1	.00367	.001548
29	.95362	591.1	.00527	.002222
30	.96621	605.5	.00659	.002779
31	.97803	619.5	.00734	.003095
32	.96733	607.5	.00731	.003083
33	.97860	613.8	.00694	.002927
34	1.00112	592.5	.00040	.000169
35	1.01126	598.5	.00041	.000173
36	.98197	582.8	.00060	.000253
37	.94819	576.5	.00359	.001514
38	.97353	613.8	.00764	.003222
39	.97916	614.8	.00739	.003117
40	.98254	614.8	.00648	.002733
41	.99098	589.8	.00093	.000392
42	.97972	585.1	.00112	.000472
43	.96114	577.8	.00205	.000865
44	.94988	579.8	.00361	.001522
45	.96452	596.5	.00535	.002256
46	.97296	611.5	.00616	.002598
47	.97465	614.1	.00783	.003302
50	.94706	567.8	.00197	.000831
51	.96114	580.1	.00253	.001067
52	.97747	607.8	.00573	.002416
53	1.00337	634.1	.00568	.002395
54	1.00675	637.5	.00727	.003066
55	.94368	566.5	.00187	.000789
56	.95044	578.8	.00346	.001459
57	.97296	602.8	.00468	.001974
58	.99774	630.5	.00559	.002357
59	1.00168	640.8	.00731	.003083
62	.98423	581.8	.00038	.000160
63	.96677	573.8	.00089	.000375
64	.95438	571.5	.00176	.000742
65	.94199	573.1	.00330	.001392
66	.95438	592.5	.00554	.002336
67	.96902	613.8	.00710	.002994
68	.98141	619.1	.00794	.003348
69	.98085	616.8	.00777	.003277
70	.98366	616.1	.00661	.002788
71	1.03322	610.8	.00038	.000160
72	1.02365	605.8	.00028	.000118
73	.99211	587.1	.00052	.000219
74	.97522	579.1	.00078	.000329
75	.95663	576.1	.00174	.000734
76	.95044	577.1	.00312	.001316
77	.96395	601.1	.00534	.002252
78	.96959	608.5	.00706	.002977
79	.98423	621.8	.00828	.003492
80	.98366	616.5	.00787	.003319
81	.99887	622.5	.00611	.002577
83	1.03097	609.8	.00041	.000173
84	.99549	589.5	.00048	.000202
85	1.01182	601.8	.00085	.000358
86	.96170	574.8	.00145	.000611
87	.95663	579.1	.00303	.001278
88	.95269	586.8	.00527	.002222
89	.96902	608.1	.00717	.003024
90	.98085	619.8	.00855	.003606
91	.99718	625.5	.00711	.002998
93	.97634	578.1	.00042	.000177
94	.96790	575.5	.00073	.000308
95	.94706	569.1	.00150	.000633
96	.94650	572.5	.00286	.001206
97	.94875	587.1	.00544	.002294
98	.96395	604.8	.00752	.003171
99	.98085	628.8	.00893	.003766





TABLE VII. - TABULATION OF HEAT-TRANSFER MEASUREMENTS  
FOR CONFIGURATION 2 - Concluded

(d)  $M = 4.65$ ;  $P_{t, \text{nom}} = 12,240 \text{ lb/sq ft}$

Thermo- couple	$T_e/T_t$	$T_w$ , OR	$h$ , Btu	$N_{St}$
			$\frac{\text{sec-ft}^2}{\text{OR}}$	
$\alpha' = 45.00$ ; $T_f = 674.0 \text{ R}$ ; $P_t = 12,229.0 \text{ lb/sq ft}$				
4	.96086	576.1	.00145	.000433
5	.94691	570.1	.00278	.000830
6	.95369	588.5	.00448	.001338
7	.96950	609.1	.00667	.001992
8	.98305	623.8	.00824	.002461
9	.98475	583.1	.00080	.000239
10	.97402	577.1	.00077	.000230
11	.96272	572.5	.00116	.000346
12	.94635	568.8	.00230	.000687
13	.94665	582.1	.00420	.001255
14	.95538	600.1	.00672	.002007
15	.97232	617.8	.00832	.002485
16	.98079	623.8	.00875	.002614
17	.98305	621.5	.00969	.002894
18	.99830	591.1	.00068	.000203
19	.98249	582.5	.00083	.000248
20	.93844	580.8	.00479	.001431
21	.97684	624.8	.00934	.002790
22	.97797	622.1	.01115	.003330
23	1.00564	595.1	.00063	.000188
24	1.00282	593.1	.00065	.000194
25	.98701	585.5	.00087	.000260
26	.97119	579.8	.00136	.000406
27	.95143	573.1	.00247	.000738
28	.93562	575.8	.00446	.001332
29	.95595	603.5	.00798	.002384
30	.96837	615.1	.01041	.003109
31	.97910	623.8	.01089	.003253
32	.96893	621.1	.01053	.003145
33	.98023	623.5	.01118	.003339
34	1.01694	600.1	.00047	.000140
35	1.02428	604.8	.00055	.000164
36	.99209	588.5	.00083	.000248
37	.95143	584.8	.00490	.001464
38	.97628	623.1	.01129	.003372
39	.98136	628.5	.01023	.003056
40	.98418	623.8	.00967	.002888
41	.99943	595.1	.00120	.000358
42	.98927	590.8	.00149	.000445
43	.96668	583.1	.00276	.000824
45	.96837	610.5	.00686	.002049
46	.97684	623.8	.00887	.002649
47	.97854	627.1	.00986	.002945
50	.94747	570.1	.00258	.000771
51	.95990	582.8	.00316	.000944
52	.97628	613.5	.00686	.002049
53	1.00282	636.9	.00826	.002467
54	1.00734	643.1	.00841	.002512
55	.94691	570.1	.00260	.000777
56	.95143	583.5	.00416	.001243
57	.97345	609.1	.00663	.001980
58	.99717	636.5	.00836	.002497
59	1.00282	640.8	.00870	.002599
60	1.04517	614.1	.00026	.000078
61	1.03388	608.1	.00028	.000084
62	.98418	582.1	.00071	.000212
63	.96893	576.1	.00116	.000346
64	.95482	576.8	.00253	.000756
65	.94465	579.5	.00440	.001314
66	.95820	601.8	.00782	.002336
67	.97232	627.8	.01065	.003181
68	.98418	629.5	.01238	.003698
69	.98249	631.1	.01101	.003289
70	.98531	629.5	.00943	.002817
71	1.02371	606.1	.00081	.000242
72	1.00790	595.5	.00064	.000191
73	.98814	585.8	.00077	.000230
74	.97289	578.5	.00120	.000358
75	.95482	573.1	.00222	.000663
76	.94973	580.8	.00418	.001249
77	.96555	605.1	.00778	.002324
78	.97232	618.1	.01105	.003301
79	.98701	636.1	.01214	.003626
80	.98475	633.1	.01176	.003513
81	.99943	633.8	.00811	.002422
83	1.02541	605.8	.00061	.000182
84	.99322	587.8	.00073	.000218
85	1.00960	599.8	.00117	.000349
86	.96103	576.1	.00217	.000648
87	.95708	583.5	.00386	.001153
88	.95595	598.1	.00724	.002163
89	.97232	617.5	.01022	.003053
90	.98475	634.5	.01187	.003546
91	.99661	636.8	.00976	.002915
93	.97684	577.8	.00067	.000200
94	.97006	575.8	.00081	.000242
95	.94973	568.5	.00187	.000559
96	.94691	576.1	.00370	.001105
97	.95199	599.5	.00738	.002204
98	.96724	627.5	.01154	.003447
99	.98418	634.5	.01261	.003767







TABLE VIII. - TABULATION OF HEAT-TRANSFER MEASUREMENTS FOR CONFIGURATION 3 - Continued

(a)  $M = 3.51$ ;  $P_{t, \text{nom}} = 5,040 \text{ lb/sq ft}$

Thermo-couple	$T_e/T_t$	$T_w, \text{OR}$	$h,$	$N_{St}$	$T_e/T_t$	$T_w, \text{OR}$	$h,$	$N_{St}$
			$\text{sec-ft}^2 \cdot \text{OR}^{-1}$				$\text{sec-ft}^2 \cdot \text{OR}^{-1}$	
$\alpha' = 37.5^\circ; T_t = 702^\circ \text{R};$					$\alpha' = 45.0^\circ; T_t = 702^\circ \text{R};$			
$P_t = 5,042.0 \text{ lb/sq ft}$					$P_t = 5,039.0 \text{ lb/sq ft}$			
1	.91464	562.1	.00580	.001604	.93134	558.5	.00307	.000850
2	.92897	591.5	.00932	.002577	.94278	577.8	.00497	.001376
3	.94443	623.5	.01565	.004328	.95765	610.1	.00782	.002165
4	.91522	555.1	.00286	.000791	.92790	551.5	.00157	.000435
5	.91064	554.5	.00453	.001253	.92161	554.1	.00253	.000701
6	.92725	582.1	.00732	.002024	.93534	569.5	.00428	.001185
7	.93698	607.5	.01147	.003172	.94450	589.8	.00694	.001922
8	.94042	618.8	.01520	.004203	.95079	609.5	.00881	.002439
9	.92897	551.5	.00151	.000418	.92790	550.8	.00128	.000354
10	.92381	546.5	.00138	.000382	.92561	546.5	.00104	.000288
11	.91751	543.8	.00194	.000536	.92447	544.8	.00114	.000316
12	.91751	554.8	.00367	.001015	.92332	550.1	.00228	.000631
13	.92209	572.8	.00598	.001654	.92504	562.1	.00396	.001096
14	.93240	594.1	.00875	.002420	.93534	588.5	.00628	.001739
15	.94959	611.8	.01058	.002926	.95537	605.8	.00839	.002323
16	.95990	620.8	.01181	.003266	.97024	619.5	.00976	.002702
17	.95990	629.5	.01334	.003689	.97194	632.1	.01045	.002893
18	.94099	556.5	.00116	.000321	.94335	557.8	.00114	.000316
19	.93527	549.5	.00084	.000232	.93935	554.1	.00108	.000299
20	.92209	570.1	.00530	.001466	.92390	563.5	.00432	.001196
21	.95589	608.1	.00905	.002503	.96795	629.5	.01062	.002941
22	.96505	626.8	.01141	.003155	.98054	643.1	.01163	.003220
23	.93813	555.8	.00125	.000346	.94736	559.5	.00108	.000299
24	.94558	555.8	.00080	.000221	.94850	559.5	.00107	.000296
25	.93527	551.5	.00085	.000235	.94278	555.8	.00108	.000299
26	.92209	544.8	.00131	.000362	.93076	549.8	.00136	.000377
27	.92266	554.8	.00279	.000772	.92576	556.8	.00245	.000678
28	.91407	561.8	.00445	.001231	.91245	555.5	.00434	.001202
29	.94214	597.1	.00623	.001723	.93820	587.8	.00722	.001999
30	.95131	601.5	.00711	.001966	.95079	613.5	.00926	.002564
31	.96734	608.1	.00708	.001958	.97368	628.1	.01095	.003032
32	.94787	599.5	.00805	.002226	.96166	631.1	.01204	.003334
33	.96219	633.5	.00954	.002638	.97825	646.8	.01284	.003555
34	.94615	560.5	.00123	.000340	.95880	566.5	.00103	.000285
35	.96677	567.8	.00073	.000202	.97139	571.8	.00094	.000260
36	.93756	550.8	.00091	.000252	.94507	556.1	.00096	.000266
37	.93240	571.1	.00416	.001150	.92619	562.8	.00425	.001177
38	.96563	608.8	.00698	.001930	.96795	633.1	.01156	.003201
39	.96563	604.8	.00661	.001828	.97825	642.1	.01218	.003372
40	.96792	626.1	.01010	.002793	.98512	655.1	.01363	.003774
44	.92438	571.5	.00540	.001493	.92046	560.5	.00448	.001240
60	.96792	570.8	.00100	.000277	.96567	567.1	.00079	.000219
61	.96333	565.8	.00074	.000205	.96223	564.1	.00068	.000188
62	.95245	562.1	.00114	.000315	.95651	565.5	.00089	.000246
63	.94271	559.1	.00171	.000473	.94907	559.1	.00127	.000352
64	.93298	564.1	.00335	.000921	.93877	559.1	.00215	.000595
65	.92897	580.8	.00632	.001768	.93134	573.8	.00452	.001252
66	.94099	607.8	.01054	.002915	.94335	598.5	.00732	.002027
67	.95703	631.5	.01262	.003490	.96280	618.8	.00995	.002755
68	.96448	639.8	.01640	.004535	.97253	635.1	.01108	.003068
69	.97594	650.1	.01798	.004972	.98855	649.8	.01264	.003500
70	.96964	619.8	.00836	.002312	.99141	664.5	.01652	.004574
71	.97823	575.5	.00093	.000257	.97425	571.8	.00075	.000208
72	.96162	564.5	.00074	.000205	.95765	561.1	.00059	.000163
73	.95016	558.8	.00091	.000252	.95079	558.1	.00084	.000233
74	.93756	553.5	.00129	.000357	.94278	554.1	.00102	.000282
75	.92553	553.5	.00264	.000730	.93477	553.5	.00178	.000493
76	.91579	566.5	.00538	.001488	.92447	560.8	.00405	.001121
77	.93928	600.5	.00907	.002508	.94793	592.1	.00671	.001858
78	.95016	622.1	.01297	.003587	.96166	615.8	.00963	.002666
79	.96448	636.1	.01490	.004120	.97768	638.1	.01106	.003062
80	.96734	642.5	.01728	.004778	.98512	649.8	.01351	.003741
81	.97536	627.1	.00722	.001997	.99427	668.1	.01722	.004768
82	.97422	577.5	.00135	.000373	.97539	577.5	.00141	.000390
83	.97193	571.8	.00086	.000238	.96738	568.8	.00086	.000238
84	.94472	557.8	.00095	.000263	.94944	559.1	.00101	.000280
85	.96448	569.1	.00128	.000354	.97024	571.8	.00111	.000307
86	.92381	551.1	.00246	.000680	.93420	553.1	.00167	.000462
87	.92438	568.5	.00494	.001366	.93534	565.5	.00389	.001077
88	.92954	590.8	.00865	.002392	.94106	585.8	.00664	.001839
89	.94558	616.5	.01235	.003415	.95994	613.1	.00967	.002677
90	.95360	627.1	.01425	.003941	.97024	632.8	.01097	.003037
91	.97479	643.1	.01551	.004289	.99256	643.8	.01303	.003608
92	.97880	638.8	.00866	.002395	.99427	665.8	.02032	.005626
93	.95016	561.8	.00118	.000326	.95308	563.1	.00129	.000357
94	.94615	559.8	.00150	.000415	.95193	562.1	.00142	.000393
95	.93469	560.5	.00236	.000653	.94507	559.5	.00183	.000507
96	.92266	564.1	.00439	.001214	.93362	567.1	.00341	.000944
97	.92897	587.5	.00749	.002071	.94106	582.8	.00609	.001686
98	.94615	612.8	.01115	.003083	.95994	609.1	.00874	.002420
99	.95646	627.5	.01364	.003772	.97253	633.1	.01074	.002974











TABLE VIII. - TABULATION OF HEAT-TRANSFER MEASUREMENTS  
FOR CONFIGURATION 3 - Continued

(b)  $M = 3.51$ ;  $P_{t, \text{nom}} = 7,200 \text{ lb/sq ft}$

Thermo- couple	$T_e/T_t$	$T_w$ , OR	$h$ ,	$N_{St}$
			$\frac{\text{Btu}}{\text{sec-ft}^2 \cdot \text{OR}}$	
$\alpha' = 45.00$ ; $T_t = 704.0 \text{ R}$ ;				
$p_t = 7,205.0 \text{ lb/sq ft}$				
1	.92835	557.8	.00367	.000712
2	.93867	577.5	.00582	.001129
3	.95472	605.1	.00960	.001862
4	.92606	555.1	.00196	.000380
5	.91918	550.1	.00310	.000601
6	.93236	570.1	.00504	.000978
7	.94211	591.1	.00812	.001575
8	.94956	606.1	.01084	.002103
9	.93064	555.1	.00174	.000338
10	.92950	548.8	.00140	.000272
11	.92950	549.5	.00162	.000314
12	.92721	554.5	.00264	.000512
13	.92663	567.1	.00480	.000931
14	.93638	588.5	.00824	.001598
15	.95644	633.8	.01113	.002159
16	.97019	627.5	.01316	.002553
17	.97134	633.1	.01425	.002764
18	.94727	560.8	.00155	.000301
19	.94268	558.1	.00162	.000314
20	.92377	567.5	.00533	.001073
21	.96790	630.1	.01444	.002801
22	.97936	645.1	.01664	.003228
23	.94898	561.5	.00148	.000287
24	.94956	561.8	.00148	.000287
25	.94440	558.8	.00162	.000314
26	.93236	555.5	.00195	.000378
27	.92721	569.5	.00329	.000638
28	.91116	557.5	.00525	.001018
29	.93867	612.5	.00839	.001627
30	.95128	612.8	.01199	.002326
31	.97306	653.8	.01445	.002803
32	.96159	630.5	.01589	.003082
33	.97764	648.8	.01829	.003548
34	.95644	567.1	.00134	.000260
35	.96962	572.5	.00133	.000258
36	.94440	557.5	.00149	.000289
37	.92491	564.5	.00514	.000997
38	.96733	632.1	.01527	.002962
39	.97707	640.5	.01607	.003117
40	.98337	657.5	.02038	.003953
44	.92033	562.5	.00523	.001014
60	.95816	563.1	.00099	.000192
61	.95300	559.5	.00093	.000180
62	.95529	562.5	.00107	.000208
63	.94956	560.8	.00114	.000273
64	.93921	560.8	.00294	.000570
65	.93060	570.8	.00542	.001051
66	.94322	596.8	.00951	.001845
67	.96215	624.1	.01360	.002638
68	.97189	634.1	.01488	.002886
69	.98739	649.1	.01701	.003299
70	.98911	664.5	.02323	.004506
71	.96503	566.8	.00092	.000178
72	.94956	557.1	.00080	.000155
73	.94784	558.8	.00098	.000190
74	.93981	558.1	.00132	.000256
75	.93179	552.8	.00215	.000417
76	.92205	562.5	.00503	.000976
77	.94727	597.1	.00898	.001742
78	.96102	621.8	.01312	.002545
79	.97650	637.1	.01498	.002906
80	.98223	657.8	.01757	.003408
81	.99197	669.1	.02478	.004806
82	.96790	573.5	.00163	.000316
83	.95987	565.1	.00112	.000217
84	.94555	559.5	.00134	.000260
85	.96561	569.8	.00145	.000281
86	.93122	552.5	.00204	.000396
87	.93351	567.5	.00454	.000881
88	.94039	591.1	.00852	.001653
89	.95873	619.8	.01298	.002518
90	.96847	632.8	.01533	.002973
91	.98968	651.1	.01717	.003330
92	.99254	673.8	.02728	.005291
93	.94898	561.5	.00161	.000312
94	.94841	561.1	.00170	.000330
95	.94268	559.5	.00205	.000394
96	.93122	563.8	.00437	.000848
97	.93981	588.1	.00794	.001540
98	.95930	616.5	.01203	.002333
99	.97191	633.1	.01458	.002828













TABLE VIII. - TABULATION OF HEAT-TRANSFER MEASUREMENTS FOR CONFIGURATION 3 - Concluded

(d)  $M = 4.65$ ;  $P_{t, nom} = 12,240 \text{ lb/sq ft}$

Thermo-couple	$T_e/T_t$	$T_w$ , OR	$\frac{h, \text{Btu}}{\text{sec-ft}^2\text{-}^\circ\text{R}}$	$N_{St}$	$T_e/T_t$	$T_w$ , OR	$\frac{h, \text{Btu}}{\text{sec-ft}^2\text{-}^\circ\text{R}}$	$N_{St}$
	$\alpha' = 37.5^\circ$ ; $T_t = 680^\circ \text{R}$ ; $P_t = 12,228.0 \text{ lb/sq ft}$				$\alpha' = 45.0^\circ$ ; $T_t = 675^\circ \text{R}$ ; $P_t = 12,243.0 \text{ lb/sq ft}$			
1	.91600	572.1	.00498	.001495	.94440	565.5	.00246	.000735
2	.92879	594.8	.00802	.002408	.95461	579.5	.00363	.001085
3	.94548	623.5	.01184	.003556	.96936	602.5	.00531	.001587
4	.92268	565.8	.00221	.000464	.95007	564.8	.00117	.000350
5	.91544	568.1	.00388	.001165	.94043	561.8	.00207	.000619
6	.92991	590.1	.00634	.001904	.95007	575.1	.00330	.000986
7	.93825	608.8	.00979	.002940	.95518	588.1	.00497	.001486
8	.94270	621.8	.01240	.003724	.96142	604.5	.00611	.001826
9	.94659	570.1	.00079	.000237	.97447	575.8	.00064	.000191
10	.93547	566.5	.00119	.000357	.96709	571.1	.00070	.000209
11	.92991	567.1	.00191	.000574	.95802	567.5	.00114	.000341
12	.92490	571.8	.00334	.001003	.94553	564.5	.00194	.000580
13	.92546	586.8	.00537	.001613	.93873	570.8	.00332	.000992
14	.93491	599.8	.00744	.002294	.94383	580.5	.00508	.001519
15	.95049	615.8	.00968	.002907	.96142	602.5	.00656	.001961
16	.96161	624.8	.01087	.003264	.97730	615.8	.00768	.002296
17	.96106	635.8	.01110	.003333	.97957	620.1	.00807	.002412
18	.96551	580.1	.00054	.000162	.99773	588.1	.00047	.000140
19	.94882	572.5	.00076	.000228	.98127	579.8	.00063	.000188
20	.92601	582.5	.00467	.001402	.93703	570.8	.00336	.001004
21	.95828	616.8	.00872	.002619	.97503	616.8	.00818	.002445
22	.94551	632.5	.01033	.003102	.98695	628.8	.00898	.002684
23	.97274	583.5	.00034	.000102	1.00850	593.5	.00048	.000143
24	.96829	581.8	.00047	.000141	1.00397	591.5	.00043	.000129
25	.95160	574.5	.00083	.000249	.98184	580.1	.00078	.000233
26	.95881	569.8	.00144	.000432	.96312	571.1	.00114	.000341
27	.93269	574.1	.00259	.000778	.94724	566.1	.00204	.000610
28	.92323	578.1	.00406	.001219	.92681	561.5	.00337	.001007
29	.94715	602.8	.00600	.001802	.94383	583.1	.00551	.001647
30	.95661	613.1	.00696	.002090	.95518	601.1	.00715	.002137
31	.97051	620.5	.00722	.002168	.97730	619.8	.00870	.002601
32	.95271	614.8	.00805	.002417	.97106	618.8	.00962	.002876
33	.96273	628.8	.00957	.002874	.98525	631.5	.01012	.003025
34	.98776	591.5	.00028	.000084	1.02269	600.8	.00033	.000099
35	.99165	594.8	.00044	.000132	1.02779	604.5	.00045	.000135
36	.95327	575.5	.00098	.000294	.98071	578.8	.00069	.000206
37	.93547	589.5	.00506	.001520	.93589	566.8	.00341	.001019
38	.94606	631.5	.01166	.003501	.97163	618.1	.00914	.002732
39	.96884	620.5	.00790	.002372	.98468	628.5	.01001	.002992
40	.96829	631.5	.00893	.002682	.99149	638.1	.01064	.003181
44	.92824	593.1	.00613	.001841	.92965	564.8	.00382	.001142
60					1.04822	615.1	.00021	.000063
61	.99777	597.1	.00021	.000063	1.03630	608.1	.00025	.000075
62	.95939	579.8	.00095	.000285	.98184	579.8	.00076	.000227
63	.94826	576.5	.00149	.000447	.96709	573.1	.00105	.000314
64	.93547	576.5	.00321	.000964	.94837	567.1	.00208	.000622
65	.93046	593.1	.00573	.001721	.93646	573.8	.00391	.001169
66	.94048	613.1	.00916	.002751	.94553	591.5	.00644	.001925
67	.95661	628.8	.01231	.003697	.96482	609.8	.00862	.002577
68	.96551	639.8	.01383	.004153	.97617	622.5	.00953	.002849
69	.97329	650.5	.01541	.004628	.99432	638.1	.01162	.003474
70	.96829	628.8	.01016	.003051	1.00453	652.8	.01531	.004577
71	1.00277	602.5	.00041	.000123	1.01872	599.8	.00052	.000155
72	.98442	589.5	.00033	.000099	1.00397	589.5	.00031	.000093
73	.95049	573.1	.00084	.000252	.96823	571.8	.00070	.000209
74	.93658	567.5	.00143	.000429	.95575	566.1	.00108	.000323
75	.92379	566.5	.00256	.000769	.94383	562.8	.00186	.000556
76	.91600	580.1	.00527	.001583	.93362	567.5	.00385	.001151
77	.93380	602.1	.00806	.002420	.95177	590.8	.00643	.001922
78	.94826	621.5	.01209	.003631	.96823	611.1	.00859	.002568
79	.96161	637.1	.01421	.004267	.98411	628.5	.01024	.003061
80	.96662	644.5	.01790	.005375	.99886	643.1	.01294	.003868
81	.97051	646.1	.02206	.006625	1.00944	658.8	.01856	.005448
82	.98943	597.1	.00083	.000249	.99602	591.5	.00103	.000308
83	.98386	591.5	.00055	.000165	.99205	586.1	.00082	.000245
84	.94882	572.8	.00103	.000309	.96823	574.8	.00104	.000311
85	.96050	582.5	.00130	.000390	.98354	583.8	.00129	.000386
86	.92323	567.5	.00237	.000712	.94837	565.5	.00186	.000556
87	.92268	578.1	.00482	.001447	.94724	574.8	.00369	.001103
88	.92768	602.8	.00792	.002378	.95291	594.5	.00623	.001862
89	.94381	616.5	.01189	.003571	.97143	612.8	.00909	.002717
90	.95216	629.5	.01353	.004063	.98241	627.8	.01034	.003091
91	.97218	644.5	.01530	.004595	1.01021	648.8	.01217	.003638
92	.97608	657.1	.02731	.008201	1.00964	661.1	.02186	.006535
93	.95049	575.5	.00121	.000363	.97050	575.5	.00084	.000251
94	.94437	572.8	.00141	.000423	.96709	573.1	.00112	.000335
95	.93046	569.1	.00242	.000727	.95688	570.1	.00167	.000499
96	.92045	577.5	.00436	.001309	.94780	572.8	.00324	.000969
97	.92657	596.5	.00729	.002189	.95518	593.5	.00586	.001752
98	.94326	613.8	.01093	.003262	.97447	612.1	.00813	.002430
99	.95104	630.1	.01732	.005201	.98411	627.1	.01123	.003357









TABLE IX. - TABULATION OF HEAT-TRANSFER MEASUREMENTS  
FOR CONFIGURATION 4 - Continued

(a)  $M = 3.51$ ;  $P_{t, \text{nom}} = 5,040 \text{ lb/sq ft}$

Thermo- couple	$T_e/T_t$	$T_w$ OR	$h$	$N_{St}$
			$\frac{\text{Btu}}{\text{sec-ft}^2\text{-}^\circ\text{R}}$	
$\alpha' = 45.0^\circ$ ; $T_t = 711^\circ \text{R}$ ;				
$P_t = 5,049.0 \text{ lb/sq ft}$				
4	.95237	570.8	.00170	.000472
5	.94376	564.5	.00292	.000812
6	.95639	584.1	.00469	.001303
7	.96671	605.1	.00701	.001948
8	.97819	620.5	.00899	.002499
9	.97934	577.5	.00135	.000375
10	.97130	570.8	.00112	.000311
11	.95983	564.5	.00113	.000314
12	.94835	568.1	.00228	.000634
13	.94663	575.5	.00401	.001114
14	.95753	594.8	.00612	.001701
15	.97417	615.5	.00747	.002076
16	.98450	632.5	.00859	.002332
17	.98335	637.8	.00905	.002515
18	.98795	635.1	.00136	.000378
19	.97130	573.1	.00142	.000395
20	.93860	573.8	.00481	.001337
21	.97647	649.8	.00759	.002109
22	.98795	642.1	.01184	.003291
23	.98737	588.5	.00174	.000484
24	.98163	579.8	.00139	.000386
25	.97475	575.5	.00145	.000403
26	.96385	570.1	.00164	.000456
27	.95524	571.5	.00270	.000750
28	.93573	572.5	.00465	.001292
29	.96040	602.8	.00750	.002084
30	.96557	625.8	.00913	.002547
31	.96049	639.5	.01014	.002818
32	.96671	635.5	.01131	.003143
33	.98795	654.5	.01185	.003293
34	.98508	580.5	.00131	.000364
35	.99024	583.5	.00139	.000386
36	.97532	574.5	.00125	.000347
37	.94491	578.5	.00483	.001342
38	.97647	637.8	.01022	.002840
39	.98909	649.8	.01101	.003060
40	.99368	663.1	.01294	.003596
41	.98565	578.1	.00100	.000278
42	.96786	569.1	.00121	.000336
43	.95122	566.5	.00261	.000725
44	.94032	573.8	.00459	.001276
45	.96155	603.1	.00705	.001959
46	.97073	629.1	.00903	.002510
47	.97934	637.8	.00951	.002643
50	.94261	569.5	.00236	.000661
51	.94950	585.5	.00533	.001481
52	.96786	623.5	.00803	.002232
53	.99196	644.8	.00925	.002571
54	.99713	649.1	.00953	.002649
55	.94434	561.1	.00228	.000634
56	.94147	574.5	.00446	.001240
57	.96499	611.8	.00817	.002271
58	.98335	641.5	.00910	.002529
59	.98967	644.8	.00980	.002724
60	.98795	577.8	.00075	.000208
61	.97934	572.5	.00073	.000203
62	.97360	570.5	.00083	.000231
63	.96614	567.5	.00109	.000303
64	.95007	564.5	.00219	.000609
65	.93975	573.1	.00442	.001228
66	.94950	604.1	.00723	.002009
67	.96901	624.1	.00964	.002679
68	.97991	643.1	.01104	.003068
69	.99081	655.8	.01277	.003549
70	.99483	672.1	.01657	.004605
71	1.00344	586.5	.00072	.000200
72	.98680	576.1	.00068	.000189
73	.96614	575.8	.00152	.000422
74	.95409	565.8	.00138	.000384
75	.94376	557.1	.00182	.000506
76	.92999	563.5	.00413	.001148
77	.95007	594.5	.00710	.001973
78	.96385	619.5	.01044	.002902
79	.98163	645.5	.01171	.003255
80	.98737	656.5	.01362	.003785
81	.99483	676.5	.01794	.004986
82	.99311	586.1	.00141	.000392
83	.98737	580.1	.00111	.000309
84	.96040	562.5	.00084	.000233
85	.97188	570.5	.00093	.000258
86	.94147	559.5	.00182	.000506
87	.94204	569.5	.00386	.001073
88	.94893	591.8	.00662	.001840
89	.96270	616.8	.00957	.002660
90	.97360	638.5	.01098	.003052
91	.99770	658.1	.01206	.003352
92	1.00057	685.5	.02019	.005611
93	.95696	562.8	.00122	.000339
94	.95925	566.1	.00113	.000314
95	.95007	561.1	.00174	.000484
96	.93917	565.1	.00343	.000953
97	.94491	586.1	.00616	.001712
98	.96327	612.8	.00864	.002401











TABLE IX. - TABULATION OF HEAT-TRANSFER MEASUREMENTS  
FOR CONFIGURATION 4 - Continued

(b)  $M = 3.51$ ;  $Pt, nom = 7,200 \text{ lb/sq ft}$

Thermo- couple	$T_e/T_t$	$T_w$ OR	$h$	$N_{St}$
			$\frac{Btu}{sec-ft^2-OR}$	
$\alpha' = 45.0^\circ$ ; $T_t = 714^\circ R$ ; $Pt = 7,203.0 \text{ lb/sq ft}$				
4	.95427	570.5	.00182	.000356
5	.94227	570.8	.00373	.000729
6	.95256	591.1	.00584	.001141
7	.96285	614.1	.00898	.001754
8	.97485	630.8	.01085	.002120
9	.97999	585.1	.00141	.000275
10	.97313	574.1	.00114	.000223
11	.96170	570.8	.00152	.000297
12	.94742	570.1	.00295	.000576
13	.94399	583.8	.00511	.000998
14	.95370	605.1	.00786	.001535
15	.97085	627.5	.00982	.001918
16	.98171	636.1	.01111	.002170
17	.98056	643.8	.01220	.002383
18	.98799	591.5	.00198	.000487
19	.97256	578.5	.00182	.000356
20	.93313	579.8	.00596	.001164
21	.97371	639.8	.01234	.002411
22	.98514	656.1	.01418	.002770
23	.98514	591.5	.00221	.000432
24	.97942	587.8	.00235	.000459
25	.97256	580.8	.00211	.000412
26	.96170	584.5	.00187	.000365
27	.95085	576.8	.00374	.000731
28	.93141	580.5	.00608	.001188
29	.95656	613.1	.00912	.001782
30	.96342	630.1	.01141	.002229
31	.97771	643.8	.01275	.002467
32	.96513	640.5	.01432	.002797
33	.98456	661.1	.01509	.002948
34	.98114	583.8	.00172	.000336
35	.98628	587.1	.00183	.000357
36	.97199	578.1	.00174	.000340
37	.94056	586.1	.00620	.001211
38	.97428	641.8	.01264	.002469
39	.98514	653.5	.01401	.002757
40	.99028	669.1	.01586	.003098
41	.97942	580.5	.00155	.000303
42	.96456	573.8	.00194	.000379
43	.94856	572.1	.00335	.000654
44	.93770	582.1	.00587	.001147
45	.95942	613.5	.00905	.001768
46	.96799	632.5	.01116	.002180
47	.97656	641.8	.01159	.002264
50	.94227	565.8	.00506	.000958
51	.94513	591.8	.00674	.001317
52	.96570	626.1	.00904	.001766
53	.98799	652.8	.01124	.002196
54	.99314	656.8	.01132	.002211
55	.94342	576.5	.00307	.000600
56	.93770	580.1	.00562	.001098
57	.96113	618.8	.00907	.001772
58	.97999	642.5	.01058	.002067
59	.98628	644.1	.01127	.002202
60	.97942	577.5	.00105	.000205
61	.96970	572.1	.00106	.000207
62	.96913	574.5	.00132	.000258
63	.96399	572.8	.00143	.000279
64	.94742	570.5	.00294	.000574
65	.93656	582.1	.00572	.001117
66	.94742	608.8	.00944	.001844
67	.96628	636.8	.01288	.002516
68	.97713	647.8	.01395	.002725
69	.98742	659.5	.01622	.003169
70	.99199	676.8	.02144	.004188
71	.99085	585.1	.00111	.000217
72	.97485	575.1	.00107	.000209
73	.95999	570.5	.00133	.000260
74	.94913	565.1	.00148	.000289
75	.94941	564.8	.00234	.000457
76	.92627	570.5	.00528	.001031
77	.94799	605.5	.00913	.001784
78	.96170	632.5	.01305	.002549
79	.97885	649.8	.01504	.002938
80	.98399	660.8	.01811	.003538
81	.99085	680.8	.02382	.004653
82	.98514	587.5	.00186	.000363
83	.97656	579.8	.00145	.000283
84	.95427	564.5	.00141	.000275
85	.96742	574.1	.00161	.000315
86	.93599	564.1	.00257	.000502
87	.93656	576.5	.00534	.001043
88	.94513	602.8	.00877	.001713
89	.96056	630.1	.01274	.002489
90	.97085	651.5	.01375	.002668
91	.99314	663.1	.01671	.003264
92	.99771	690.8	.02666	.005208
93	.95142	564.5	.00157	.000307
94	.95485	566.1	.00155	.000303
95	.94684	564.8	.00226	.000441
96	.93599	572.5	.00463	.000904
97	.94342	597.5	.00804	.001571
98	.96170	635.1	.01140	.002227











TABLE IX. - TABULATION OF HEAT-TRANSFER MEASUREMENTS  
FOR CONFIGURATION 4 - Continued

(c)  $M = 4.65$ ;  $p_{t, \text{nom}} = 8,640 \text{ lb/sq ft}$

Thermo- couple	$T_e/T_t$	$T_w$ , OR	$h$ , Btu	$N_{St}$
			$\frac{\text{sec-ft}^2}{\text{OR}}$	
$\alpha' = 45.0^\circ$ ; $T_t = 671^\circ \text{R}$ ; $p_t = 8,641.0 \text{ lb/sq ft}$				
4	.96527	568.5	.00076	.000320
5	.95559	567.5	.00162	.000682
6	.96755	580.5	.00282	.001188
7	.97210	590.8	.00426	.001795
8	.98690	604.1	.00511	.002153
9	.98918	580.8	.00051	.000215
10	.98235	576.8	.00039	.000164
11	.96926	569.8	.00061	.000257
12	.95901	567.5	.00127	.000535
13	.95161	569.5	.00224	.000944
14	.95844	579.8	.00357	.001504
15	.97495	595.1	.00461	.001942
16	.98463	603.1	.00502	.002115
17	.98576	606.8	.00584	.002460
18	1.00683	591.1	.00046	.000194
19	.98747	580.1	.00069	.000291
20	.94193	564.5	.00265	.001116
21	.97495	600.1	.00589	.002481
22	.98918	613.1	.00698	.002941
23	1.01366	596.1	.00067	.000282
24	1.00683	593.5	.00073	.000308
25	.99032	583.8	.00064	.000270
26	.97153	572.8	.00083	.000350
27	.95958	568.8	.00139	.000586
28	.93661	561.1	.00248	.001045
29	.95730	581.5	.00427	.001799
30	.96470	592.1	.00441	.001858
31	.98235	605.8	.00617	.002599
32	.97039	601.1	.00699	.002945
33	.98918	616.1	.00763	.003214
34	1.02447	601.1	.00045	.000190
35	1.02447	601.1	.00045	.000190
36	.99203	583.1	.00069	.000291
37	.94933	570.8	.00299	.001260
38	.97723	603.8	.00553	.002330
39	.99316	615.8	.00698	.002941
40	.99829	624.5	.00828	.003488
41	1.00170	588.5	.00059	.000249
42	.98178	578.1	.00085	.000358
43	.96015	569.1	.00160	.000674
44	.94478	567.1	.00284	.001196
45	.96129	585.1	.00416	.001753
46	.97096	597.1	.00587	.002473
47	.98064	605.5	.00606	.002553
50	.95616	568.1	.00146	.000615
51	.96015	581.5	.00298	.001255
52	.97609	604.1	.00454	.001913
53	.99772	618.5	.00632	.002663
54	1.00396	626.8	.00664	.002797
55	.95503	567.5	.00149	.000628
56	.95389	571.8	.00271	.001142
57	.97438	595.1	.00416	.001753
58	.99032	611.5	.00585	.002456
59	.98068	615.8	.00630	.002654
60	1.05009	614.5	.00027	.000114
61	1.03415	605.1	.00040	.000169
62	.98861	581.1	.00062	.000261
63	.97723	576.5	.00072	.000303
64	.95446	565.5	.00143	.000602
65	.94136	565.5	.00294	.001239
66	.94819	583.1	.00467	.001967
67	.96641	597.8	.00651	.002743
68	.97893	608.8	.00772	.003252
69	.99715	630.5	.00808	.003404
70	1.01081	638.5	.01055	.004445
71	1.03073	604.8	.00059	.000249
72	1.01252	594.1	.00054	.000227
73	.98007	581.5	.00165	.000695
74	.96584	571.1	.00155	.000653
75	.95332	565.1	.00190	.000800
76	.93624	561.1	.00315	.001327
77	.95673	583.8	.00465	.001959
78	.96926	599.8	.00683	.002877
79	.98690	613.1	.00788	.003320
80	1.00056	626.8	.00889	.003745
81	1.01195	644.1	.01365	.005751
82	1.01764	596.5	.00054	.000227
83	1.00740	591.5	.00062	.000261
84	.97723	575.5	.00081	.000341
85	.99146	585.5	.00097	.000409
86	.95446	566.5	.00148	.000624
87	.95446	571.8	.00273	.001150
88	.96015	584.8	.00430	.001812
89	.97324	600.8	.00637	.002684
90	.98406	611.8	.00742	.003126
91	1.01366	632.1	.00814	.003429
92	1.01536	649.5	.01562	.006581
93	.97552	573.1	.00061	.000257
94	.97495	573.8	.00087	.000367
95	.96243	569.8	.00149	.000628
96	.95104	570.5	.00239	.001007
97	.95673	581.1	.00437	.001841
98	.97438	600.1	.00597	.002515



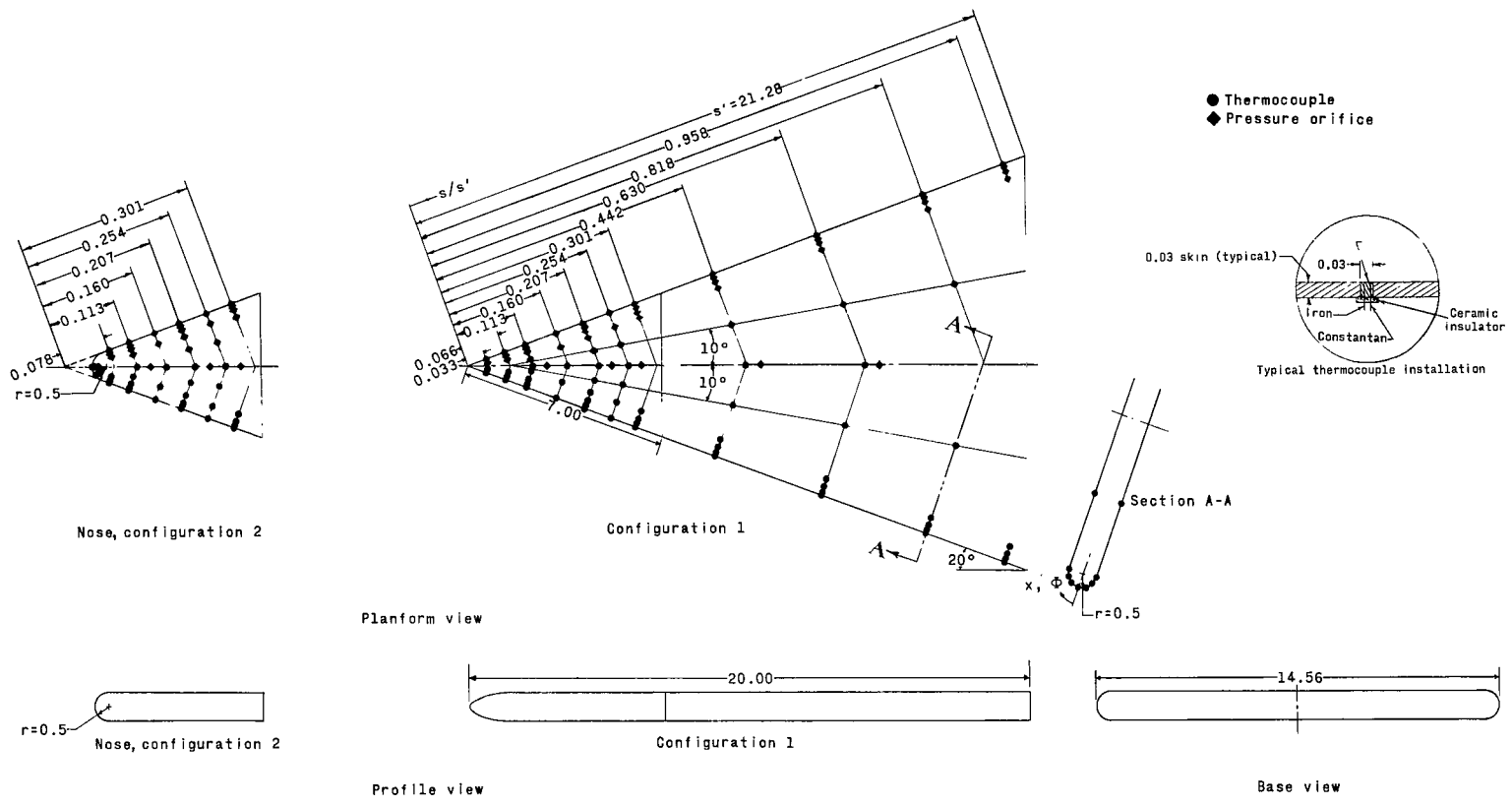






TABLE IX. - TABULATION OF HEAT-TRANSFER MEASUREMENTS  
 FOR CONFIGURATION 4 - Concluded  
 (d)  $M = 4.65$ ;  $p_{t,nom} = 12,240$  lb/sq ft

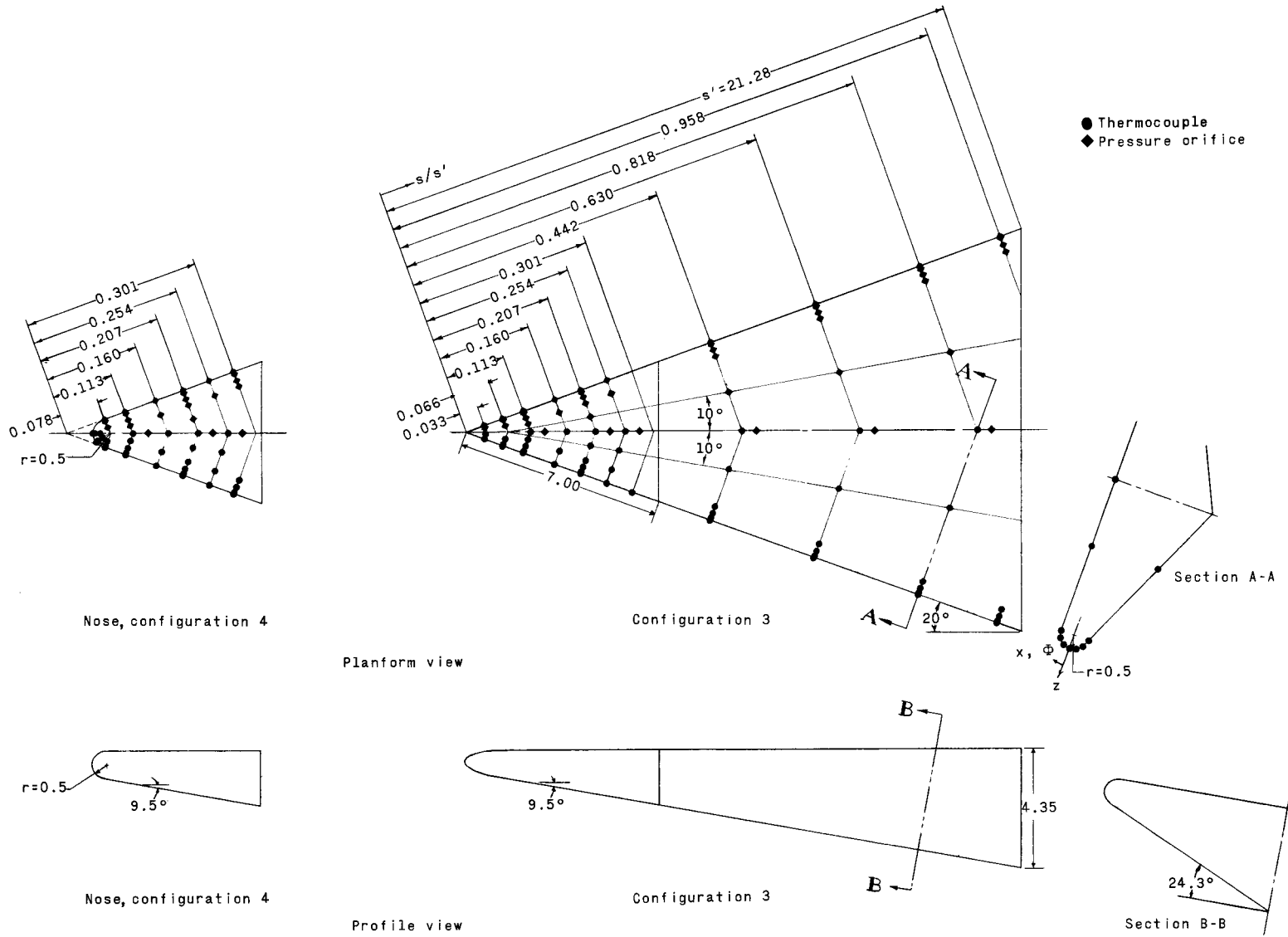
Thermo- couple	$T_e/T_t$	$T_w$ OR	$h$	$N_{St}$
			$\frac{Btu}{sec-ft^2-OR}$	
$\alpha' = 45.0^\circ$ ; $T_t = 875^\circ R$ ; $p_e = 12,231.0$ lb/sq ft				
4	.97137	571.1	.00103	.000308
5	.95820	570.1	.00217	.000648
6	.96794	583.8	.00334	.000997
7	.97481	597.8	.00523	.001562
8	.98797	611.5	.00619	.001848
9	.99771	583.8	.00059	.000176
10	.99026	579.8	.00066	.000197
11	.97767	573.5	.00073	.000218
12	.96278	570.1	.00164	.000490
13	.95477	574.1	.00276	.000824
14	.96107	586.8	.00426	.001272
15	.97767	603.8	.00567	.001693
16	.98797	612.8	.00637	.001902
17	.98855	616.8	.00711	.002123
18	1.01200	593.8	.00077	.000230
19	.99427	583.8	.00107	.000320
20	.94504	570.5	.00751	.001048
21	.97996	611.5	.00692	.000966
22	.99313	624.8	.00799	.002386
23	1.01771	599.8	.00103	.000308
24	1.01200	595.8	.00101	.000302
25	.99656	586.5	.00115	.000343
26	.97939	578.1	.00144	.000430
27	.96565	574.5	.00212	.000633
28	.94160	568.5	.00349	.001042
29	.96336	591.5	.00493	.001472
30	.96965	603.1	.00639	.001908
31	.98568	616.5	.00737	.002201
32	.97423	612.8	.00853	.002547
33	.99313	628.5	.00880	.002628
34	1.02628	601.8	.00068	.000203
35	1.02800	603.1	.00068	.000203
36	.99771	585.5	.00095	.000284
37	.95191	576.5	.00385	.001150
38	.98168	614.5	.00720	.002150
39	.99599	626.5	.00820	.002449
40	1.00000	636.5	.00970	.002897
41	1.00285	589.1	.00088	.000263
42	.98626	579.8	.00103	.000308
43	.96336	574.5	.00222	.000663
44	.94733	572.1	.00347	.001036
45	.96565	593.8	.00520	.001553
46	.97481	607.5	.00658	.001965
47	.98454	615.8	.00691	.002063
50	.96049	568.8	.00194	.000579
51	.96164	583.1	.00353	.001054
52	.97767	604.8	.00537	.001604
53	.99828	626.1	.00641	.001914
54	1.00514	634.5	.00707	.002111
55	.95992	568.8	.00190	.000567
56	.95420	577.8	.00312	.000932
57	.97595	601.1	.00488	.001457
58	.99198	621.1	.00571	.001705
59	.99828	623.8	.00678	.002025
60	1.04629	610.8	.00043	.000128
62	.99255	582.1	.00078	.000233
63	.98168	577.8	.00104	.000311
64	.95763	569.1	.00202	.000603
65	.94332	574.1	.00380	.001135
66	.95246	588.5	.00597	.001783
67	.97023	608.8	.00728	.002174
68	.98339	620.5	.00920	.002747
69	.99942	634.5	.01038	.003100
70	1.01200	652.1	.01433	.004279
71	1.02286	600.1	.00081	.000242
72	1.00628	590.1	.00060	.000179
73	.98053	578.5	.00179	.000535
74	.96679	571.1	.00183	.000546
75	.95420	565.8	.00248	.000741
76	.93817	567.1	.00420	.001254
77	.95935	593.1	.00648	.001935
78	.97252	611.8	.00903	.002696
79	.99084	626.5	.00995	.002971
80	1.00285	639.8	.01198	.003577
81	1.01428	656.8	.01665	.004972
82	1.01028	593.5	.00085	.000254
83	1.00114	586.8	.00081	.000242
84	.97652	574.8	.00101	.000302
85	.99141	584.5	.00119	.000355
86	.95334	566.1	.00205	.000612
87	.95591	576.5	.00374	.001117
88	.96393	593.5	.00590	.001762
89	.97767	613.1	.00815	.002434
90	.98912	624.5	.00949	.002834
91	1.01428	644.8	.01084	.003237
92	1.01771	662.8	.01965	.005868
93	.97595	572.5	.00085	.000254
94	.97595	573.1	.00112	.000334
95	.96393	573.8	.00170	.000508
96	.95248	572.1	.00325	.000970
97	.95992	589.8	.00560	.001672



(a)  $0^\circ$  dihedral.

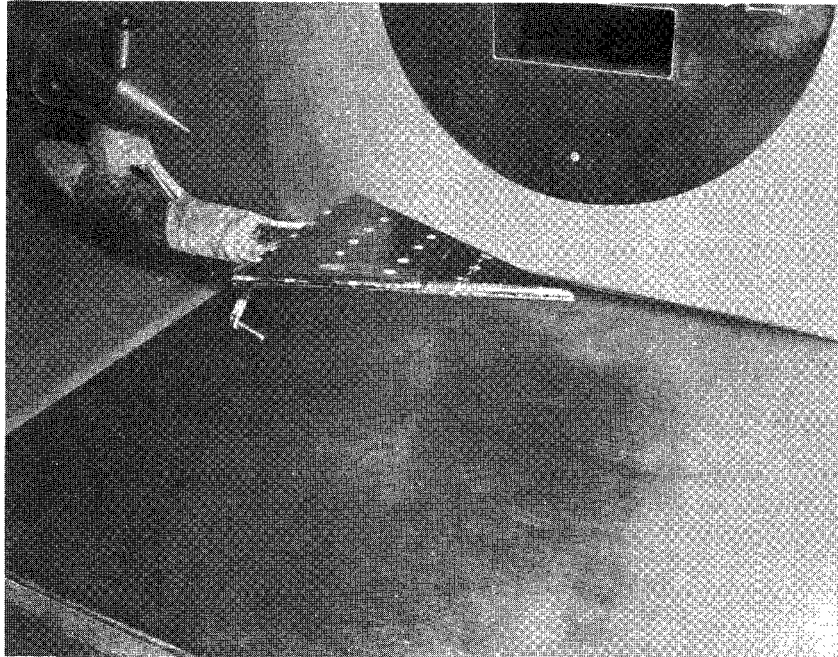
Figure 1.- Thermocouple and pressure-orifice locations on models. (All dimensions are in inches unless otherwise indicated.)





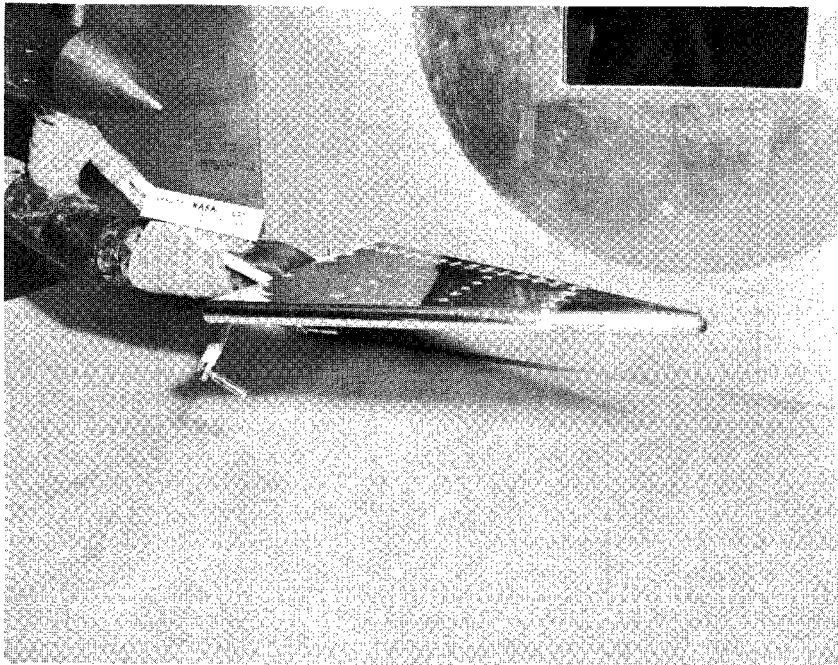
(b)  $24.3^\circ$  dihedral.

Figure 1.- Concluded.



(a) Configuration 1.

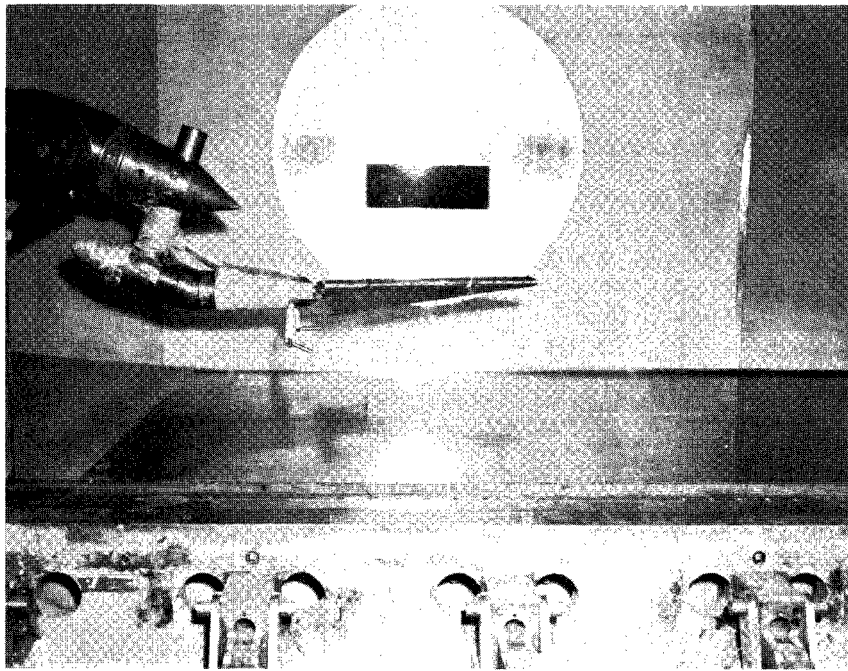
L-59-1674



(b) Configuration 2.

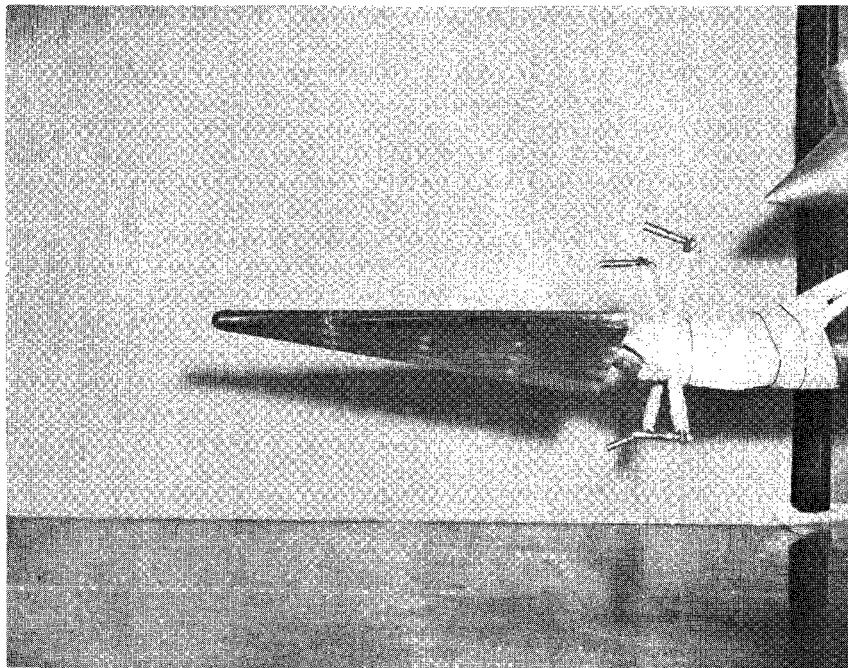
L-59-1683

Figure 2.- Installation of models in wind tunnel.



(c) Configuration 3.

L-59-1684



(d) Configuration 4.

L-59-1679

Figure 2.- Concluded.

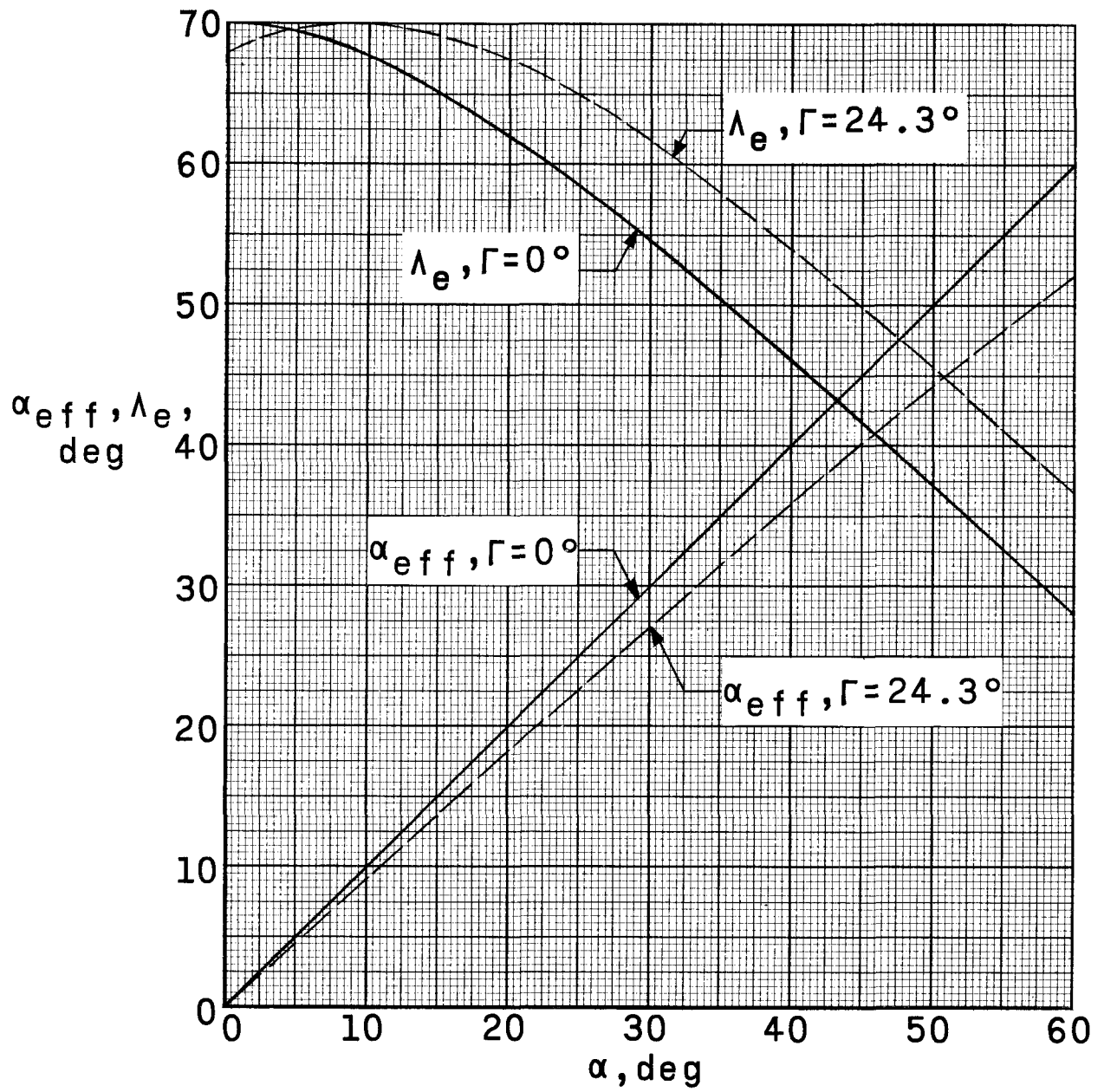


Figure 3.- Variation of wing effective geometry with angle of attack.



$\alpha' = 0^\circ$



$\alpha' = 7.5^\circ$



$\alpha' = 15.0^\circ$



$\alpha' = 22.5^\circ$

(a)  $M = 3.51$ ;  $R \approx 2.90 \times 10^6$ .

L-64-3040

Figure 4.- Typical schlieren photographs of configuration 1.



$\alpha' = 30.0^\circ$



$\alpha' = 37.5^\circ$



$\alpha' = 45.0^\circ$

(a) Concluded.

L-64-3041

Figure 4.- Continued.



$\alpha' = 0^\circ$



$\alpha' = 7.5^\circ$



$\alpha' = 15.0^\circ$

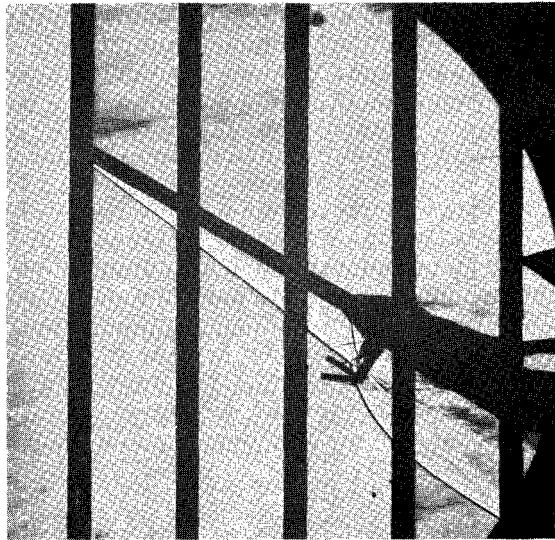


$\alpha' = 22.5^\circ$

(b)  $M = 4.65$ ;  $R \approx 2.90 \times 10^6$ .

L-64-3042

Figure 4.- Continued.



$\alpha' = 30.0^\circ$



$\alpha' = 37.5^\circ$



$\alpha' = 45.0^\circ$

(b) Concluded.

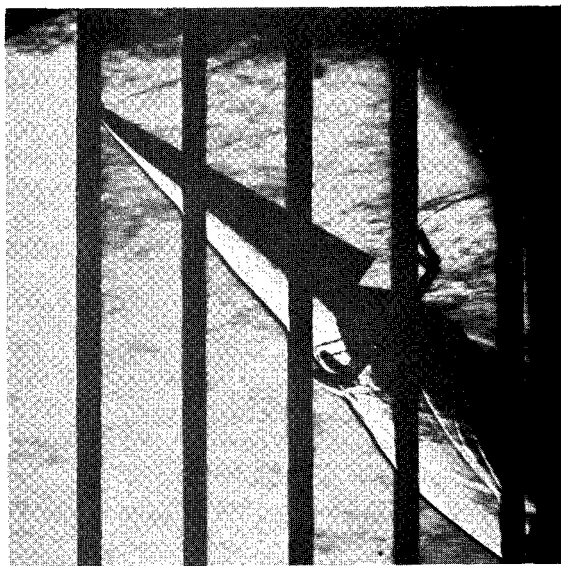
L-64-3043

Figure 4.- Concluded.





$\alpha' = -45.0^\circ$



$\alpha' = -37.5^\circ$

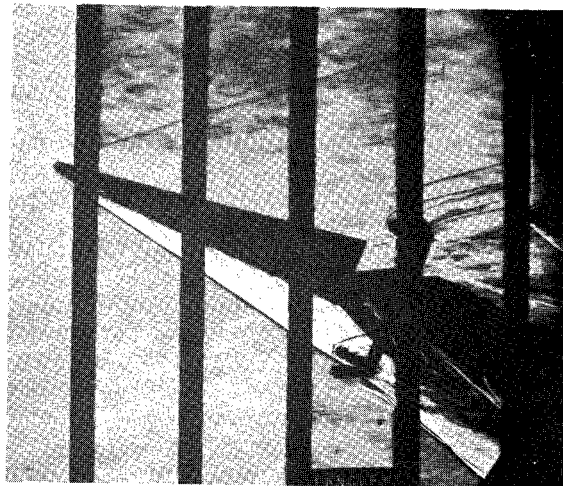


$\alpha' = -30.0^\circ$

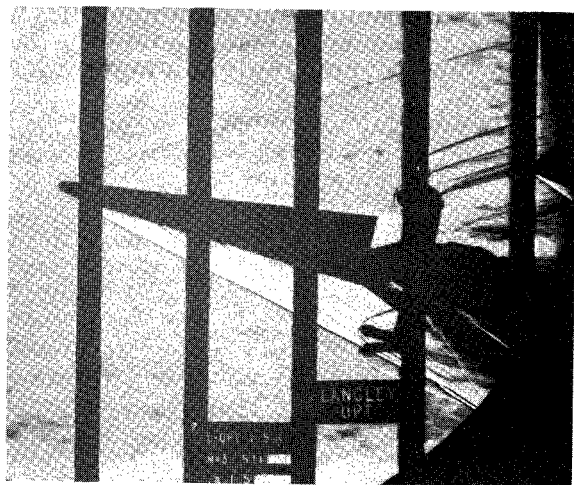
(a)  $M = 3.51$ ;  $R \approx 2.90 \times 10^6$ .

L-64-3044

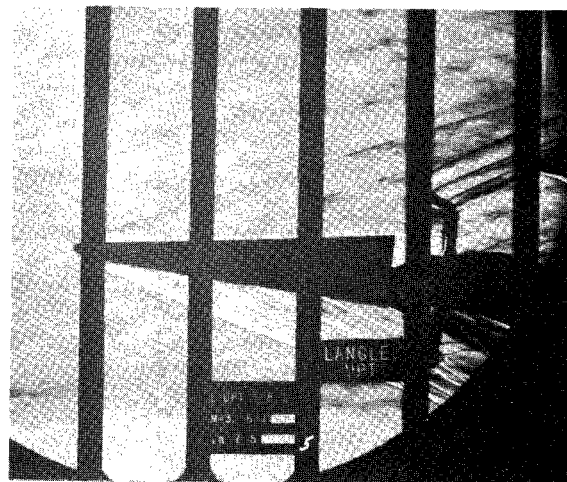
Figure 5.- Typical schlieren photographs of configuration 3.



$\alpha' = -22.5^\circ$



$\alpha' = -15.0^\circ$

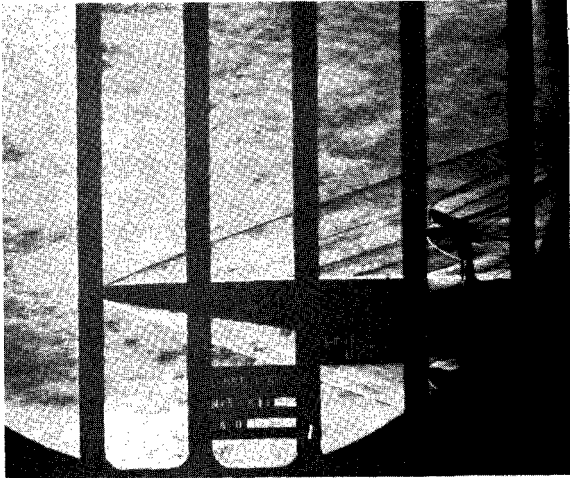


$\alpha' = -7.5^\circ$

(a) Continued.

L-64-3045

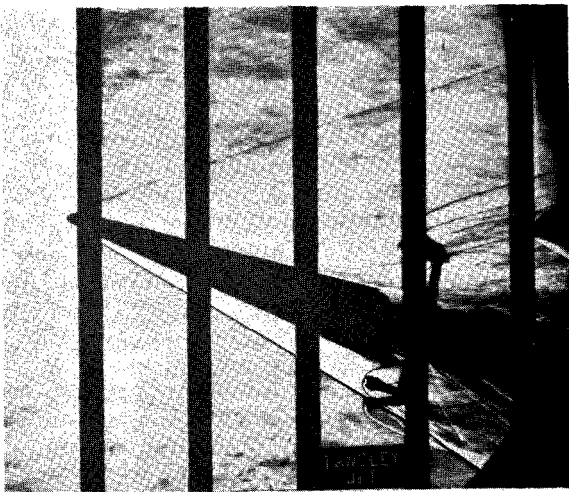
Figure 5.- Continued.



$\alpha' = 0^\circ$



$\alpha' = 7.5^\circ$



$\alpha' = 15.0^\circ$



$\alpha' = 22.5^\circ$

(a) Continued.

L-64-3046

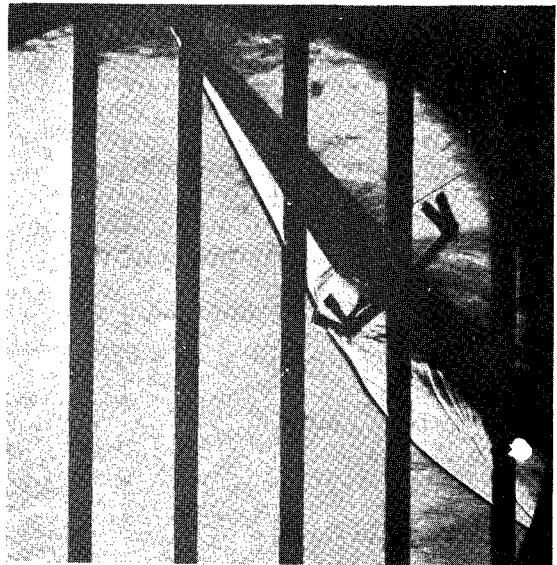
Figure 5.- Continued.



$\alpha' = 30.0^\circ$



$\alpha' = 37.5^\circ$



$\alpha' = 45.0^\circ$

(a) Concluded.

L-64-3047

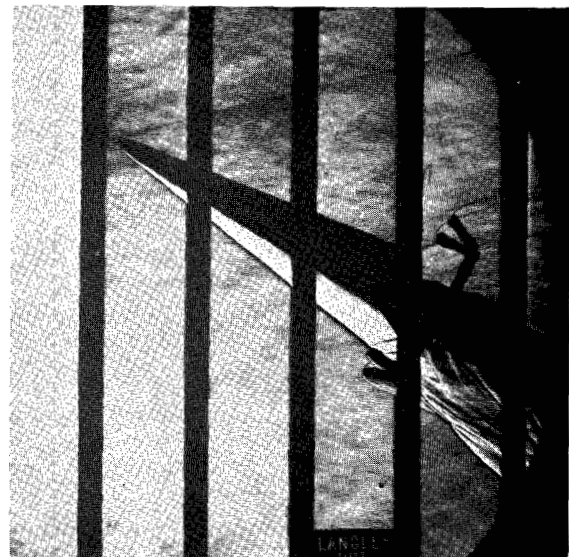
Figure 5.- Continued.



$\alpha' = -45.0^\circ$



$\alpha' = -37.5^\circ$



$\alpha' = -30.0^\circ$

(b)  $M = 4.65$ ;  $R \approx 2.90 \times 10^6$ .

I-64-3048

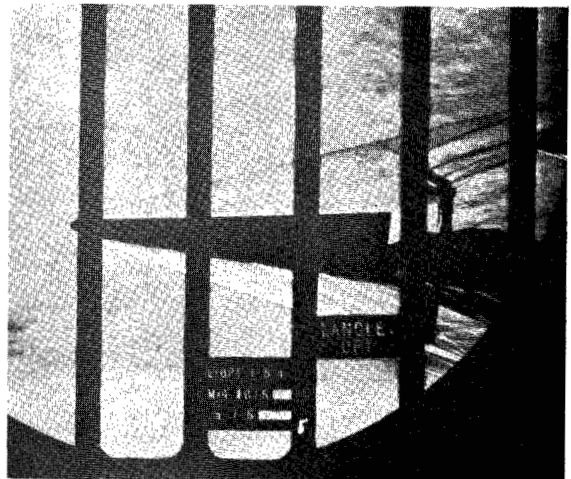
Figure 5.- Continued.



$\alpha' = -22.5^\circ$



$\alpha' = -15.0^\circ$



$\alpha' = -7.5^\circ$

(b) Continued.

L-64-3049

Figure 5.- Continued.



$\alpha' = 0^\circ$



$\alpha' = 7.5^\circ$



$\alpha' = 15.0^\circ$

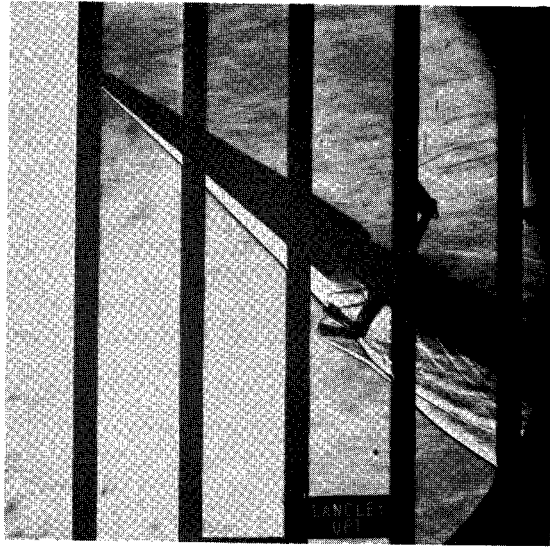


$\alpha' = 22.5^\circ$

(b) Continued.

L-64-3050

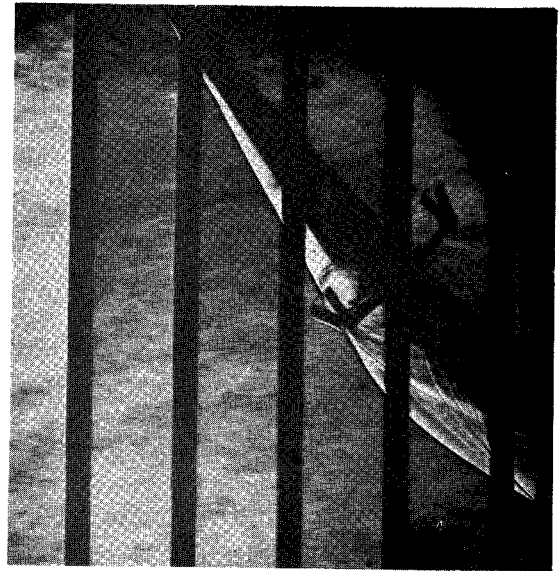
Figure 5.- Continued.



$\alpha' = 30.0^\circ$



$\alpha' = 37.5^\circ$



$\alpha' = 45.0^\circ$

(b) Concluded.

L-64-3051

Figure 5.- Continued.





$\alpha' = 0^\circ$



$\alpha' = 7.5^\circ$



$\alpha' = 15.0^\circ$

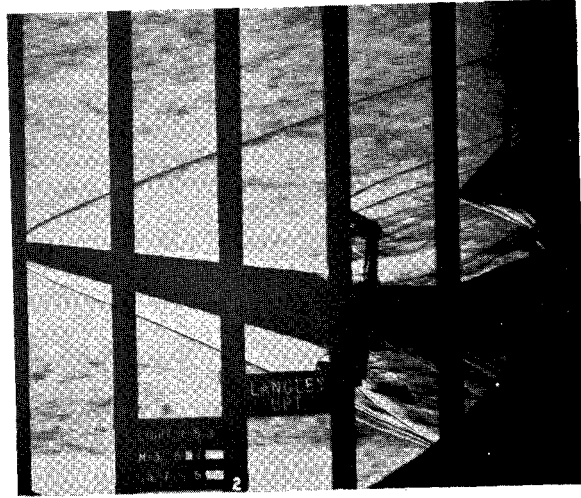


$\alpha' = 20.0^\circ$

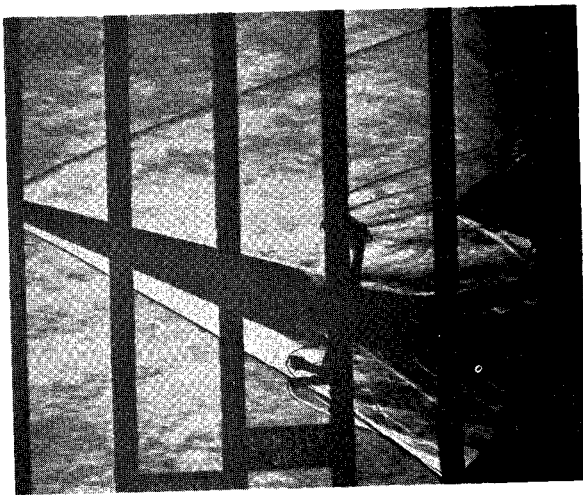
(c) Planform view;  $M = 3.51$ ;  $R \approx 2.90 \times 10^6$ .

L-64-3052

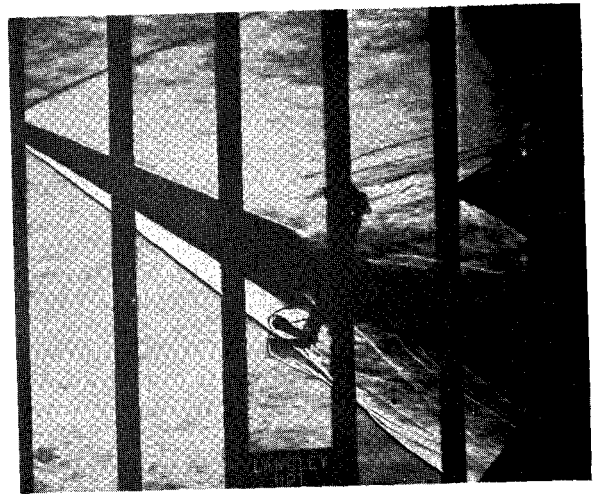
Figure 5.- Concluded.



$\alpha' = 7.5^\circ$



$\alpha' = 15.0^\circ$



$\alpha' = 22.5^\circ$

Figure 6.- Typical schlieren photographs of configuration 4.  $M = 3.51$ ;  $R \approx 2.90 \times 10^6$ . L-64-3053



$\alpha' = 30.0^\circ$



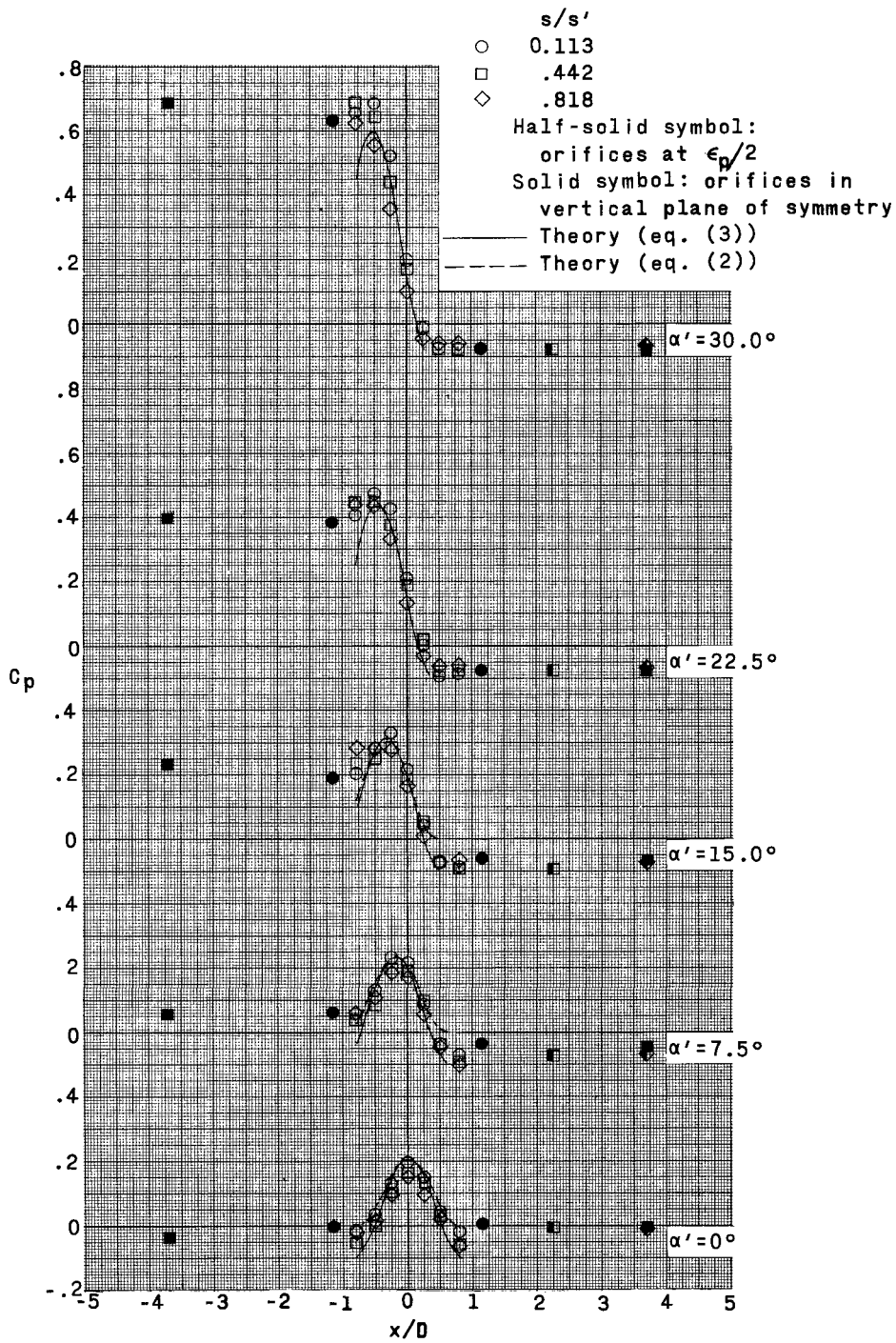
$\alpha' = 37.5^\circ$



$\alpha' = 45.0^\circ$

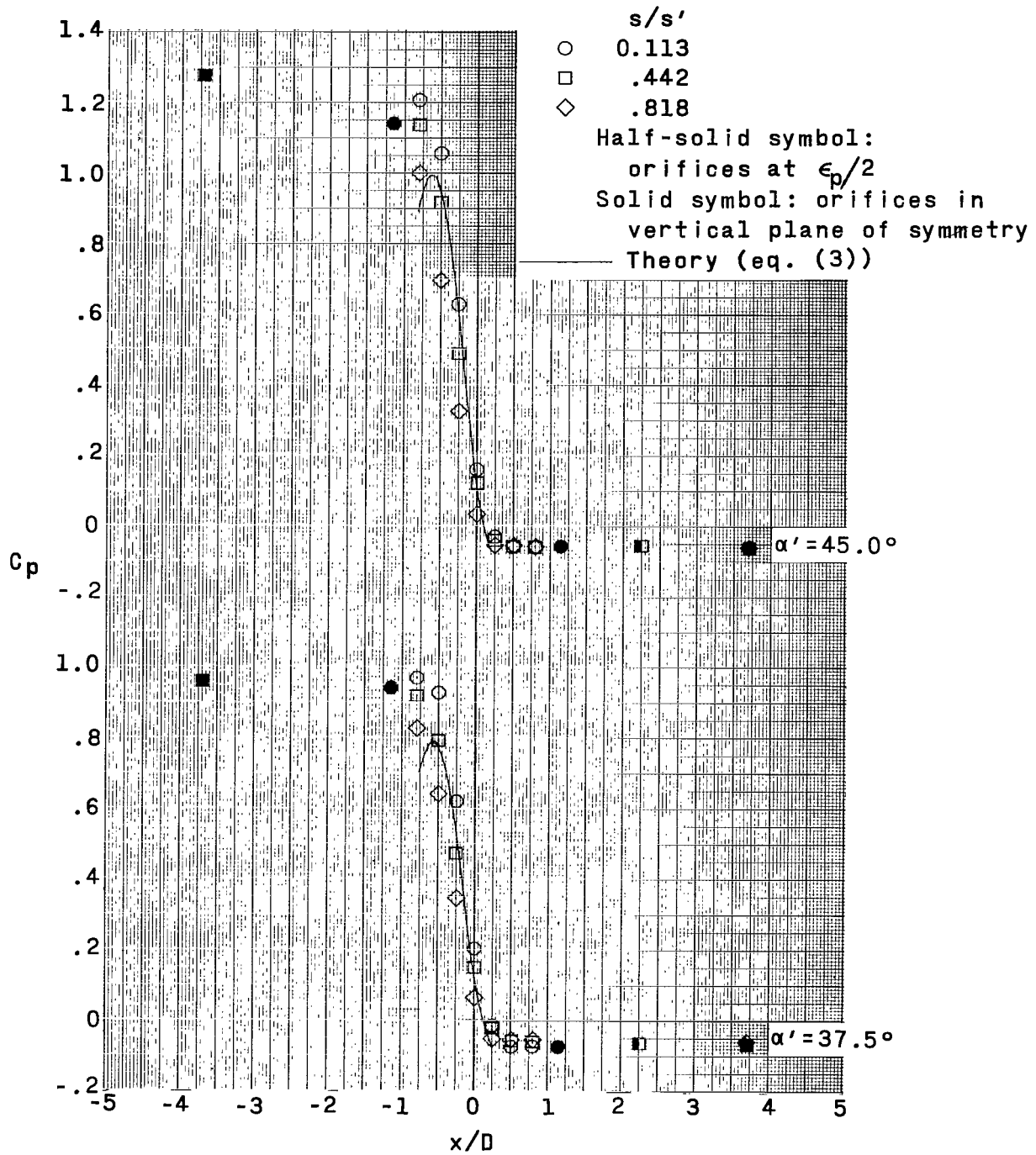
Figure 6.- Concluded.

L-64-3054



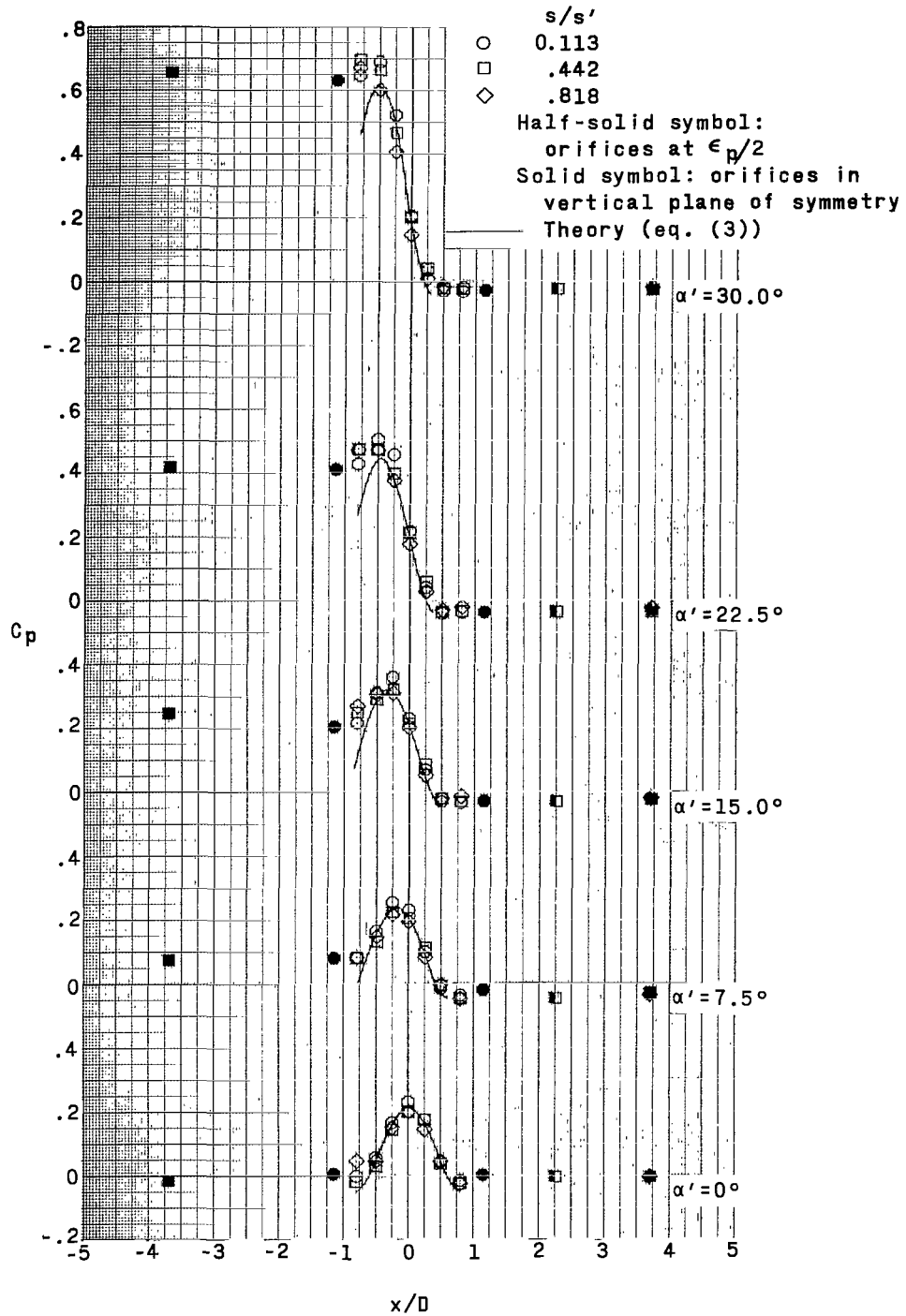
(a)  $M = 3.51$ .

Figure 7.- Effect of angle of attack on pressure-coefficient distribution normal to wing leading edge of configuration 1.  $R \approx 4.00 \times 10^6$ .



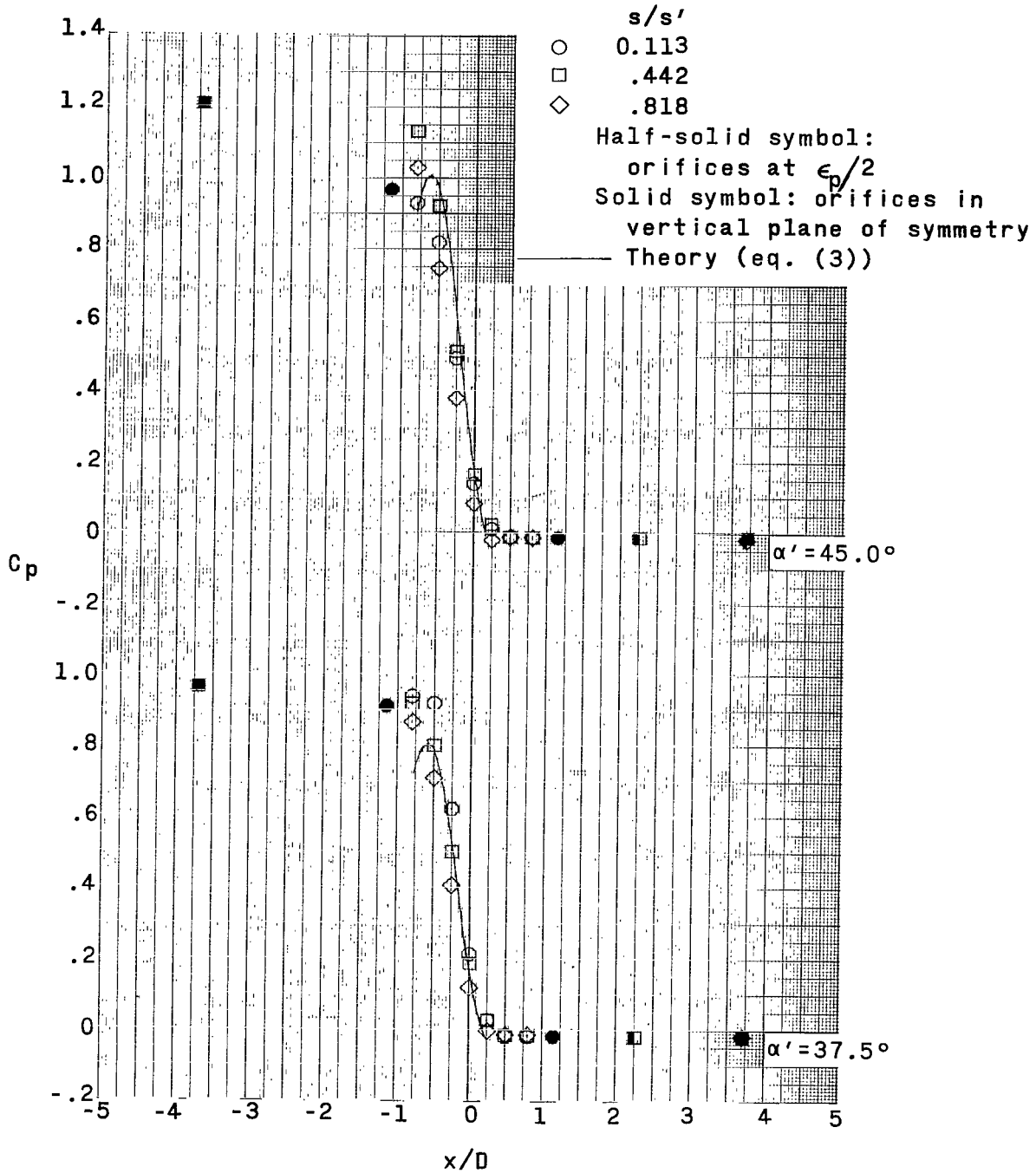
(a) Concluded.

Figure 7.- Continued.



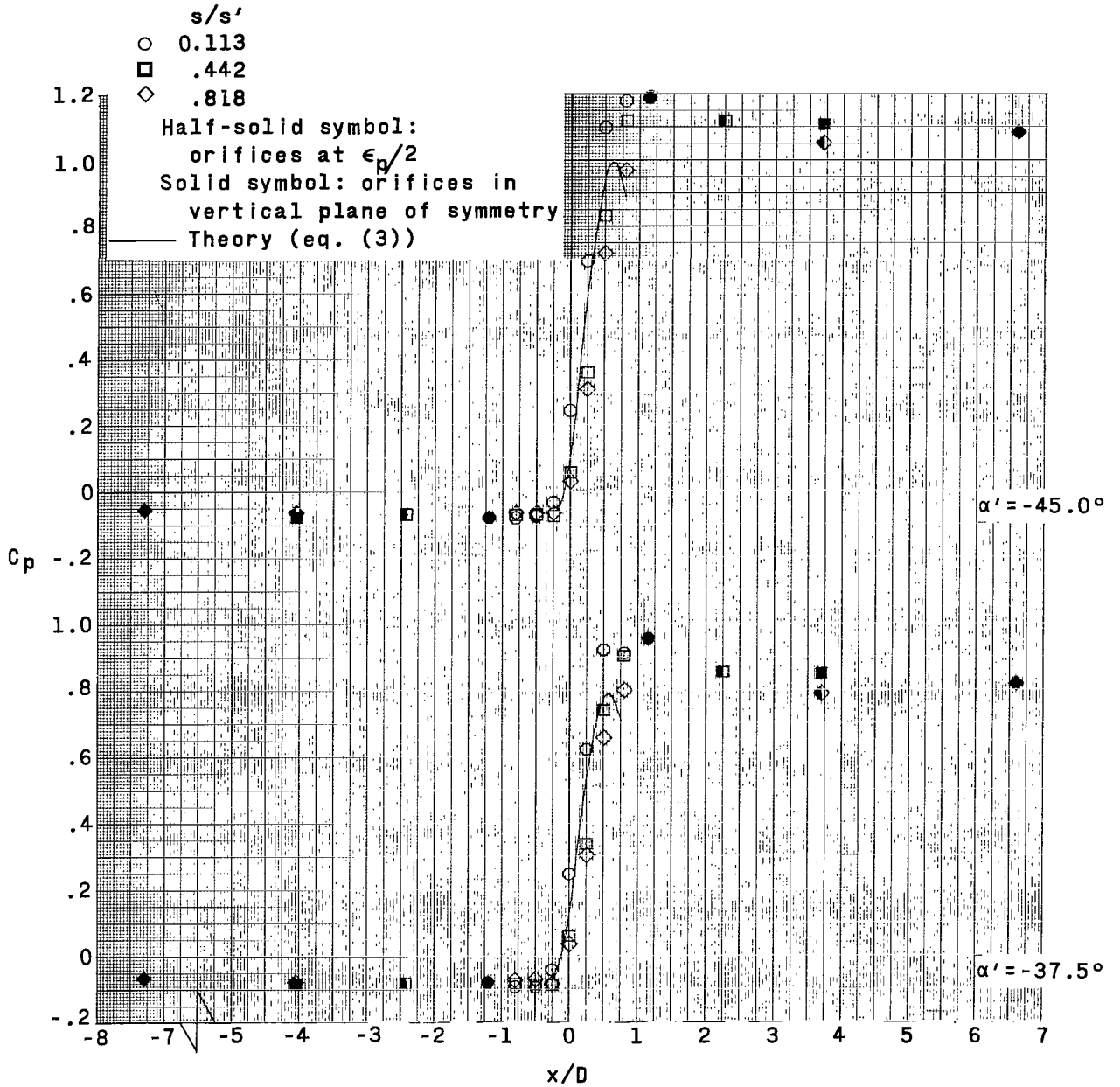
(b)  $M = 4.65$ .

Figure 7.- Continued.



(b) Concluded.

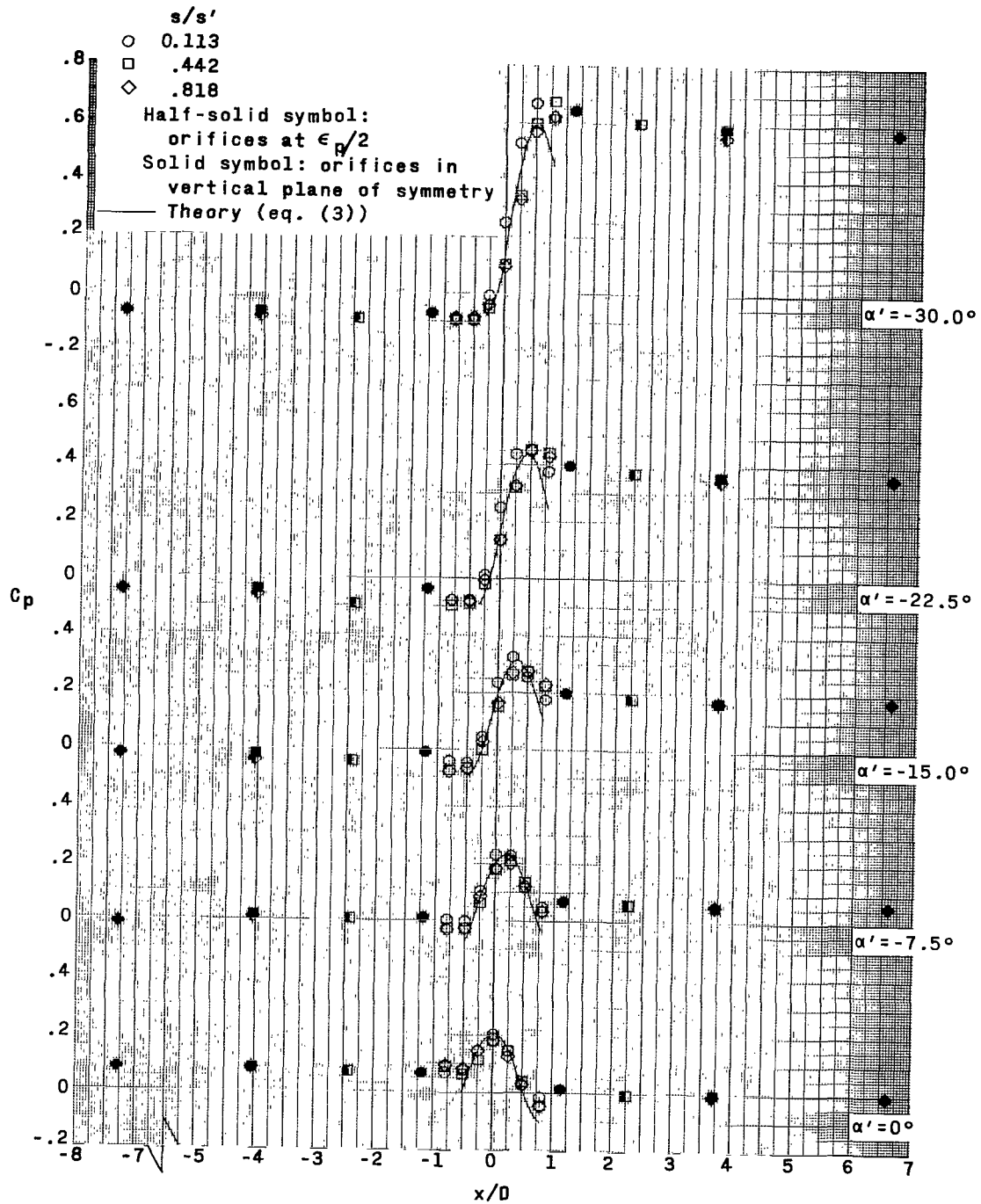
Figure 7.- Concluded.



(a)  $M = 3.51$ .

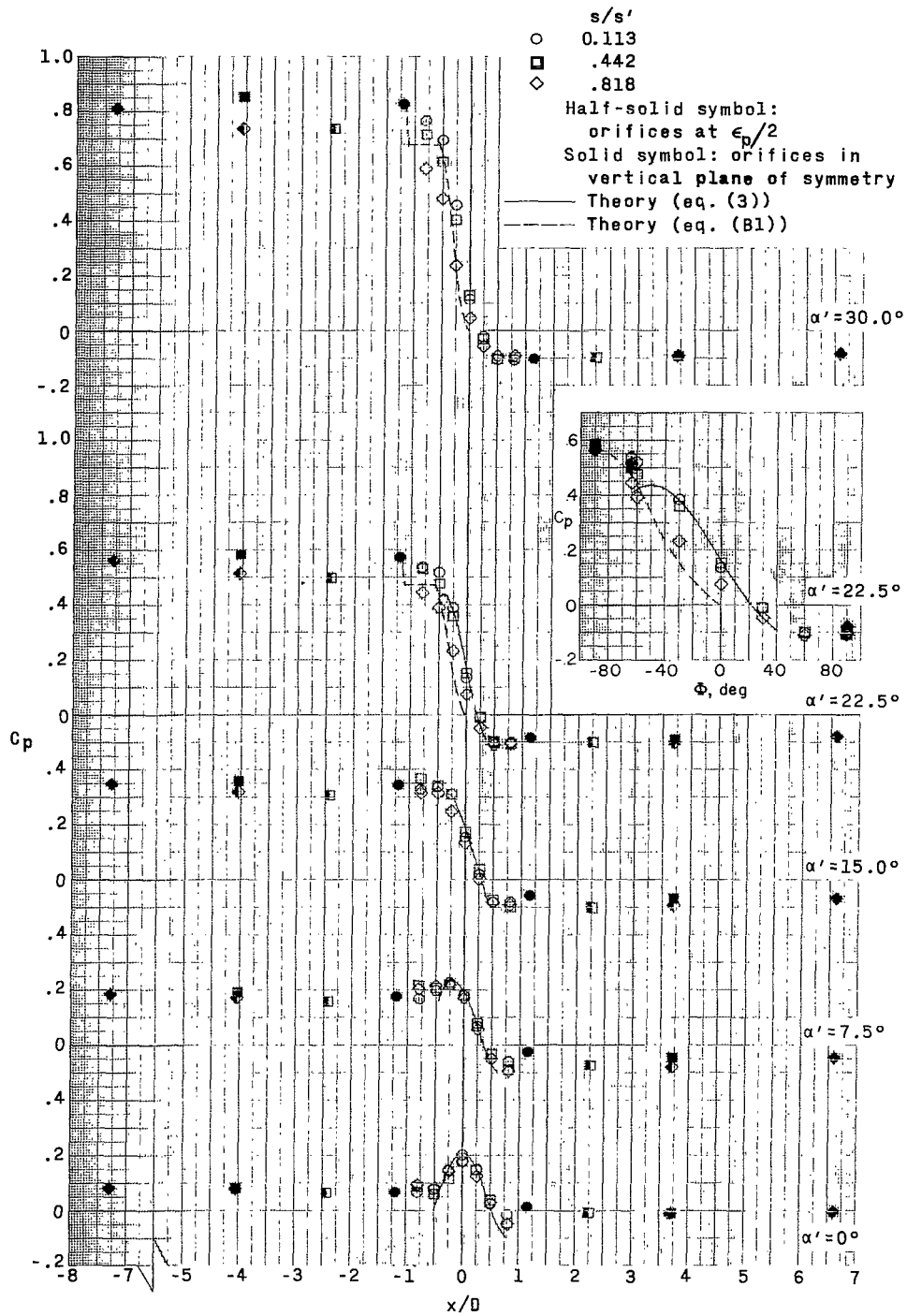
Figure 8.- Effect of angle of attack on pressure-coefficient distribution normal to wing leading edge of configuration 3.  $R \approx 4.00 \times 10^6$ .





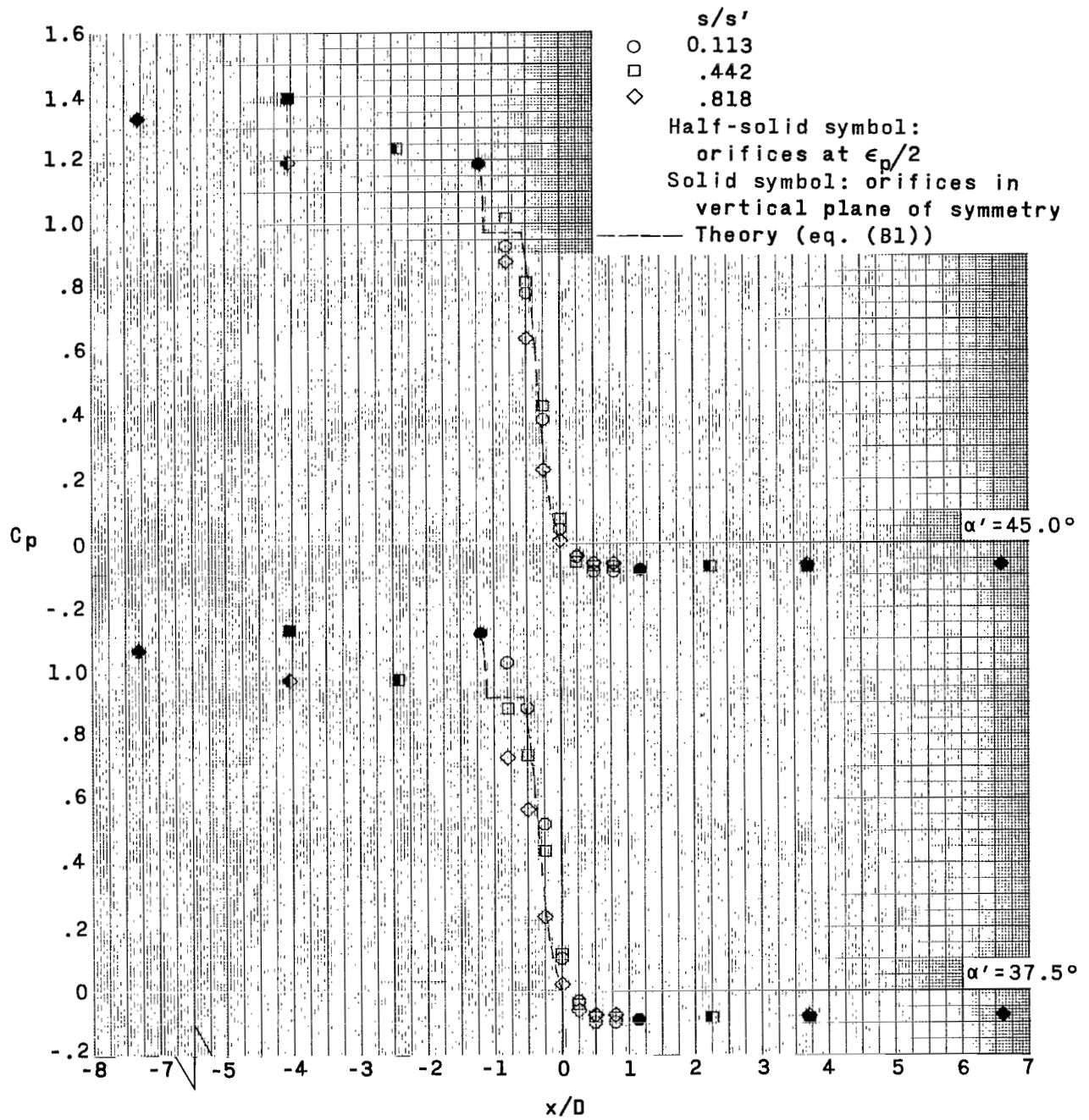
(a) Continued.

Figure 8.- Continued.



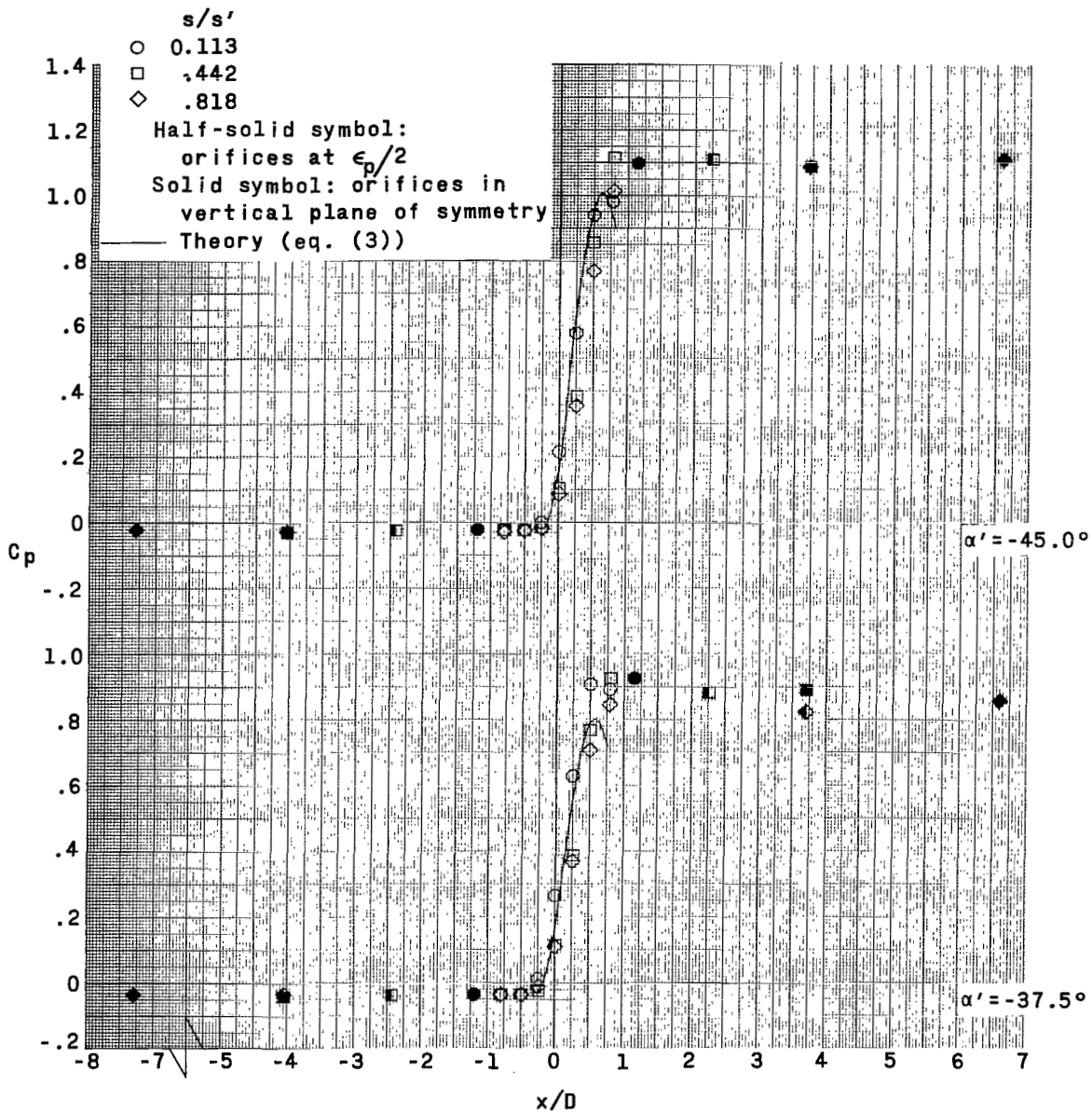
(a) Continued.

Figure 8.- Continued.



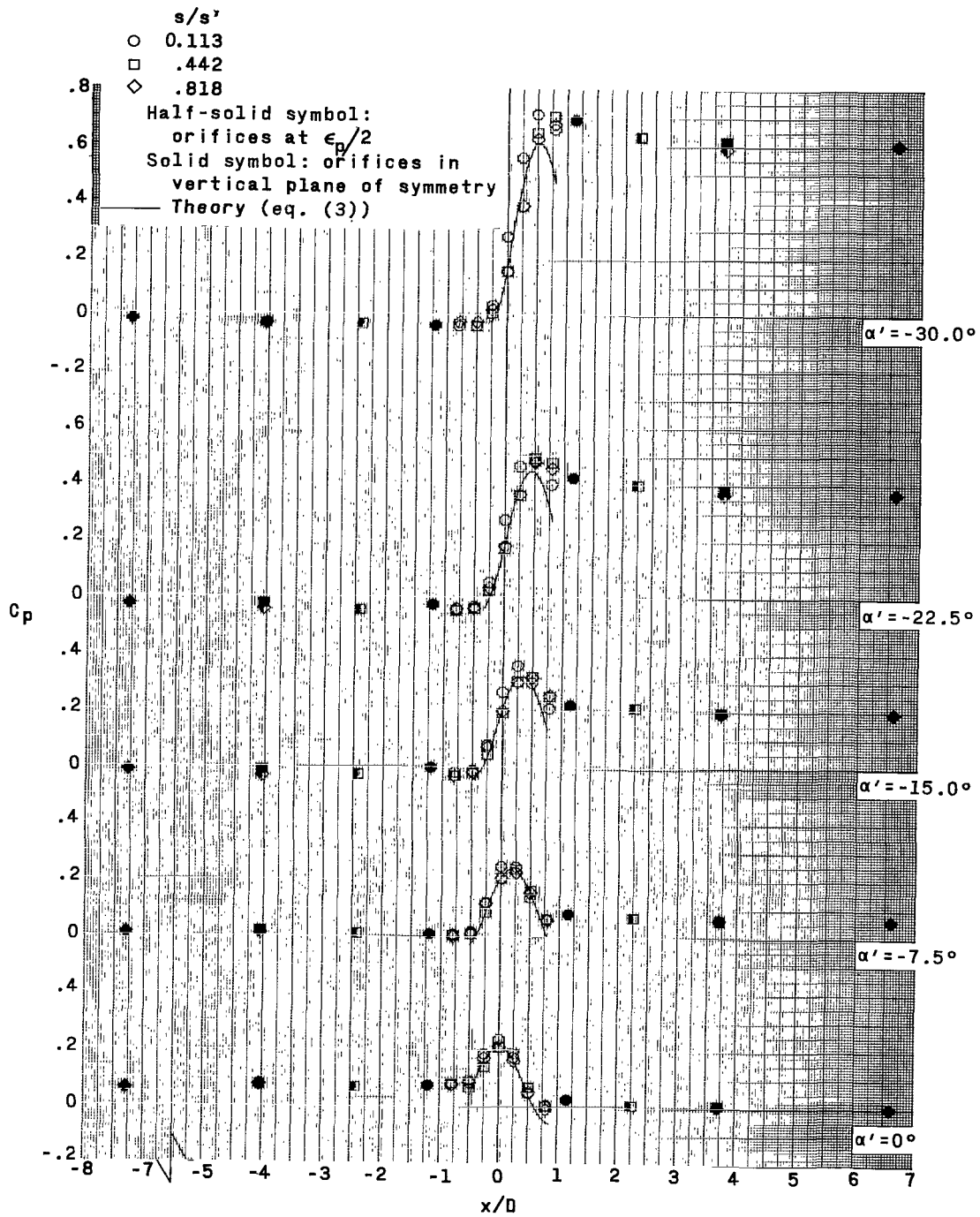
(a) Concluded.

Figure 8.- Continued.



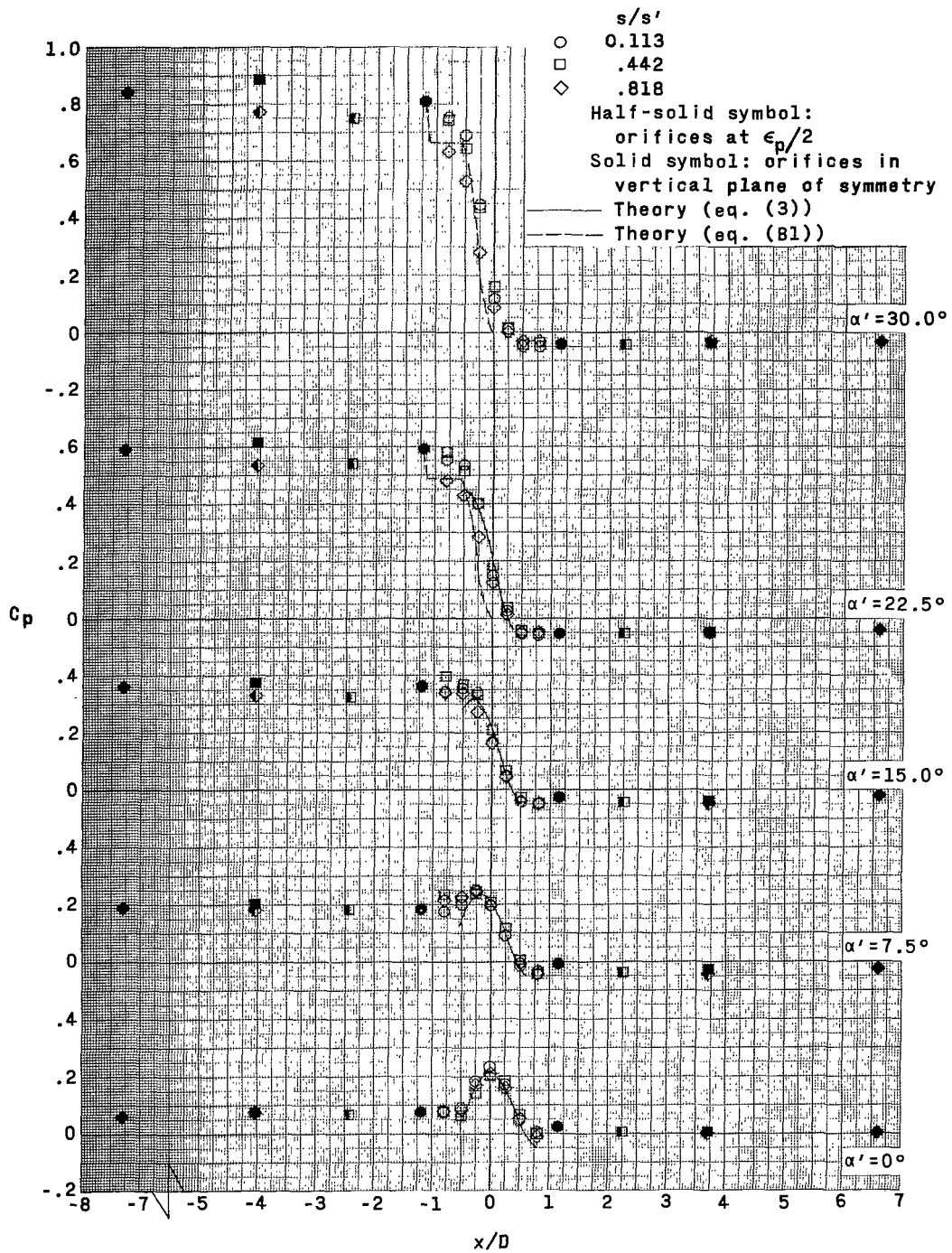
(b)  $M = 4.65$ .

Figure 8.- Continued.



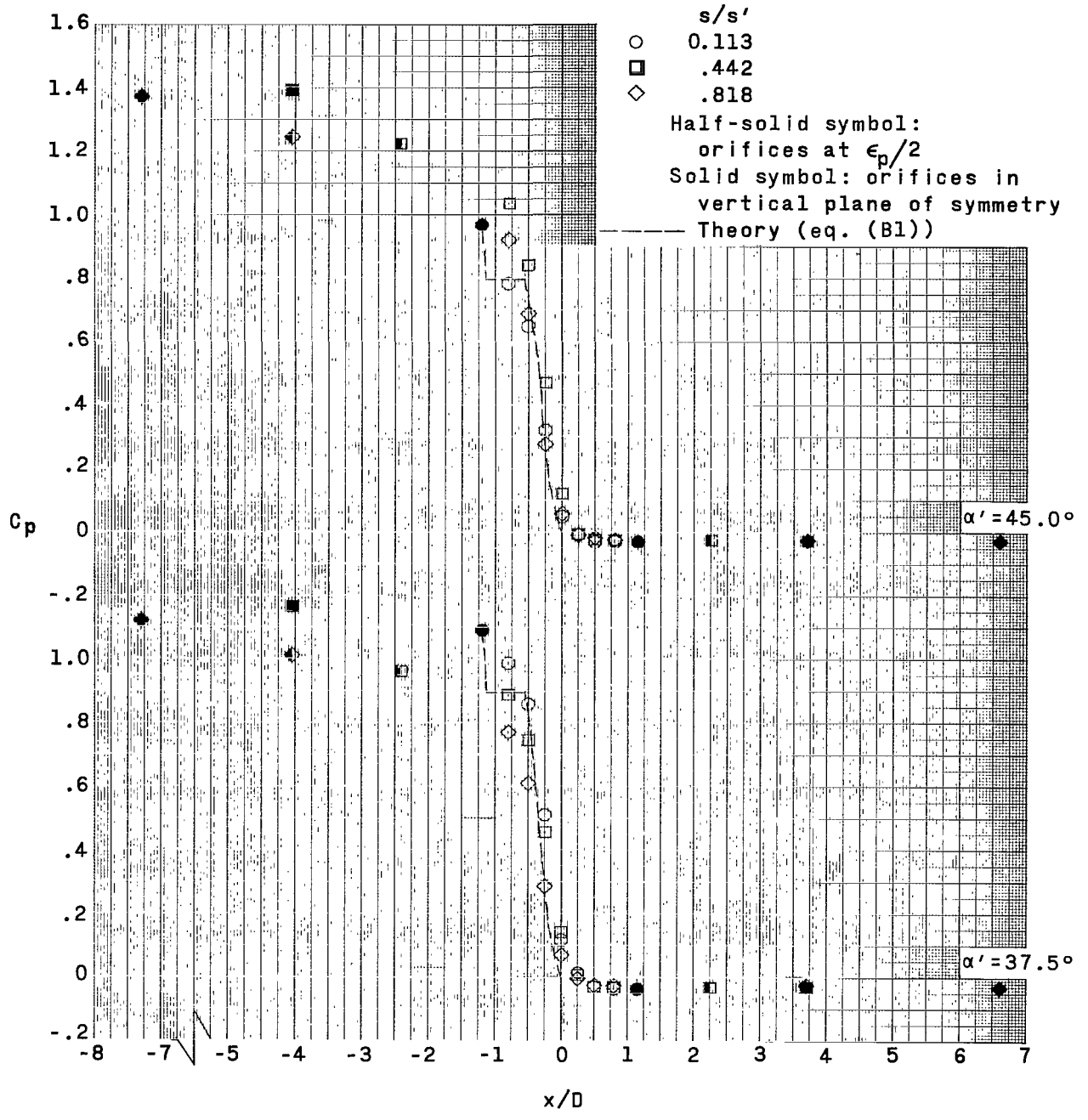
(b) Continued.

Figure 8.- Continued.



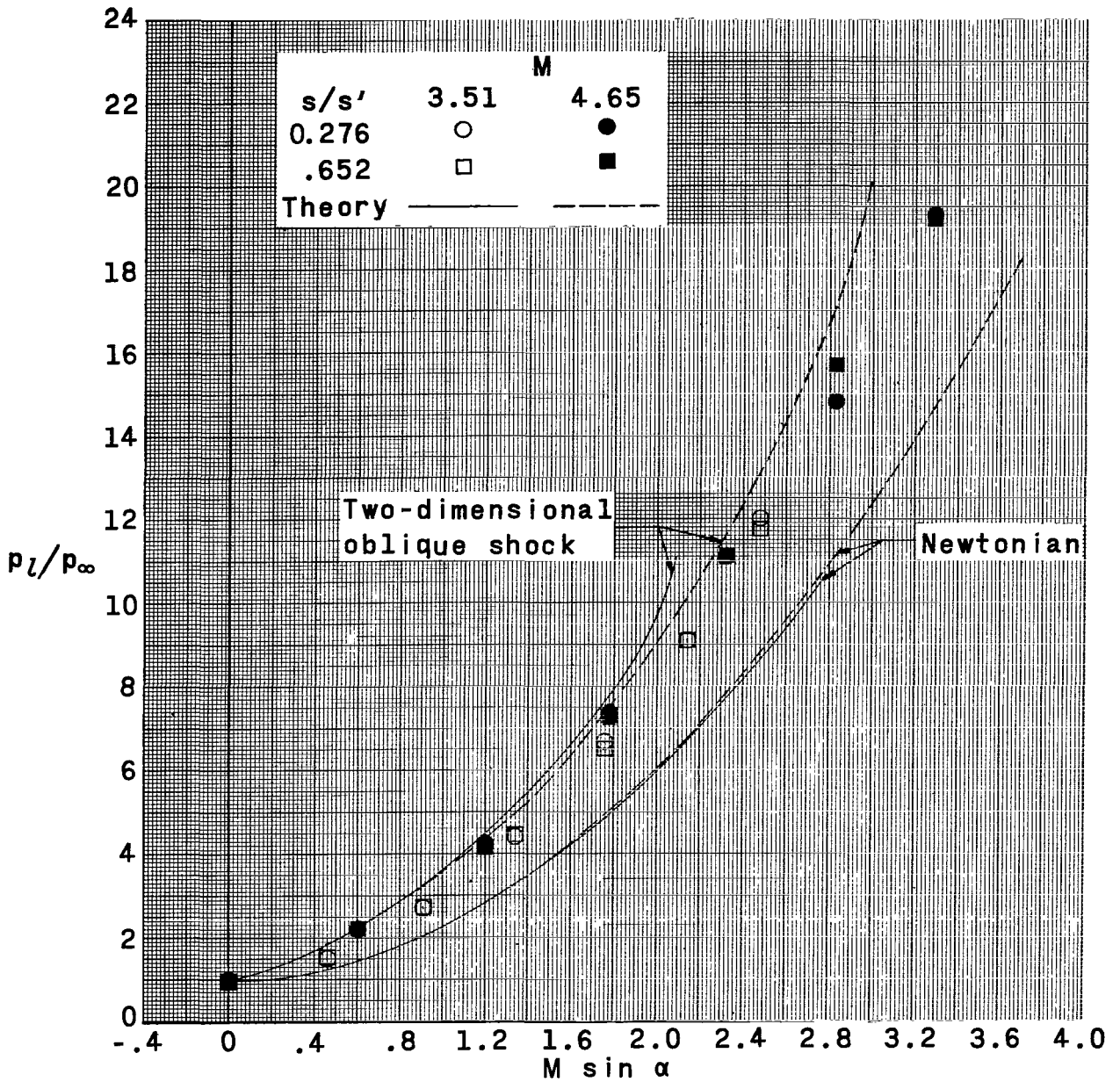
(b) Continued.

Figure 8.- Continued.



(b) Concluded.

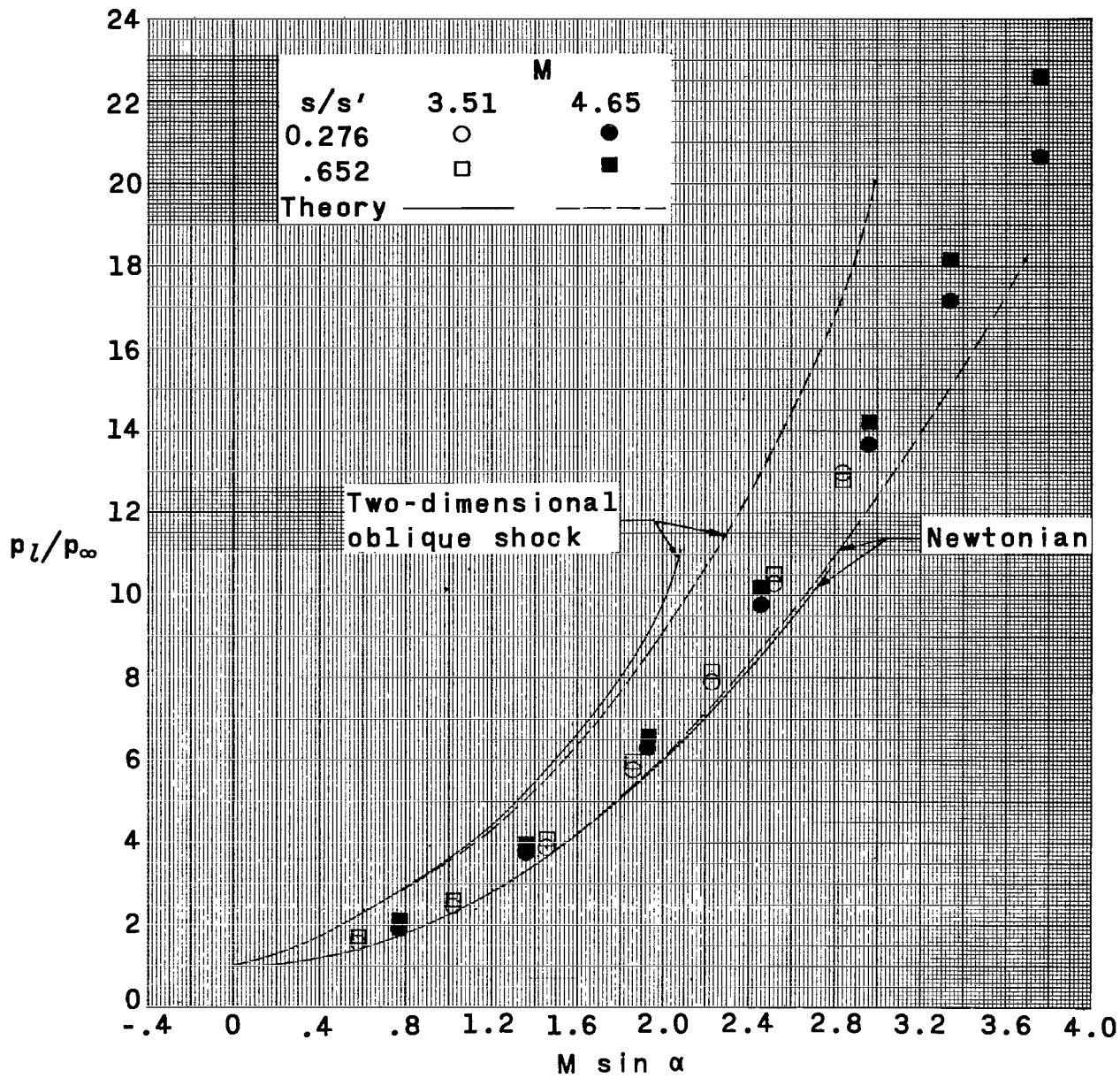
Figure 8.- Concluded.



(a) Configuration 1.

Figure 9.- Correlation of experimental data along windward center line of configurations 1 and 3 at Mach numbers 3.51 and 4.65 through an angle-of-attack range from  $0^\circ$  to  $45^\circ$ .





(b) Configuration 3.

Figure 9.- Concluded.

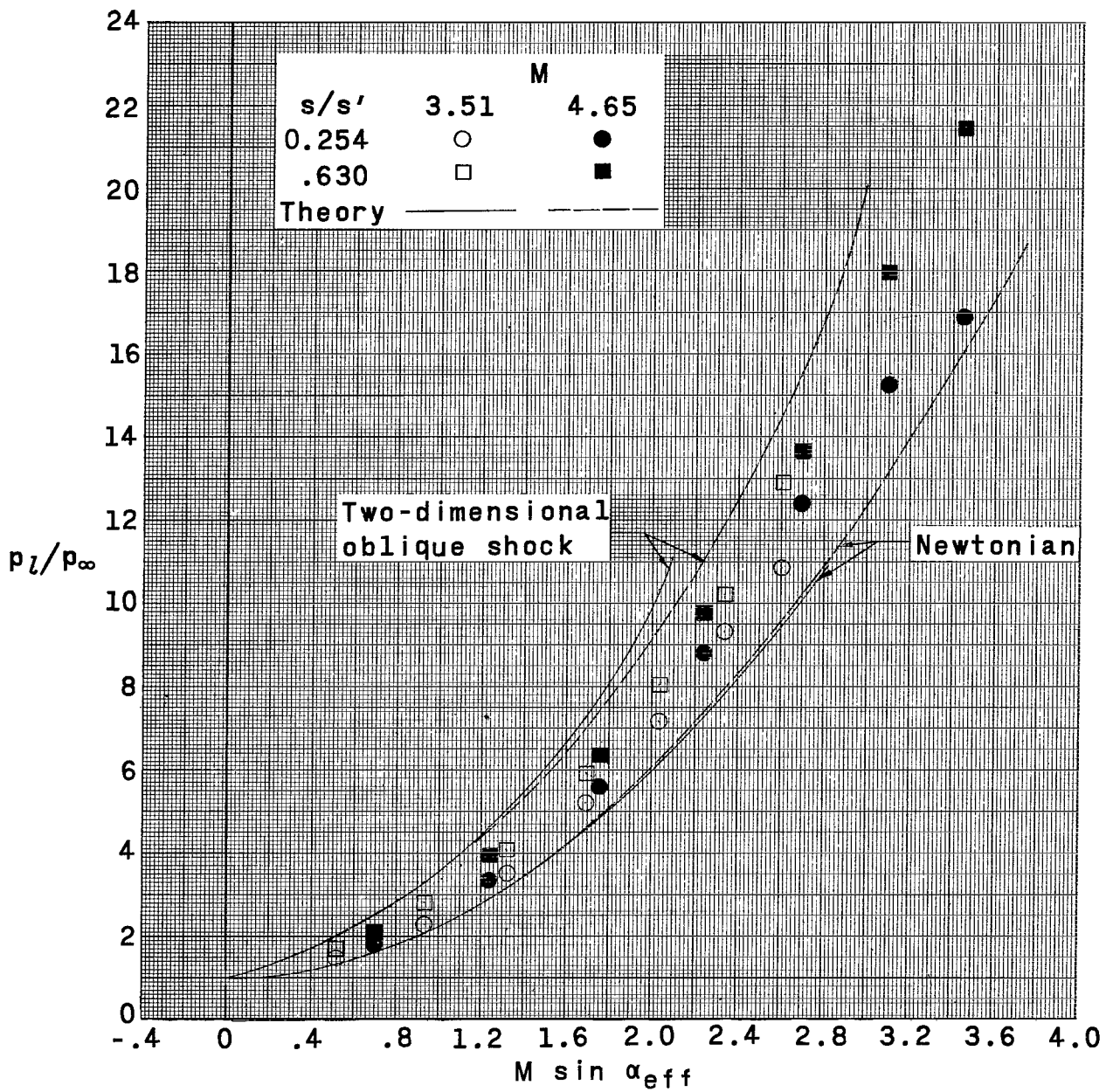
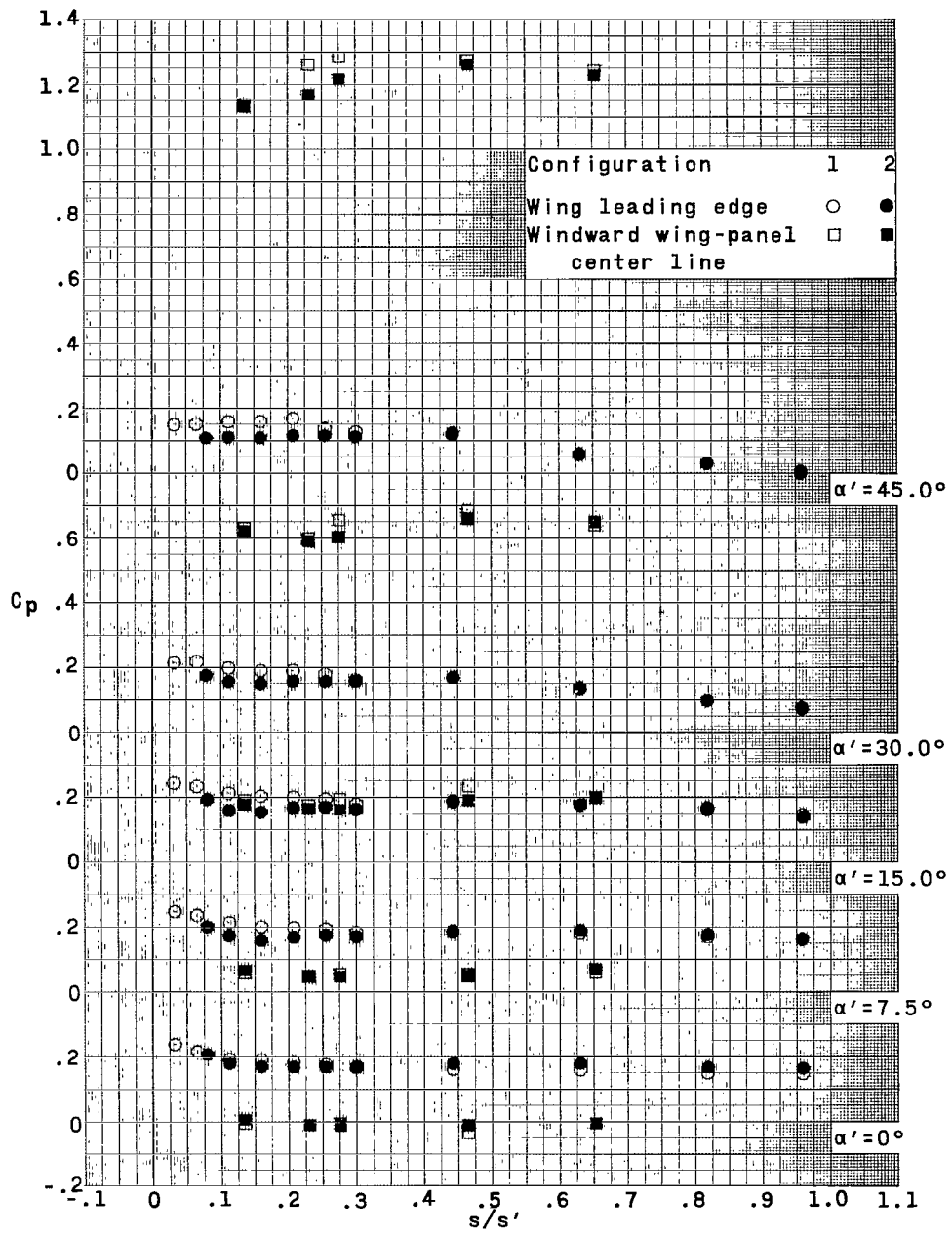
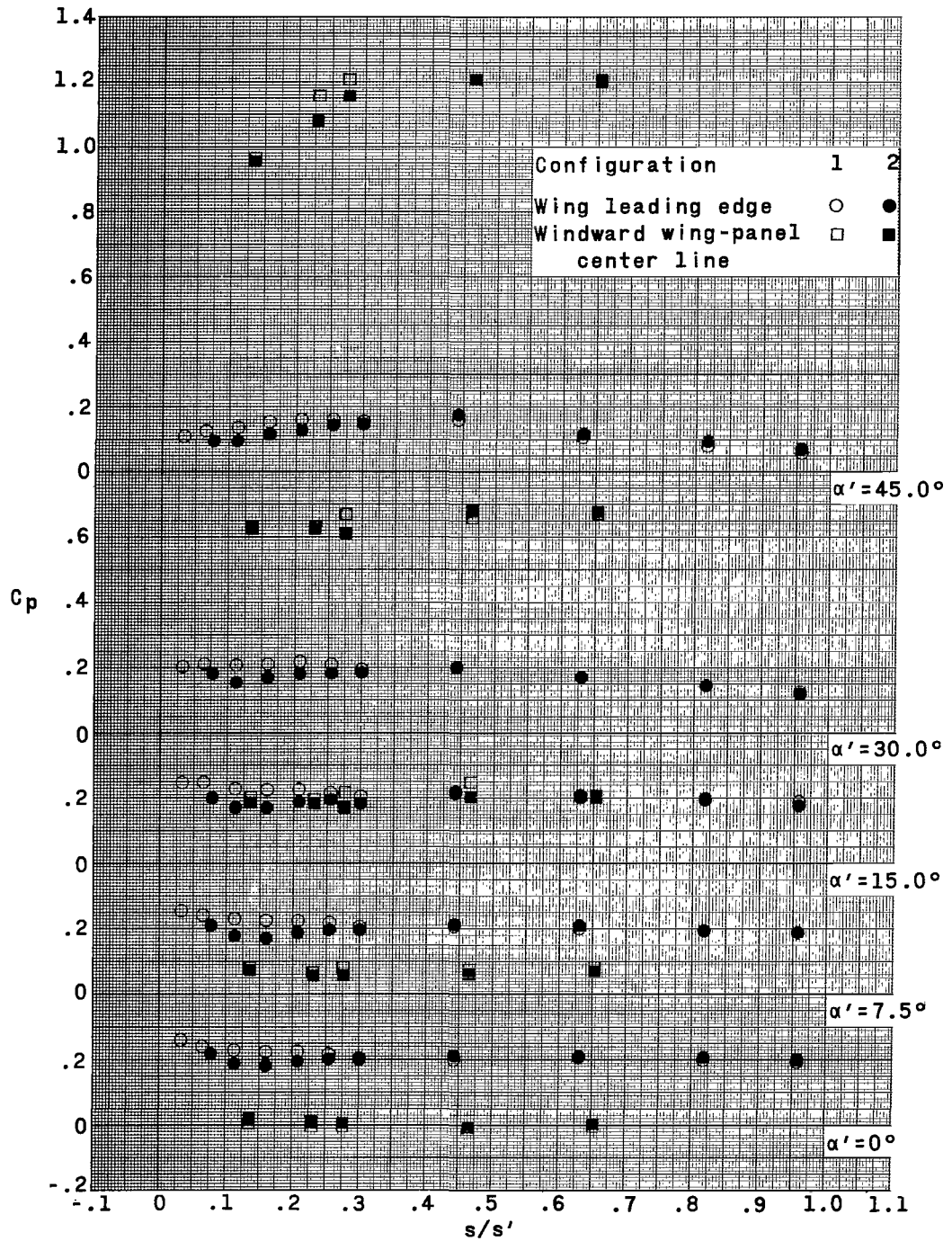


Figure 10.- Correlation of experimental data on windward surface at  $\epsilon_p/2$  of configuration 3 at Mach numbers 3.51 and 4.65 through an angle-of-attack range from  $0^\circ$  to  $45^\circ$ .



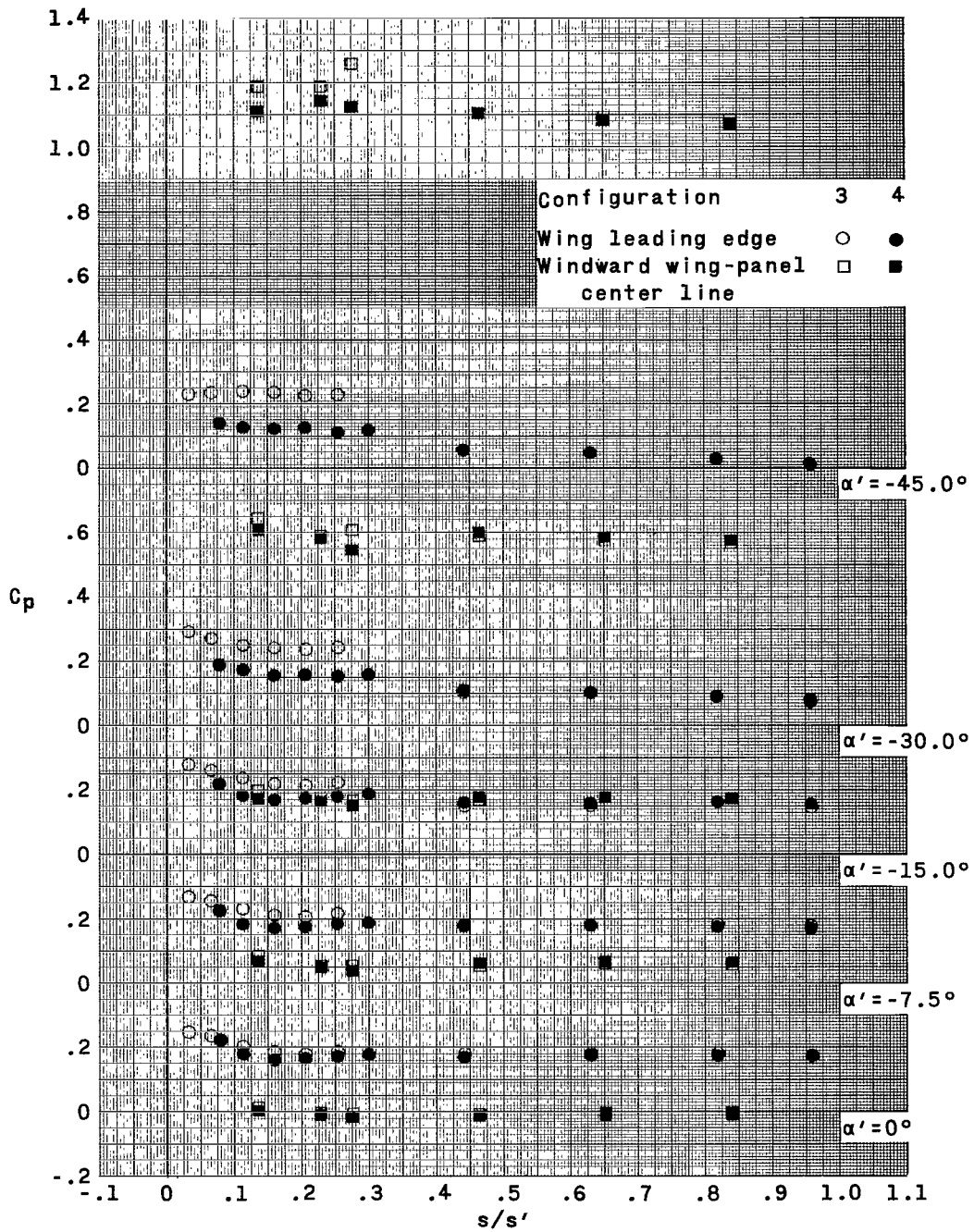
(a)  $M = 3.51$ ;  $R \approx 4.00 \times 10^6$ .

Figure 11.- Effect of nose bluntness on  $C_p$  distribution along windward center line and wing leading edge of models with  $0^\circ$  dihedral.



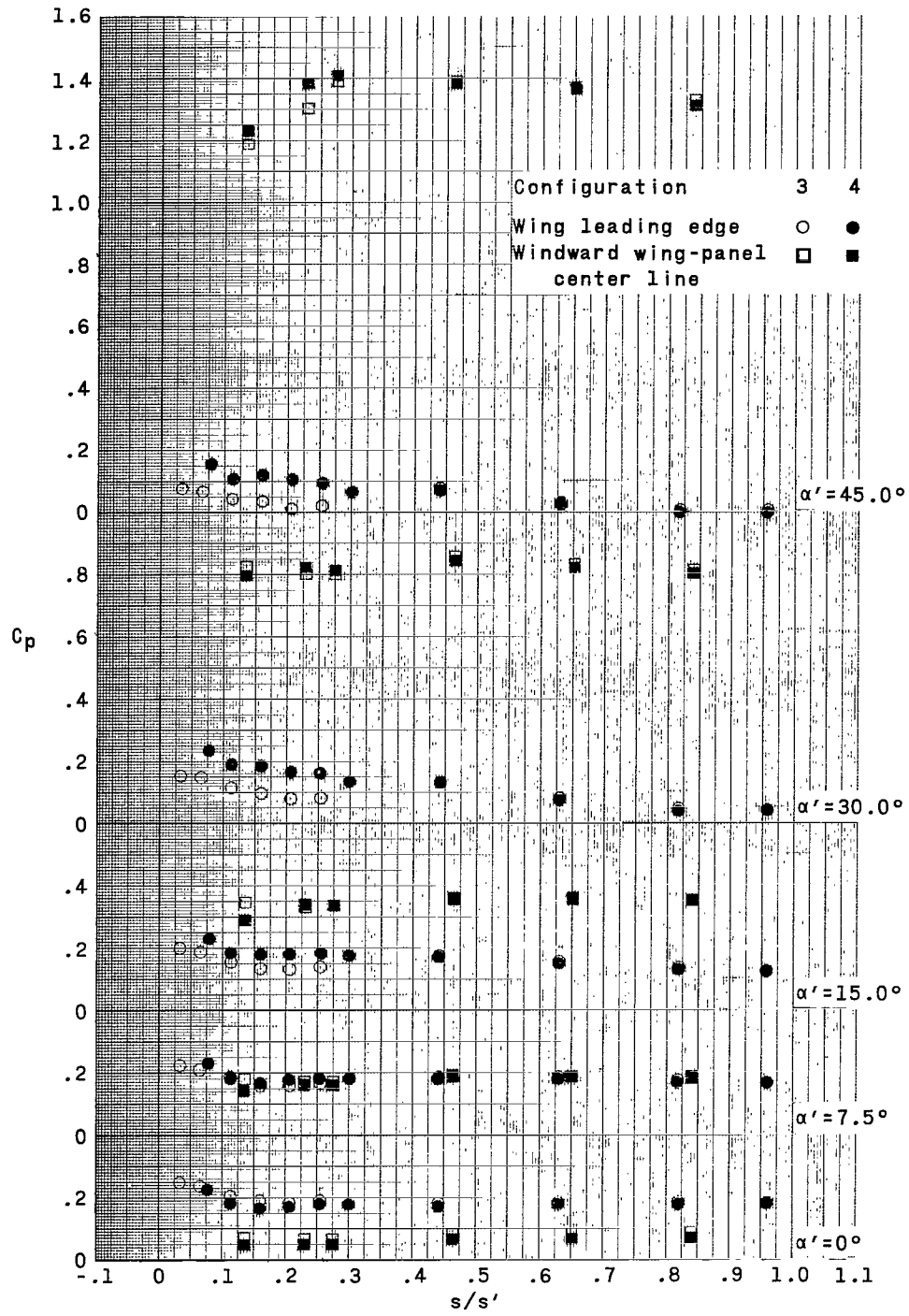
(b)  $M = 4.65$ ;  $R \approx 4.00 \times 10^6$ .

Figure 11.- Concluded.



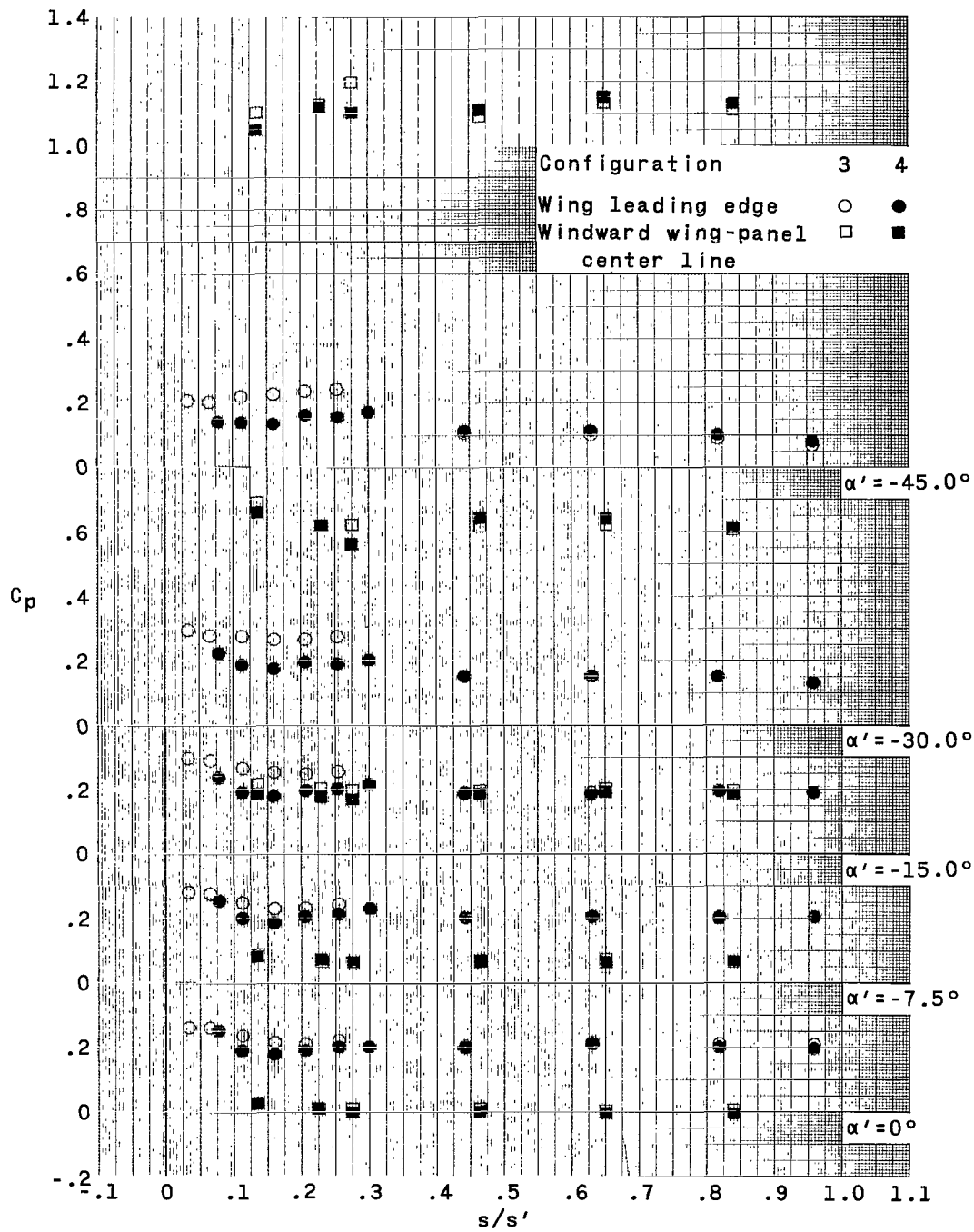
(a)  $M = 3.51$ ;  $R \approx 4.00 \times 10^6$ .

Figure 12.- Effect of nose bluntness on  $C_p$  distribution along windward center line and wing leading edge of models with  $24.3^\circ$  dihedral.



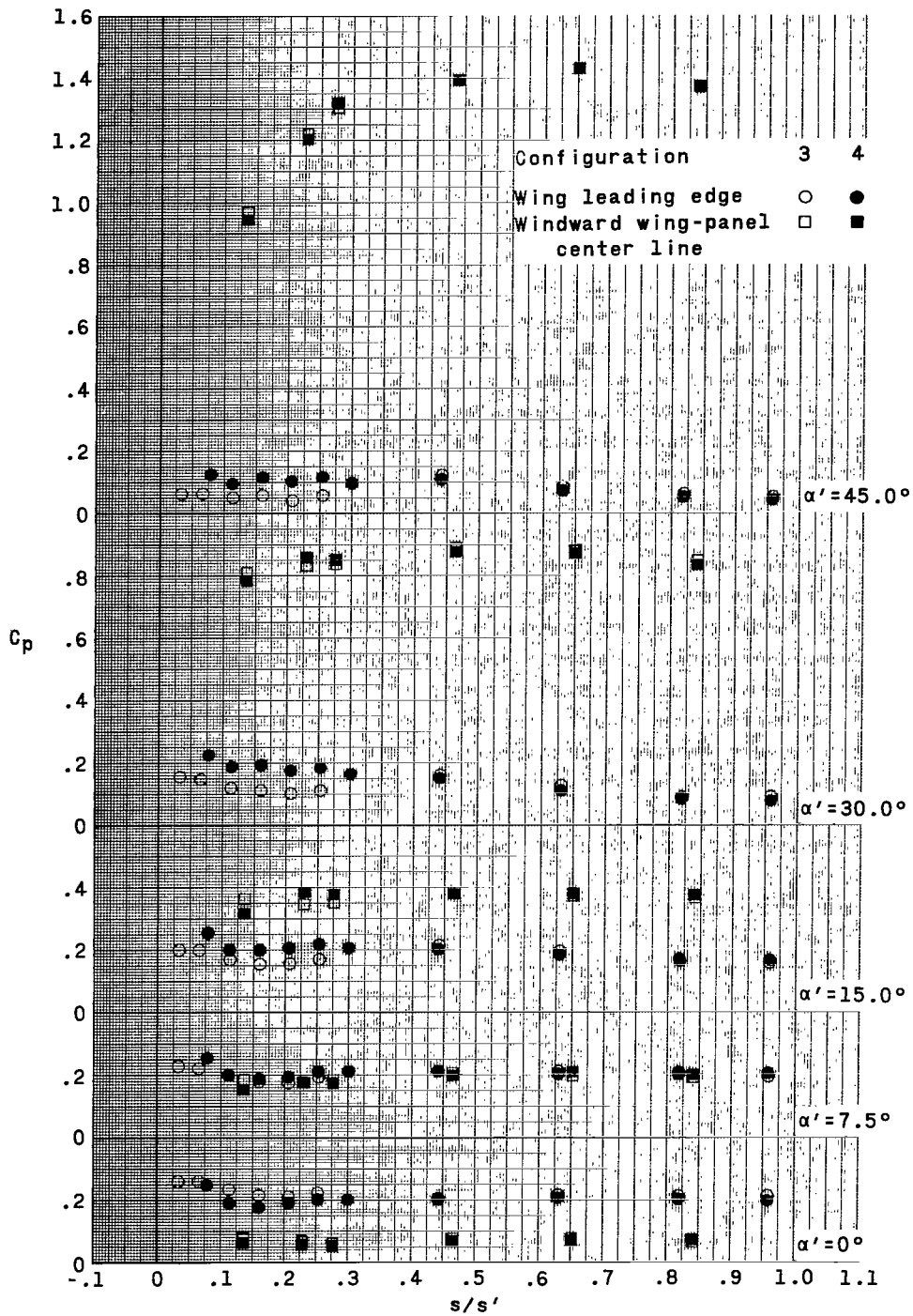
(a) Concluded.

Figure 12.- Continued.



(b)  $M = 4.65$ ;  $R \approx 4.00 \times 10^6$ .

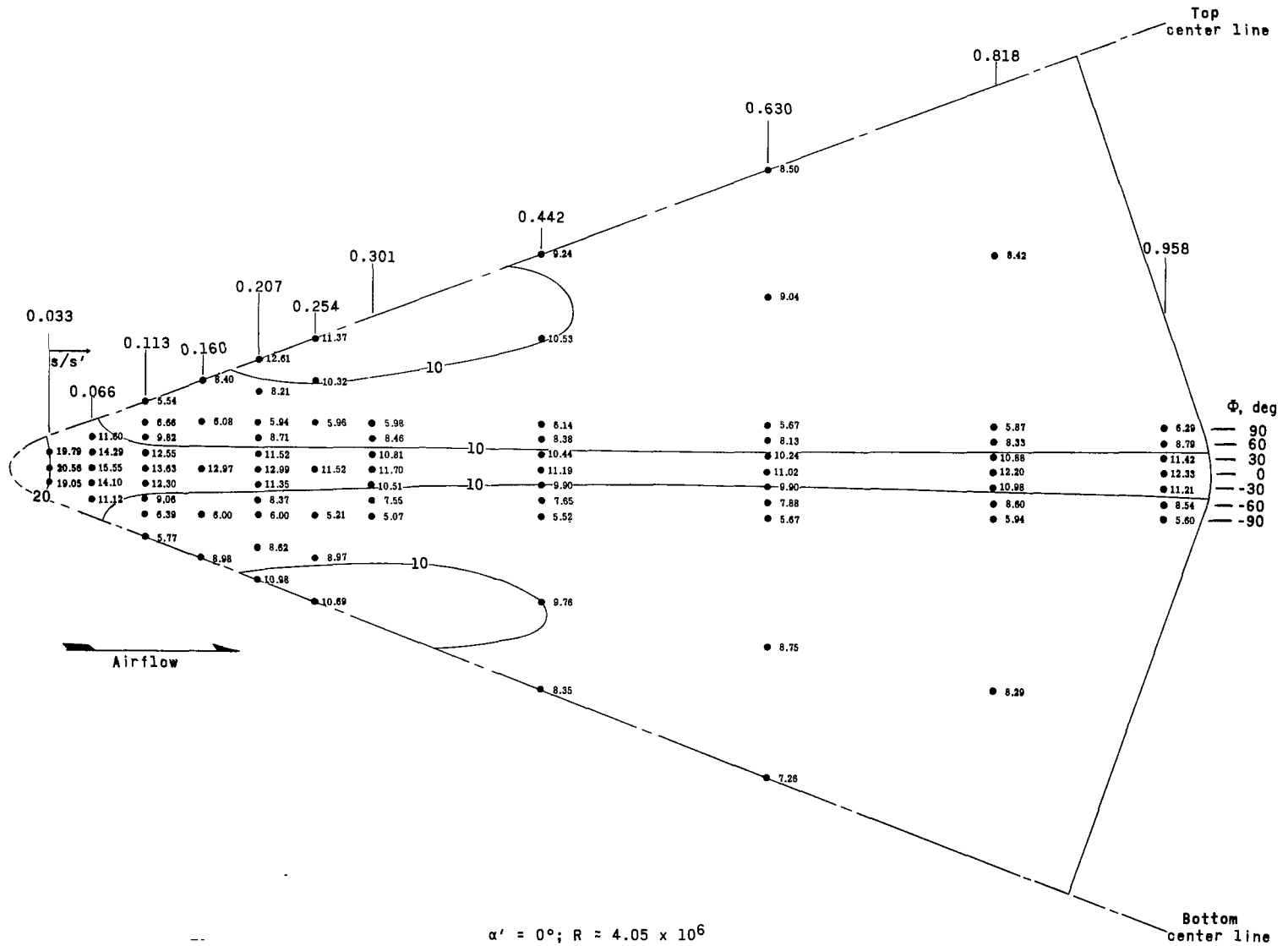
Figure 12.- Continued.



(b) Concluded.

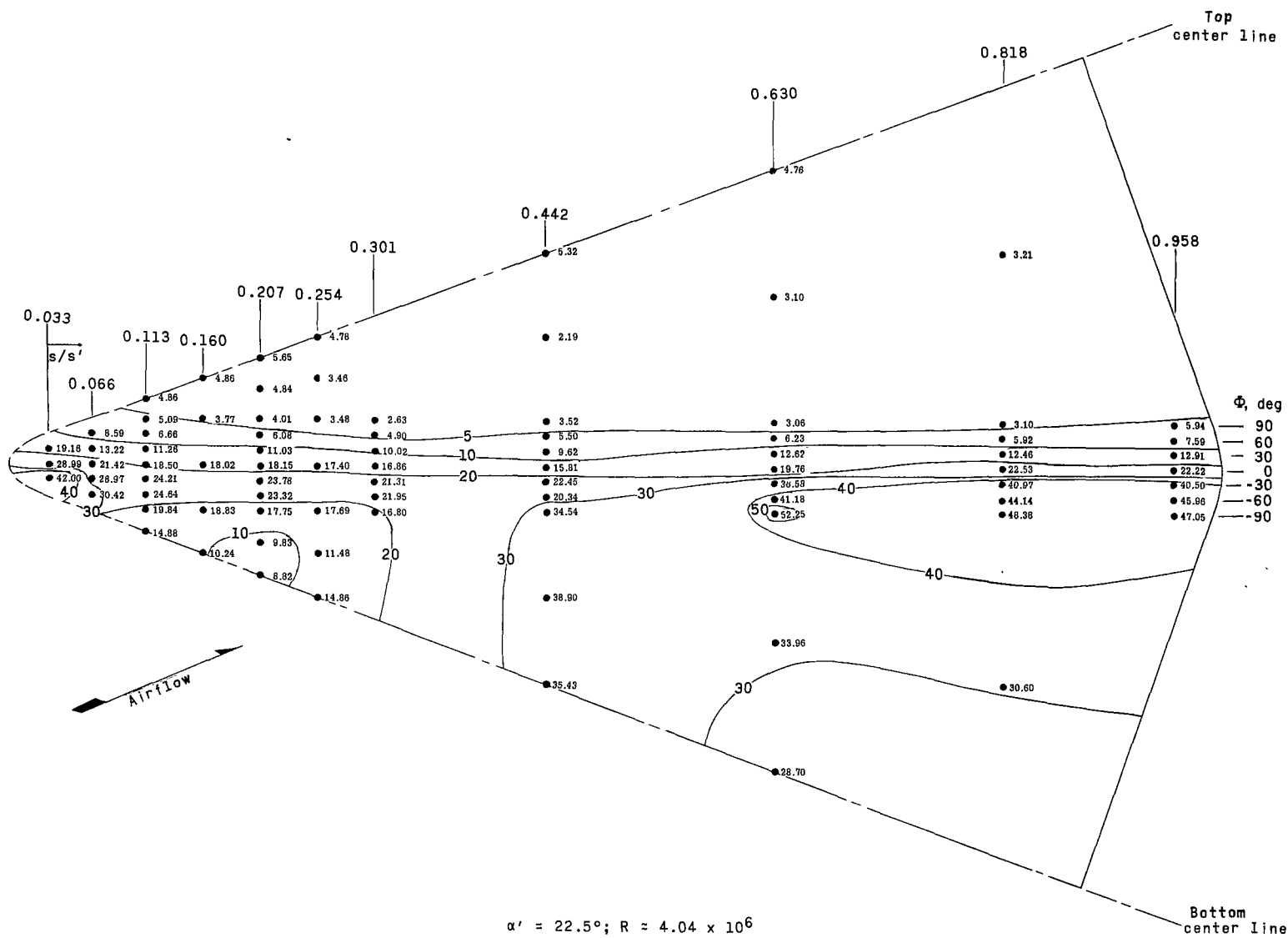
Figure 12.- Concluded.





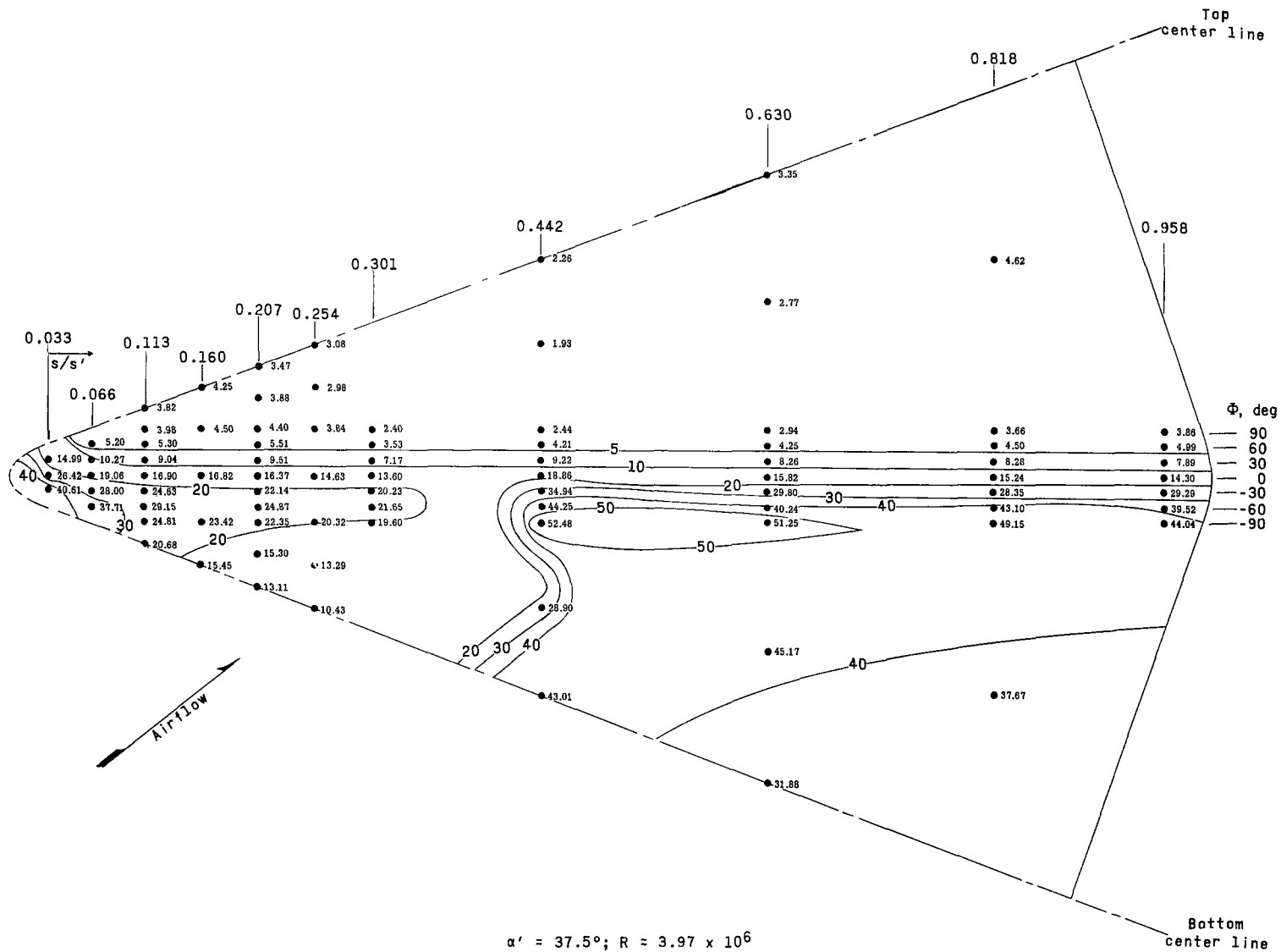
(a) Configuration 1;  $M = 3.51$ .

Figure 13.- Effect of angle of attack on Stanton number distribution ( $N_{St} \times 10^{-4}$ ).



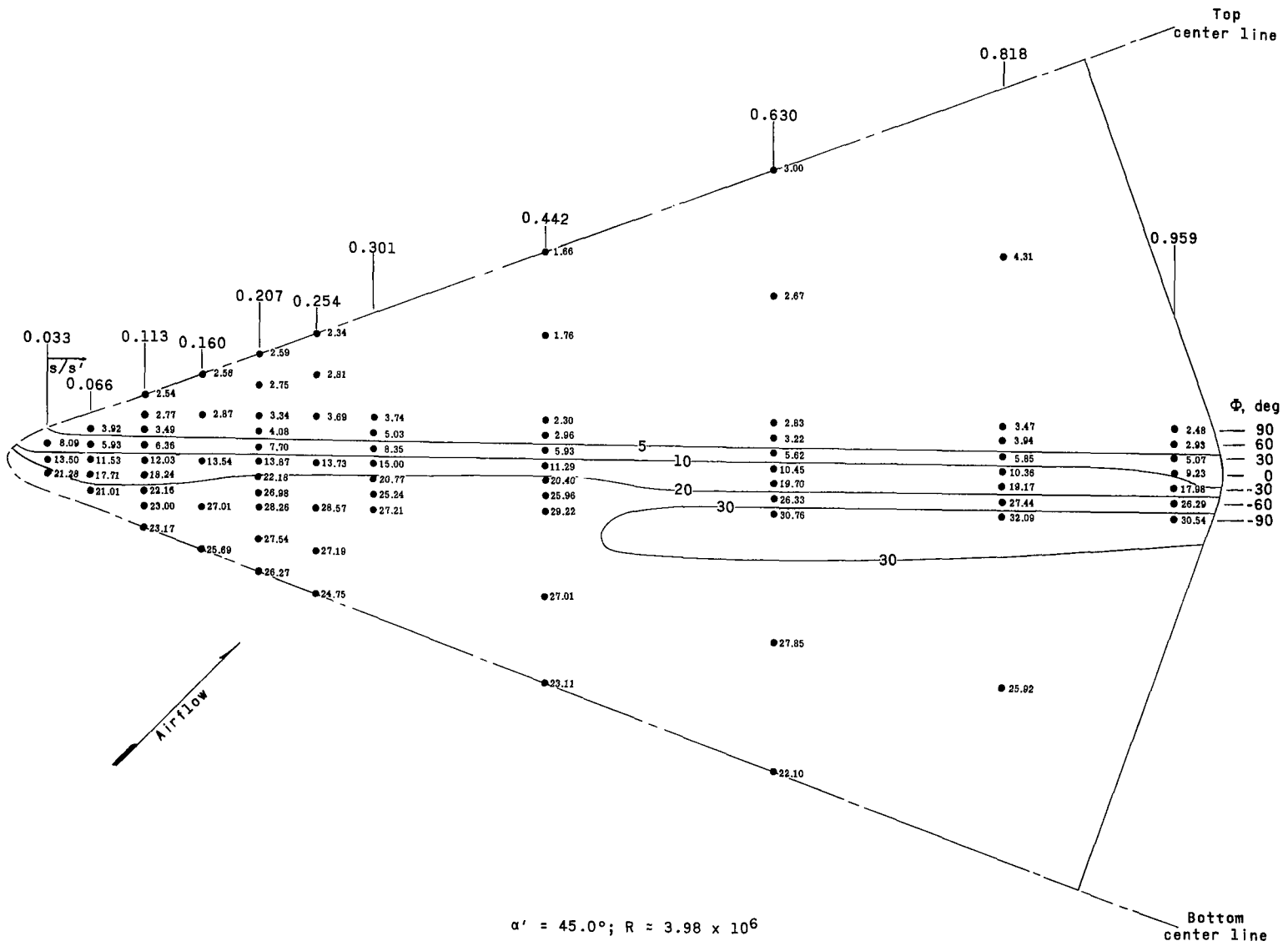
(a) Continued.

Figure 13.- Continued.

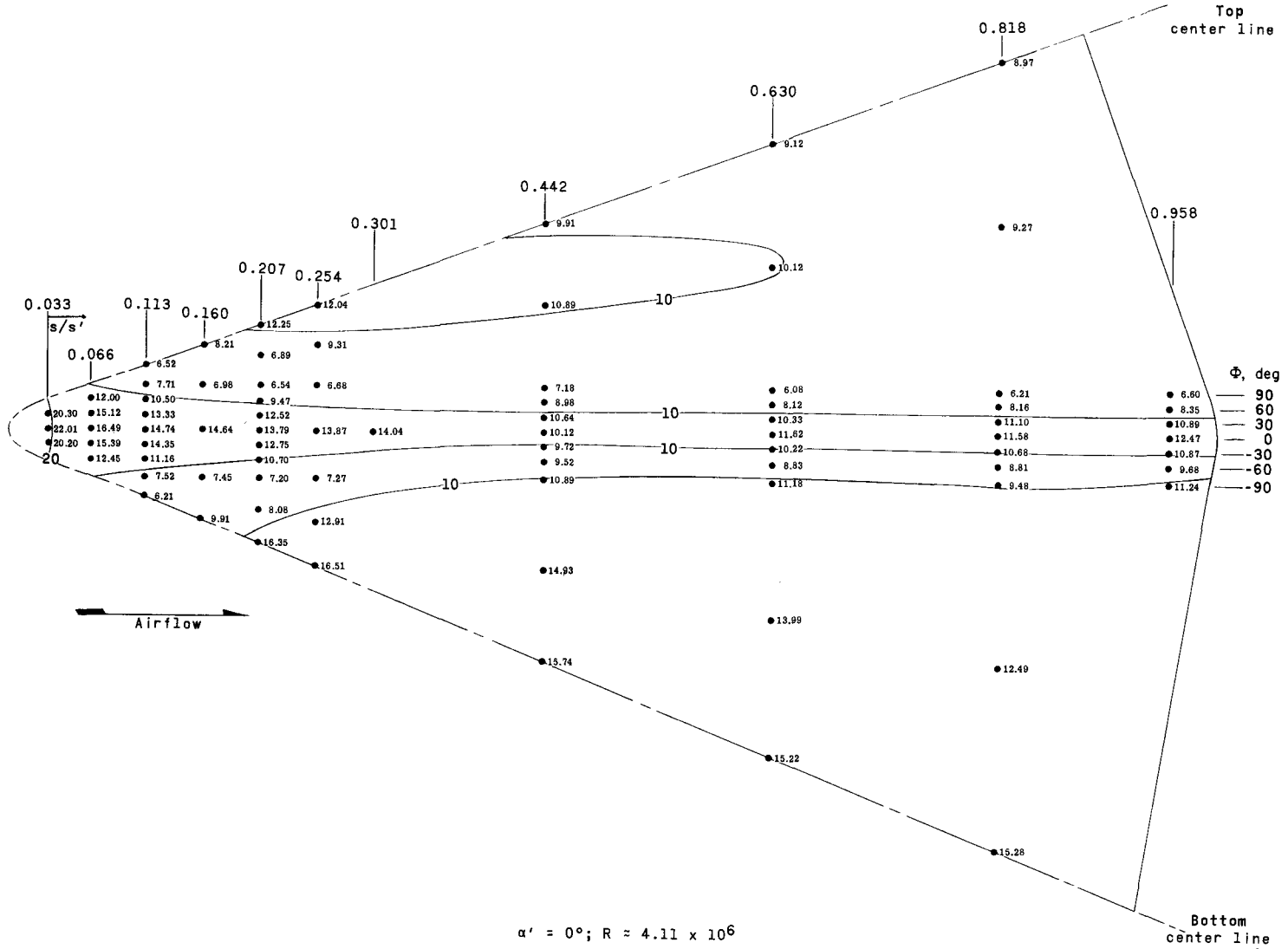


(a) Continued.

Figure 13.- Continued.

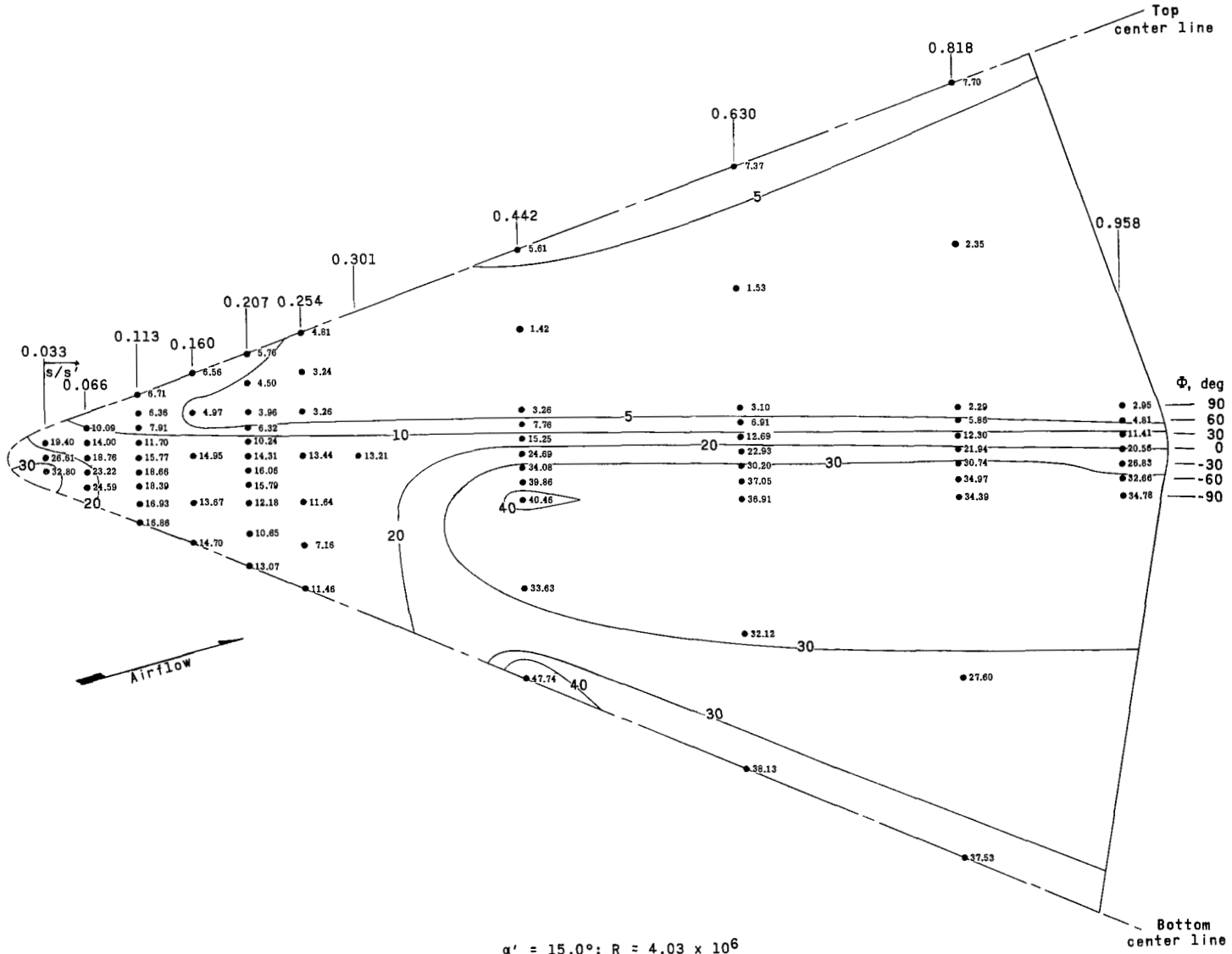


(a) Concluded.  
 Figure 13.- Continued.



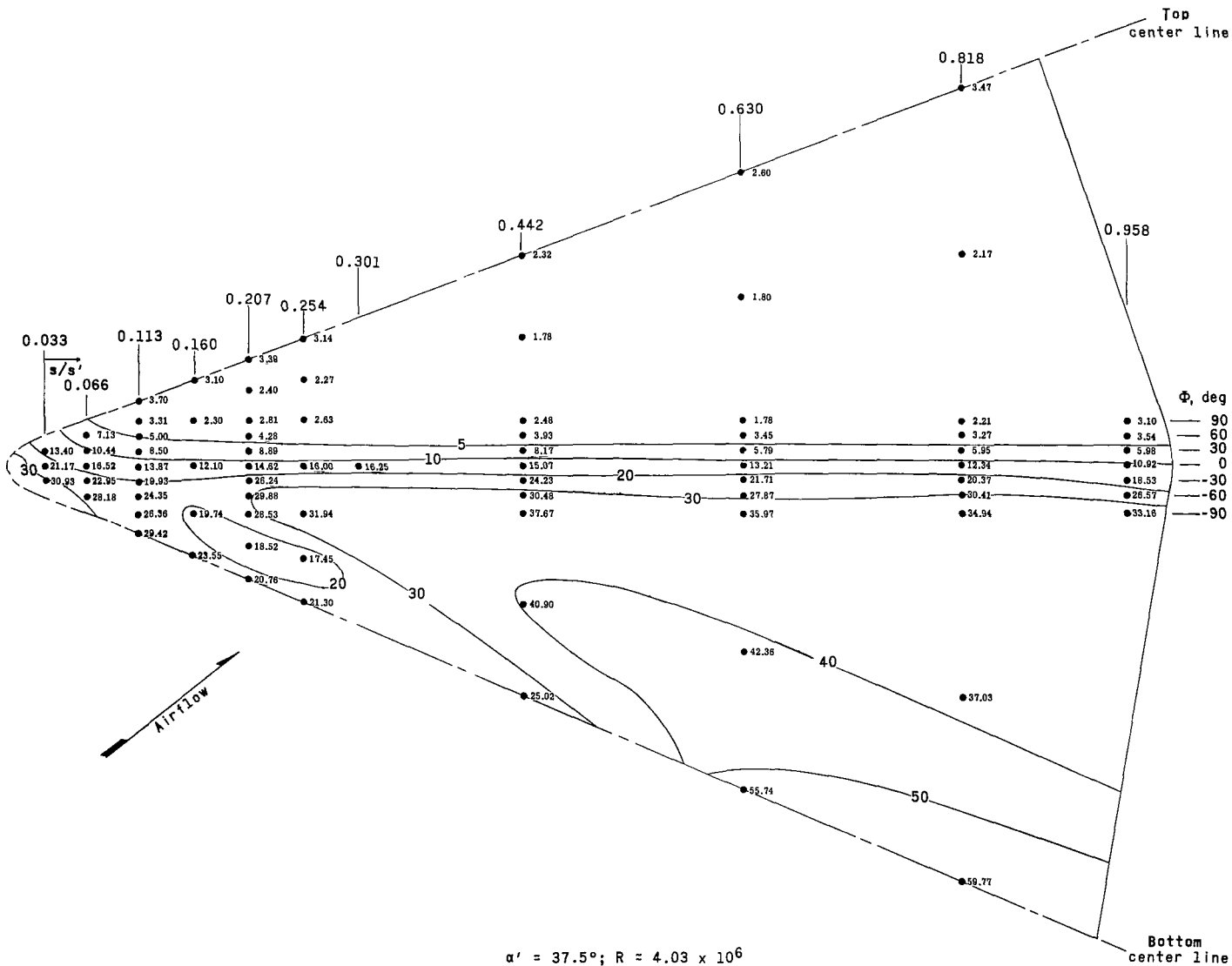
(b) Configuration 3;  $M = 3.51$ .

Figure 13.- Continued.



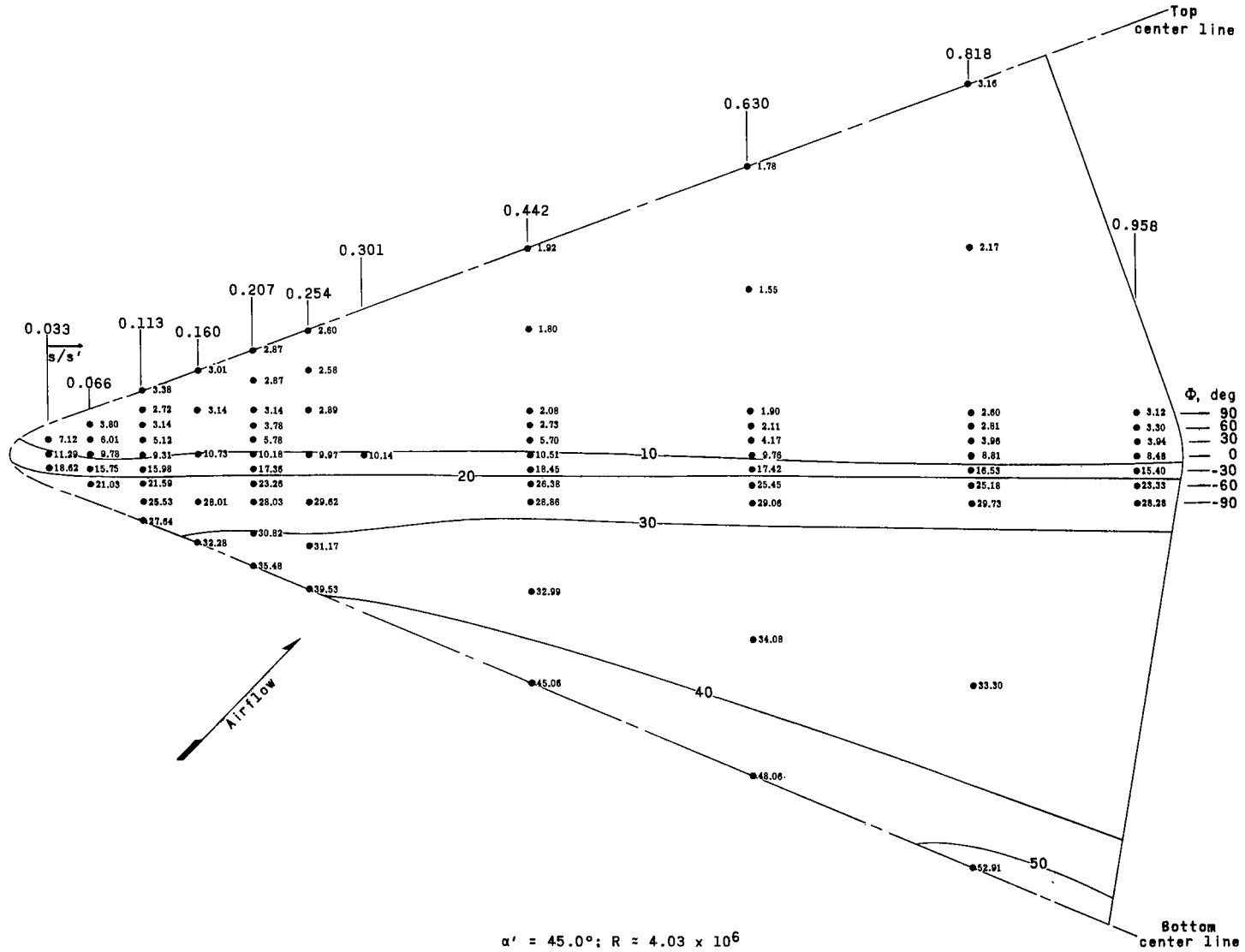
(b) Continued.

Figure 13.- Continued.



(b) Continued.

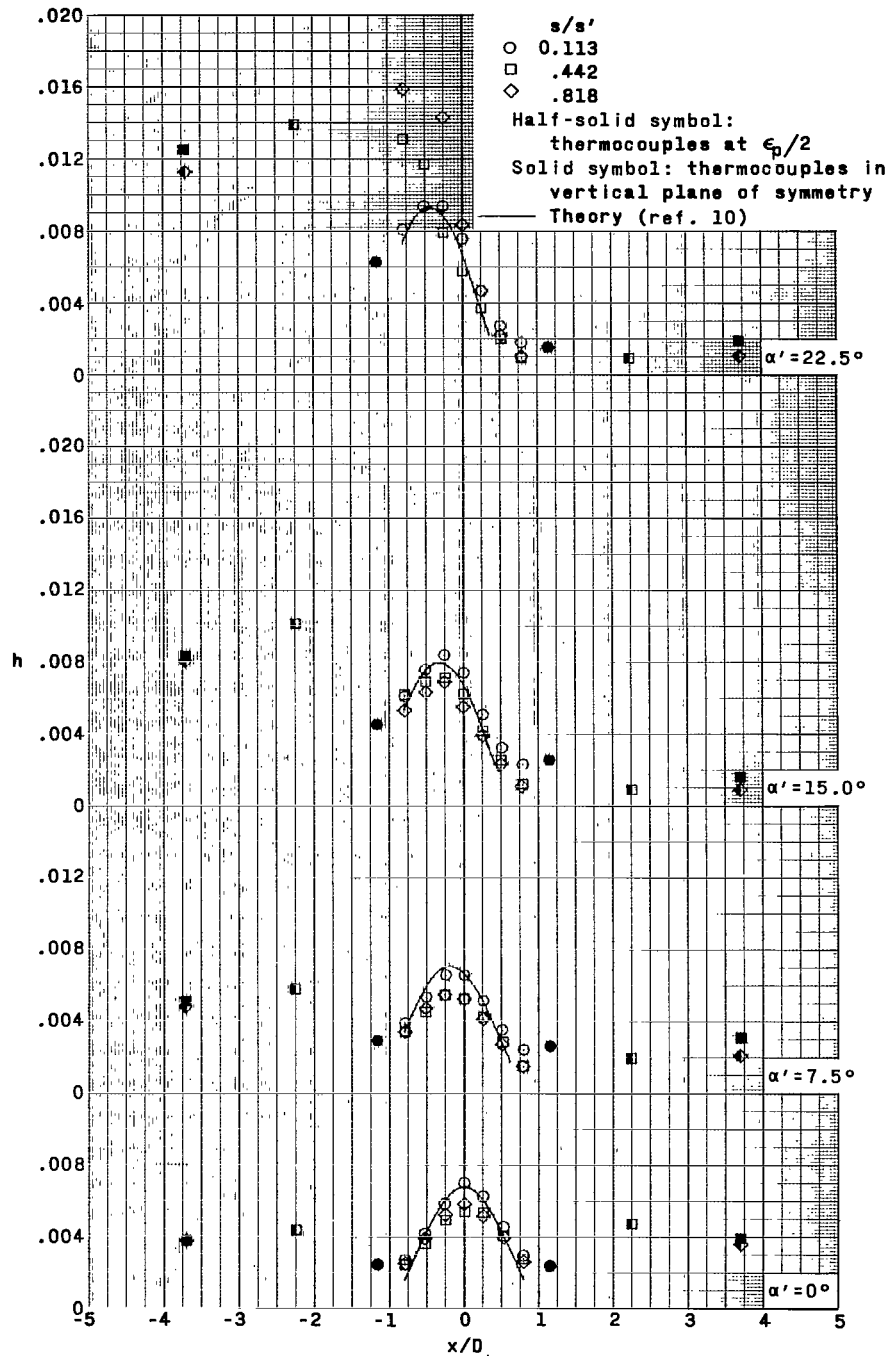
Figure 13.- Continued.



(b) Concluded.

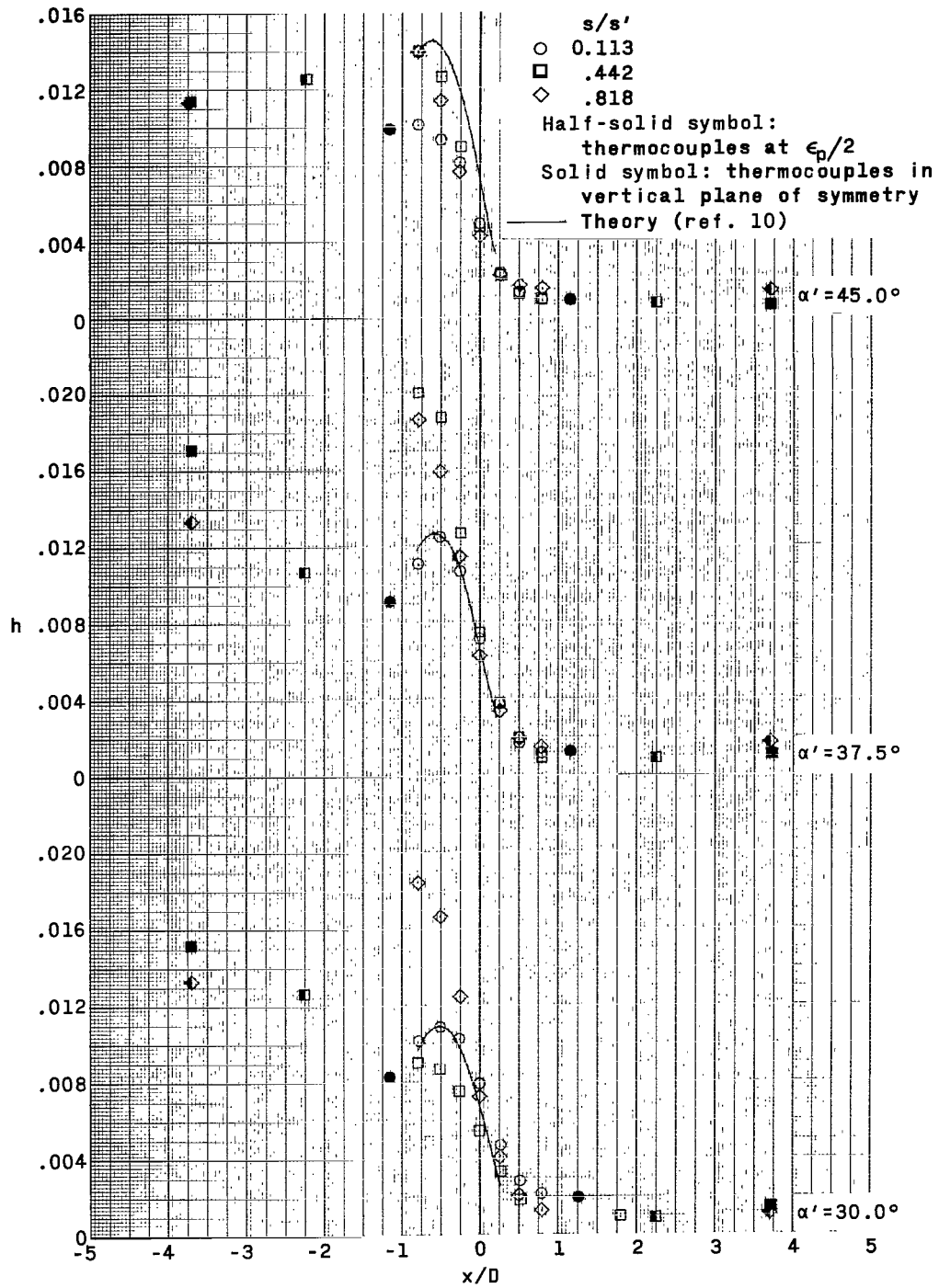
Figure 13.- Concluded.





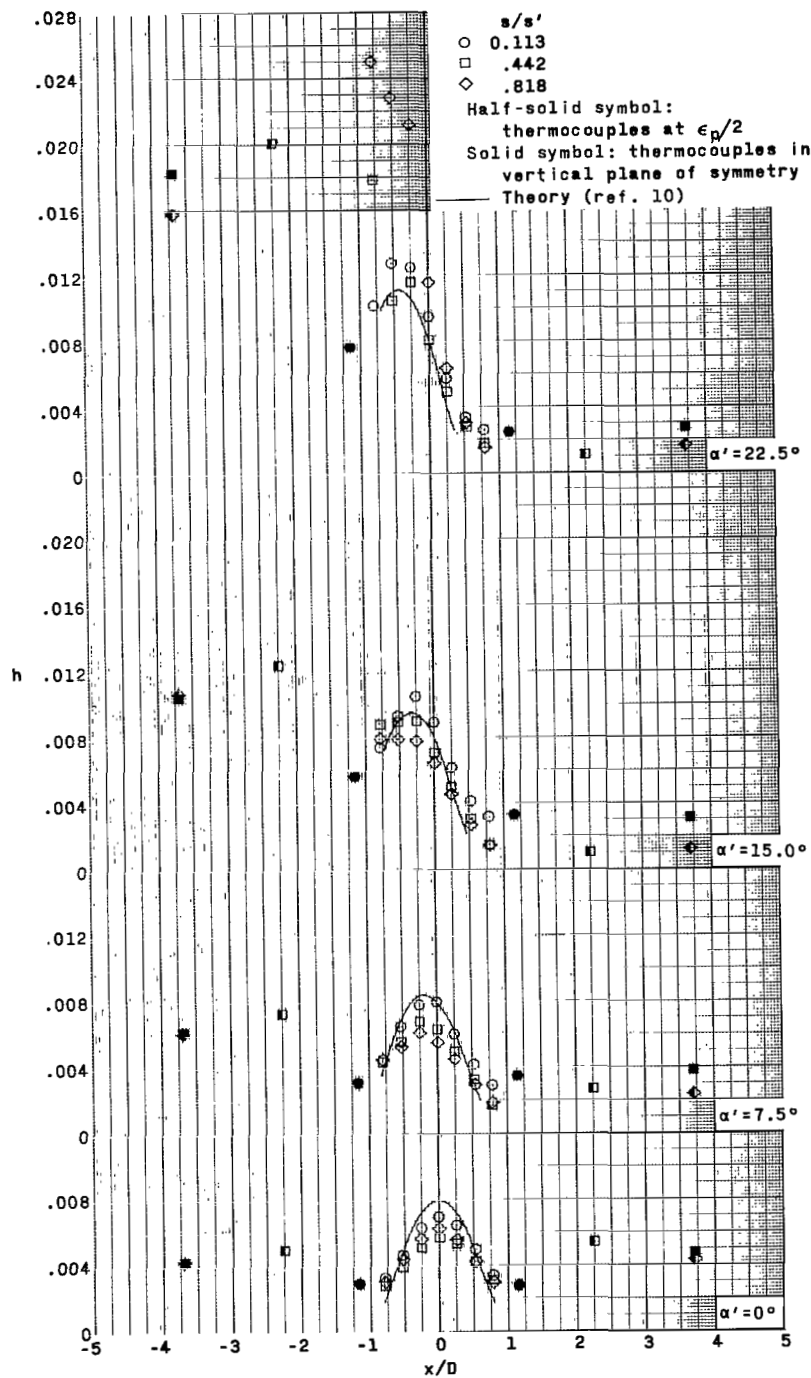
(a)  $M = 3.51$ ;  $R \approx 2.90 \times 10^6$ .

Figure 14.- Effect of angle of attack, Mach number, and Reynolds number on heat-transfer-coefficient distribution normal to wing leading edge of configuration 1.



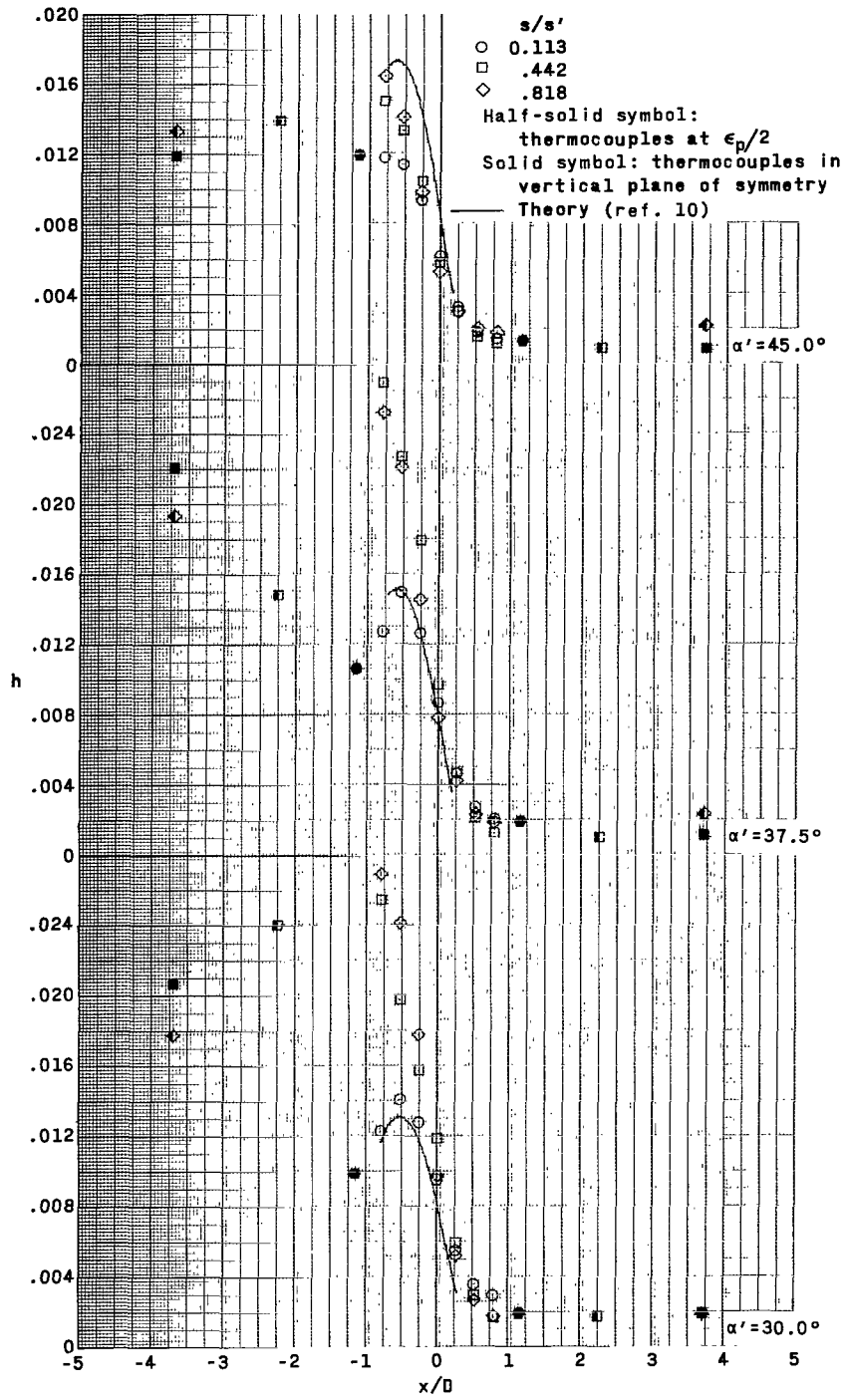
(a) Concluded.

Figure 14.- Continued.



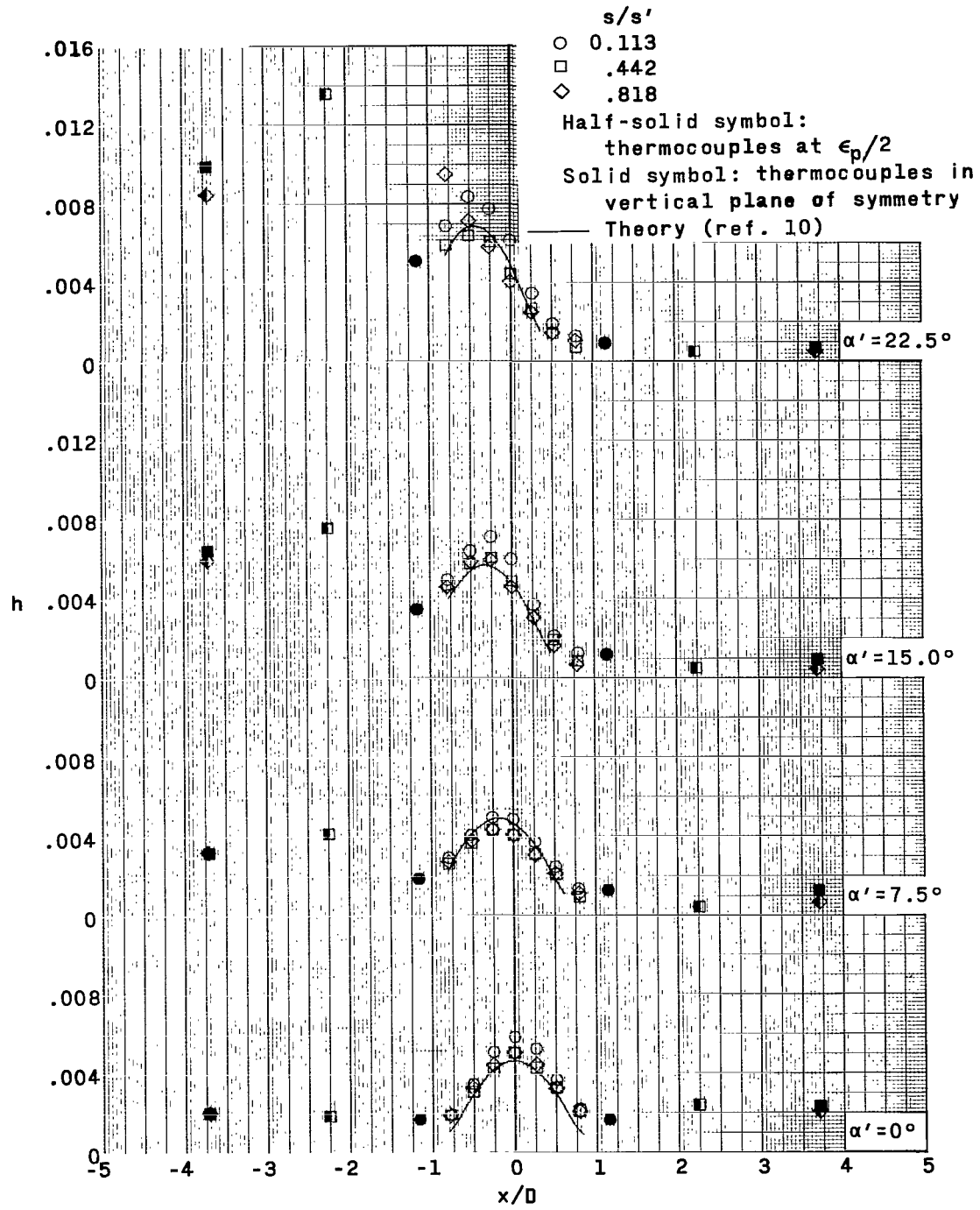
(b)  $M = 3.51$ ;  $R \approx 4.00 \times 10^6$ .

Figure 14.- Continued.



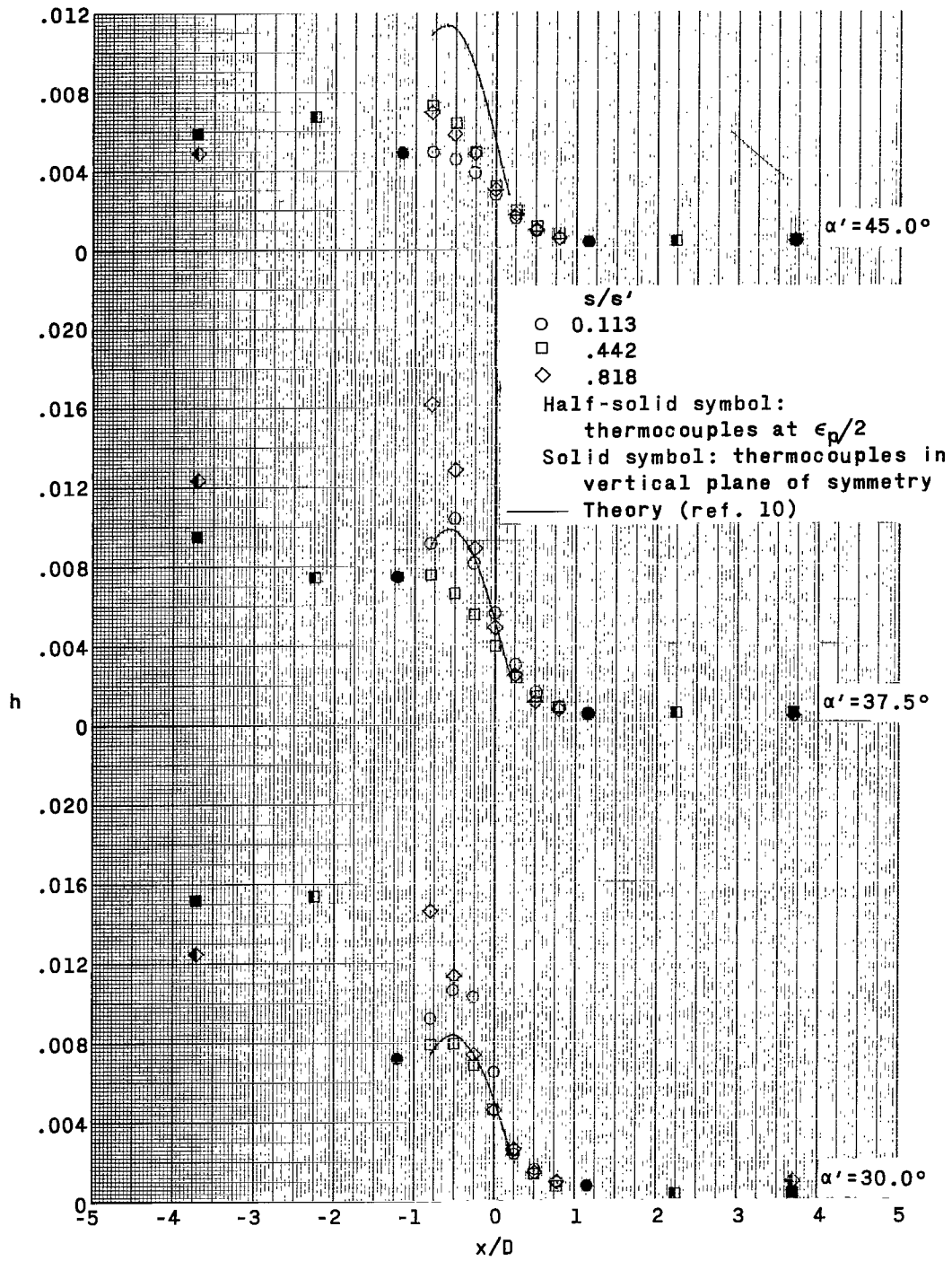
(b) Concluded.

Figure 14.- Continued.



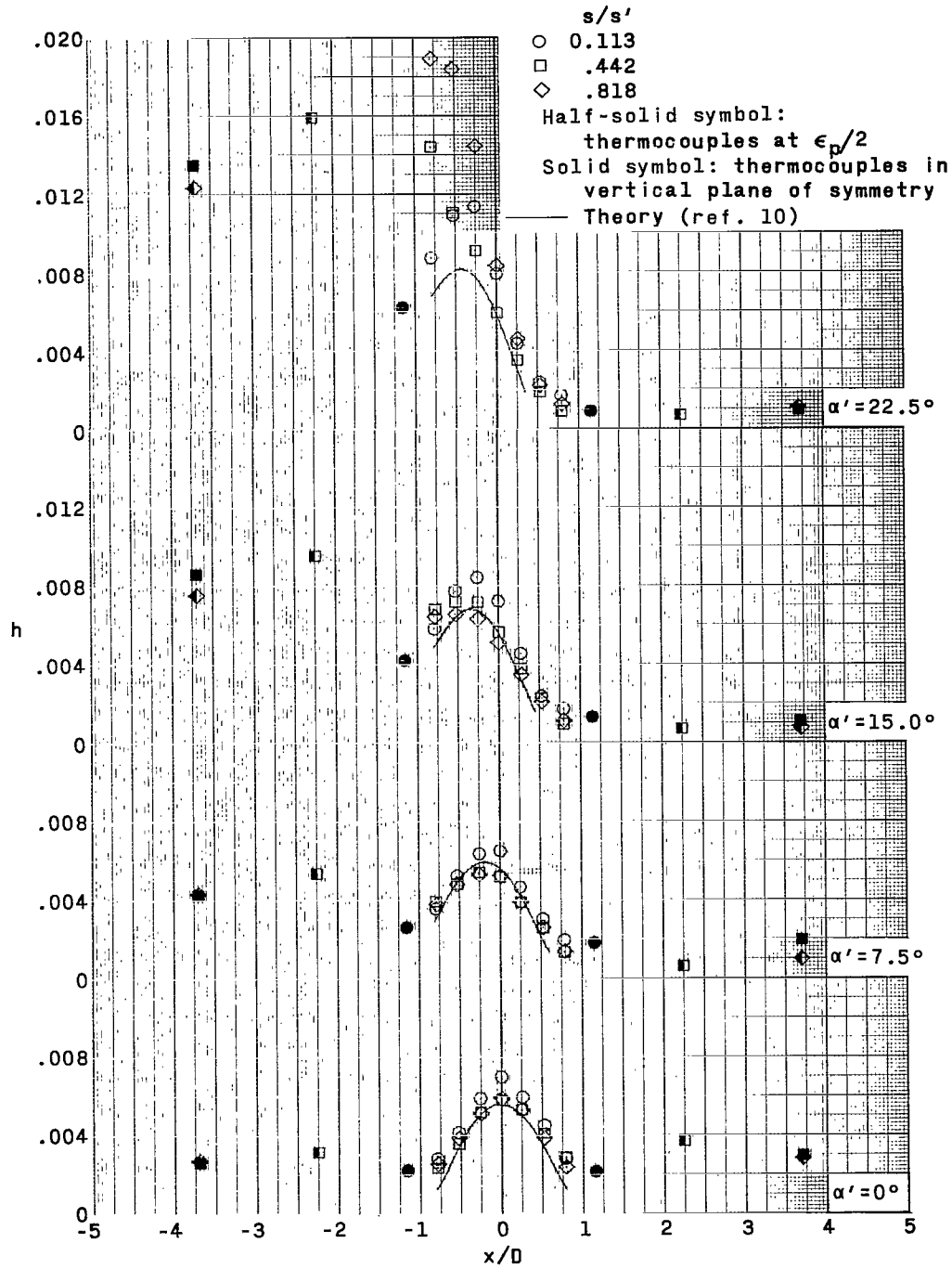
(c)  $M = 4.65$ ;  $R \approx 2.90 \times 10^6$ .

Figure 14.- Continued.



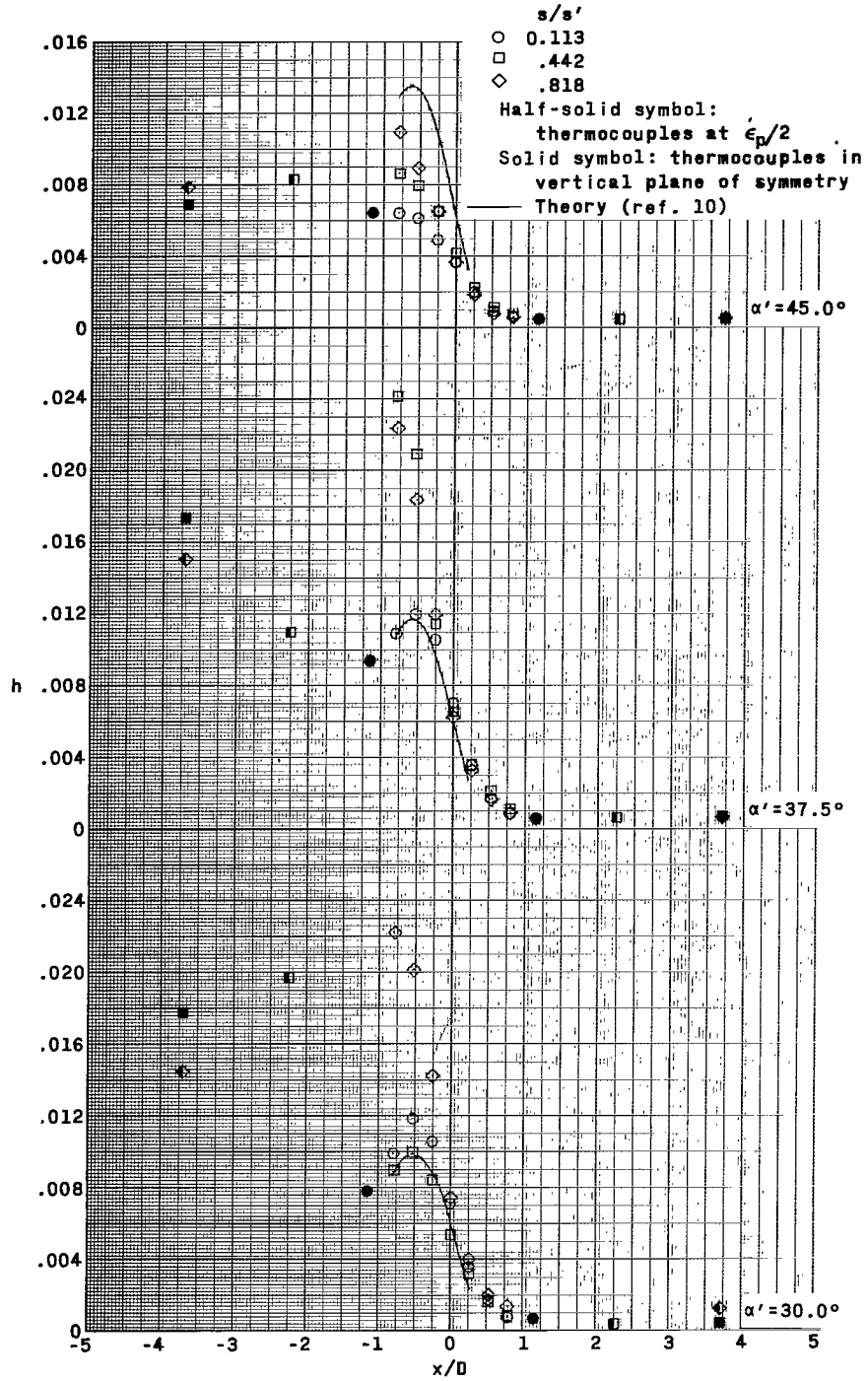
(c) Concluded.

Figure 14.- Continued.



(d)  $M = 4.65$ ;  $R \approx 4.10 \times 10^6$ .

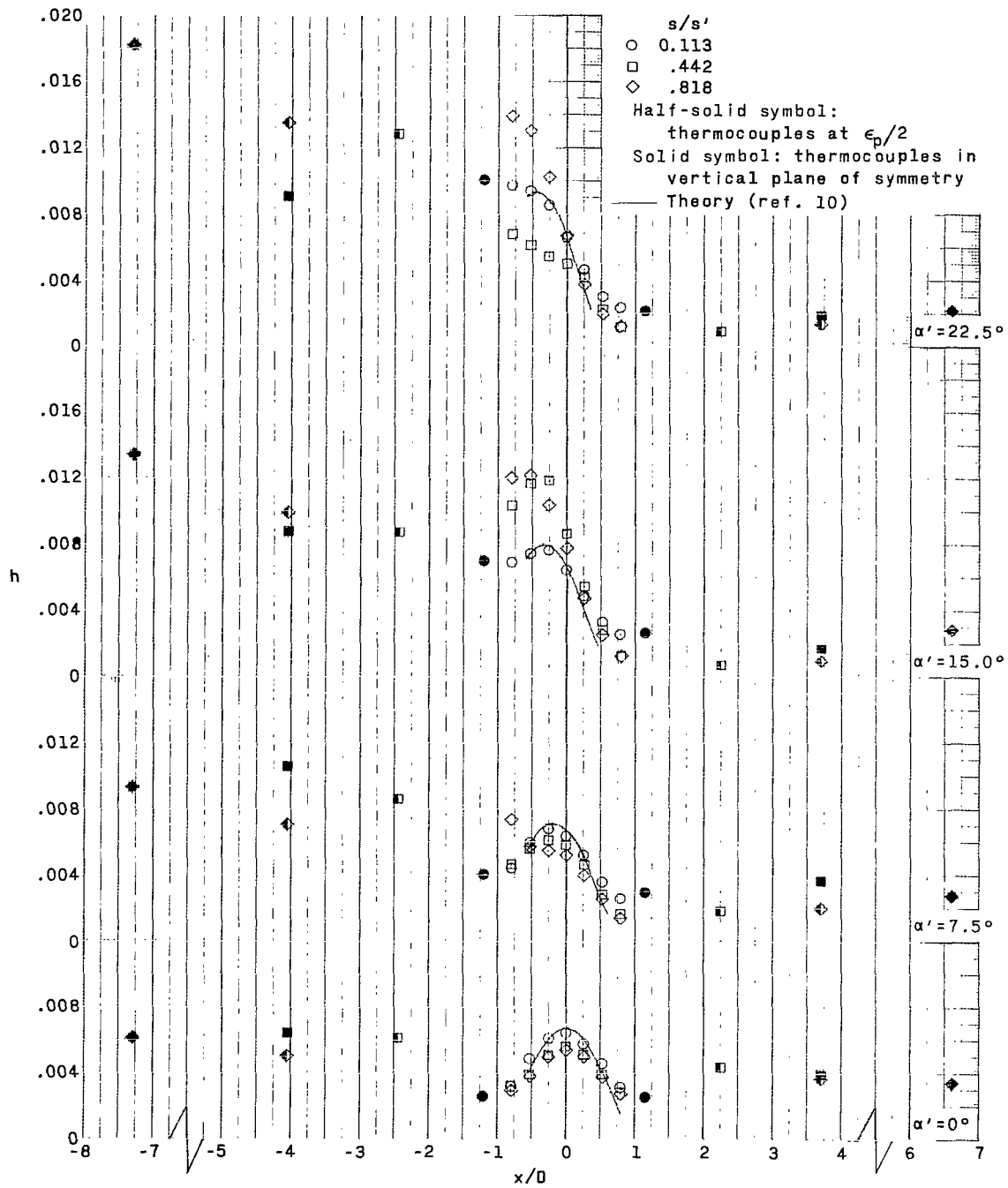
Figure 14.- Continued.



(d) Concluded.

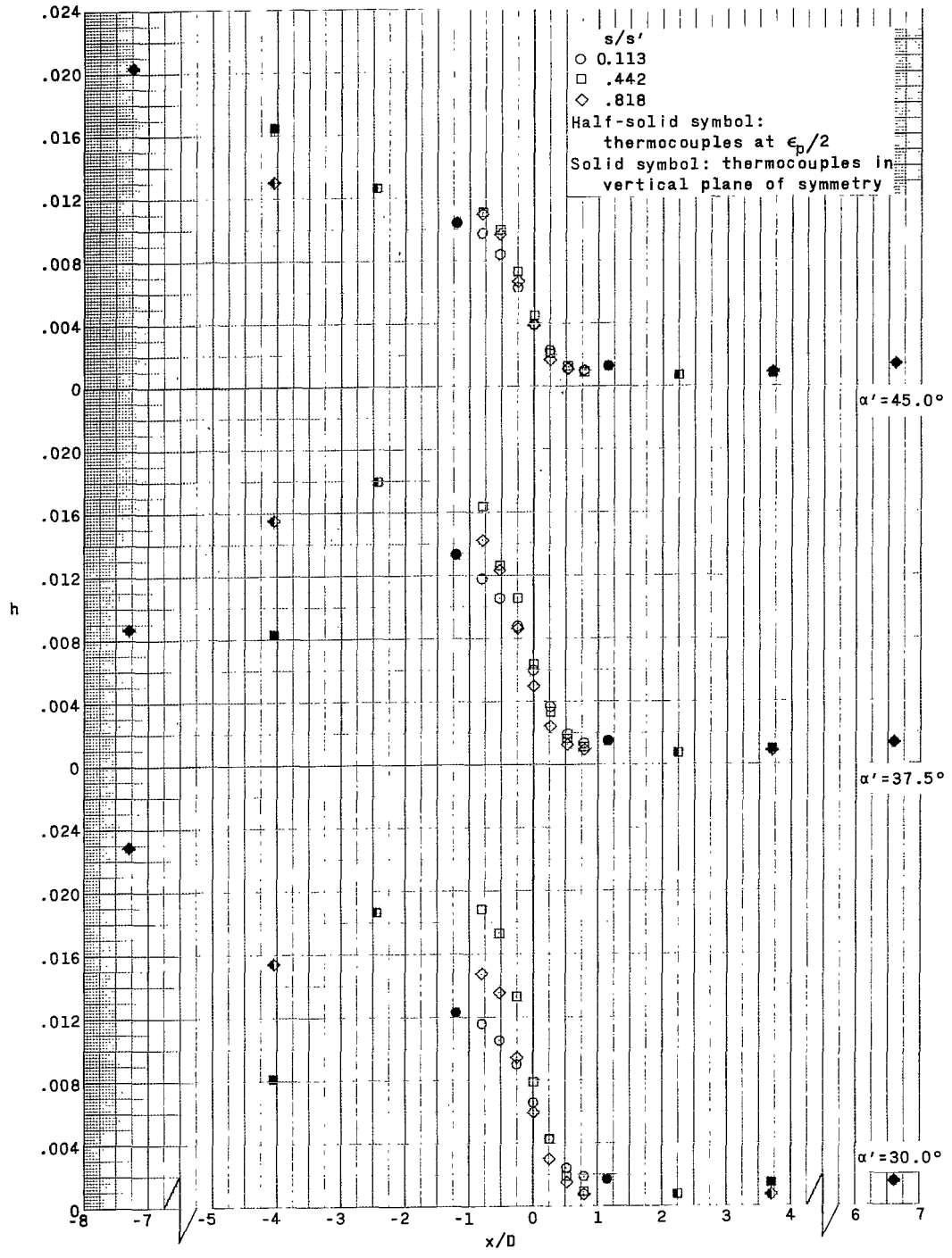
Figure 14.- Concluded.





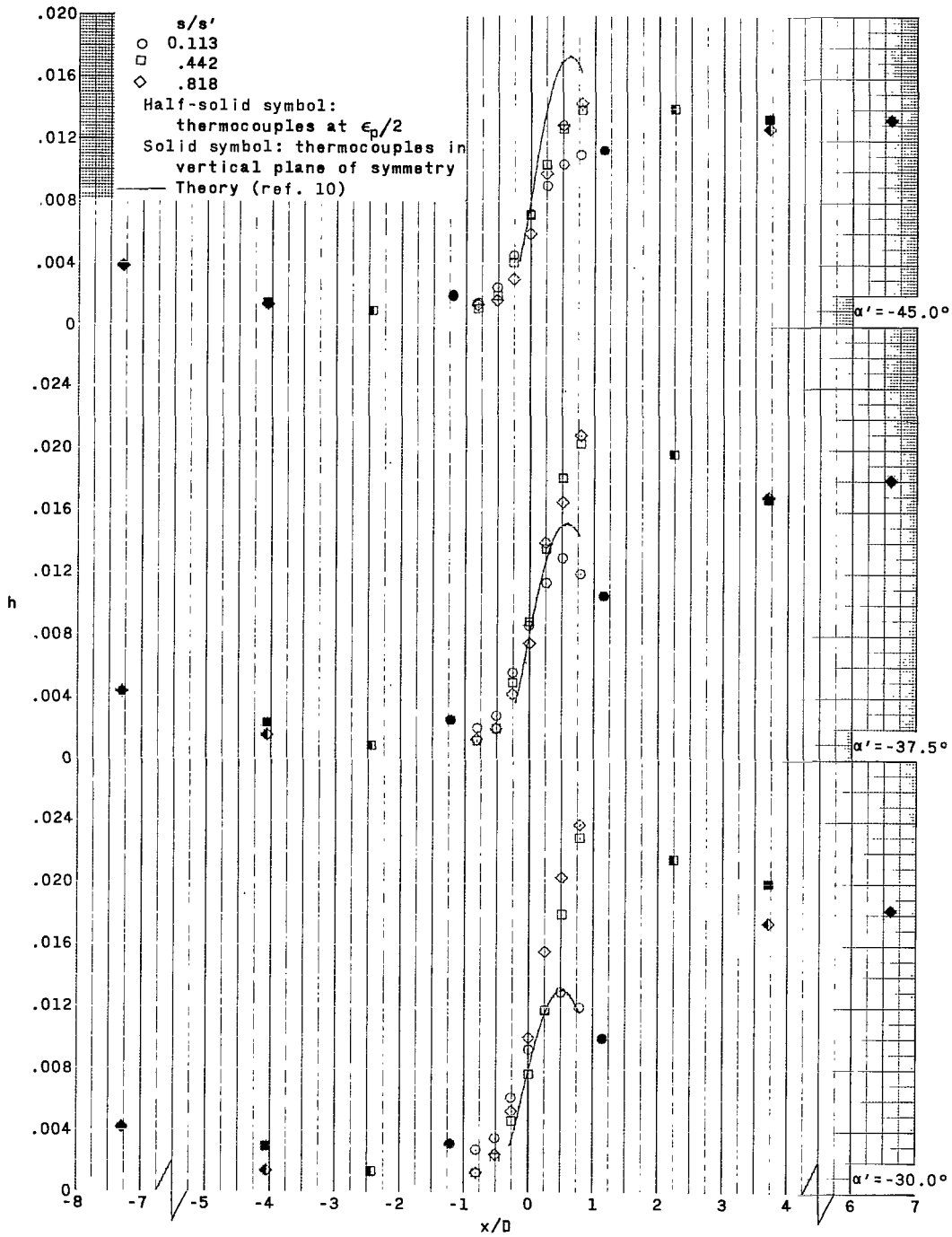
(a)  $M = 3.51$ ;  $R \approx 2.90 \times 10^6$ .

Figure 15.- Effect of angle of attack, Mach number, and Reynolds number on heat-transfer-coefficient distribution normal to wing leading edge of configuration 3.



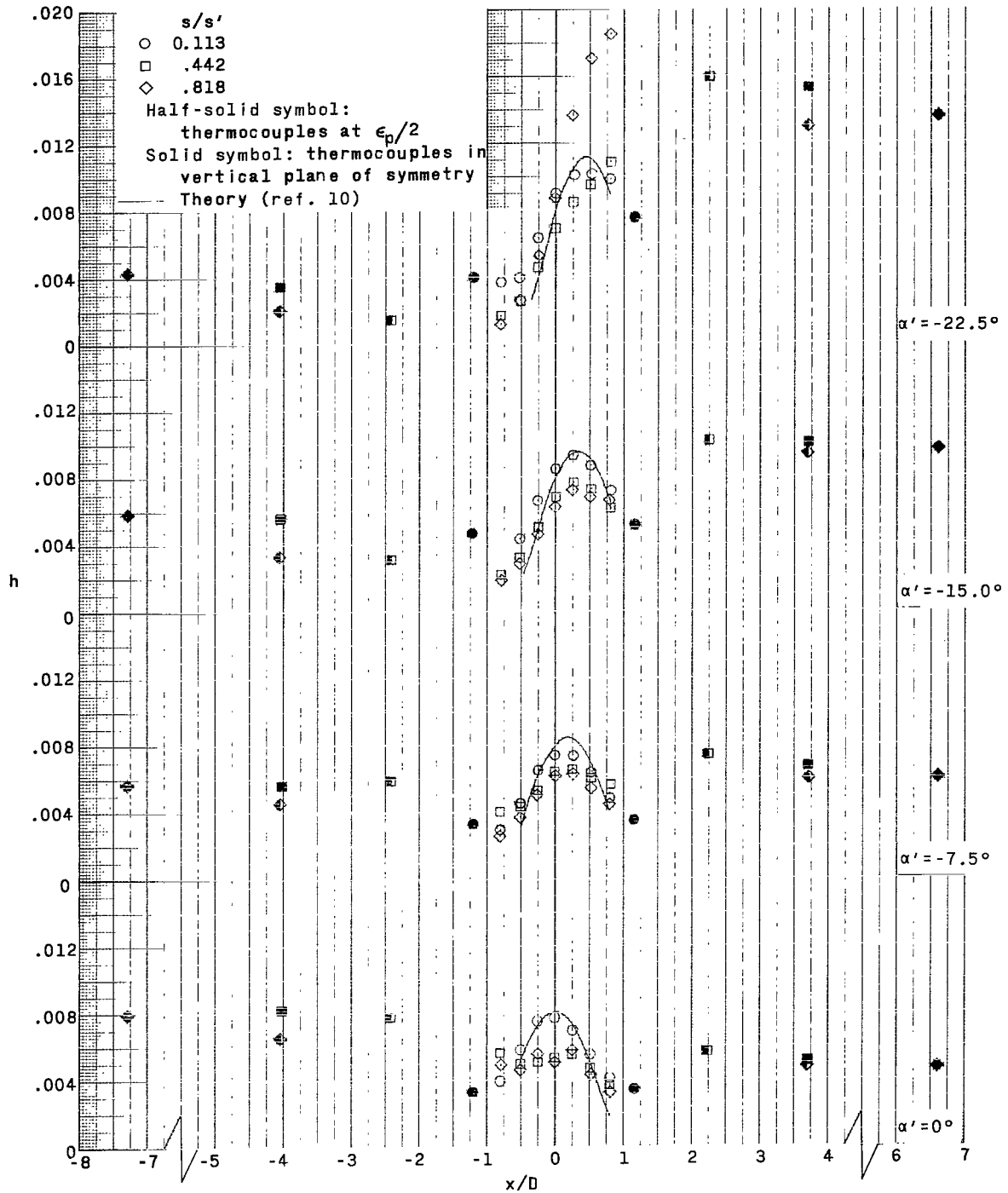
(a) Concluded.

Figure 15.- Continued.



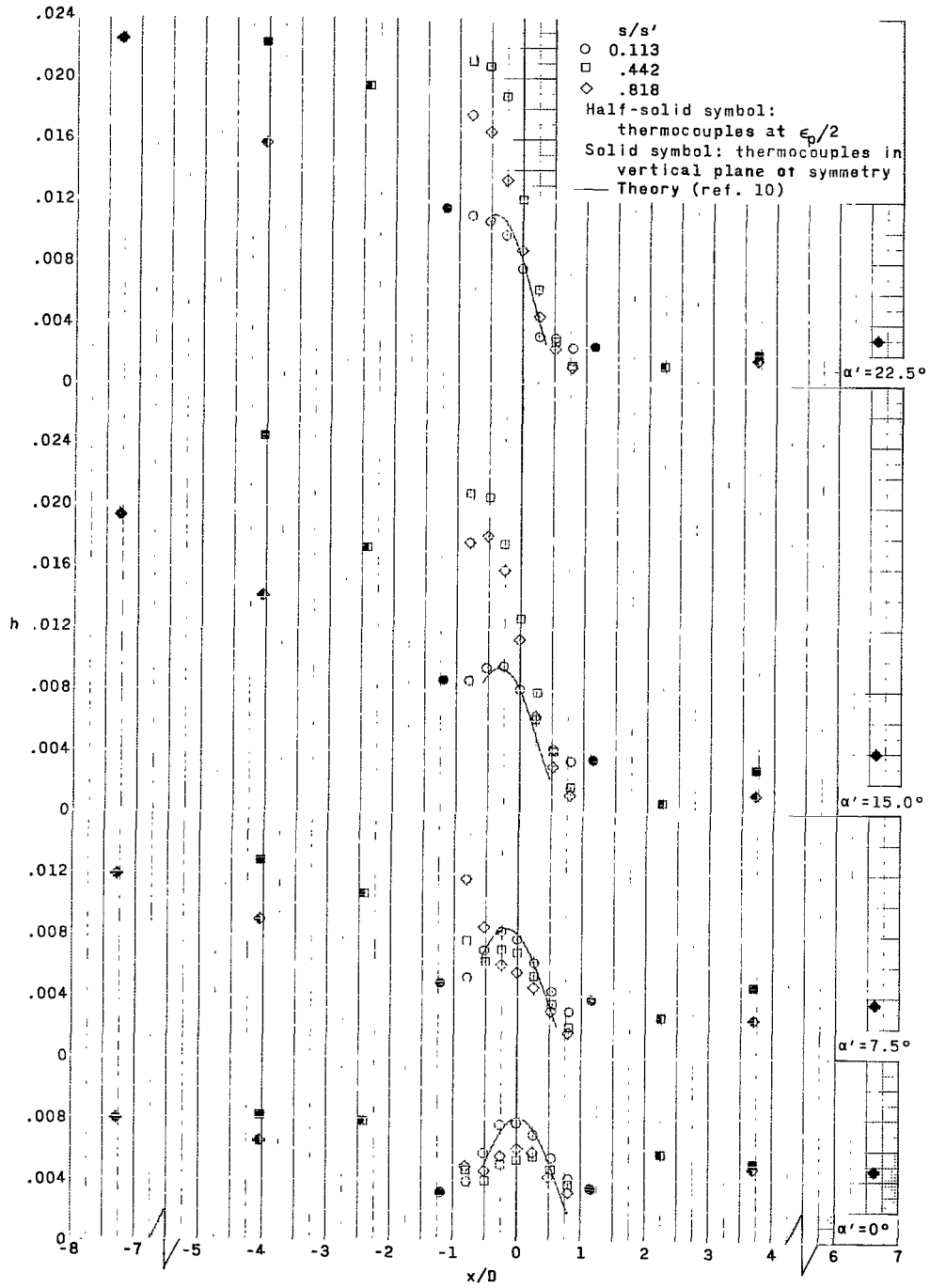
(b)  $M = 3.51$ ;  $R \approx 4.00 \times 10^6$ .

Figure 15.- Continued.



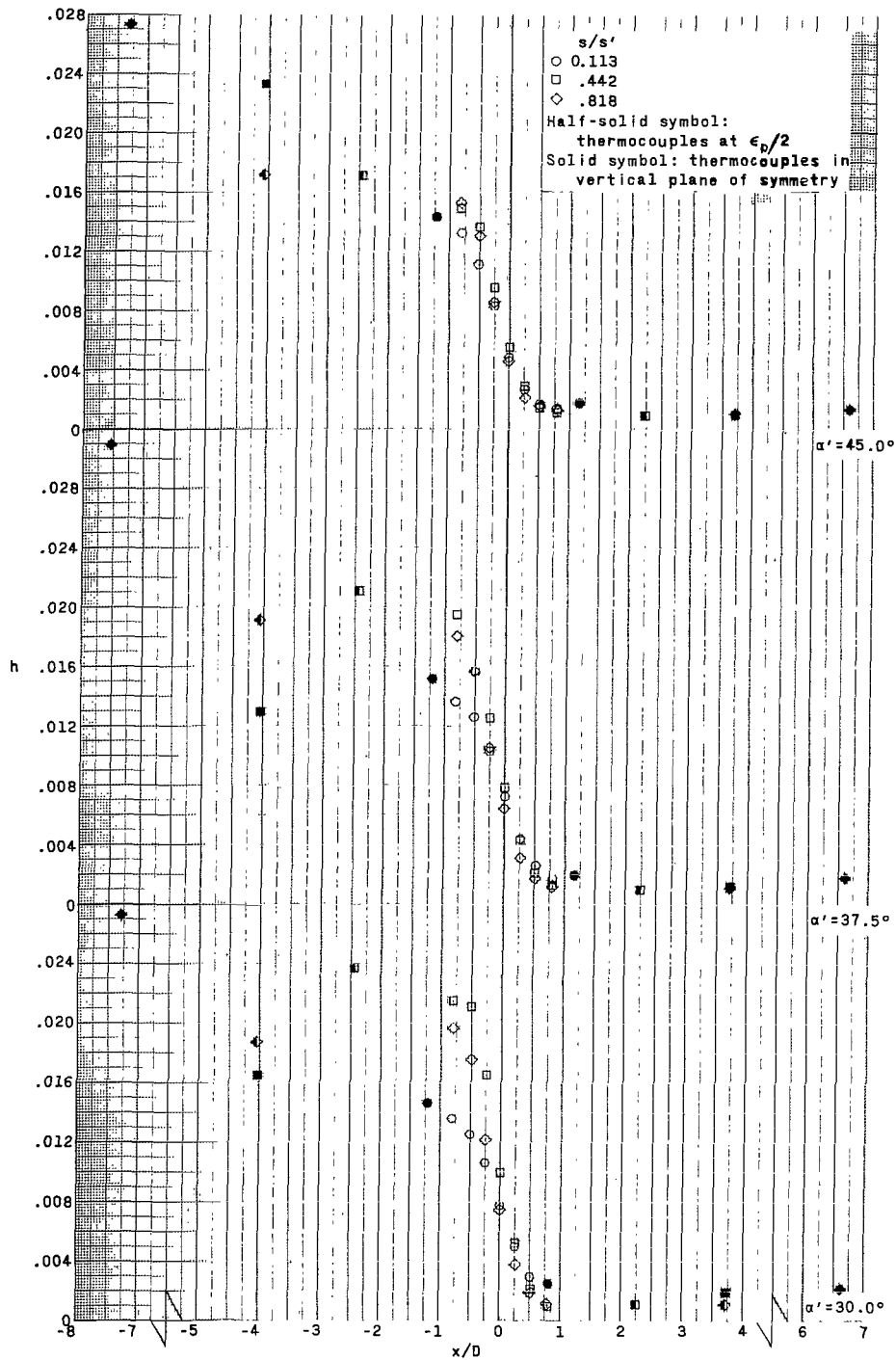
(b) Continued.

Figure 15.- Continued.



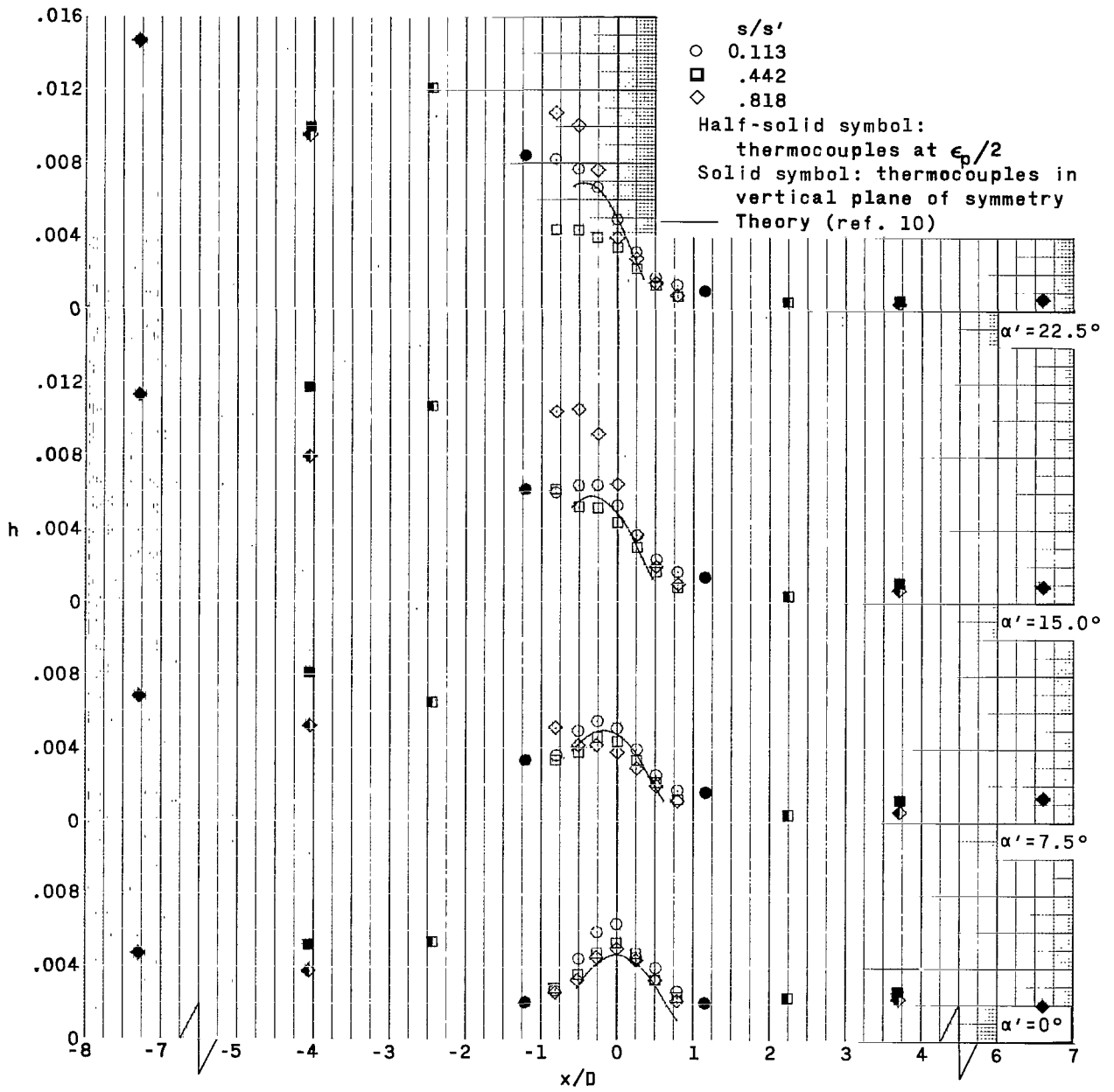
(b) Continued.

Figure 15.- Continued.



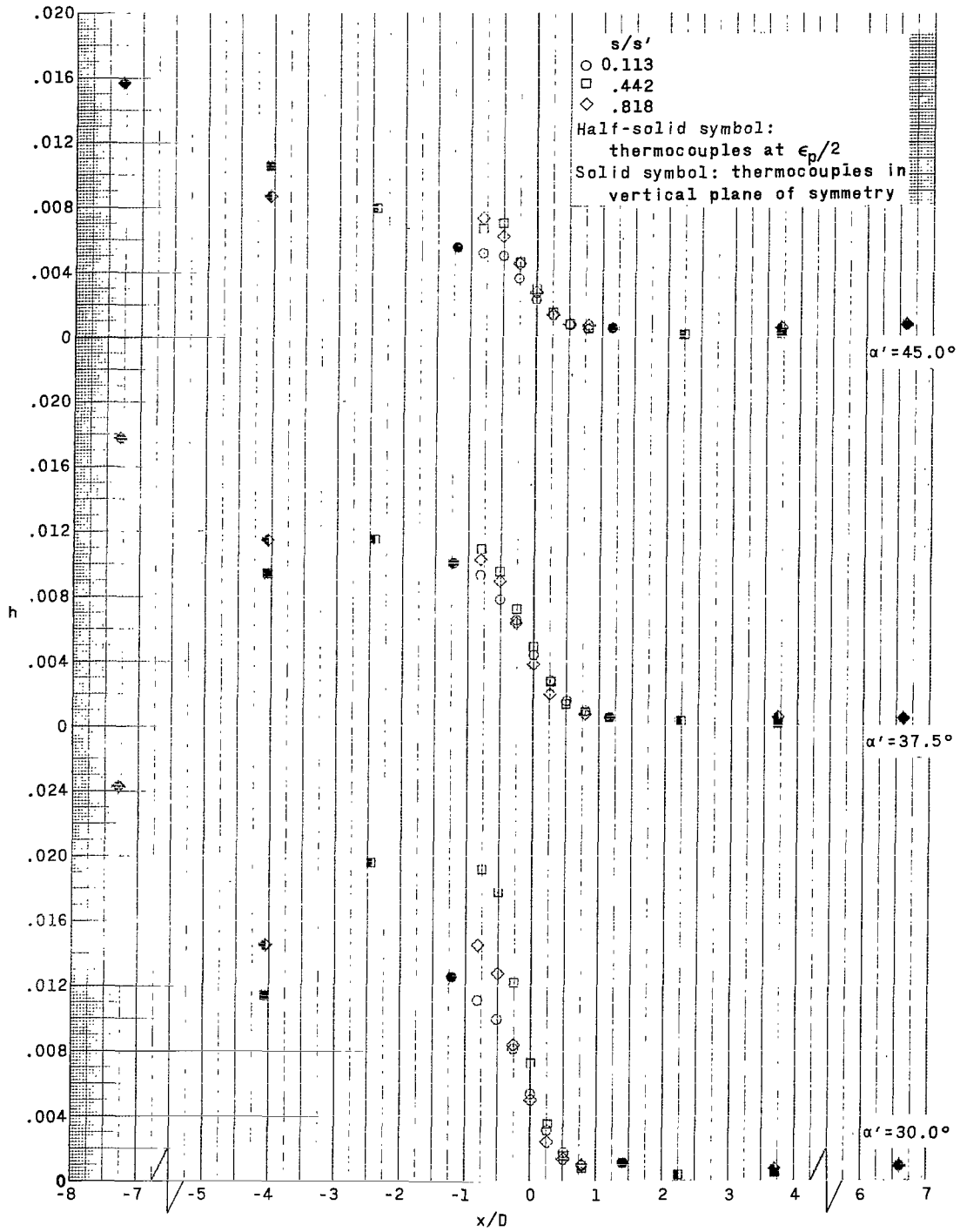
(b) Concluded.

Figure 15.- Continued.



(c)  $M = 4.65$ ;  $R \approx 2.90 \times 10^6$ .

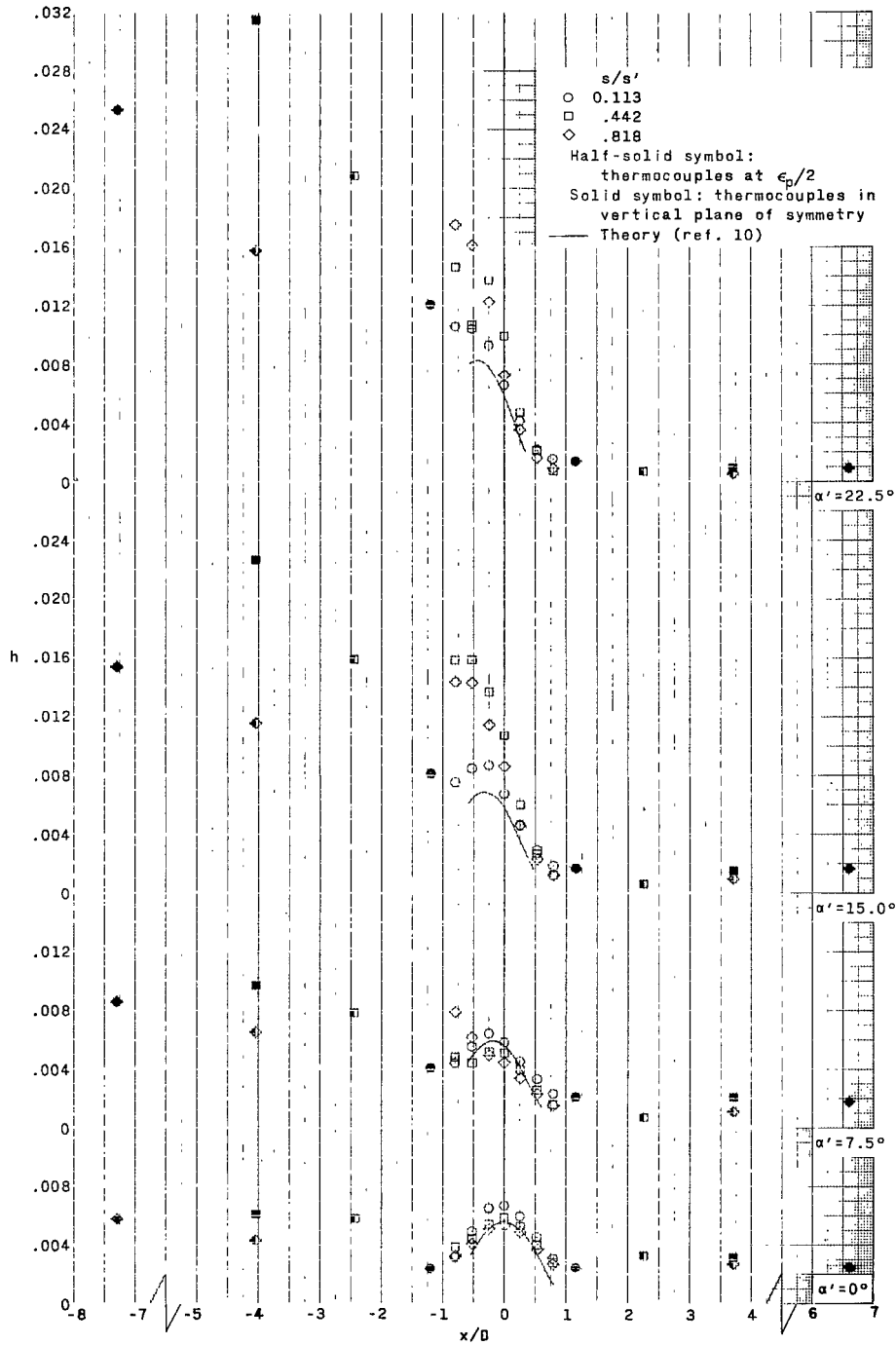
Figure 15.- Continued.



(c) Concluded.

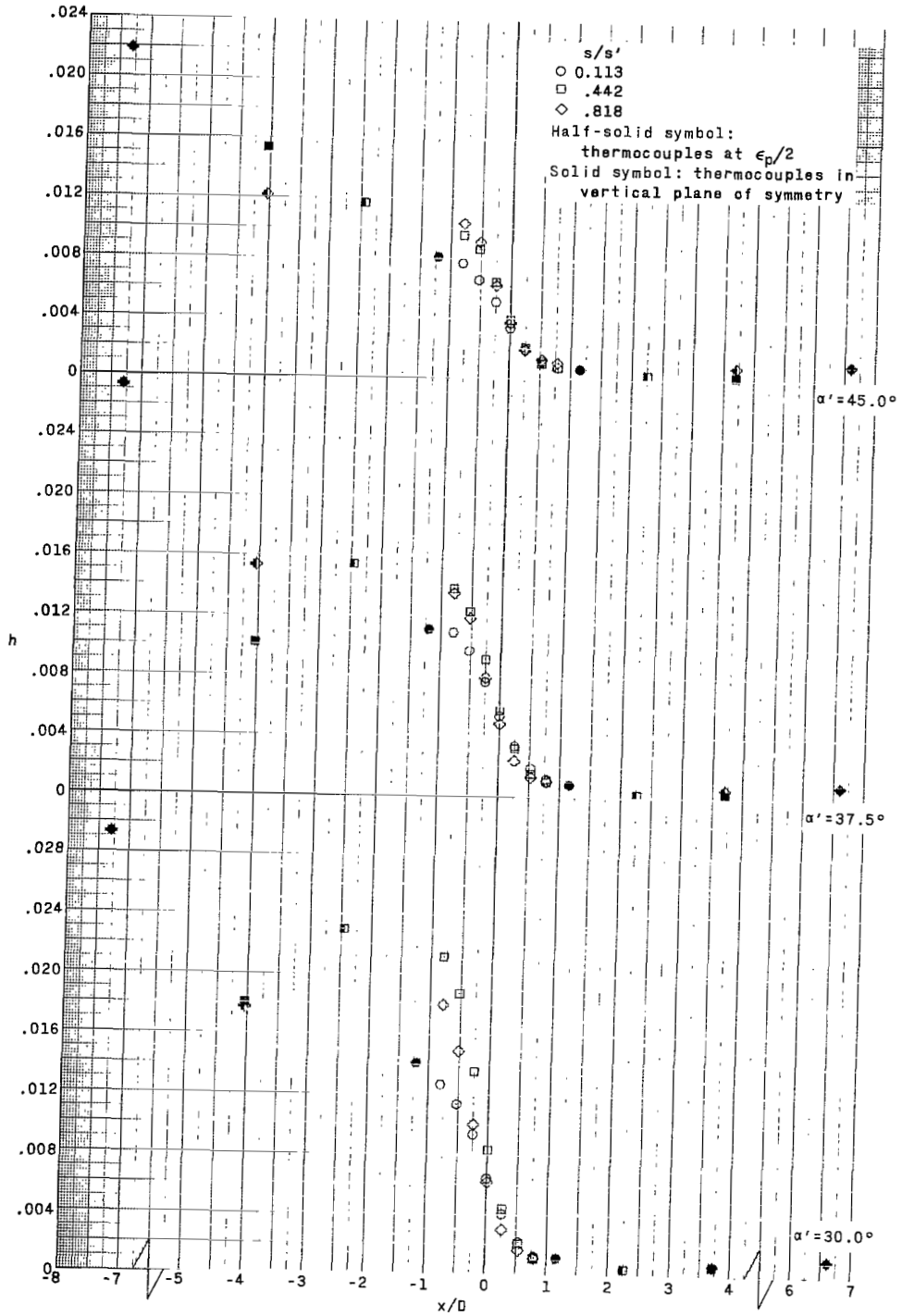
Figure 15.- Continued.





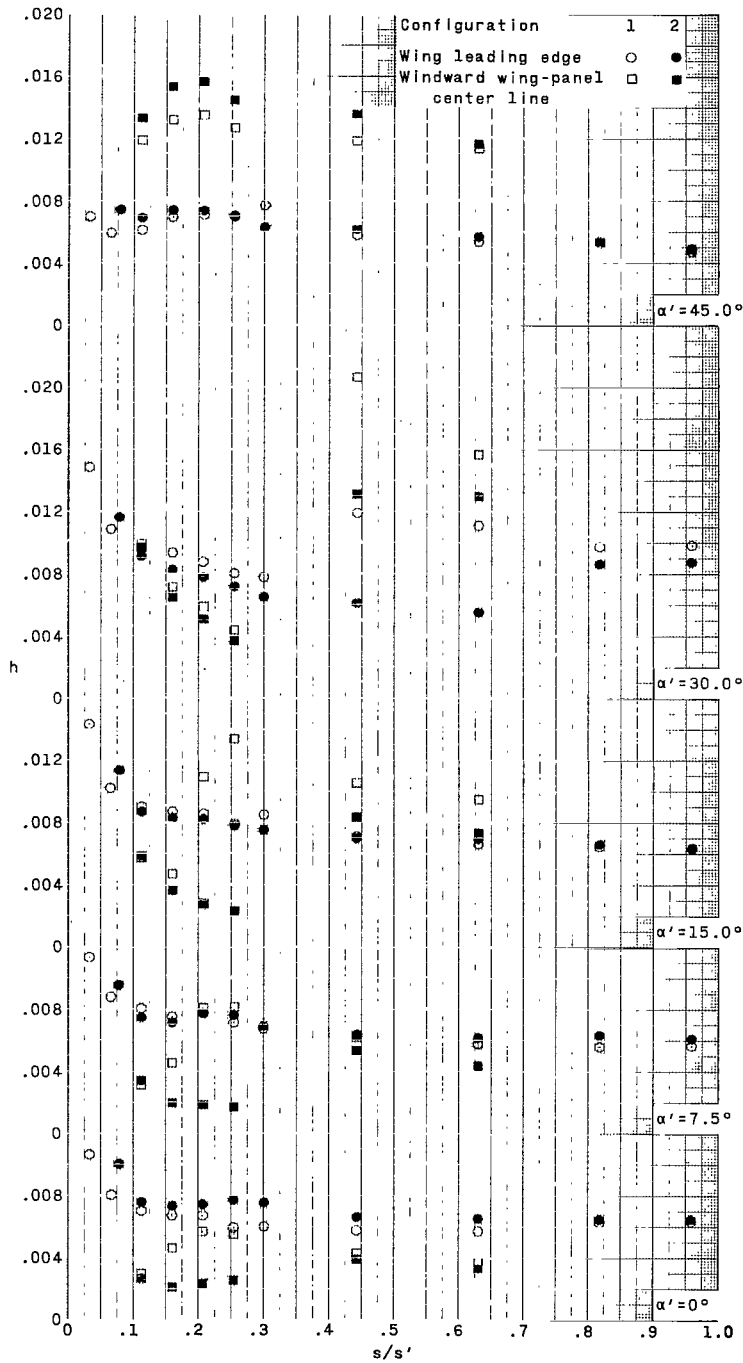
(d)  $M = 4.65$ ;  $R \approx 4.10 \times 10^6$ .

Figure 15.- Continued.



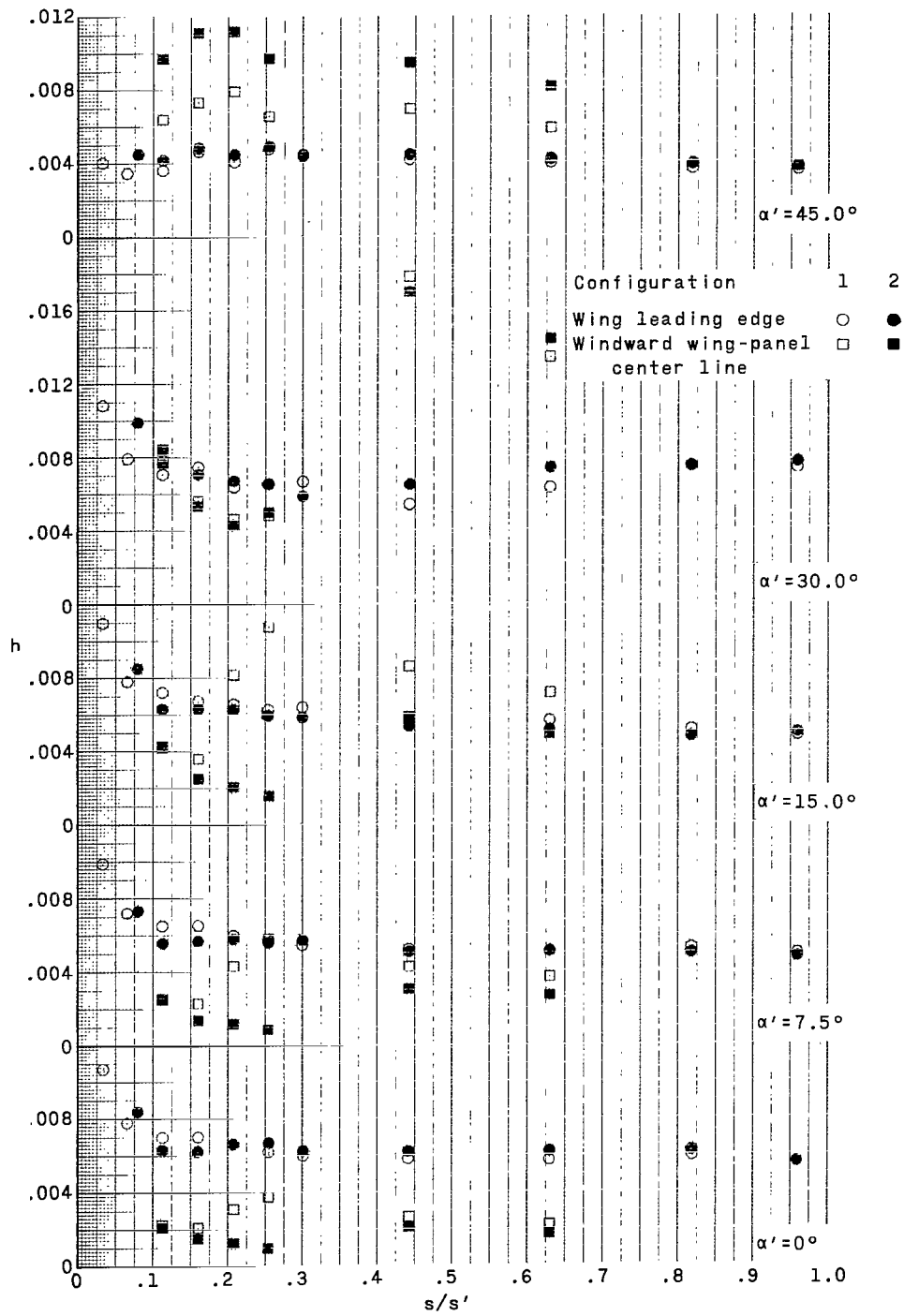
(d) Concluded.

Figure 15.- Concluded.



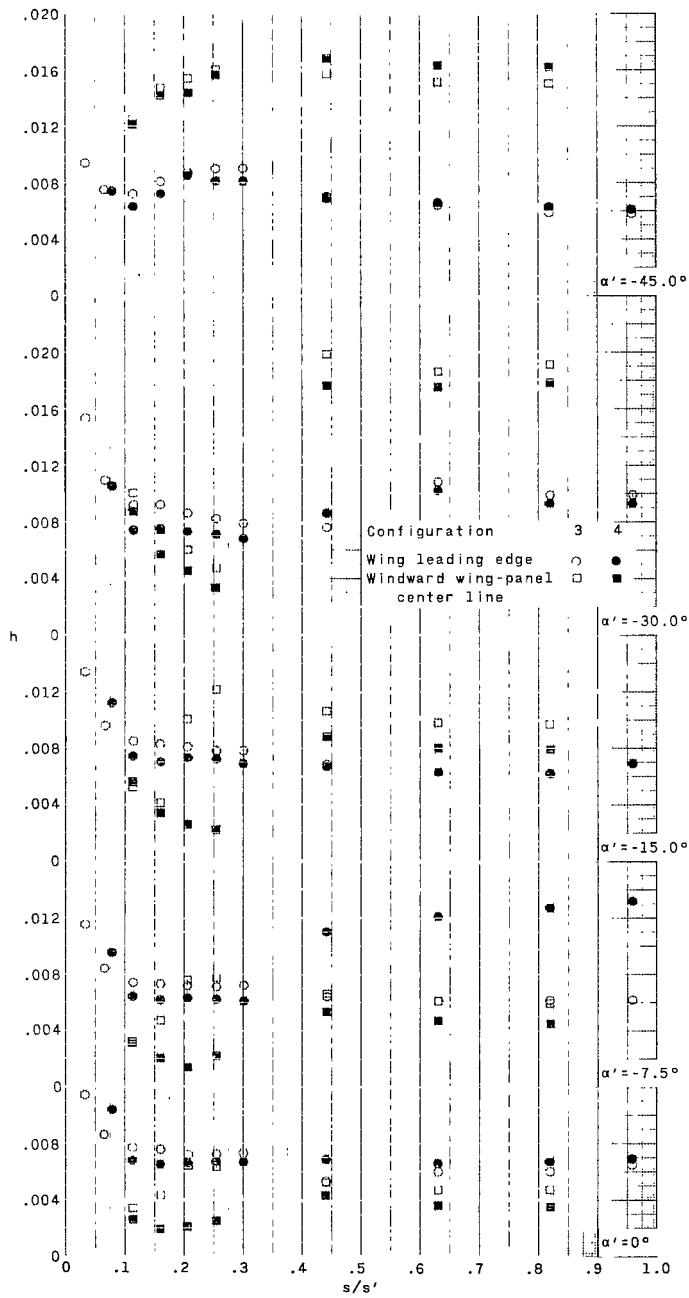
(a)  $M = 3.51$ ;  $R \approx 4.00 \times 10^6$ .

Figure 16.- Effect of nose bluntness on heat-transfer-coefficient distribution along windward center line and wing leading edge of models with  $0^\circ$  dihedral.



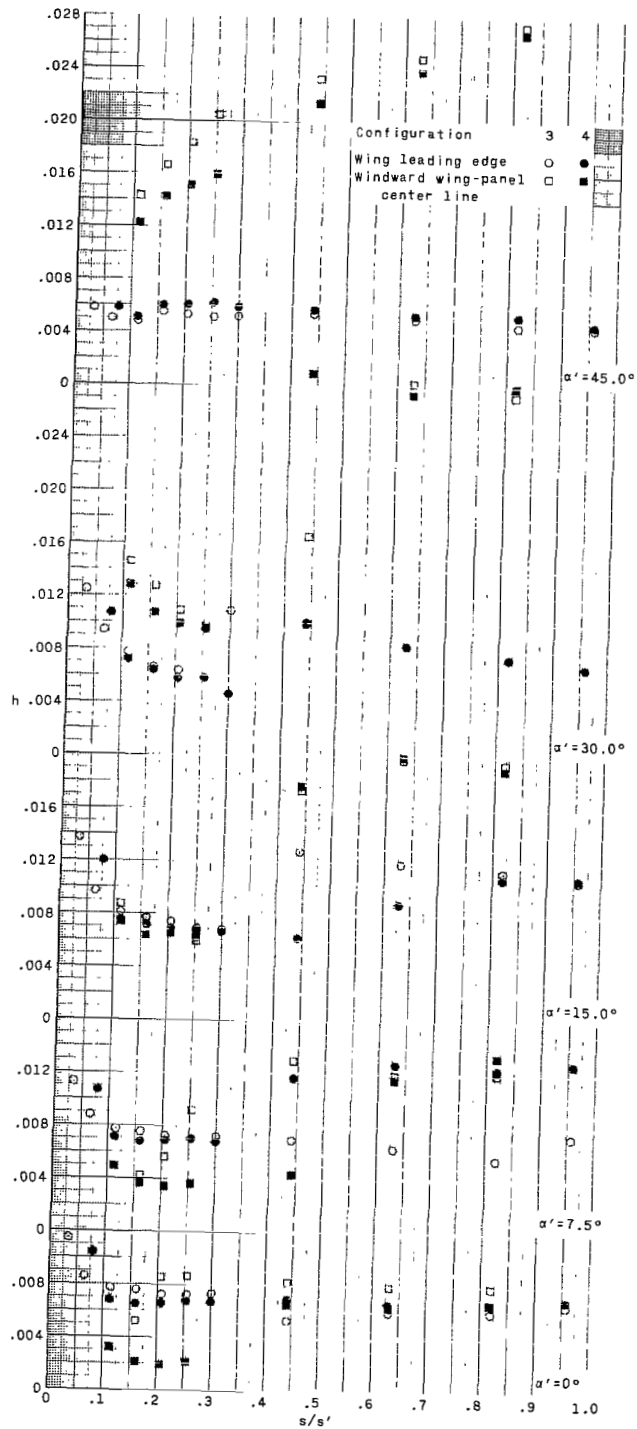
(b)  $M = 4.65$ ;  $R \approx 4.10 \times 10^6$ .

Figure 16.- Concluded.



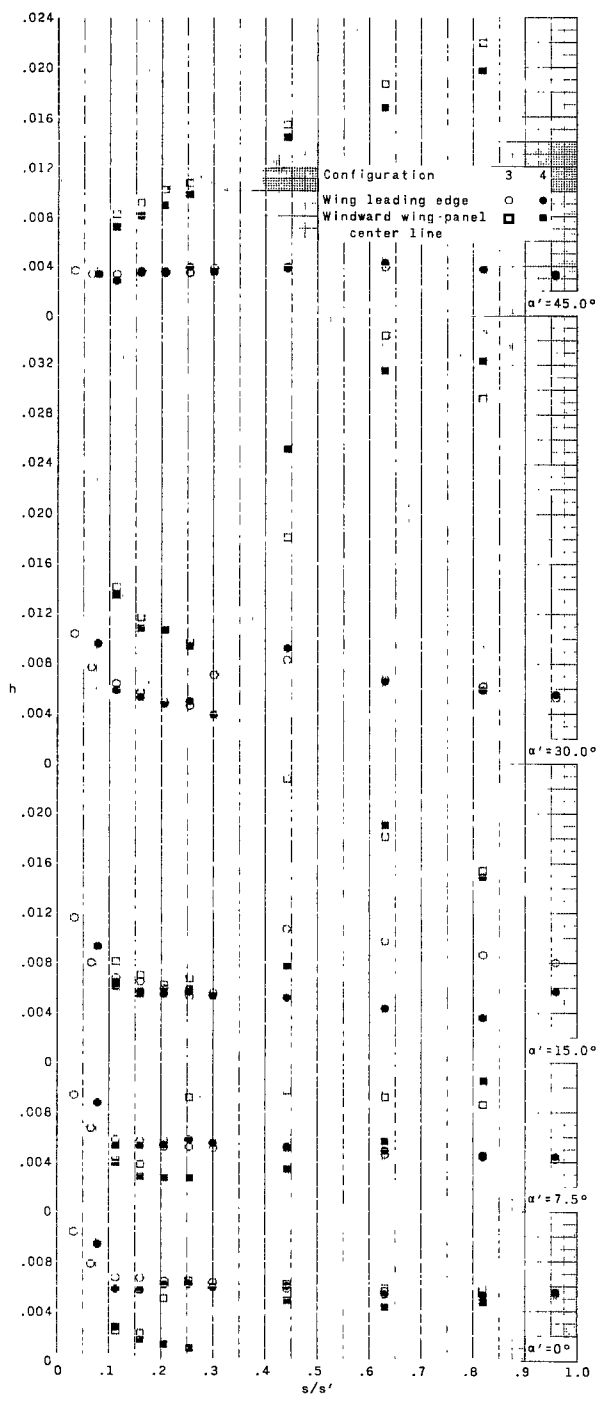
(a)  $M = 3.51$ ;  $R \approx 4.00 \times 10^6$ .

Figure 17.- Effect of nose bluntness on heat-transfer-coefficient distribution along windward center line and wing leading edge of models with  $24.3^\circ$  dihedral.



(a) Concluded.

Figure 17.- Continued.



(b)  $M = 4.65$ ;  $R \approx 4.10 \times 10^6$ .

Figure 17.- Concluded.

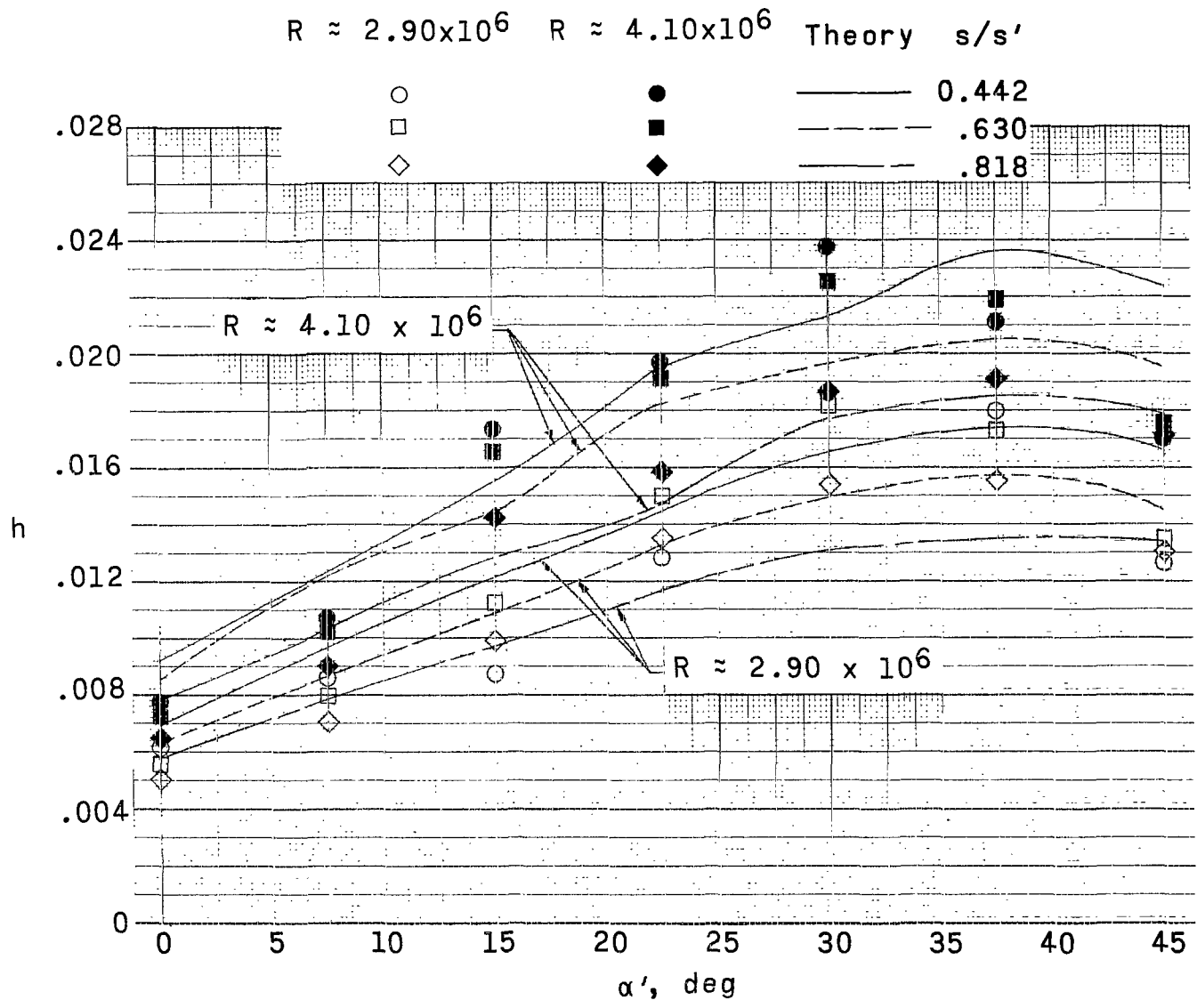
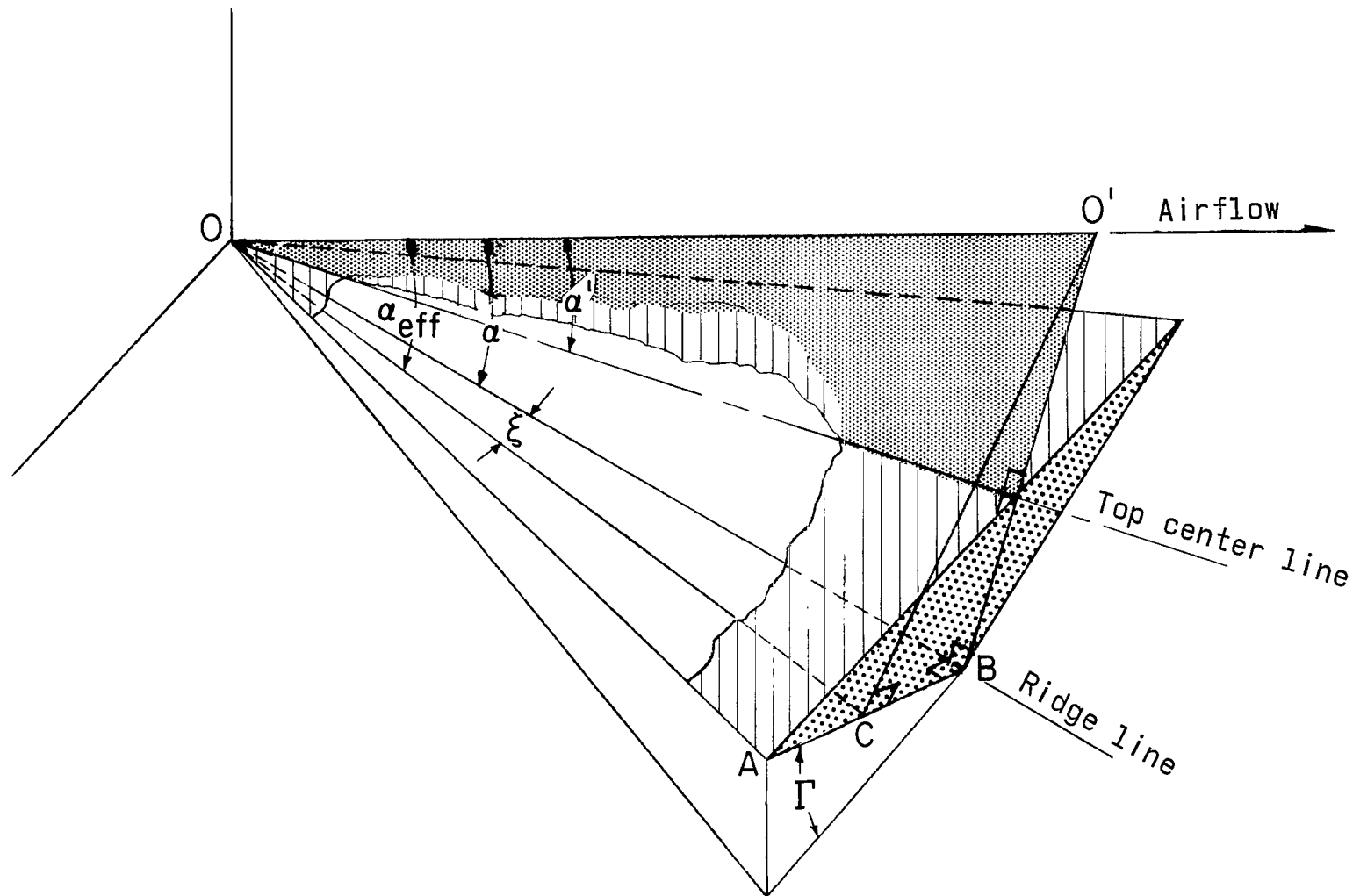


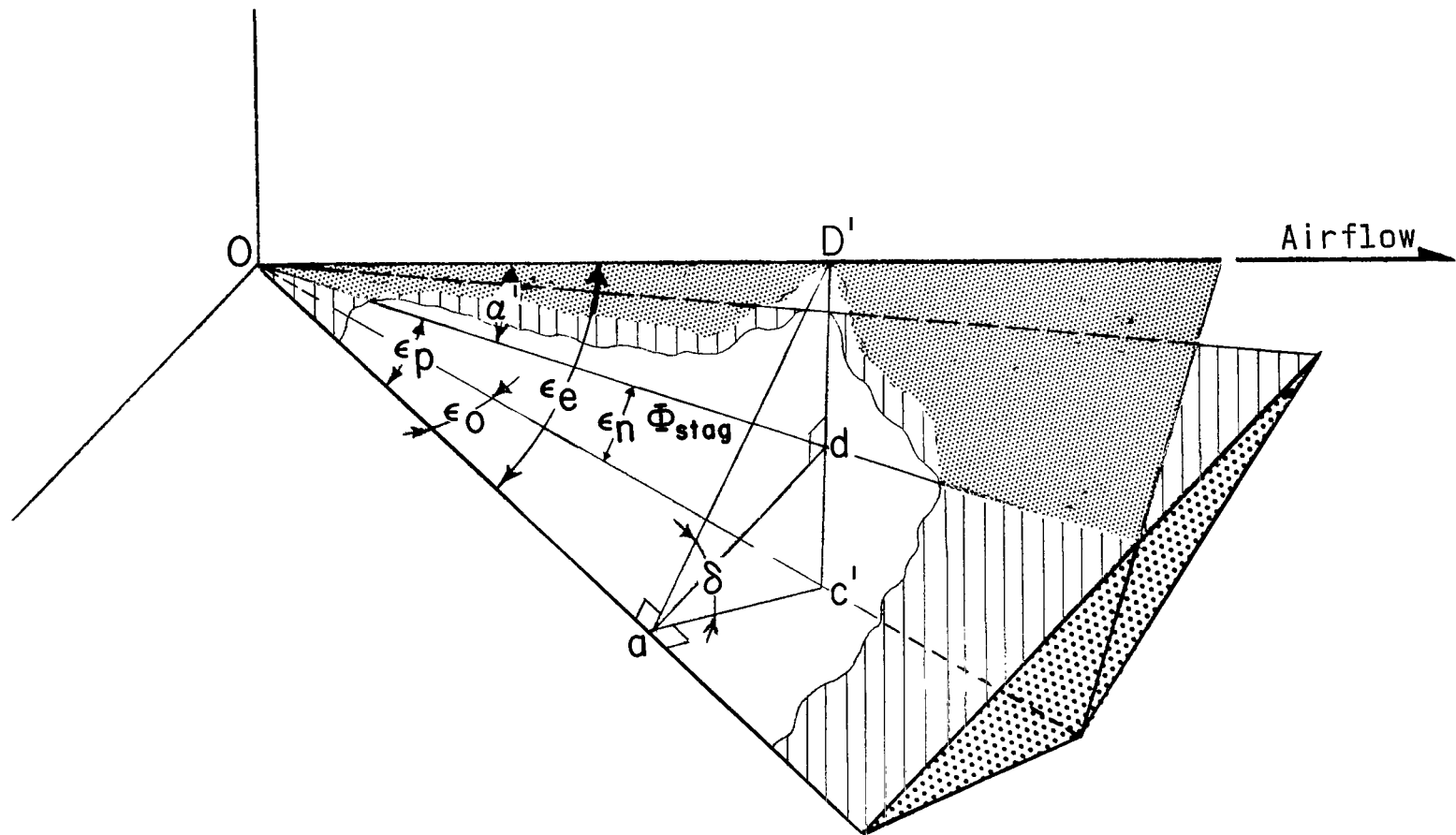
Figure 18.- Effect of angle of attack on heat-transfer-coefficient distribution along windward wing panel at  $\epsilon_p/2$  of configuration 3.  $M = 3.51$ .





(a) In plane perpendicular to ridge line.

Figure 19.- Wing geometry.



(b) In plane perpendicular to wing leading edge.

Figure 19.- Concluded.

2/7/85  
of

*"The aeronautical and space activities of the United States shall be conducted so as to contribute . . . to the expansion of human knowledge of phenomena in the atmosphere and space. The Administration shall provide for the widest practicable and appropriate dissemination of information concerning its activities and the results thereof."*

—NATIONAL AERONAUTICS AND SPACE ACT OF 1958

## NASA SCIENTIFIC AND TECHNICAL PUBLICATIONS

**TECHNICAL REPORTS:** Scientific and technical information considered important, complete, and a lasting contribution to existing knowledge.

**TECHNICAL NOTES:** Information less broad in scope but nevertheless of importance as a contribution to existing knowledge.

**TECHNICAL MEMORANDUMS:** Information receiving limited distribution because of preliminary data, security classification, or other reasons.

**CONTRACTOR REPORTS:** Technical information generated in connection with a NASA contract or grant and released under NASA auspices.

**TECHNICAL TRANSLATIONS:** Information published in a foreign language considered to merit NASA distribution in English.

**TECHNICAL REPRINTS:** Information derived from NASA activities and initially published in the form of journal articles.

**SPECIAL PUBLICATIONS:** Information derived from or of value to NASA activities but not necessarily reporting the results of individual NASA-programmed scientific efforts. Publications include conference proceedings, monographs, data compilations, handbooks, sourcebooks, and special bibliographies.

*Details on the availability of these publications may be obtained from:*

SCIENTIFIC AND TECHNICAL INFORMATION DIVISION  
NATIONAL AERONAUTICS AND SPACE ADMINISTRATION  
Washington, D.C. 20546